Cape Peninsula
University of Technology

TREATMENT OF BIODIESEL WASTEWATER IN A HYBRID ANAEROBIC BAFFLED REACTOR MICROBIAL FUEL CELL (ABR-MFC) SYSTEM

by
LOREEN GROBBELAAR

Thesis submitted in fulfilment of the requirements for the degree
Master of Engineering: Chemical Engineering

in the Faculty of
Engineering

at the
Cape Peninsula University of Technology

Supervisor: Dr. Debbie De Jager

Co-supervisors: Prof. Marshall S. Sheldon
Dr. Buntu Godongwana

Cape Town
March 2019

DECLARATION

I, Loreen Grobbelaar, declare that the contents of this thesis represent my own unaided work, and that the thesis has not previously been submitted for academic examination towards any qualification. Furthermore, it represents my own opinions and not necessarily those of the Cape Peninsula University of Technology.

Signed **Date**

ABSTRACT

The biodiesel industry produces large volumes of biodiesel wastewater (BDWW) during the purification of crude biodiesel. This wastewater is characterised by high concentrations of chemical oxygen demand (COD), biological oxygen demand (BOD), total suspended solids (TSS), and fats, oils and greases (FOG) which in turn defines BDWW as a highly polluted effluent. The low nitrogen and phosphorous content of BDWW creates an unfavourable environment for the growth of microorganisms, thereby making it difficult to degrade naturally.

Biodiesel companies discharge untreated non-compliant wastewater directly to the municipal sewer system. Treatment prior to discharge is a necessity since the disposal of untreated BDWW may raise serious environmental concerns (i.e. disturbance of biological ecosystems) resulting in penalties liable by non-compliant companies due to the implementation of the waste discharge charge system (WDCS) which is regulated by the industrial waste discharge standard limits in South Africa (SA).

This study aimed to combine the advantages of the conventional anaerobic baffled reactor (ABR) system with microbial fuel cell (MFC) technology resulting in an innovative technology used to treat high strength industrial BDWW at ambient conditions. Many studies have reported effective treatment of BDWW, however to date literature implementing an ABR equipped with MFC technology has not been reported.

The main objectives of the study were to determine which parameters do not meet the industrial wastewater discharge standard limits, whether pH and carbon:nitrogen:phosphorous (C:N:P) ratio adjustments will suffice prior to treatment with the ABR-MFC, the maximum power density (PD) as well as to determine the treatment efficiency of the ABR-MFC.

BDWW obtained from a local biodiesel production plant employing alkali-transesterification of waste vegetable oil, was fed to the ABR-MFC at three organic loading rates (OLR) (1.15, 1.98 and 3.46 kg COD/m^3.day) as well as a constant hydraulic retention time (HRT) of 10 days. The ABR-MFC successfully reduced the COD, FOG and TSS by 64.55%, 99.96% and 98.55%, respectively during OLR 3 while achieving a maximum PD of 296 mW/m^2 at a current density of 4.69 mA/m^2 and an internal resistance of 280.69 Ω.

The COD concentration of the BDWW was the only parameter after treatment to not meet the industrial wastewater discharge standard limits. The COD could be further reduced by including a post-treatment step to further reduce the COD contained in BDWW.

The 6-compartment single-chamber membrane-less ABR-MFC successfully treated industrial BDWW while simultaneously generating electricity without the need for a pre-treatment step and the implementation of a recycle stream. However, more research should be conducted to increase system efficiency regarding COD removal and the maximum PD achieved by the laboratory scale ABR-MFC system.

This research would benefit biodiesel industries in the Western Cape (South Africa), with an option to meet the industrial wastewater discharge standard limits imposed by the City of Cape Town. Biodiesel industries could potentially reduce their carbon footprint (i.e. reduce their environmental impact) and benefit financially by potentially eliminating or reducing penalties resulting from the implementation of the waste discharge charge system. Ultimately, this research would provide baseline information for future researchers in the field of BDWW treatment with MFC technology since this research could be fundamental for scale-up to pilot- and full-scale systems.

ACKNOWLEDGEMENTS

I wish to thank:

- Cape Peninsula University of Technology (CPUT) for the financial support and for giving me the opportunity to pursue my dream.
- My supervisor Dr. Debbie De Jager, for her understanding, integrity, humility, patience, professional guidance and continuous support, for sharing her knowledge and wisdom, and for inspiring me throughout my research.
- My co-supervisor Dr. Buntu Godongwana for his professional assistance, guidance, knowledge and financial support throughout this project, whom without this project would not have been possible.
- My co-supervisor Prof. Marshall Sheldon for her financial and emotional assistance, integrity and humility.
- Mr. Alwyn Bester, Mrs. Hannelene Small and Mrs. Elizma Alberts for their continuous support and assistance throughout my studies at CPUT.
- Our industrial partner for agreeing to supply us with biodiesel wastewater and thereby giving me the opportunity to gain invaluable experience.
- Athlone Wastewater Treatment Works for their assistance in supplying aerobic granules and for allowing us to use their facilities.
- South African Breweries (SAB) for their assistance in supplying anaerobic granules from their upflow anaerobic sludge bed (UASB) reactor.
- Cabot Corporation for supplying us with activated carbon and carbon black.
- My fellow postgraduate colleagues at CPUT for their support and encouragement.
- My family and friends, for your much-needed love, support and continuous motivation.
- The holy trinity, God the Father, God the Son and God the Holy Spirit, for giving me the faith, wisdom and strength needed.

The financial assistance of the National Research Foundation (NRF) towards this research is acknowledged. Opinions expressed in this thesis and the conclusions arrived at, are those of the author, and are not necessarily to be attributed to the National Research Foundation.

DEDICATION

This thesis is dedicated to my father, mother and brother.
Without your unconditional love, constant support and encouragement, and utmost faith in me,
I would not be where I am today.

TABLE OF CONTENTS

LIST OF FIGURES

LIST OF TABLES

LIST OF SYMBOLS

Roman Symbols	Definition
A_{brush}	Brush area [cm^2]
A_{fibre}	Fibre area [cm^2]
$C_{available}$	Available carbon concentration in wastewater used as substrate [$mg\ COD/l$]
$C_{optimal}^{ratio}$	Optimal carbon ratio for C:N:P ratio
C_p	Total number of coulombs [C]
C_T	Theoretical amount of coulombs that can be produced from the COD contained in the wastewater used as substrate [C]
E	Measured potential difference of cell [$V\ or\ mV$]
E°	Standard cell electromotive force [V]
E_{emf}	Maximum electromotive force [V]
F	Faraday's Constant [$96\,485\ Coulombs/mol$]
H	Height [m or cm or mm]
H_{void}^{ABR}	ABR void height [m or cm or mm]
H_{void}^{Baffle}	Baffle void height [m or cm or mm]
HRT	Hydraulic retention time [days]
I	Current [A]
IR_{int}	Product of current and internal resistance [V]
J_{ACV}	Current density normalised to anodic chamber volume [A/m^3]
J_{ASA}	Current density normalised to anode surface area [A/m^2]
K'	Kelvin
K	Potassium
L	Length [m or cm or mm]
$L_{Separator}$	Length of one separator [m^3 or l or ml]

L_{void}^{ABR}	ABR void length [m or cm or mm]
L_{void}^{Baffle}	Baffle void length [m or cm or mm]
m	Mass [mg]
$m_{combust}$	Mass after combustion [mg]
m_{post}	Mass after drying [mg]
m_{pre}	Mass before addition of sample [mg]
Mr	Molar mass [g/mol]
n	Number of electrons transferred
$N_{available}$	Available nitrogen concentration in wastewater used as substrate [$mg\ N/l$]
$N_{optimal}^{ratio}$	Optimal nitrogen ratio for C:N:P ratio
$N_{optimal}^{sample}$	Optimal amount of nitrogen for C:N:P ratio [$mg\ N/l$]
$N_{required}$	Amount of nitrogen to be added in order to achieve an optimal C:N:P ratio [$mg\ N/l$]
OC_{feed}^{COD}	Organic matter (COD) concentration of the feed substrate [mg/l]
$OC_{Product}^{COD}$	Organic matter (COD) concentration in the product [mg/l]
OC_{feed}^{FOG}	Organic matter (FOG) concentration of the feed substrate [mg/l]
$OC_{Product}^{FOG}$	Organic matter (FOG) concentration in the product [mg/l]
$OC_{feed}^{NO_3^-}$	NO_3^- concentration of the feed substrate [mg/l]
$OC_{Product}^{NO_3^-}$	NO_3^- concentration in the product [mg/l]
OC_{feed}^{TP}	TP concentration of the feed substrate [mg/l]
$OC_{Product}^{TP}$	TP concentration in the product [mg/l]
OC_{feed}^{TSS}	TSS concentration of the feed substrate [mg/l]
$OC_{Product}^{TSS}$	TSS concentration in the product [mg/l]
OC_{feed}^{VSS}	VSS concentration of the feed substrate [mg/l]
$OC_{Product}^{VSS}$	VSS concentration in the product [mg/l]
OCV	Open circuit voltage [V]

OCV^*	Open circuit voltage calculated from the slope of the polarization curve [V]
OLR	Organic loading rate [$kg\ COD/m^3.day$]
p	Stoichiometric coefficient of products
P	Power generated [W]
P	Phosphorous
P_{max}	Maximum power generated [W]
$P_{available}$	Available phosphorous concentration in wastewater used as substrate [$mg\ P/l$]
$P_{optimal}^{ratio}$	Optimal phosphorous ratio for C:N:P ratio
$P_{optimal}^{sample}$	Optimal amount of phosphorous for C:N:P ratio [$mg\ P/l$]
$P_{required}$	Amount of phosphorous to be added in order to achieve an optimal C:N:P ratio [$mg\ P/l$]
PD	Power density [W/m^3 or W/m^2]
PD_{ACV}	Power density normalised to anodic chamber volume [W/m^3]
$PD_{ACV}^{ABR-MFC}$	Power density normalised to anodic chamber volume for ABR-MFC [W/m^3]
PD_{ACV}^{C1-C6}	Power density normalised to anodic chamber volume for compartments 1 to 6 [W/m^3]
PD_{CSA}	Power density normalised to cathode surface area [W/m^2]
$PD_{CSA}^{ABR-MFC}$	Power density normalised to cathode surface area for ABR-MFC [W/m^3]
PD_{CSA}^{C1-C6}	Power density normalised to cathode surface are for compartments 1 to 6 [W/m^2]
PD_{ASA}	Power density normalised to anode surface area [W/m^2]
$PD_{ASA}^{ABR-MFC}$	Power density normalised to anode surface area for ABR-MFC [W/m^3]
PD_{ASA}^{C1-C6}	Power density normalised to anode surface area for compartments 1 to 6 [W/m^2]
$[products]^p$	Concentration of products
Q_{feed}	Influent flow rate [l/day or ml/min or m^3/day]
r	Stoichiometric coefficient of reactants

R	Universal Gas Constant [$8.31447\ J/mol.K$]
R_{ext}	External resistance of the cell [Ω]
$[reactants]^r$	Concentration of reactants
R_{int}	Internal resistance of the cell [Ω]
$SA_{Electrode}$	Electrode surface area [cm^2]
SA_A	Anode electrode surface area [cm^2]
SA_T^{Anode}	Total anode electrode surface area [cm^2]
SA_C	Cathode electrode surface area [cm^2]
SVI	Sludge volume index [ml/g]
T	Absolute temperature [K]
TSS	Total suspended solids [mg/l]
t_{ave}	Average time [s or min or hr]
V_{ave}	Average volume [ml]
V_{Baffle}	Volume of one baffle [m^3 or l or ml]
V_T^{Baffle}	Total volume of all baffles [m^3 or l or ml]
$V_{Electrode}$	Electrode volume [m^3 or l or ml]
V_{sample}	Sample volume [ml]
$V_{separator}$	Volume of one separator [m^3 or l or ml]
$V_{settled}$	Settled sludge volume [ml/l]
$V_T^{separator}$	Total volume of all separators [m^3 or l or ml]
V_T	Net liquid volume of the anodic chamber (i.e. working volume of the reactor) [m^3 or l or ml]
V_T^{ABR}	Total ABR volume [m^3 or l or ml]
V_T^{Anode}	Total anodic chamber volume [m^3 or l or ml]
$V_T^{Cathode}$	Total cathodic chamber volume [m^3 or l or ml]
V_{Void}	Void volume [m^3 or l or ml]

V_{Void}^{ABR}	Void volume of ABR [m^3 or l or ml]
$V_{Total\ void}^{Baffles}$	Total void volume of baffles [m^3 or l or ml]
V_W	Working volume [m^3 or l or ml]
V_W^{ABR}	Working volume of ABR [m^3 or l or ml]
$V_W^{ABR-MFC}$	Working volume of ABR-MFC [m^3 or l or ml]
V_W^{Anode}	Anodic chamber working volume [m^3 or l or ml]
$V_W^{Cathode}$	Cathodic chamber working volume [m^3 or l or ml]
W	Width [m or cm or mm]
W_{void}^{ABR}	ABR void width [m or cm or mm]
W_{void}^{Baffle}	Baffle void width [m or cm or mm]
$W_{separator}$	Separator width [m or cm or mm]
#	Amount or number

Greek Symbols	**Definition**
ε_{COD}	Organic matter (i.e. COD) removal efficiency [%]
ε_c	Coulombic efficiency [%]
ε_{FOG}	Organic matter (i.e. FOG) removal efficiency [%]
ε_{NO_3}	Nitrate nitrogen (NO_3-N) removal efficiency [%]
ε_{TP}	Total phosphorous removal efficiency [%]
ε_{TSS}	Total suspended solids (TSS) removal efficiency [%]
ε_{VSS}	Volatile suspended solids (VSS) removal efficiency [%]
μ	Micron
Ω	Resistance [ohm]
π	Pi [3.142]
Π	Reaction quotient

LIST OF ABBREVIATIONS

Terms/Acronyms/Abbreviations	Definition/Explanation
A	Ampère [A]
ABR	Anaerobic Baffled Reactor
ABR*	Algal Bioreactor
ABS-MFC	Anaerobic Baffled Stacking Microbial Fuel Cell
AC	Activated Carbon
ACV	Anode Chamber Volume
AD-MFC	Anaerobic Digester Microbial Fuel Cell
AGS	Anaerobic Granular Sludge
$Al(OH)_3$	Aluminium Hydroxide
$Al_2Cl(OH)_5$	Polyaluminium Chloride [mg/l]
AM	Ante Meridiem (Before Noon)
A/m^2	Ampère per Square Meter
AS	Activated Sludge
As	Arsenic [mg/l]
ASA	Anode Surface Area
ASBR	Anaerobic Sequencing Batch Reactor
ASTN	American Standards
Au	Gold [mg/l]
B	Boron [mg/l]
BDWW	Biodiesel Wastewater
BEMR	Bioelectrochemical Membrane Reactor
BFC	Biofilter Circuit
BI	Biodegradability Index
BOD	Biological Oxygen Demand [mg/l]

BOD_5	Biological Oxygen Demand after 5 days incubation [mg/l]
BOD:COD	Biological Oxygen Demand:Chemical Oxygen Demand
BOD_n	Biological Oxygen Demand after n days incubation [mg/l]
C	Carbon
C	Coulombs
C1	Compartment 1
C2	Compartment 2
$C_2Cl_3F_3$	Trichlorotrifluoroethane
$C_2H_3Cl_3$	1,1,1-Trichloroethane
C3	Compartment 3
C_3H_3N	Acrylonitrile
C_3H_6O	Allyl Alcohol
C4	Compartment 4
C5	Compartment 5
C6	Compartment 6
$C_6FeN_6^{3-}$	Ferricyanide
$(C_6H_4NH_2)_2$	Benzidene
CB	Carbon Black
CCl_3F	Trichlorofluoromethane
CCl_4	Carbon Tetrachloride
Cd	Cadmium [mg/l]
CE-MFC	Cassette Electrode Microbial Fuel Cell
$CHCl_3$	Chloroform
CH_2Cl_2	Methylene Chloride
$CH_3CH_2CO_2H$	Propionic Acid
CH_3CH_2OH	Ethanol

$CH_3(CH_2)_7OH$	Octanol
$CH_3CO_2^-$	Acetate
CH_3CO_2H	Acetic Acid
CH_3OH	Methanol
CH_4	Methane [mg/l]
CH_4N_2O	Urea [mg/l]
Cl	Chlorine [mg/l]
cm	Centimetre
cm^2	Square Centimetre
CN^-	Cyanide [mg/l]
C:N:P	Carbon:Nitrate:Phosphate
C:N:P:Fe	Carbon:Nitrate:Phosphate:Iron
CO_2	Carbon Dioxide
CoCT	City of Cape Town
COD	Chemical Oxygen Demand [mg/l]
CPUT	Cape Peninsula University of Technology
Cr	Chromium [mg/l]
Cr^{3+}	Chromium Cations
Cr^{6+}	Chromium Cations
CSA	Cathode Surface Area
CSTR	Continuous Stirred Tank Reactor
Cu	Copper
DAF	Dissolved Air Floatation
dm	Decimetre
dm^3	Cubic Decimetre
DMAc	N,N - Dimethylacetamide
DO	Dissolved Oxygen [mg/l]

DSVI	Diluted Sludge Volume Index [ml/g]
e^-	Electron
EC	Electrical Conductivity [mS/cm]
E_{emf}	Maximum Cell Voltage [V or mV]
EIS	Electrochemical Impedance Spectrometry
EN	European Standards
FAME	Fatty Acid Methyl Ester
Fe	Iron [mg/l]
Fe^{2+}	Iron(II)
$FeCl_2$	Iron(II) Chloride
FFA	Free Fatty Acid
FOG	Fats, Oils and Grease [mg/l]
FPMFC	Flat Plate Microbial Fuel Cell
FT-MFC	Floating Type Microbial Fuel Cell
g	Gram
g/g COD	Gram per Gram Chemical Oxygen Demand
g COD/l.day	Gram Chemical Oxygen Demand per Litre per Day
g COD/m^3.day	Gram Chemical Oxygen Demand per Cubic Metre per Day
g/l	Gram per Litre
g/mol	Grams per Mol
GTMFC	Graphite-granule Tubular Air-Cathode Microbial Fuel Cell
h	Hour(s)
H	Hydrogen
H^+	Proton
H_2	Hydrogen
H_2S	Hydrogen Sulphide [mg/l]

h/day	Hours per Day
H_2O	Water (molecular)
H_2O_2	Hydrogen Peroxide
H_2SO_4	Sulphuric Acid
H_3PO_4	Phosphoric Acid
Hg	Mercury [mg/l]
HRT	Hydraulic Retention Time [days]
K	Kilo
kg	Kilogram
kg COD/m^3.day	Kilogram Chemical Oxygen Demand per Cubic Metre per Day
K_2HPO_4	Dipotassium Hydrogen Phosphate
KH_2PO_4	Potassium Dihydrogen Orthophosphate
KOH	Potassium Hydroxide
kW	Kilowatt
kW/m^3	Kilowatt per Cubic Metre
kW/kg COD treated	Kilowatt per kg Treated Chemical Oxygen Demand
L	Litres
l/day	Litres per Day
l/min	Litres per Minute
m	Metres
mA	Milli-Ampère
mA/A	Milli-Ampère per Ampere
mA/m^2	Milli-Ampère per Square Metre
mm	Millimetre
mM	Millimolar
m^2	Square Metres

m^3	Cubic Metres
MBR	Membrane Bioreactor
MFC	Microbial Fuel Cell
MFC-AFMBR	Microbial Fuel Cell Anaerobic Fluidised Bed Membrane Bioreactor
MFC-BM	Batch Mode Microbial Fuel Cell
MFC-CM	Continuous Mode Microbial Fuel Cell
MFC-SCM	Semi-Continuous Mode Microbial Fuel Cell
Mg^{2+}	Magnesium Cations
mg	Milligrams
mg BOD/l	Milligram Biological Demand per Litre
mg/g	Milligram per Gram
mg/l	Milligrams per Litre
min	Minute(s)
ml	Millilitre
MLAC-MFC	Membrane-Less Air-Cathode Microbial Fuel Cell
ml/dm^3	Millilitres per Cubic Decimetre
ml/g	Millilitres per Gram
ml/l	Millilitres per Litre
MLMFC	Membrane-Less Microbial Fuel Cell
ml/min	Millilitres Per Minute
MW	Megawatt
mW	Milliwatt
mW/m^2	Milliwatt per Square Metre
mW/m^3	Milliwatt per Cubic Metre
mW/W	Milliwatt per Watt
N	Nitrogen

Na	Sodium [mg/l]
Na^+	Sodium Cations
$NaHCO_3$	Sodium Bicarbonate
Na_2HPO_4	Dibasic Sodium Phosphate
NaOH	Sodium Hydroxide
NDP	National Development Plan
NEMA	National Environmental Management Act
NERSA	National Energy Regulator of South Africa
NF	Nanofiltration
NH_3	Ammonia [mg/l]
$NH_4H_2PO_4$	Diammonium Hydrogen Phosphate
$(NH_4)_2SO4$	Ammonium Sulphate
Ni	Nickel [mg/l]
No.	Number
NO_3^-	Nitrate [mg/l]
NO_3-N	Nitrate Nitrogen [mg/]
NRF	National Research Foundation
n/s	Not Specified
NTU	Nephelometric Turbidity Unit
NWA	National Water Act
•OH	Hydroxyl Radical
O	Oxygen (Elemental) [mg/l]
O_2	Oxygen [mg/l]
OCM	Open Circuit Mode
OCV	Open Circuit Voltage (mV)
OLR	Organic Loading Rate [kg COD/m^3.day]
OP	Ortho-phosphate [mg/l]

P	Phosphorous [mg/l]
Pb	Lead [mg/l]
PD	Power Density [W/m^2 or W/m^3]
PEM	Proton Exchange Membrane
PM	Post Meridiem (After Noon)
PO_4	Phosphate
PO_4-P	Ortho-phosphate [mg/l]
pp	Per Person
ppm	Parts per Million
Pt	Platinum
PTFE	Polytetrafluoroethylene
PVDF	Polyvinylidene Fluoride
RO	Reverse Osmosis
rpm	Revolutions per Minute
RSA	Republic of South Africa
S	Sulphide [mg/l]
s	Second(s)
S^{2-}	Sulphide Anions
SA	South Africa
SAB	South African Breweries
Salt	Salinity [mg/l]
SANAS	South African National Accreditation System
Sat	Saturday
SBR	Sequencing Batch Reactor
sCOD	Soluble Chemical Oxygen Demand [mg/l]
Se	Selenium [mg/l]

SEA	Separator Electrode Assembly
SMBR	Submerged Membrane Bioreactor
SMF	Submersible Microbial Fuel Cell
SO_4^{2-}	Sulphate [mg/l]
SPA	Spaced Electrode Assembly
SRT	Sludge Retention Time [days]
SS	Settleable Solids [mg/l]
SSV	Settled Sludge Volume [ml]
SSVI	Stirred Sludge Volume Index [ml/g]
SVI	Sludge Volume Index [ml/g]
tCOD	Total Chemical Oxygen Demand [mg/l]
TDS	Total Dissolved Solids [ppm or mg/l]
Ti	Titanium [mg/l]
TKN	Total Kjeldahl Nitrogen [mg/l]
TP	Total Phosphate [mg/l]
TSS	Total Suspended Solids [mg/l]
Tue	Tuesday
UASB	Up-flow Anaerobic Sludge Blanket
UBFC	Up-flow Bio-filter Circuit
UCT	University of Cape Town
UF	Ultrafiltration
UFAF	Up-flow Anaerobic Filter
USD	United States Dollar
USD/m^3	United States Dollar per Cubic Metre
V	Voltage/Volts
VFA	Volatile Fatty Acid [mg/l]
VSS	Volatile Suspended Solids [mg/l]

W	Watt
WDCS	Waste Discharge Charge System
WISA	Water Institute of Southern Africa
W/kg	Watt per Kilogram
W/kg COD treated	Watt per Kilogram Treated Chemical Oxygen Demand
W/m^2	Watt per Square Metre
WSA	Water Services Act
WVO	Waste Vegetable Oil
WW	Waste Water
YWP	Young Water Professionals
Zn	Zinc [mg/l]
%	Percentage

GLOSSARY

Terms	Definition/Explanation
Acetogenesis	Process where acetate-forming bacteria produce acetate (Gerardi, 2003).
Activated Carbon	A highly porous substance produced via heat treatment of raw materials in the absence of air in order to increase its adsorptive power (Nill, 2016).
Activated Sludge (AS)	Active biomass in the form of solids which are formed during the treatment of wastewater via the activated sludge process (Spellman, 2014).
Alkalinity	Measure of the ability of water to neutralise acids [ppm $CaCO_3$] (Spellman, 2014).
Anaerobic	Pertains to conditions where there is an absence of oxygen/air (Judd, 2010).
Anaerobic Baffled Reactor (ABR)	Watertight chamber equipped with a series of baffles which directs the flow of wastewater through active biomass (i.e. sludge) (Judd, 2010).
Anode	Negative electrode where oxidation occurs (Garverick, 1994).
Biological Oxygen Demand (BOD)	Measure of the oxygen, necessary to maintain sufficient levels of living microorganisms, present in water [mg/l] (Spellman, 2014).
Catalyst	Substances that increase the rate of a chemical reaction (Gerardi, 2003).

Cathode	Positive electrode where reduction occurs (Garverick, 1994).
Chemical Oxygen Demand (COD)	Measure of the organic compounds present in water [mg/l] (Judd, 2010).
Contamination	Deterioration of the quality of water sources (Spellman, 2014).
Current (i.e. electric current)	Rate at which electrons move through an external circuit [A] (Pletcher & Walsh, 1993).
Current Density	Amount of electric current flowing per unit of electrode surface area [A/m^2] (Garverick, 1994).
Coulombic Efficiency	The number of electrons recovered as electrical current compared to the total number of electrons in the substrate (Logan, 2008).
Diffusion	A spontaneous process that occurs in order to obtain a uniform concentration gradient between a site of higher concentration and a site of lower concentration [m^2/s] (Spellman, 2014).
Fats, Oils and Grease (FOG)	Measure of dispersed and dissolved oil contained in the wastewater (Stewart & Arnold, 2009).
Fouling	Process which causes a decrease in system performance due to accumulation of deposits (Judd, 2010).
Hydraulic Retention Time (HRT)	Measure of the average length of time which a soluble particle remains within the reactor [days] (Drioli & Giorno, 2010).

Mediator	A substance used to assist electron transfer from the cellular membrane of a microorganism to an (external) electrode (Liu & Ramnarayanan, 2004).
Methanogens	Methane producing microorganism (Judd, 2010).
Microbial Fuel Cell (MFC)	An electrochemical device which converts chemical energy into electrical energy through metabolic processes executed by microorganisms responsible for the degradation of wastewater (Permana *et al*., 2015).
Open Circuit Voltage (OCV)	Maximum voltage in the charged state at zero current. Maximum voltage reachable by a system (Kumar & Sarakonsri, 2010) at infinite resistance (i.e. open circuit mode) (An *et al*., 2009).
Organic Loading Rate (OLR)	Rate at which organic material is introduced into a system [kg COD/m^3.day] (Bitton, 1998).
Potential difference (i.e. voltage)	Measure of the amount of energy dissipated per unit charge between two points in an electric circuit [V] (Bretschneider & De Weille, 2006).
Power (i.e. electric power)	Measure of the rate of energy (produced or consumed) per unit time [W] (Von Meier, 2006).
Power Density (PD)	Measure of electrical power per unit area or per unit volume [W/m^2 or W/m^3] (Smil, 2015).

OUTPUTS FROM THIS STUDY

- **Articles Submitted for Publication**

Grobbelaar, L., De Jager, D., Godongwana, B. & Sheldon, M.S. 2018. Is it possible to successfully treat biodiesel wastewater and produce electricity simultaneously? *Water Science and Technology*: Submitted 19 February 2018 [Paper ID: FIWA1-IYWP2017-3749873; Manuscript number: WST-EM18464].

- **Conference Oral Presentations**

Grobbelaar, L., De Jager, D., Godongwana, B. & Sheldon, M.S. 2017. Anaerobic baffled reactor equipped with microbial fuel cell technology – A promising approach for industrial biodiesel wastewater treatment. Water Institute of Southern Africa (WISA) Water Sustainability Symposium, The Lord Charles, Somerset West, South Africa, 7 – 10 May 2017.

Grobbelaar, L., De Jager, D., Godongwana, B. & Sheldon, M.S. 2017. Is it possible to successfully treat biodiesel wastewater and produce electricity simultaneously? 8th International Young Water Professionals (YWP) Conference, Cape Town International Convention Centre, Cape Town, South Africa, 10 – 13 December 2017.

CHAPTER ONE

INTRODUCTION

CHAPTER ONE:
INTRODUCTION

1.1. Background

The generation of biodiesel wastewater (BDWW) increases as the international demand for biodiesel fuel increases due to higher oil prices, government targets and incentives (Department of Minerals and Energy, 2007). Large amounts of highly polluted wastewater (i.e. high strength wastewater) is produced during the purification of crude biodiesel (Atadashi *et al*., 2011; Phukingngam *et al*., 2011; Siles *et al*., 2010). It has been reported that the wet washing process (i.e. purification of crude biodiesel) can result in 3 litres of wastewater per litre of biodiesel produced (Steiman *et al*., 2016). In 2011 the global biodiesel industry generated an estimate of 13 000 m^3 to 193 000 m^3 of BDWW per day (Veljković *et al*., 2014).

The commercial biodiesel production company (i.e. industrial partner), that agreed to supply BDWW for the duration of this research study, discharges non-compliant wastewater directly to the municipal sewer system. Currently, this company is using an ineffective wastewater treatment system prior to disposal of the produced BDWW. The treatment system currently used by the company does not reduce the organic contaminants (i.e. chemical oxygen demand (COD) and fats, oils and grease (FOG)) contained in the BDWW to within the industrial wastewater discharge standard limits. BDWW has many other characteristics besides the COD and FOG, which might not meet the industrial wastewater discharge standards (Daud *et al*., 2014; Austic & Lobdell, 2009).

If the company continues to discharge the ineffectively treated BDWW, which has significant impact on the environment, they will soon have to deal with penalties resulting from the implementation of the waste discharge charge system (WDCS) (Pegram *et al*., 2014) which in turn will increase the cost of their biodiesel production process. It is therefore necessary to analyse the BDWW to determine which parameters do not meet the industrial wastewater discharge standard limits and run a preliminary evaluation of a modified anaerobic baffled reactor (ABR) equipped with microbial fuel cell (MFC) technology for the possible treatment of industrial BDWW.

1.2. Problem statement

A commercial biodiesel production company, located in the Western Cape, discharges non-compliant BDWW with regard to COD and FOG, directly into the municipal sewer system. Direct

discharge of large amounts of non-compliant BDWW to municipal sewer systems can cause serious environmental problems (Steiman *et al*., 2016; Daud *et al*., 2014; Veljković *et al*., 2014; Atadashi *et al*., 2011), such as reduced microbial activity and clogging of municipal sewer systems (Veljković *et al*., 2014). Appropriate treatment of this wastewater is therefore a necessity for environmental sustainability due to the high pollution levels and large amounts of wastewater associated with biodiesel production (Daud *et al*., 2014; Veljković *et al*., 2014; Austic & Lobdell, 2009; Suehara *et al*., 2005).

1.3. Research questions

The following research questions will be answered during this research study:

1. Is it possible to reduce the COD and FOG in BDWW to a value which is acceptable for discharge into the municipal sewer system by only adjusting the pH and carbon:nitrate:phosphate (C:N:P) ratio of industrial BDWW prior to treatment with the ABR-MFC system?
2. How does changes to the organic loading rate (OLR) of the system feed influence the power generated by the ABR-MFC system?

1.4. Aim and objectives

The focus of this study was to successfully reduce the organic matter concentration (i.e. COD and FOG) in industrial BDWW, so as to meet the South African (SA) industrial wastewater discharge standard limits, using a hybrid ABR-MFC system at ambient conditions while simultaneously generating electricity.

The objectives of this study were to:

1. Evaluate and determine which parameters do not meet the industrial wastewater discharge standards in the BDWW.
2. Evaluate and determine whether pH and C:N:P ratio adjustments are required prior to treatment with the ABR-MFC system.
3. Determine the maximum power output generated by the ABR-MFC system.
4. Determine the treatment efficiency of the ABR-MFC system.

1.5. Research design and methodology

Biological treatment was applied to industrial BDWW in order to evaluate the organic matter (i.e. COD and FOG) removal efficiency of a 6-compartment bench-scale ABR equipped with MFC technology. Activated sludge (AS) and anaerobic granular sludge (AGS) was used as inoculum and biocatalyst in the treatment system. An existing bench-scale ABR, with a working volume of 90.41 litres, was modified into a bench-scale ABR-MFC system where the ABR was used as the anodic chamber. The single-chamber membrane-less ABR-MFC consisted of the ABR, 6 carbon fibre brush electrodes and 6 floating air-cathode electrodes.

Daily samples were collected from the ABR-MFC feed and product tanks. The following parameters were analysed in duplicate: temperature, pH, total dissolved solids (TDS), salinity (salt), electrical conductivity (EC), turbidity, total COD, total suspended solids (TSS), volatile suspended solids (VSS), total- and ortho-phosphate (TP and OP) concentration and total nitrogen (as NO_3^--N) concentration. Biological oxygen demand (BOD) and FOG were analysed by an independent South African National Accreditation System (SANAS) accredited laboratory.

The potential difference of the ABR-MFC system was monitored and recorded daily in order to determine the maximum power density of the system. Volumetric flow rate was monitored for each experimental condition so as to ensure that the correct hydraulic retention time (HRT) was being applied to the system.

The following engineering aspects were covered during this study:

1. Mass transfer via diffusion of:
    a. protons (i.e. cations) from wastewater (i.e. bulk solution/oxidised substrate) to the gas diffusion layer;
    b. protons (i.e. cations) from the gas diffusion layer to air;
    c. dissolved oxygen (DO) in the air to the cathode electrode;
    d. electrons from AS and AGS (i.e. microorganism cell structure) to the anode electrode;
    e. electrons from the anode electrode to the copper wire;
    f. electrons from the copper wire to the cathode electrode; and
    g. oxygen to the anode (possibility) (Jang *et al*., 2004).
2. Current generation.

1.6. Significance

The main purpose of this research project was to successfully treat industrial BDWW containing high levels of COD and FOG in a hybrid ABR-MFC treatment system while generating electricity as a by-product. Since industrial BDWW was used for this study, this research project will be beneficial to biodiesel companies in SA, using alkali-transesterification of waste vegetable oil (WVO) and employing the wet washing step to purify the crude biodiesel produced.

Biodiesel production companies will benefit from the implementation of a system which effectively treats industrial BDWW to within the SA government industrial wastewater discharge standard limits. These companies will benefit due to a possible elimination or reduction of penalties resulting from the implementation of the WDCS (Austic & Lobdell, 2009).

This research will contribute to avoiding a reduction in microbial activity in wastewater treatment plants, due to the large amounts of high strength industrial wastewater being disposed of, as well as the plugging of municipal sewer systems (Veljković *et al*., 2014). This innovative biotechnological treatment system will therefore contribute to reducing environmental toxicity thereby contributing to environmental remediation and promoting environmental sustainability.

This research project also contributes to ensuring that all South Africans have access to clean running water in their homes thereby contributing to SA's National Development Plan (NDP) (National Planning Commision, 2011) which aims to alleviate poverty and inequality by promoting social inclusion. Since the treatment system generates electricity as a by-product via the use of a biocatalyst (i.e. microorganisms), energy in the form of electricity will contribute to SA's design for sustainability thereby contributing to SA's energy security in an environmentally friendly manner. This relates to SA's NDP which promotes the production of sufficient energy to support industries at competitive prices and aims to ensure access to electricity for poor households thereby contributing to the country's transition to a low-carbon economy.

This study will also provide baseline information for future researchers in the field of BDWW treatment with MFC technology, since limited research on this topic is available. This study could therefore be fundamental for scale-up to pilot- and full-scale systems, thereby creating opportunities for economic growth and jobs, as well as increasing opportunities for growth and development in rural areas. This research project contributes to expanding SA's economic infrastructure, international competitiveness and in turn allows all South Africans to play a leading role in continental development.

1.7. Delineation

Although electricity generation was observed in the ABR-MFC system, the focus of this research remained wastewater treatment. The following was therefore not covered during this study:

- Assessment of the efficiency of the electrical energy produced as an energy source (i.e. energy recovery);
- Biogas capture and analysis;
- Determination of the coulombic efficiency of the ABR-MFC system;
- Microbial metabolic activity;
- Microorganism identification;
- Optimisation and scale-up;
- Product purification (i.e. ultrafiltration (UF) and reverse osmosis (RO) systems, as well as disinfection);
- The use of a catalyst (i.e. Platinum (Pt)) on the cathode;
- The use of artificial electron mediators (i.e. methylene blue and neutral red) which can be added to the anodic chamber of an MFC to enhance the efficiency of this treatment technology;
- The use of a proton exchange membrane (PEM) which allows for proton exchange between the bulk anode (i.e. substrate) and cathode (i.e. air) solutions; and
- The use of double-chambered MFC systems.

CHAPTER TWO

LITERATURE REVIEW

CHAPTER TWO:
LITERATURE REVIEW

2.1. Introduction

It is well-known that South Africa (SA) is currently experiencing a water (Singh, 2016) and energy (Cameron, 2015) crisis. In turn, water restrictions and load shedding have been implemented over the past decade. SA is a water scarce country thus conserving water for future generations is therefore every resident's responsibility (Hawker, 2015). However, the daily water usage per capita in SA exceeds the global average. Nonetheless, South Africans disregard the fact that it is likely that there will not be enough clean water in the near future (Cloete, 2016).

Municipal by-laws are becoming stricter with regard to the industrial discharge standard limits. As a result, South African industries are severely penalised if they do not meet these limits. Additional treatment costs are associated with the disposal of high strength industrial wastewater with chemical oxygen demand (COD) concentrations of more than 1 000 mg/l (HWT, 2013). In addition, there would be a reduction in water usage and discharge when methods for treating and re-using wastewater is implemented thereby assisting in reducing the operational cost of biodiesel producing companies (Kleine *et al*., 2002). Mahendra and Mahavarkar (2013), suggested that the possibility of reducing the treatment costs of biodiesel wastewater (BDWW) exists through combining biological wastewater treatment and electricity generation by using microbial fuel cell (MFC) technology.

MFC technology may create more affordable wastewater treatment by offsetting operating costs if electricity generation in these systems can be increased (Liu & Ramnarayanan, 2004). This could result in affordable on-site wastewater treatment systems for biodiesel production plants. Mahendra and Mahavarkar (2013) therefore regard MFC technology as the ultimate solution for a sustainable renewable source of energy.

2.2. South Africa's water and energy crisis

SA is a water scarce country with a low average rainfall (De la Harpe & Ramsden, 2008). Drought is a natural hazard of the country's climate and will potentially intensify resulting in an increase of drought area coverage to 90% by 2100 (Water Research Commission, 2015). In 2015, five out of the nine provinces had been declared disaster areas (Hawker, 2015) with weeks of no water supply reported in some areas in the Free-State (Singh, 2016). Water restrictions have been

implemented in the past decade to relieve the water crisis currently being experienced in the country.

South African citizens and industries have a major impact on the country's water resources on a daily basis (De la Harpe & Ramsden, 2008). Innovations regarding wastewater treatment technologies and water efficiency measures could alleviate the South African water crisis (Cloete, 2016) so as to ensure the availability and accessibility of sufficient amounts of water for future generations, which is the responsibility of every SA resident (Hawker, 2015).

Thelwell (2014) reported that 98% of the available water supply in the country is being used, while 36% of the country's clean water is being misused (Thelwell, 2014). This amounts to R7-billion in potable water lost annually (Hawker, 2015). SA's social and economic development is therefore dependent on the country's available water resources (De la Harpe & Ramsden, 2008). The economic effects of the SA water crisis affect industries, municipalities and households. Food production is compromised, transportation costs increase, unemployment rates increase and insufficient amounts of power is available for industrial use (Water Research Commission, 2016).

Level 1 (Table 2.1) water restrictions were in place prior to the implementation of Level 2 water restrictions on 1 January 2016, due to the Western Cape region being water-scarce (City of Cape Town, 2016b). The Western Cape received substantially low rainfall in 2016/2017 resulting in the region being declared a disaster area on 22 May 2017 (Payi, 2017). Consequently, the City of Cape Town (CoCT) implemented more stringent water restrictions (Level 4a) in the Western Cape which restricted residential (i.e. domestic) users to 100 litres per person per day (Table 2.1) (City of Cape Town, 2017b). Nonetheless, the CoCT was unable to achieve the overall target for collective consumption of 500 million litres per day and therefore implemented Level 4b water restrictions (Table 2.1) which further restricted residential users to 87 litres per person per day (City of Cape Town, 2017b; City of Cape Town, 2017c). Although the CoCT received assistance from residential users, additional restrictions (Level 5) (Table 2.1) were implemented (City of Cape Town, 2017a) with the aim to reduce consumption in the commercial (i.e. industrial) sector by 20% (News24, 2017). Level 6a water restrictions, implemented on 1 January 2018, restricted the commercial and industrial sector to reduce their consumption by 45% in order for them to comply with level 6 water restrictions (Denita, 2018). On 17 January 2018, Cape Town's Mayor, Patricia de Lille, announced that the Western Cape was guaranteed a "Day Zero" situation where the municipal water supply would not be able to endure the demand (Davis, 2018). Desperately, the CoCT implemented Level 6B water restrictions on 1 February 2018, which further restricted Western Cape residents to 50 L per person per day in order to reach a collective daily consumption target of 450 million litres per day (City of Cape Town, 2018).

The country is facing important challenges as the growth in electricity demand occasionally outpaces supply. As a result of maintenance backlogs and failure to meet the demand of the increasing growth in the economic and social development of SA, the country's largest supplier of electricity, Eskom, implemented load shedding to prevent complete failure of the national power system (Van der Nest, 2015).

Table 2.1: Western Cape water restrictions as implanted by the CoCT (City of Cape Town, 2016a; City of Cape Town, 2017a; City of Cape Town, 2017b; City of Cape Town, 2017c; City of Cape Town, 2017d)

Restriction Effective	**Irrigation**	**Filling pools**	**Washing vehicles**	**Usage pp/day**	**Sector Affected**
Level 1 Prior to 1 Jan 2016	Allowed	Allowed	Allowed	CoCT Tariffs	Domestic
Level 2 1 Jan 2016	Allowed	Allowed	Allowed	CoCT Tariffs	Domestic
Level 3a 1 Nov 2016	Allowed - using bucket Prohibited - within 24 hours of rainfall; using hosepipes / automatic sprinkler systems	Allowed	Use bucket	CoCT Tariffs	Domestic
Level 3b 1 Feb 2017	Allowed - using bucket (Tue and Sat between 6PM and 9AM (1 hour/day)) Prohibited - within 48 hours of rainfall; using hosepipes / sprinkler systems	Manual top-up if fitted with pool cover	Use non-potable water/ commercial carwash	CoCT Tariffs	Domestic
Level 4a 1 Jun 2017	Allowed - using non-potable water (Tue and Sat between 6PM and 9AM (1 hour/day)) Prohibited - within 7 days of rainfall	Prohibited	Prohibited	100 L	Domestic
Level 4b 1 Jul 2017	Prohibited	Prohibited	Prohibited	87 L	Domestic
Level 5 3 Sep 2017	Prohibited	Prohibited	Prohibited	87 L	Industrial
Level 6a 1 Jan 2018	Prohibited	Prohibited	Prohibited	87 L	Industrial & Commercial
Level 6b 1 Feb 2018	Prohibited	Prohibited	Prohibited	50 L	Domestic

*pp = per person

South Africans were first introduced to load shedding in November 2007 (Mushwana & Fourie, 2009) when the stability of the national grid was at risk mainly due to electricity demand outpacing supply (Van der Nest, 2015). Lasting until the end of January 2008, the electricity supply crisis of 2007/2008 had major impacts on SA traffic, schools, hospitals, industry and business operations which suffered significant financial losses resulting in the discomfort of thousands of South Africans (Mushwana & Fourie, 2009). The 2007/2008 electricity supply crisis was largely attributed

to a lack of skills at Eskom and coal-shortages which affected Eskom's coal-fired power plants at the time (Van der Nest, 2015).

In November 2014 a coal storage silo at the Majuba power plant, providing SA with approximately 10% of its electricity, collapsed attributing to the recent electricity supply crisis of 2015 (Van der Nest, 2015). Consequently, it has been reported that the new coal-fired power plants, Medupi and Kusile, which could contribute a nominal 4 800 megawatt (MW) to the grid once completed (Environment News South Africa, 2015) were put on hold (wracked) in February 2015 since construction delays and budget overruns affected the synchronisation of the power plants with the national grid (Van der Nest, 2015). It is expected that these power plants will only be fully operational in 2019/2020 (Environment News South Africa, 2015; Van der Nest, 2015).

Eskom's total capacity is approximately 45 000 MW of electricity (Van der Nest, 2015) while variations in actual capacity are experienced on a daily basis (Environment News South Africa, 2015). The latter can be as a result of planned and unplanned maintenance as in the case in April 2015 when Eskom lost nearly half of its available capacity (Environment News South Africa, 2015) forcing the country into stage-three load shedding (Van der Nest, 2015).

Statistics revealed that electricity produced by independent electricity producers increased by 8.51% compared to a 1.82% decrease in electricity production by Eskom in 2013/14. Electricity imports and exports have increased by 18.55% and decreased by 0.67%, respectively. A 9.4% increase in the average tariff for standard tariff customers has been announced by the National Energy Regulator of South Africa (NERSA) for the 2016/17 financial year (Pretorius & Le Cordeur, 2016). Development of electricity outside Eskom can therefore be expected (Van der Nest, 2015). Investing in renewable energy (i.e. wind and solar) could relieve the country from its energy crisis as a short to medium term solution since the construction and implementation of these systems are relatively faster than the implementation of the new coal-fired power plants (Van der Nest, 2015).

Access to electricity is one of SA's contributing factors to the country's economic activity. SA's economic growth and international competitiveness are therefore affected by the inability of the country to supply the amount of electricity demanded by consumers (Van der Nest, 2015). The 2015 electricity supply crisis contributed to the closing down of major mining operations in SA (Mushwana & Fourie, 2009) which strongly affected the exchange rate since the country relies on its precious metal exports (Van der Nest, 2015).

2.3. SA environmental legislation on industrial wastewater discharge

Section 24 (a) and (b)(1) in the Bill of Rights contained in the Constitution of the Republic of South Africa (RSA) states that: “Everyone has the right to an environment that is not harmful to their health or well-being, and to have the environment protected, for the benefit of present and future generations, through reasonable legislative and other measures that prevent pollution and ecological degradation” (Republic of South Africa, 1996). Furthermore, Section 41 (1)(b) of the Constitution of the RSA stipulates that it is the responsibility of the SA government to secure the well-being of residents of the country (Republic of South Africa, 1996).

The National Environmental Management Act (NEMA) [No. 107 of 1998] was implemented in support of Sections 24 and 41 of the Constitution. The purpose of the Act is to protect the environment by means of the principles set out in the Act thereby ensuring environmental sustainability for present and future generations. The two most important principles set out in the Act is the precautionary principle (Section 2 (4)(a)(vii)) and the polluter pays principle (Section 2 (4)(p)). The precautionary principle stipulates that decisions are approached in a risk-averse and cautious manner while considering all the relevant factors. The polluter pays principle obliges those responsible for harming the environment to cover the costs of remedying pollution and environmental degradation (Republic of South Africa, 1998a).

The National Water Act (NWA) [No. 36 of 1998] was implemented in 1998 in order to ensure that SA water resources are effectively protected, used, controlled, conserved and managed, thereby assuring the sustainability of SA water resources (Republic of South Africa, 1998b). The NWA supports Section 27 of the Constitution which stipulates that “everyone has the right to sufficient food and water” (Republic of South Africa, 1996). Pollution prevention contributes to the protection of water resources. The polluter pays principle therefore also applies to the NWA. The person(s) responsible for polluting a water resource is responsible to cover the costs of remedying the pollution. It is therefore the responsibility of the person(s) who uses, controls, occupies or owns a water resource to ensure that pollution is prevented or corrected once polluted (De la Harpe & Ramsden, 2008).

Unlike the NWA which governs the protection, use, control, conservation and management of water resources in South Africa, the Water Services Act (WSA) [No. 108 of 1997] governs the rules followed by local municipalities (De la Harpe & Ramsden, 2008). National standards and tariffs for water services should be provided by local municipalities since it is the responsibility of these municipalities as per the rules set out by the WSA (Republic of South Africa, 1998b). The WSA stipulates in Section 7 (2) that: “no person may dispose of industrial effluent in any manner

other than that approved by the water services provider nominated by the water services authority having jurisdiction in the area". The Wastewater and Industrial Effluent By-law imposed by the City of Cape Town stipulates the industrial wastewater discharge standard limits which are indicated in Table 2.2.

Table 2.2: Industrial wastewater discharge standard limits (City of Cape Town, 2012)

Variables and Substances	Maximum Standard
COD	5 000 mg/l
pH	Between 5.5 and 12.0
Settleable Solids (SS) [60 minutes]	50 mg/l
Suspended Solids	1 000 mg/l
Total Dissolved Solids (TDS)	4 000 mg/l
Fats, Oils and Grease (FOG)	400 mg/l
Conductivity (EC)	5 mS/cm
Chlorine (as Cl)	1 500 mg/l
Total Sulphates (as SO_4^{2-})	1 500 mg/l
Total Chromium (as Cr)	10 mg/l
Total Copper (as Cu)	20 mg/l
Phenolic Index	50 mg/l
Total Phosphates (as TP)	25 mg/l
Sodium (as Na)	1 000 mg/l
Total Iron (as Fe)	50 mg/l
Total Cyanides (as CN^-)	20 mg/l
Total Sulphides (as S)	50 mg/l
Total Sugars and Starches (as glucose)	1 500 mg/l
Total Zinc (as Zn)	30 mg/l
Total Arsenic (as As)	5 mg/l
Total Boron (as B)	5 mg/l
Total Lead (as Pb)	5 mg/l
Total Selenium (as Se)	5 mg/l
Total Mercury (as Hg)	5 mg/l
Total Titanium (as Ti)	5 mg/l
Total Cadmium (as Cd)	5 mg/l
Total Nickel (as Ni)	5 mg/l

2.4. Treatment of BDWW

2.4.1. BDWW generation and characteristics

Biodiesel is typically produced via four main processing steps using various feedstocks which include edible oils (e.g. palm oil, sunflower oil, and olive oil), non-edible oils (e.g. poultry, castor, and rubber seed) and wastes (e.g. waste cooking oil and municipal sewage sludge) (Daud *et al*., 2014). According to Veljković *et al*. (2014), the first step in biodiesel production includes the conversion of triglycerides and alcohol into glycerol and fatty acid methyl esters (FAME). Separation of crude biodiesel from crude glycerol follows the first step of biodiesel production. Consequently, crude biodiesel is purified and separated from the wastewater generated during the purification step of the production process. The final product is then obtained by drying the separated biodiesel using ion exchange. In some cases, the process also involves further processing of crude glycerol (Povrenović *et al*., 2014; Veljković *et al*., 2014).

The purification step of biodiesel production via the alkali-catalysed transesterification process of waste vegetable oil (WVO) is responsible for the generation of BDWW (Leung *et al*., 2009). It is claimed that the wet washing process used for biodiesel purification is the most effective method to remove excess contaminants and impurities contained within the crude biodiesel (Veljković *et al*., 2014). Depending on the amount of impurities in the crude biodiesel the wet washing process is usually repeated two to five times with fresh water (Veljković *et al*., 2014; Phukingngam *et al*., 2011; Chavalparit & Ongwandee, 2009) in order to ensure that the final product meets the stringent international standard biodiesel specifications (Daud *et al*., 2014; Povrenović *et al*., 2014; Berrios & Skelton, 2008) such as the European (EN 14214) and American (ASTM D6751) standards for biodiesel fuel (Daud *et al*., 2014; Povrenović *et al*., 2014). The wet washing process therefore results in a large amount of wastewater (Phukingngam *et al*., 2011).

Typical impurities contained within BDWW include unconverted triglycerides, sodium salts, soap, glycerol, methanol, and remaining catalyst (Veljković *et al*., 2014). These impurities contribute to the high content of biological oxygen demand (BOD), COD, total suspended solids (TSS) and FOG (Daud *et al*., 2014) which characterise this wastewater as a highly polluted effluent (Veljković *et al*., 2014; Suehara *et al*., 2005). Consequently, these characteristics are responsible for the BDWW's high viscosity and opaque white colour (Daud *et al*., 2014; Veljković *et al*., 2014).

Although the FOG content in BDWW is generally very high (Table 2.3), the high content of other major organic matter contributors (i.e. methanol and glycerol) deems this wastewater significantly different from other oil-containing wastewater (Phukingngam *et al*., 2011). The nitrogen and phosphorous content in this wastewater is extremely low (i.e. 39 mg/l and 4.5 mg/l, respectively

(Kakarla *et al*., 2015)) with pH varying between 5.0 and 11.0, thus creating an unfavourable environment for the growth of microorganisms, and making it difficult for the wastewater to be degraded naturally (Suehara *et al*., 2005). Table 2.3 indicates typical values of the main pollutants present in BDWW, produced during the alkali-catalysed transesterification of different feedstocks, as reported in literature.

Table 2.3: Typical characteristics of BDWW, produced during the alkali-catalysed transesterification of various feedstocks, reported in literature

Biodiesel Feedstock	Country	Parameter					Reference
		pH	COD	BOD	FOG	TSS	
		-	[mg/l]	[mg/l]	[mg/l]	[mg/l]	
Tallow	Thailand	*10.0*	*218 000*	-	-	*79 390*	Sukkasem *et al*., 2011
Palm Oil	Thailand	10.3	*56 400*	-	3 270	*400*	Phukingngam *et al*., 2011
WVO	Japan	11.0	*14 800*	-	*15 100*	*2 670*	Suehara *et al*., 2005
WVO	Thailand	*9.8*	*41 979*	*1 889*	*1 375*	*680*	Pitakpoolsil & Hunsom, 2013
Palm Oil	Malaysia	*5.0*	5900	-	2 680	348	Daud *et al*., 2015
WVO	Spain	*10.4*	*428 000*	-	-	-	Siles *et al*., 2010
WVO	Spain	*10.4*	*428 000*	-	-	-	Siles *et al*., 2011
WVO	Thailand	8.9	30 980	-	6 020	340	Chavalparit & Ongwandee, 2009
Palm Oil	Thailand	*9.5*	*105 000*	*45 000*	*11 000*	-	Rattanapan *et al*., 2011
WVO	United Kingdom	6.7	183 62	-	-	8 850	Berrios & Skelton, 2008

* All figures in *italics* have been calculated or converted from the original data by the author of the thesis according to the calculations shown in Appendix A (section A.1).

2.4.2. Overview of current treatment technologies for BDWW

Several physical and chemical treatment processes have proven to effectively treat oily wastewater, including the conventional treatment methods such as floatation, coagulation, biological treatment and membrane separation technology (Yu *et al*., 2013). Although the combination of these conventional processes might be costly, improved treatment efficiency is achieved when treating oily wastewater (Padaki *et al*., 2015). According to Veljković *et al*. (2014) a typical BDWW treatment process should consist of a physico-chemical process followed by flotation or sedimentation, a biological treatment process and a reverse osmosis (RO) system. Similarly, Austic and Lobdell (2009) explain that BDWW treatment requires physical, chemical and biological treatment steps. Table 2.4 depicts typical BDWW characteristics after various final treatment processes along with the removal efficiencies of these processes.

2.4.2.1. Physico-chemical treatment technologies

The physico-chemical treatment method is usually conducted as a pre-treatment step prior to biological treatment. It involves chemical addition and physical separation of BDWW. In this method physical treatment such as sedimentation, filtration or floatation usually precedes chemical treatment which involves adsorption, acidification and flocculation-coagulation or a combination of these processes (Veljković *et al*., 2014). According to Daud *et al*., (2015), flocculation-coagulation is a promising method that can be used as a pre-treatment step for BDWW since high removal percentages (refer to Table 2.4) have been obtained using this treatment method. Similarly, Pitakpoolsil and Hunsom (2013) obtained high removal percentages (Table 2.4) in their study, which aimed at removing pollutants from BDWW using commercial chitosan flakes as an adsorbent. The major purpose of chemical treatment for BDWW is to cause coagulation via acidification, prior to the addition of a coagulant or a cationic polymer, thereby favouring flocculation (Veljković *et al*., 2014).

Table 2.4: Typical removal efficiencies of different treatment processes used for BDWW treatment accompanied with influent and effluent pH values

Process	pH		COD	BOD	FOG	TSS	Reference
	In	Out	Removal [%]				
Up-flow Bio-Filter Circuit (UBFC)	10.0	7.0	50	-	-	-	Sukkasem *et al*., 2011
Anaerobic Baffled Reactor (ABR)	10.3	7.3	99	-	84	-	Phukingngam *et al*., 2011
Biological Treatment System	11.0	-	-	-	-	-	Suehara *et al*., 2005
Adsorption	9.8	4.1	90	76	67	*89.7*	Pitakpoolsil & Hunsom, 2013
Coagulation-flocculation	5.0	-	81	-	97	97	Daud *et al*., 2015
Electrocoagulation	8.9	6.1	55.4	-	98.4	96.6	Chavalparit & Ongwandee, 2009
Dissolved Air Floatation (DAF)	9.5	6.0	85.7	85	99.6	-	Rattanapan *et al*., 2011

* All figures in *italics* have been calculated or converted from the original data by the author of the thesis according to the calculations shown in Appendix A (section A.1).

Another process which is very effective in separating oily materials from emulsions after chemical pre-treatment (i.e. acidification and coagulation-flocculation) includes dissolved air floatation (DAF) (Daud *et al*., 2014). This method is often employed by dissolving compressed air in BDWW in order to remove oily materials and solid particles as well as to reduce turbidity (Veljković *et al*., 2014). In a study conducted by Rattanapan *et al*. (2011), DAF was combined with an acidification-coagulation pre-treatment step so as to optimise the operational parameters of DAF for BDWW

thereby enhancing the efficiency of the treatment system. Removal percentages for their study can be found in Table 2.4.

2.4.2.2. Electrochemical treatment technologies

Electrochemical treatment is employed as either electrocoagulation or hydrothermal electrolysis (Veljković *et al*., 2014). During the electrocoagulation treatment process, metallic hydroxide flocs are formed at the anode and cathode of an electrochemical cell once the wastewater is exposed to electric current (Veljković *et al*., 2014). Soluble organic compounds and colloids are rapidly adsorbed and trapped within these large flocs (Siles *et al*., 2010) which can then either be removed by sedimentation (Daud *et al*., 2014) or floatation which is supported by hydrogen produced at the cathode (Siles *et al*., 2010). Although this treatment process seems promising; it can only be used as a pre-treatment step for BDWW (Veljković *et al*., 2014). The latter is supported by the results obtained (Table 2.4) in a study conducted by Chavalparit and Ongwandee (2009) who attempted to optimise the electrocoagulation process for the treatment of BDWW. In their study, a COD removal percentage of 55.43% was obtained at optimal process conditions.

Siles *et al*. (2011) evaluated the effect of acidification-electrocoagulation and acidification-coagulation-flocculation pre-treatments of BDWW, in which the COD was found to be 428 000 mg/l (Table 2.3), with an anaerobic digestion as post-treatment on laboratory scale. The combination of acidification-electrocoagulation with an anaerobic digestion process achieved a total COD removal of 99% and was identified as the best process (Siles *et al*., 2011). The BDWW was firstly acidified to a pH less than 4.0 by adding sulphuric acid (H_2SO_4). The BDWW was then centrifuged at 8 000 rpm for 5 minutes prior to neutralising the aqueous phase with sodium hydroxide (NaOH) to a fixed pH of 8.07. Prior to conducting the acidification-electrocoagulation pre-treatment process, the BDWW had a total COD of 252 000 mg/l. Current (12 V (1.5 A)) was applied to the BDWW via 8 aluminium electrodes in a 5 L continuous stirred tank reactor (CSTR) for 30 minutes. Metal hydroxide ions were produced from the aluminium ions generated in the process and hydrolysed in the electrochemical cell. Neutralised particles trapped in the aluminium hydroxide ($Al(OH)_3$) flocks were efficiently removed by floatation and/or centrifugation after the metal compounds reacted with the negatively charged particles contained in the BDWW (Siles *et al*., 2011).

During hydrothermal electrolysis performed in sub-critical BDWW, ions in the form of free hydroxyl radicals (•OH), and occasionally hydrogen atoms, are formed when water vapour molecules surrounding the anode are ionised and subsequently collide. In addition, several liquid water

molecules are broken and reformed into gaseous products such as hydrogen (H_2), hydrogen peroxide (H_2O_2) and oxygen (O_2) which can oxidise many stable organic compounds (Veljković *et al*., 2014). Nonetheless, post-treatment is a necessity since both methods cannot effectively reduce contaminants below the industrial wastewater discharge standard limits (Veljković *et al*., 2014). Electrochemical treatment technologies can however be improved by combining this treatment technology with other treatment methods; developing innovative, inexpensive electrode materials; and optimising process conditions and reactor design so as to increase the efficiency of these systems (Veljković *et al*., 2014).

2.4.2.3. Advanced oxidation treatment technologies

Advanced oxidation processes include ozonation, heterogeneous photocatalysis and the photo-Fenton process, all of which are considered to be highly efficient physico-chemical processes. These processes involve the generation of highly reactive oxidising species, such as hydroxyl radicals (•OH), which are able to degrade organic compounds. It was however reported that these processes are not appropriate technologies to treat BDWW due to low removal efficiencies (Veljković *et al*., 2014).

Further investigation regarding all three advanced oxidation processes for BDWW is therefore required. Additionally, development of innovative devices with larger surface areas; efficient photocatalysis and innovative catalysts are required for the respective advanced oxidation treatment technologies. Larger surface areas are required for efficient ozone-wastewater contact whereas innovative catalysts should function at neutral pH without removal from treated wastewater (Veljković *et al*., 2014).

2.4.2.4. Biological treatment technologies

Biological treatment technologies have the advantage of effectively treating wastewater with high organic content while requiring minor operating conditions (Veljković *et al*., 2014). The high content of biodegradable organic compounds present in BDWW therefore gives the impression of this wastewater being a promising raw material for microbial degradation (Veljković *et al*., 2014). However, the characteristics of BDWW can inhibit the growth of microorganisms which makes biological treatment of this wastewater challenging (Suehara *et al*., 2005).

According to Daud *et al*. (2014), the study of biological treatment technologies for the treatment of BDWW is limited. This straightforward treatment technology however has low capital investment and operating costs which deem biological treatment technologies economically favourable when compared to conventional treatment methods (Veljković *et al*., 2014). In a review conducted by Veljković *et al*. (2014) it was identified that optimal process conditions are yet to be established while optimisation of reactor configurations and pre-treatment (i.e. acidification, coagulation, and electrocoagulation) processes for anaerobic treatment should be investigated in the near future.

Phukingngam *et al*. (2011) who developed an anaerobic biological treatment system using an ABR combined with a physico-chemical pre-treatment step (i.e. chemical coagulation and sedimentation) for the treatment of BDWW reported high removal percentages (Table 2.4) when the system operated at optimal conditions. In the biological treatment system, an optimal organic loading rate (OLR) of 1.5 kg COD/m^3.day was reported when the treatment system operated at a hydraulic retention time (HRT) of 10 days. Hence, optimal conditions are a necessity when commencing biological treatment of BDWW (Veljković *et al*., 2014). Pre-treatment methods are therefore usually employed prior to biological treatment (Daud *et al*., 2014). These pre-treatment methods are usually accompanied with nutrient (i.e. nitrogen and phosphorous) addition and pH adjustment (Suehara *et al*., 2005) due to the excessive amount of carbon sources (i.e. residual oil, methanol and glycerol) contained within BDWW (Veljković *et al*., 2014).

2.4.2.5. MFC treatment technologies

The use of MFC technology has also been investigated for the efficient treatment of BDWW (Daud *et al*., 2014). A COD removal percentage of 50% was reported (Table 2.4) in a study conducted by Sukkasem *et al*. (2011) who developed an UBFC system combined with a fermentation pre-treatment step. In a study conducted by Liu and Ramnarayanan (2004), the authors claimed that their study was the first to report wastewater treatment accompanied by electricity generation using a single chamber MFC.

During degradation of the substrate (i.e. wastewater) which is used as fuel in the MFC, microorganisms generate electrons while protons are generated during oxidation of the substrate (Mahendra & Mahavarkar, 2013). Electrons are transported through an external circuit consisting of an anode, resistor (i.e. power user) and consequently a cathode (Ravindra, 2015). Water is generated in the cathodic chamber of the MFC as a result of diffusion of the protons contained within the solution in the anodic chamber through the proton exchange membrane (PEM) or salt bridge which separates the two compartments (Mahendra & Mahavarkar, 2013). Figure 2.1

depicts the basic working principle of an MFC. The anodic and cathodic chemical reactions taking place in the MFC are shown in Equations 2.1 and 2.2.

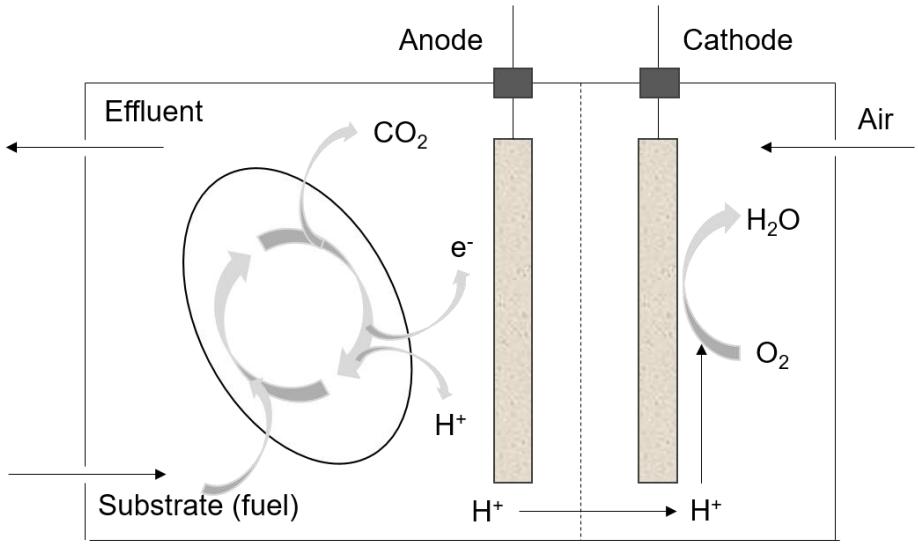

Figure 2.1: Working principle of an MFC adopted from Garche *et al*. (2009)

Anodic reaction (Garche *et al*., 2009):

$$C_{12}H_{22}O_{11} + 13H_2O \rightarrow 12CO_2 + 48H^+ + 48e^- \quad \text{(Eq. 2.1)}$$

Cathodic reaction (Garche *et al*., 2009):

$$O_2 + 4e^+ + 4H^+ \rightarrow 2H_2O \quad \text{(Eq. 2.2)}$$

Although limited research has been conducted using this treatment technology future perspectives include the use of inexpensive materials since existing MFCs are equipped with proton exchange membranes (PEM), precious metal catalysts (i.e. gold (Au) or platinum (Pt)), mediators and graphite electrodes (Daud *et al*., 2014).

2.5. Biological wastewater treatment

Biological wastewater treatment became an accepted wastewater treatment practice in the 1930s (Yang, 2013). Since then, this wastewater treatment method has been extensively utilised to effectively remove organic contaminants from wastewater (Cheremisinoff, 1996). The main purpose of biological treatment for industrial wastewater is to reduce the concentration of organic

and inorganic contaminants present in the wastewater (Tchobanoglous *et al*., 2003; Cheremisinoff, 1996). Biological treatment technologies require no chemical addition while producing low amounts of sludge by consuming minimal energy (Chavalparit & Ongwandee, 2009). This treatment technology is therefore regarded as the most cost effective method for treating wastewater containing organic impurities (Cheremisinoff, 1996).

The type of biological treatment used is influenced by one of the three existing redox conditions for biological treatment, namely; aerobic, anoxic and anaerobic (Judd, 2010). Aerobic and anaerobic processes are the two most familiar types of biological wastewater treatment processes available (Warden Biomedia, 2014) both of which have been widely utilised for domestic and industrial wastewater treatment (Yang, 2013).

Aerobic conditions are characterised by the presence of oxygen and are therefore oxygen dependent (Judd, 2010). Aerobic treatment is considered to be the most effective biological treatment process with regard to removing organic impurities contained within wastewater (Templeton & Butler, 2011). The aerobic process is therefore the most frequently used biological treatment process (Amjad, 2010).

Anaerobic conditions are characterised by the complete absence of oxygen and are therefore oxygen independent (Judd, 2010). According to Liu and Ramnarayanan (2004), anaerobic treatment processes are generally used for the treatment of high strength industrial wastewater. This statement is supported by Judd and Judd (2006) who also stipulated that anaerobic treatment is usually only considered for high strength waste. The extent of pollution can be controlled by employing anaerobic treatment (Siles *et al*., 2010) that could possibly reduce treatment costs (Liu & Ramnarayanan, 2004) since a potential thermal energy source, in the form of methane, is produced as a product (Judd, 2010).

According to Spellman (2013), anaerobic treatment comprises two steps. Facultative microorganisms feed on the organic matter present in the wastewater and produce more microorganisms, volatile fatty acids (VFA), hydrogen sulphide (H_2S), carbon dioxide (CO_2), some stable solids and other gases in the first step. The VFA produced in the first step then becomes a food source for the anaerobic microorganisms in the second step where more microorganisms, stable solids and methane gas are produced thus completing the anaerobic treatment process (Spellman, 2013).

2.5.1. Anaerobic digestion

Although anaerobic treatment may be a time-consuming process associated with long start-up periods which might produce a prominent odour while generating an effluent with a high organic concentration, the process has many advantages compared to the conventional aerobic process (Veljković *et al*., 2014). This energy efficient treatment process requires minimal nutrient addition and produces small amounts of sludge while converting organic waste into methane (CH_4) (Faisal & Unno, 2001). The anaerobic digestion process involves four degradation stages (Seijan *et al*., 2016) which at equal digestion rates, results in efficient anaerobic treatment (Gerardi, 2003).

During the first stage of the process, hydrolysis, hydrolytic bacteria are responsible for the degradation of complex organic waste (i.e. particulate and colloidal (Gerardi, 2003)) into simpler soluble organic compounds (Seijan *et al*., 2016) so that the microorganisms can more readily digest these compounds (Yadav *et al*., 2015; Gerardi, 2003). The second stage of the process, acidogenesis, involves the degradation of simple soluble organic compounds to volatile acids (e.g. propionic acid ($CH_3CH_2CO_2H$) (Gerardi, 2003)) and alcohol (e.g. ethanol (CH_3CH_2OH) (Gerardi, 2003)) by acidogenic bacteria (Seijan *et al*., 2016). Acetogenic bacteria are then responsible for converting volatile acids and alcohol into hydrogen gas and acids (i.e. acetic acid (CH_3CO_2H) and acetate ($CH3CO_2^-$)) in the third stage of the process, acetogenesis (Seijan *et al*., 2016; Gerardi, 2003). The fourth stage, methanogenesis, involves the production of methane and carbon dioxide as a result of consumption of hydrogen gas and acids by methanogenic bacteria (Seijan *et al*., 2016).

Cheremisinoff (1996) describes this four-staged process as a two-phase process consisting of concurrent absorption and degradation of organic compounds by anaerobic and facultative microorganisms. The first phase involves the conversion of organic compounds to volatile acids (i.e. acetic-, propionic- and butyric acids) and results in a decrease in pH. The second phase involves the conversion of these volatile acids to methane and carbon dioxide.

2.5.2. Implementation of an ABR for the treatment of wastewater

In 1982, Bachmann and co-workers developed the ABR and at the time specified that this treatment technology showed excellent promise for the treatment of industrial wastewater. Since then, the ABR has been used to effectively treat a variety of wastewaters varying from low to high strength (Barber & Stuckey, 1999). This treatment technology is considered to be a robust, high rate anaerobic digester which has the ability to reduce organic material contained within

wastewater (Bwapwa *et al*., 2010). The ABR is equipped with a series of vertical baffles which reduces microbial washout while directing the flow of wastewater (Figure 2.2) through active biomass which is likely to rise and settle as gas is produced in the system (Bachmann *et al*., 1985).

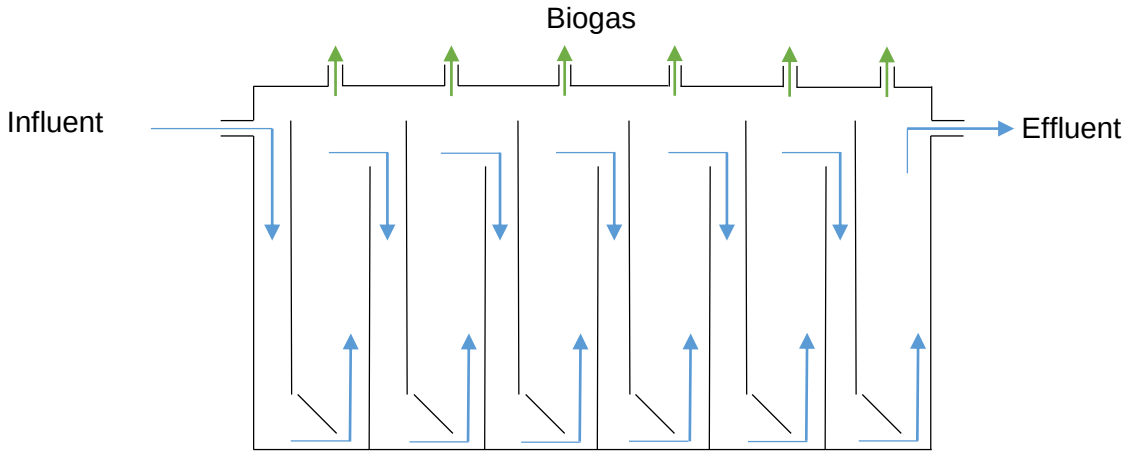

Figure 2.2: Schematic of an ABR adopted from Barber & Stuckey (1999)

Various microbial communities may develop within each compartment of the ABR treatment system due to its unique design. Generally, acidogenic bacteria will dominate in the front compartments of the ABR where substrate concentrations are higher, while methanogenic bacteria will dominate towards the end of the reactor. The development of these microbial communities are however dependent on the type and amount of substrate present along with the pH and temperature of the system (Barber & Stuckey, 1999). Although the ABR can tolerate major changes in OLR, the performance of the ABR is largely dependent on the hydrodynamic behaviour of the treatment system which consequently influences the extent of contact between the wastewater and microorganisms contained within the reactor (Barber & Stuckey, 1999). It is recommended that low OLRs and long HRTs be used during the start-up of an ABR treatment system so as to promote the development of methanogenic bacteria in every compartment of the reactor (Barber & Stuckey, 1999).

BDWW generated during the purification of crude biodiesel, produced by a small-scale biodiesel production plant employing alkali-catalysed transesterification of palm oil, was treated by Phukingngam *et al*. (2011). In this study a physico-chemical pre-treatment step (i.e. chemical coagulation and sedimentation) combined with an anaerobic biological treatment system using an ABR was developed. During the study, they detected a decrease in the pH level of the wastewater while employing biological treatment with OLRs above 1.5 kg COD/m^3.day. These conditions were regarded as unfavourable for methanogenesis and were attributed to an excessive build-up of

VFAs. Effective consumption of VFAs was however observed when the ABR was operated at an optimum OLR of 1.5 kg COD/m^3.day. This was established when the pH levels in the respective compartments of the ABR remained at approximately 7. The overall treatment process (i.e. physico-chemical pre-treatment combined with an ABR) resulted in removal efficiencies of 99% for COD, and 100% for both methanol and glycerol when the ABR operated at this OLR.

Grobicki and Stuckey (1991) specified that a recycle stream is usually implemented when influent wastewater contains large amounts of toxic substances. Typical organic and inorganic substances accompanied with their respective toxic concentration levels associated with anaerobic wastewater treatment are depicted in Table 2.5. The type of wastewater being treated will therefore encourage whether or not to make use of a recycle stream (Barber & Stuckey, 1999).

Table 2.5: Toxic concentration levels of various organic and inorganic substances usually associated with anaerobic wastewater treatment (Gerardi, 2003)

	Substance / Compound	Toxic concentration (mg/L)
Organic substances	Allyl Alcohol (C_3H_6O)	100
	Acrylonitrile (C_3H_3N)	5
	Benzidine ($(C_6H_4NH_2)_2$)	5
	Chloroform ($CHCl_3$)	10 - 16
	Carbon tetrachloride (CCl_4)	10 - 20
	Methylene chloride (CH_2Cl_2)	100 - 500
	Octanol ($CH_3(CH_2)_7OH$)	200
	1,1,1-Trichloroethane ($C_2H_3Cl_3$)	1
	Trichlorofluoromethane (CCl_3F)	20
	Trichlorotrifluoroethane ($C_2Cl_3F_3$)	5
Inorganic substances	Ammonia (NH_3)	1 500
	Arsenic (As)	1.6
	Boron (B)	2
	Cadmium (Cd)	0.02
	Chromium cations (Cr^{6+})	5-50
	Chromium cations (Cr^{3+})	50 - 5 000
	Copper (Cu)	1 - 10
	Cyanide (CN-)	4
	Iron (Fe)	5
	Magnesium cations (Mg^{2+})	1 000
	Sodium cations (Na^{+})	3 500
	Sulphide anions (S^{2-})	50
	Zinc (Zn)	5-20

Bachmann *et al*. (1985) incorporated a recycle stream into a 5 compartment ABR treating complex protein carbohydrate wastewater, with the aim of reducing the amount of acid produced in the first compartment. The incorporation of the recycle stream however resulted in a decrease in system pH since the ABR was allowed to behave as a completely mixed system. In contrast to the latter, Barber and Stuckey (1999) stated in their review of ABR treatment systems, that the advantage of the implementation of a recycle stream is that the pH in the front compartments of the ABR is increased thereby reducing the toxicity and inhibition of the influent wastewater. A recycle stream can be used to alter the pH and to dilute high strength influent wastewater (Grobicki & Stuckey, 1991), therefore higher OLRs are possible (Barber & Stuckey, 1999). Although the implementation of a recycle stream may seem beneficial, the incorporation thereof may cause the ABR treatment system to return to a single-phase digestion system, resulting in a decrease in overall efficiency while microbial communities are disrupted and hydraulic dead space is increased (Barber & Stuckey, 1999).

2.5.3. Advantages and disadvantages of the ABR

2.5.3.1. ABR advantages

According to Barber and Stuckey (1999), the ABR has a number of advantages when compared with other anaerobic digestion systems (i.e. up-flow anaerobic sludge blanket (UASB) reactor and an anaerobic filter). They also specified that one of the major advantages of the ABR system is that it can separate the various stages of anaerobic digestion, specifically acidogenesis and methanogenesis, longitudinally down the ABR. This allows for the development of different microbial populations depending on the conditions within the treatment system (Wang, 2004). The system therefore performs as a two-phase system (Barber & Stuckey, 1999). Other advantages that are related to the use of ABR treatment systems include:

- Alternating operation is possible (Barber & Stuckey, 1999);
- Effluent can be reused for horticulture purposes (Bwapwa *et al*., 2010);
- Highly efficient in treating medium strength, soluble organic waste (Barber & Stuckey, 1999; Bachmann *et al*., 1985);
- High void volume (Barber & Stuckey, 1999; Bachmann *et al*., 1985); simple design and inexpensive construction (Faisal & Unno, 2001; Barber & Stuckey, 1999; Bachmann *et al*., 1985);
- Long solid retention time (SRT), resulting in low sludge production (Faisal & Unno, 2001; Barber & Stuckey, 1999; Bachmann *et al*., 1985);

- Low capital and operating costs (Barber & Stuckey, 1999);
- Low HRT due to high loading rate capability (Faisal & Unno, 2001; Barber & Stuckey, 1999);
- Minimal clogging (Barber & Stuckey, 1999; Bachmann *et al*., 1985); and
- No mechanical mixing (Barber & Stuckey, 1999), therefore no moving parts (Bachmann *et al*., 1985).

2.5.3.2. ABR disadvantages

Due to its simple design, problems are usually associated with maintaining an even distribution of the influent (i.e. feed) stream in pilot and full-scale systems. It therefore becomes necessary to construct shallow reactors so as to maintain acceptable liquid and gas up-flow velocities (Barber & Stuckey, 1999). The ABR treatment system is associated with the following disadvantages:

- Appropriate discharge and/or further treatment of effluent and sludge is required due to low reduction of pathogens and nutrients (Bwapwa *et al*., 2010; Wafler, 2010);
- Long start-up periods (Wafler, 2010); and
- Needs expert design (Wafler, 2010).

2.6. Factors affecting biological wastewater treatment

2.6.1. Temperature and pH

Degradation in biological systems can be significantly affected by temperature fluctuations and microbial metabolism may even be altered if temperatures exceed 39˚C. Optimum temperature for microbial growth is therefore between 15˚C and 39˚C (Jou & Huang, 2003). On the contrary, Khanal (2008) stipulated that anaerobic treatment systems can operate at temperatures ranging between 10 and 60 °C. There are two main types of microorganisms (i.e. acidogens and methanogens) present during wastewater treatment. The optimum pH for methanogenesis (i.e. production of methane by methanogenic bacteria) is between 7.8 and 8.2, while the optimum pH for acidogenesis (i.e. production of acid by acidogenic bacteria) is between 5.5 and 6.5. The optimum pH for the co-existence of methanogens and acidogens is between 6.8 and 7.4. When these microorganisms co-exist during wastewater treatment, it is necessary to maintain a neutral pH since methanogenesis is the rate-limiting step during the co-existence of these microorganisms. The optimum pH for microbial growth therefore ranges between 6.5 and 7.5 for

bioreactor systems (Water and Wastewater Measuring Solutions, 2002), although common wastewater bacteria can function between pH levels ranging from 6.0 to 8.5 (Jou & Huang, 2003).

2.6.2. Nutrient concentration

According to Gray (2004), biological wastewater treatment is largely dependent on the amount of nutrients (i.e. nitrogen and phosphorous) present in the wastewater. Microorganisms responsible for the degradation of organic impurities in wastewater requires a balanced supply of nutrients such as nitrogen (as ammonia or nitrates) and phosphorous (as orthophosphate) in order for these microorganisms to survive (Gerardi, 2003). Microbial metabolism is significantly affected if these nutrients are not present (Khanal, 2008). Phosphorous can be supplied in the form of dibasic sodium phosphate (Na_2HPO_4) whereas nitrogen and sulphur can be supplied in the form of ammonium sulphate ($(NH_4)_2SO4$) (Jou & Huang, 2003). It is therefore necessary to consider the carbon:nitrate:phosphate (C:N:P) ratio of the wastewater prior to implementing biological treatment in order to obtain the most favourable aerobic and anaerobic conditions (Thompson *et al*., 2006). It should be noted that there are major differences with regard to nutrient requirements for these two processes (Gerardi, 2003). Depending on the biological treatment process used, it often becomes necessary to supply the wastewater with the required nutrients in order to ensure that the optimal C:N:P ratio is obtained for adequate biological oxidation (Gray, 2004). Optimal C:N:P ratios reported by literature for aerobic and anaerobic treatment processes are 100:5:1 and 250:5:1, respectively (Ajeng *et al*., 2010; Thompson *et al*., 2006; Ammary, 2004).

Phukingngam *et al*. (2011) biologically treated BDWW that initially contained 14.0 mg/l total Kjeldahl nitrogen (TKN) and undetected amounts of phosphorous in an ABR. The BDWW in this study was pre-treated with chemical coagulation and sedimentation due to the significantly high FOG content in the raw wastewater. The FOG content of the wastewater was reduced from 3 300 mg/l to 130 mg/l by adding sulphuric acid (H_2SO_4) to adjust the pH from 10.3 to 4.0 prior to adding 62.5 mg/l polyaluminium chloride ($Al_2Cl(OH)_3$) and 1.25 mg/l cationic polymer. Nutrients (i.e. $NH_4H_2PO_4$ (diammonium hydrogen phosphate), dipotassium hydrogen phosphate (K_2HPO_4), and iron(II) (Fe_2^+) chloride ($FeCl_2$)) were added to the chemically pre-treated BDWW in order to obtain an optimal carbon:nitrate:phosphate:iron (C:N:P:Fe) ratio of 150:1.1:0.2:0.33 prior to diluting the wastewater to pre-determined OLRs which ranged between 0.5 and 3.0 kg COD/m^3.day. Consequently, sodium hydroxide was added to adjust the pH to between 6.8 and 7.2 prior to anaerobic treatment with an ABR (Phukingngam *et al*., 2011).

2.6.3. Activated sludge (AS)

According to Spellman (2013), activated sludge (AS) is merely active biomass in the form of solids which are formed during the treatment of wastewater via the activated sludge process. The settling characteristics of AS can be evaluated by investigating its compressibility and settleability (Qin *et al*., 2015) and is thus a quality indicator (Spellman, 2004).

According to Judd and Judd (2006), sludge settleability defines the quality of the product. The settleability of AS can be determined by allowing the AS to settle in a measuring cylinder for 30 minutes and using the readings to determine the settled sludge volume (SSV) and sludge volume index (SVI) (Spellman, 2013). In a study conducted by Qin *et al*. (2015), where a submerged membrane bioreactor (SMBR) with pendulum type oscillation was used for the treatment of oily wastewater, it was found that the sludge initially displayed high settleability when the SVI was lower than 80 ml/g.

According to Von Sperling (2007), the settleability of the sludge is lower when a higher SVI value is obtained. Typical approximate SVI values for activated sludge can be observed in Table 2.6 where SVI values for three different methods of measuring the SVI are depicted. The three methods include performing the test without stirring the sample during the settling period (SVI), diluting the sample prior to testing (DSVI) and stirring the sample during the settling period (SSVI) (Von Sperling, 2007).

Table 2.6: Approximate SVI values for AS (Von Sperling, 2007)

	Range of values for the Sludge Volume Index (ml/g)		
Settleability	**SVI**	**DSVI**	**SSVI**
Excellent	0-50	0-45	0-50
Good	50-100	45-95	50-80
Fair	100-200	95-165	80-140
Poor	200-300	165-215	140-200
Very Poor	>300	>215	>200

Jou and Huang (2003) conducted a pilot study for oil refinery wastewater treatment using a fixed-film bioreactor. In their study, it was found that the majority of the biodegradation occurred in the first chamber of the bioreactor which showed greater than 85% COD removal at an HRT of 2h. It was found that deviations in effluent characteristics (i.e. pH fluctuations) often resulted in poor degradation of wastes; and concluded that process stability and resistance to environmental shock

increased when a high microorganism concentration (8 000 mg/l) was maintained within the bioreactor.

The SVI is dependent on the solids concentration (TSS) of the activated sludge (Von Sperling, 2007). SVI is calculated using Equation 2.3.

$$SVI = \frac{V_{settled\ sludge}}{TSS} \quad \text{(Eq. 2.3)}$$

Where, SVI is the sludge volume index [ml/g]; $V_{settled\ sludge}$ is the volume in millilitres occupied by 1 gram of activated biosolids [ml/l]; and TSS is the total suspended solids present in the sample [mg/l].

2.6.4. BOD and COD

The most commonly used parameters for the characterisation of wastewater are BOD and COD (Zaher & Hammam, 2014). According to Judd (2010), COD is a measure of the organic compounds present in water while Spellman (2014) defines BOD as a measure of the oxygen necessary to maintain sufficient levels of microorganisms present in the water.

COD can be measured either as soluble COD (sCOD) or total COD (tCOD) and the results are defined as the amount of oxygen consumed (in mg) per litre of sample. Samples are filtered through a 0.45 μm filter prior to analysis in order to eliminate biological interference when sCOD is measured. Conversely, 'straight' samples are used when measuring tCOD (Environmental Business Specialists, 2015). There are many ways in which one can determine the BOD of wastewater (Water and Wastewater Measuring Solutions, 2002) of which the most common method is known as 'determination of BOD after *n*-days (BOD_n)'. When this method is used residual oxygen after *n* days incubation at 20 (± 1) ˚C is determined according to the standards of determination of dissolved oxygen. For example, BOD_5 is determined by measuring the residual oxygen after 5 days of incubation at 20 (± 1) ˚C (Prokkola *et al*., 2007).

Although COD values are generally higher than BOD values there is a definite correlation between these two parameters. However, the BOD:COD ratio will vary due to its high dependency on the characteristics of the wastewater and may even exceed 10 for industrial wastewater. This ratio is frequently used as an indicator for biodegradation capacity (Lee & Nikraz, 2014) and is better known as the biodegradation index (BI) which is generally used to determine whether wastewater is biodegradable or non-biodegradable (Zaher & Hammam, 2014). Wastewater is considered to

be fairly biodegradable and can be effectively treated biologically when the BOD:COD ratio is more than 0.6. Seeding of the wastewater is required when the BOD:COD ratio ranges between 0.3 and 0.6 in order to treat the wastewater biologically. This is due to the fact that the microorganisms responsible for the degradation of the wastewater usually require a prolonged acclimatisation period. The process will therefore be relatively slow. Biodegradation will not proceed when the BOD:COD ratio is less than 0.3. This wastewater can therefore not be treated biologically since the toxicity and refractory properties of this wastewater inhibits metabolic activity of the bacterial seed. Plant effluent quality can be greatly affected by the type of biological wastewater treatment technology chosen. It is therefore necessary to determine the biodegradability index (BI) of the influent wastewater. The BI can also be used to evaluate the treatment process of a wastewater treatment plant in terms of its design and operation which in turn may lead to an improvement of plant performance.

Process performance can be determined by measuring the removal efficiency using Equation 2.4 (Spellman, 2014).

$$\varepsilon_{COD} = \frac{OC_{feed}^{COD} - OC_{product}^{COD}}{OC_{feed}^{COD}} \times 100 \qquad \text{(Eq. 2.4)}$$

Where, ε_{COD} is the organic matter (i.e. COD) removal efficiency [%]; OC_{feed} is the organic matter (i.e. COD) concentration of the feed substrate [mg COD/l]; and $OC_{product}$ is the organic matter (i.e. COD) concentration in the product [mg COD/l].

2.6.5. HRT and OLR

Nitrifying bacteria grow slower than carbon degraders, therefore a longer SRT and HRT is required to achieve nitrification (Judd, 2010). Conversely, Phukingngam *et al*. (2011) regards high rate anaerobic biological processes as a successful method for treating high strength industrial wastewater with the advantage of recovering biogas as fuel.

HRT is defined as the average length of time that a soluble particle remains within a reactor (Drioli & Giorno, 2010) and can be determined according to Equation 2.5.

$$HRT = \frac{V_W}{Q_{feed}} \quad \text{(Eq. 2.5)}$$

Where, HRT is the hydraulic retention time [days]; V_W is the reactor volume [l]; and Q_{feed} is the influent flow rate [l/day] (Sukkasem *et al*., 2011).

Industrial wastewaters are best known for their high organic loadings and usually contain compounds which are difficult to treat (Gil *et al*., 2011). Phukingngam *et al*. (2011) conducted a study where the performance and phase separated characteristics of an ABR was evaluated for treating BDWW at 6 different OLRs ranging from 0.5 to 3.0 kg COD/m^3.day, namely 0.5, 0.7, 1.0, 1.5, 2.1 and 3.0 kg COD/m^3.day. An HRT of ten days together with an influent flow rate of 2.2 l/day was maintained throughout the duration of the study. It was found that the ABRs operating at the lower OLRs (0.5 – 1.5 kg COD/m^3.day) were most effective in removing organic matter. The COD removal efficiencies of the ABRs decreased from approximately 99% to 80% when the OLR was higher (2.1 to 3.0 kg COD/m^3.day).

OLR is defined as the rate at which organic matter is introduced into a reactor (Bitton, 1998) and is determined according to Equation 2.6.

$$OLR = \frac{OC_{feed}}{HRT} \quad \text{(Eq. 2.6)}$$

Where, OLR is the organic loading rate [g COD/l.day]; OC_{feed} is the organic matter (i.e. COD) concentration of the feed substrate [g COD/l]; and HRT is the hydraulic retention time [days] (Sukkasem *et al*., 2011).

2.7. MFC technology

2.7.1. Introduction

An MFC is an electrochemical device which converts chemical energy into electrical energy (Permana et al., 2015; Spiegel, 2007). This direct conversion of energy occurs through the metabolic processes executed by microorganisms responsible for the degradation of wastewater (Permana *et al*., 2015). This section includes an overview of the possible applications of MFC

technology, including the treatment of wastewater, as well as the advantages and disadvantages of the implementation of MFC technology.

2.7.2. MFC fundamentals

According to Spiegel (2007), chemical fuel cells have higher (15 to 25%) electrical energy conversion rates due to the complex chemical reactions which occurs in MFCs. Spiegel (2007) also concluded that the current density per anodic chamber volume is inversely proportional to the size of the MFC while the power output of MFCs increases when microorganisms are immobilised. This section includes an overview of the basic principles of MFC technology. The section therefore includes limitations on the performance of MFC technology and the type of electrodes used in these types of technologies, as well as theory regarding the calculations associated with MFC technology.

2.7.2.1. Limitations on performance

According to Logan (2008), the performance of MFC technology is restricted due to the limited research that is available on system stability and power output associated with the technology's long-term performance. The maximum cell voltage (i.e. open circuit voltage (OCV)) generated by MFC technology is only achieved when the MFC is run in the open circuit mode (OCM) (i.e. infinite resistance) (Logan, 2008). However, the purpose of introducing MFC technology for wastewater treatment is to supply energy (in the form of electricity) to a device which consumes energy/power (i.e. a pump used to feed the MFC system). The MFC is therefore run in closed circuit mode, thereby mimicking the effect of power supply to a system.

According to Yuan *et al*. (2010), the cell OCV is the potential difference observed between the cathode and the anode when zero electric current is generated with an infinite resistance and therefore no power output. The specific microbial community used as biocatalyst limits the performance of the MFC with regard to the OCV obtained (Logan, 2008).

The maximum cell voltage (E_{emf}) that can theoretically be achieved by an air-cathode MFC under OCV conditions is 1.1 V (Logan, 2008). However, activation-, ohmic- and concentration losses influence the performance of an MFC (refer to sections 2.8.1.1. for details regarding these losses). Losses due to scavenging microorganisms also influences the performance of an MFC. This could be explained via microbial metabolism, since microorganisms lose energy while oxidising the

substrate (i.e. MFC fuel). Nonetheless, the interaction of microorganisms with inorganic components remains a challenge in MFC technology (Mahadevan *et al*., 2014).

2.7.2.1.1. Internal resistance

The internal resistance of an MFC can be determined using four different methods. These methods include; a polarisation slope, power density (PD) peak, electrochemical impedance spectrometry (EIS) or current interruption (Logan, 2008). The EIS (Logan, 2008) and current interruption (Yuan *et al*., 2010; Logan, 2008) methods, which are more accurate than the first two methods mentioned, requires the use of a potentiostat (Logan, 2008). However, since this study did not include the use of a potentiostat to determine the polarisation and PD curves, detail regarding these methods can be found in the work of Yuan *et al*. (2010) and Logan (2008).

The main objective of MFC technology is to maximise the power output of the system, thereby achieving the highest current density at OCV conditions (Logan, 2008). This is achieved by altering the external resistance of the MFC thereby achieving different cell voltages at specific external resistances (Yuan *et al*., 2010; Logan, 2008). Using the measured voltage and calculated current (or current density), a polarisation curve (i.e. voltage vs. current or voltage vs. current density) is plotted which can then be used to characterise fuel cell performance (Yuan *et al*., 2010). The curve allows for the determination of the smallest decrease in voltage, thereby maximising power generation. Prior to obtaining polarisation data it is essential that the MFC is stable under steady state conditions. It is also strongly recommended that the OCV is determined after running the MFC in OCM overnight. The MFC voltage in closed circuit mode should then be obtained by changing the external resistance of the system in increasing order. The time that each resistor should remain in the external circuit is not definite, however pseudo steady-state (i.e. stable voltage) should be achieved for the system during this time (Logan, 2008).

The times for each resistor to obtain pseudo steady-state reported in literature varies from 30 seconds (Ieropoulos *et al*., 2008), 5-10 minutes (Song *et al*., 2015), 15 minutes (Kim *et al*., 2015; Logan *et al*., 2007), 20 minutes (Yang *et al*., 2015), 1 day (Ren *et al*., 2014), as well as 1 week, 3.5 months, and 5 months (Zhang *et al*., 2014). According to Logan (2008), the time allowed for the system to reach pseudo steady-state could affect the data obtained, since a prolonged time could possibly allow for a change in microbial structure and the possibility of the system not reaching electrical equilibrium if the time allowed for stabilisation is too short.

The maximum power generated by an MFC is usually reported as the highest point of the PD curve (PD vs. current or PD vs. current density) (i.e. PD peak method) using Equation 2.7. The

PD peak method is easily used to determine the maximum power generated by the MFC. Equation 2.7 shows that the maximum power output of the MFC is achieved when the external resistance of the system (i.e. MFC) is equal to the internal resistance (Logan, 2008).

$$P_{max} = \frac{OCV^2 R_{ext}}{(R_{int} + R_{ext})^2} \quad \text{(Eq. 2.7)}$$

Where; P_{max} is the maximum power [W]; OCV is the open circuit voltage [V]; R_{ext} is the external resistance (i.e. load) of the MFC [Ω]; and R_{int} is the internal resistance of the MFC [Ω] (Logan, 2008).

The typical polarisation curve (Figure 2.3) can be divided into three regions. Regions one ("rapid voltage losses, low current"), two ("region of constant voltage drop") and three ("rapid voltage drop, high current") can respectively be attributed to activation-, ohmic- and concentration-losses (Mahadevan *et al*., 2014; Logan, 2008).

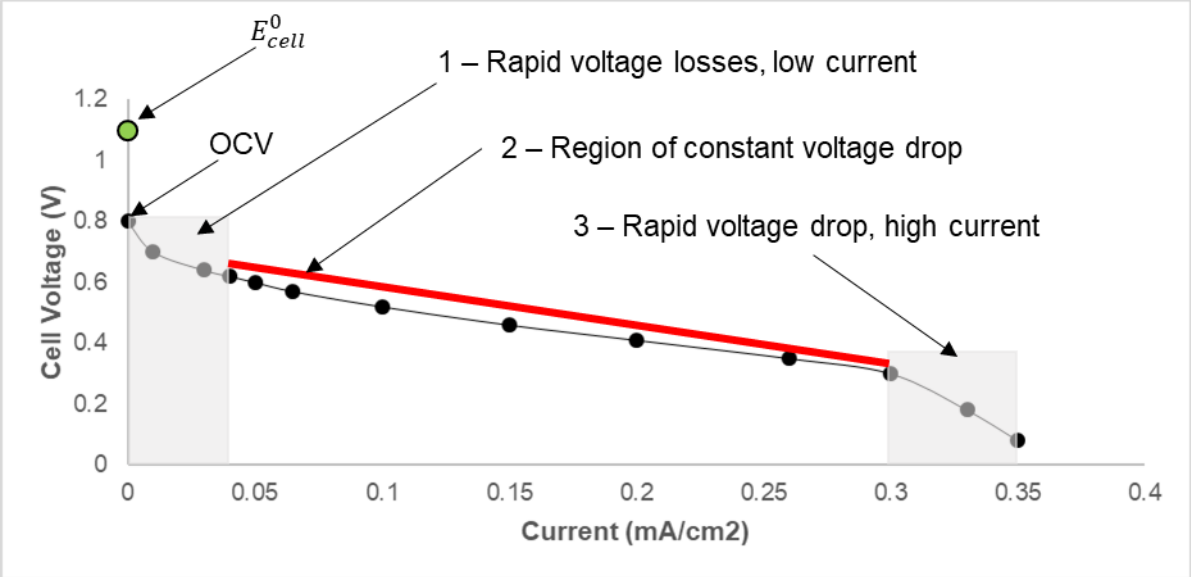

Figure 2.3: Typical characterisation of a polarisation curve adopted from Logan (2008)

2.7.2.1.2. Activation losses

The sharp decrease in MFC voltage (i.e. low polarisation and/or low current densities) initially observed in region 1 (Figure 2.3) represents the activation losses of a typical MFC system, which

occurs at both the anode and cathode electrodes. These activation losses can be attributed to the energy barrier that must be overcome when electrons are transferred from microbial shuttles, through the external circuit, to the anode electrode (Mahadevan *et al*., 2014).

Activation losses (i.e. region 1 in Figure 2.3) can be overcome by increasing the anode electrode surface area (i.e. increase surface porosity and roughness) thereby reducing current density; improving anode-microbe interactions (i.e. addition of an artificial electron mediator to enhance electron transfer); increasing operating temperature (i.e. not possible in an MFC unless the biochemical reaction is separate from the anode chamber); decreasing activation losses at the electrode surface (i.e. addition of a catalyst, such as Pt, to the electrode) (Mahadevan *et al*., 2014).

2.7.2.1.3. Ohmic losses

The polarisation curve (Figure 2.3) steadily decreases in region 2 (i.e. medium polarisation and/or intermediate current densities) which represents the ohmic losses observed in the typical MFC. These losses are a result of the interference of the flow of charge through the external circuit which is due to the anodic resistance (Mahadevan *et al*., 2014). The internal resistance of the MFC is the main cause of ohmic losses observed in region 2 of the typical polarisation curve (Figure 2.3) for an MFC (Yuan *et al*., 2010).

In region 2 of the polarisation curve (Figure 2.3) a direct linear relationship between the measured cell voltage and current density can be observed. This relationship can be expressed as Equation 2.6 which defines the characteristics of the MFC due to its relatively high internal resistance (Logan, 2008). The slope of the polarisation curve can be expressed as the product IR_{int}, thus including the sum of all internal resistance (i.e ohmic) losses (Mahadevan *et al*., 2014; Logan, 2008). Since the internal resistance of an MFC includes the electrode (i.e. anode and cathode) overpotentials which varies with current, it is assumed for calculation purposes, that the internal resistance and ohmic losses are equivalent (Logan, 2008). The internal resistance of the MFC can be determined from the slope of a linear polarisation curve (i.e. polarisation slope method) using Equation 2.8.

$$E_{emf} = OCV^{*} - IR_{int} \qquad \text{(Eq. 2.8)}$$

Where; E_{emf} is the maximum electromotive force [V]; OCV^* is the open circuit voltage (OCV) calculated from the slope of the polarisation curve (i.e. not a true OCV) [V]; I is the current generated [A]; and R_{int} is the internal resistance of the MFC [Ω].

The OVC used in Equation 2.8 (y-intercept of Figure 2.3) is not the true OCV of the MFC due to the activation losses which occurs in region 1 (Figure 2.3, explained in section 2.8.1.1.). The OCV used in Equation 2.8 is implied by extrapolation of the linear portion of the curve to the y-axis and is therefore indicated as OCV^* (Logan, 2008).

2.7.2.1.4. Concentration losses

The sudden decrease in measured cell voltage (high/maximum polarisation and/or high current densities) which is observed in region 3 (Figure 2.3) represents concentration losses (i.e. mass transfer losses) in the MFC system (Mahadevan *et al*., 2014). These losses are more noticeable at high current densities since diffusion (i.e. mass transfer) of the substrate to the anode electrode surface is limited. Concentration losses could be attributed to the MFC system not reaching electrical equilibrium (i.e. total current generation) which is dependent on the anode and cathode potential. The two main factors which contributes to the concentration losses in an MFC is the design of the anode, as well as the operating parameters of the MFC (Mahadevan *et al*., 2014).

2.7.2.2. MFC electrodes

The (electrical) performance of an MFC largely depends on microorganism interaction with the anode. Surface charges can explain the concept of microbial adhesion to anode electrodes. The microorganisms (i.e. negative charge) should adhere properly to the anode surface area (i.e. positive charge). This attraction between the microorganisms and electrodes can be simplified by modifying the electrode surface area (Mahadevan *et al*., 2014).

Substrate oxidation, electron transfer and microbial adhesion is largely dependent on the design (i.e. material and architecture) of the anode electrode (Mahadevan *et al*., 2014). The PD, dependent on the current generated, of an MFC can be increased by increasing the effective surface area of the electrodes while keeping the nominal area constant. This increase in the active surface area of the electrodes directly affects the biochemical reactions (i.e. oxidation of substrate by microorganism) within the MFC system (Kumar & Sarakonsri, 2010).

The most common type of electrodes used in MFCs are carbon-based. This is due to the excellent properties (i.e. high conductivity, flexibility, durability and eco-friendliness) that carbon possesses (Mahadevan *et al*., 2014). Common electrode materials reported in literature are depicted in Table 2.7.

The most effective anode electrode to date is the brush configuration (i.e. carbon fibre brush electrode) since microorganisms can easily adhere to the fibres of the brush which has a high porosity and a large surface area (Mahadevan *et al*., 2014). These electrodes are easily produced by winding graphite fibres into a double core of non-corrosive titanium (Mahadevan *et al*., 2014; Rabaey *et al*., 2010). Nonetheless, materials other than titanium should be investigated for the use of the core wire in these brushes to decrease the manufacturing cost of the brush configuration anode (Rabaey *et al*., 2010).

2.7.2.3. Potential difference

The potential difference of a MFC can be determined according to Equation 2.9 (Logan, 2008).

$$E = I \times R_{ext} \qquad \text{(Eq. 2.9)}$$

Where, E is the cell potential [V]; I is the current [A]; and R_{ext} is the external resistance of the cell [Ω] (Logan, 2008).

The maximum cell voltage, based on thermodynamic relationships, can be determined according to Equation 2.10 (Logan, 2008).

$$E_{emf} = E^0 - \frac{RT}{nF}\ln(\Pi) \qquad \text{(Eq. 2.10)}$$

Where, E_{emf} is the maximum electromotive force [V]; E^0 is the standard cell electromotive force [V]; R is the universal gas constant [8.31447 J/mol.K]; T is the absolute temperature [K]; n is the number of electrons transferred [#]; F is Faradays constant [96 485 Coulombs/mol]; and Π is the reaction quotient defined as $\Pi = \frac{[products]^p}{[reactants]^r}$ where p is the stoichiometric coeeficient of the products and r is the stoichiometric coefficient of the reactants (Logan, 2008).

Table 2.7: Electrode materials reported in literature

	Electrode Material		Reference
Anode	Carbon	Felt	Gajda *et al*., 2015; Kim *et al*., 2015; Martinucci *et al*., 2015; Pasupuleti *et al*., 2015; Yao *et al*., 2014; Tugtas *et al*., 2011; Zhong *et al*., 2011; Liu *et al*., 2005
		Paper	Min & Logan, 2004
		GAC	Liu *et al*., 2011; Sukkasem *et al*., 2011; Wang *et al*., 2011; Feng *et al*., 2010; You *et al*., 2007
	Graphite	Plate(s)	Wang *et al*., 2016; Feng *et al*., 2010
		Rod(s)	Mahendra & Mahavarkar, 2013; Liu *et al*., 2011; Wang *et al*., 2011; Ghangrekar & Shinde, 2007; You *et al*., 2007; Rabaey *et al*., 2005; Liu & Ramnarayanan, 2004
		Felt	Miyahara *et al*., 2015; Cha *et al*., 2010; Song *et al*., 2010; An *et al*., 2009; Jang *et al*., 2004
		Granules	Song *et al*., 2010; Zhuwei *et al*., 2008; Rabaey *et al*., 2005
		Fibre brushes	Kakarla *et al*., 2015; Zhang *et al*., 2015; Ahn *et al*., 2014; Lanas *et al*., 2014; Ren *et al*., 2014
Cathode	Carbon	Felt	Gajda *et al*., 2015; Kakarla *et al*., 2015; Kim *et al*., 2015; Martinucci *et al*., 2015; Zhang *et al*., 2015; Ahn *et al*., 2014; Lanas *et al*., 2014; Ren *et al*., 2014; Tugtas *et al*., 2011; Wang *et al*., 2011; Zhong *et al*., 2011; Feng *et al*., 2010; Song *et al*., 2010; Min & Angelidaki, 2008; You *et al*., 2007; Liu *et al*., 2005; Min & Logan, 2004
		Paper	Yao *et al*., 2014; Li *et al*., 2008; Liu *et al*., 2005
		GAC	Sukkasem *et al*., 2011
	Graphite	Rod(s)	Wang *et al*., 2016; Mahendra & Mahavarkar, 2013; Ghangrekar & Shinde, 2007
		Felt	Liu *et al*., 2011; Cha *et al*., 2010; An *et al*., 2009; Rabaey *et al*., 2005; Jang *et al*., 2004
		Granules	Zhuwei *et al*., 2008

2.7.2.4. Current and current density

Wastewater strength and coulombic efficiency strongly influences the current generated by the MFC (Logan, 2008). The current generated by the MFC can be determined by Equation 2.11 (Sukkasem *et al*., 2011).

$$I = \frac{E}{R_{ext}} \qquad \text{(Eq. 2.11)}$$

Where, I is the current [A]; E is the cell potential [V]; and R_{ext} is the external resistance [Ω].

The coulombic efficiency of the MFC can be determined using Equation 2.12 (Feng *et al*., 2010).

$$\varepsilon_c = \frac{C_p}{C_T} \times 100 \quad \text{(Eq. 2.12)}$$

Where, ε_c is the coulombic efficiency [%]; C_p is the total amount of coulombs [C]; and C_T is the theoretical amount of Coulombs that can be produced from the COD contained in the wastewater used as substrate.

The current density can be determined using Equation 2.13 (Feng *et al*., 2010).

$$J_{ACV} = \frac{E}{R_{ext} \times V_W} \quad \text{(Eq. 2.13)}$$

Where, J_{ACV} is the current density [A/m^3]; E is the measured potential difference of the cell [mV]; R_{ext} is the external resistance [Ω]; V is the net liquid volume of the anode chamber [m^3].

2.7.2.5. Power output and PD

The power generated is a measure of the rate of energy produced per unit time (Von Meier, 2006) by the MFC and can be calculated using Equation 2.14 (Sukkasem *et al*., 2011) or Equation 2.15 (Logan, 2008).

$$P = \frac{E^2}{R_{ext}} \quad \text{(Eq. 2.14)}$$

Where, P is the power generated [W]; E is the measured cell potential [V]; and R_{ext} is the external resistance [Ω].

$$P = I \times E \quad \text{(Eq. 2.15)}$$

Where, P is the power generated [W]; I is the current [A]; and E is the measured cell potential [V].

The PD is a measure of the electrical power generated per unit area or per unit volume (Smil, 2015) and can be determined by using Equation 2.16 (Feng *et al*., 2010).

$$PD = \frac{E^2}{R_{ext} \times V_W} \quad \text{(Eq. 2.16)}$$

Where, PD is the PD [W/m^3]; E is the measured cell potential [mV]; R_{ext} is the external resistance [Ω]; and V is the net liquid volume of the anode chamber [m^3].

2.7.3. MFC technology applications

According to Mahadevan *et al.* (2014), five different types of MFC technology have been developed, namely; uncoupled bioreactor MFC (i.e. separate microorganism compartment/double-chamber), integrated bioreactor MFC (i.e. single-chamber), MFC with an artificial mediator (i.e. intermediate electron transfer molecules), mediator-less MFC (i.e. direct electron transfer to electrode), as well as a mediator- and membrane-less MFC (i.e. single-chamber, absence of mediator and proton exchange membrane (PEM)). For the purpose of this study, the focus will be on single-chamber, mediator- and membrane-less MFC technology. Information regarding other MFC technology types can be found elsewhere (Mahadevan *et al*., 2014).

The main applications fo MFC technolgy includes the generation of electricity and biohydrogen, as well as the development of biosensors (i.e. BOD sensors) and wastewater treatment (Du *et al*., 2007). The application of MFC technology can potentially lead to the development of low power consumption sources, sensors based on interaction at the electrodes, as well as the electrochemical manufacture of chemicals (Spiegel, 2007). Nonetheless, the main attraction of MFC technology during the past decade is wastewater treatment.

2.7.3.1. Implementation of MFC technology for the treatment of wastewater

According to Logan (2008), the main purpose of an MFC, implemented for wastewater treatment, will be to reduce the organic matter (i.e. COD and FOG) contained within the wastewater. Since the MFC is a biological (i.e. anaerobic) system it can therefore theoretically replace biological treatment reactors such as the AS aeration tank or the trickling filter. The use of MFC technology may reduce solid production significantly, which may decrease a wastewater treatment plants' operational costs since solid treatment is regarded as an expensive process.

Low construction and operating costs are associated with single-chamber MFCs since the cathode does not require aeration. These systems therefore have a simple design (Kakarla *et al*., 2015). According to Logan (2008), 50% of the electricity used at a wastewater treatment plant can be attributed to the aeration used in the AS process. Single-chamber MFCs used for wastewater treatment therefore have an energy efficient advantage over the AS process if electricity generation in these systems can be increased.

In a study conducted by Sukkasem *et al*. (2011), an UBFC in combination with a fermentation pre-treatment step was developed. Electrode surface area was increased by immobilising microorganisms, which were used as the biocatalyst, on granular activated carbon. Different operational conditions (i.e. external resistance, OLR, HRT, pH level and aeration rate) were investigated in order to assess the treatment efficiency of the UBFC system by monitoring the alkalinity and COD removal achieved by the MFC in the absence of a PEM. In their study, full strength BDWW (COD = 218 ± 30 g/L, pH level = 10 ± 1) (refer to Table 2.2) was subjected to fermentation which resulted in a mixed liquor with a pH level of less than 7. The pre-treatment step accounted for 41.7% COD removal. The wastewater was then diluted to pre-determined OLRs ranging between 15 and 45 kg COD/m^3.day while pH levels ranged between 4.5 and 7.5 prior to feeding the wastewater to the UBFC treatment system (Sukkasem *et al*., 2011).

Although nutrient addition was not required for this treatment process, the anode could only degrade 30% of the organic matter contained within the BDWW, while the cathode required optimum influent conditions regarding the COD of the BDWW. Optimal conditions at the selected external resistance (10 kΩ) were an OLR of 30 kg COD/m^3.day; an HRT of 1.04 days, a pH level between 6.5 and 7.5 and an aeration rate of 2.0 l/min. The maximum COD removal of the UBFC system running at the optimal conditions specified was 70% thereby resulting in treated wastewater having a COD concentration of 9.02 g/l and a neutral pH level. The influent concentration of 30 kg COD/m^3.day was selected as the optimum OLR since it seemed to generate the most electricity during the investigation. Nonetheless, a small amount of electricity (0.0024

W/kg COD treated) was generated by the UBFC system. In comparison, the total power consumption of this low cost (USD 1775.7/m^3) treatment system, which achieved 50% COD removal, was estimated to be 0.152 kW/kg COD treated (2.275 kW/m^3). A 10% increase in COD removal was achieved by the UBFC system once the circuit was closed with a 10 kΩ external resistor. However, this large external resistance resulted in low electricity generation of 35.62 mW/m^3 (based on UBFC anode volume). The authors suggested that further investigation regarding the low electricity generation of the system was required as they associated it with a low degradation of substrate, microorganisms sensitivity and the long distance between the electrodes (Sukkasem *et al*., 2011).

2.7.4. Advantages and disadvantages of MFC technology

2.7.4.1. MFC advantages

According to Rabaey and Verstraete (2005), MFC technology could possibly fulfil energy requirements by increasing the amount of fuels used daily and could be useful in areas neglecting electrical infrastructure. The advantages of MFC technology include:

- Direct production of electricity (Gude, 2016; Logan, 2008) as a result of the conversion of substrate energy (Rabaey & Verstraete, 2005);
- Environmentally friendly technology (Gude, 2016; Rayment & Sherwin, 2003);
- Lower solid production when compared to aerobic treatment processes such as the activated sludge system (Logan, 2008);
- Passive aeration of cathode (Liu & Ramnarayanan, 2004).
- No energy input required (Logan, 2008).
- Operating efficiently at ambient temperatures (Gude, 2016; Spiegel, 2007; Rabaey & Verstraete, 2005) although system performance is improved at higher temperatures (Logan, 2008);
- Possible regulation of the odour generated (Logan, 2008); and
- Silent operation (Rayment & Sherwin, 2003).

2.7.4.2. MFC disadvantages

The major disadvantage of MFC technology is the high costs associated with construction of these systems (Sukkasem *et al*., 2011). 80% of the construction cost of MFCs are attributed to PEMs

and precious metals which are generally used in laboratory scale MFC systems (Arora, 2012). Other disadvantages include:

- Cathode electrolytes (e.g. ferricyanide ($C_6FeN_6^{3-}$)) have to be chemically regenerated and replaced (Logan, 2008);
- System performance is limited by an increased distance between the anode and cathode which results in a high internal resistance in the system (Kakarla *et al*., 2015); and
- System performance is decreased by the use of PEMs (Logan, 2008) and cathode electrolytes (Kakarla *et al*., 2015).

2.7.5. Combination of wastewater treatment and electricity generation

Table 2.8 summarises various literature articles with regard to the treatment of various types of wastewater using different types of MFC technologies. The literature reviews the treatment of wastewater originating from industrial (i.e. corn stover explosion process-, molasses-, dairy-, primary clarifier-, swine-, dark fermentation-, hospital-, brewery-effluent and BDWW) and domestic practices. This summary also includes the treatment of synthetic wastewater (i.e. glucose, acetic acid, glutamate). The anode chamber volumes, electrode surface areas, external resistance, power densities as well as the COD removal efficiencies are depicted by Table 2.8.

Table 2.8: Performance and characteristics of (laboratory scale) single-chambered air-cathode MFC technology used for the treatment of wastewater (WW) reported in literature

Substrate	Substrate strength	Process used	Anode Chamber		Surface area		R_{ext}	PD_{ASA}	PD_{ACV}	ε_{COD}	Reference
	mg COD/l		V_T	V_w	SA_A	SA_C	Ω	mW/m^2	mW/m^3	%	
			ml		cm^2						
Corn stover explosion process effluent	> 30 000	Graphite granule baffled air-cathode MFC	460	210		19			10.7	89.1	Feng *et al*., 2010
Molasses WW	127 500	Anaerobic baffled stacking MFC (ABSMFC)	**2 484**	690							Zhong *et al*., 2011
Domestic WW	210	MFC anaerobic fluidized bed membrane bioreactor (MFC-AFMBR)		130		35		89		92.5	Ren *et al*., 2014
Synthetic WW (glucose)	170 - 1200	Baffled MFC	**7 331**	1 500							Li *et al*., 2008
BDWW	218 000	UBFC		500					35.62	**50**	Sukkasem *et al*., 2011
Domestic WW	945	Single chamber MFC	10 000	8 000	**11.56**	**11.56**		0.84^^^^		86.6	Mahendra & Mahavarkar, 2013
Dairy WW	1 868							1.02^^^^		84.8	
Primary clarifier effluent	210 - 220	Single chamber MFC	**498**	388	**238.75**		465	26		80	Liu & Ramnarayanan, 2004
Swine WW	73828	Single chamber - coupled anaerobic digester MFC (AD-MFC)	**216**	320	15	15	500	33		80.5	Kim *et al*., 2015

Table 2.8: Performance and characteristics of (laboratory scale) single-chambered air-cathode MFC technology used for the treatment of wastewater (WW) reported in literature

Substrate	Substrate strength	Process used	Anode Chamber		Surface area		R_{ext}	PD_{ASA}	PD_{ACV}	ε_{COD}	Reference
	mg COD/l		V_T	V_w	SA_A	SA_C	Ω	mW/m^2	mW/m^3	%	
			ml		cm^2						
WW treatment plant effluent	180 - 210	Algae bioreactor MFC	210	205		30	600	*630*		n/s	Kakarla *et al*., 2015
Primary clarifier effluent	439	Cube shaped reactors	**64**	26		7	100	n/s			Zhang *et al*., 2015
Domestic WW	1 672	Submersible MFC (SMFC)	600	550	**16**		180	204		n/s	Min & Angelidaki, 2008
Synthetic WW (glucose)	n/s	MFC submersed in anodic chamber		144			51		16 700	1.1^^	Cha *et al*., 2010
Synthetic WW (glucose)	1 000	Graphite-granule tubular air-cathode MFC (GTMFC)	95	55	**48**	90	50		*50 200*	n/s	You *et al*., 2007
Synthetic WW (acetic acid^)	n/s	Bioelectrochemical Membrane Reactor (BEMR)	210	109		494	100		4 350	92.4	Wang *et al*., 2011
Synthetic WW (acetic acid)	490	Coupled sequencing batch reactor (SBR) MFC	790	410		790	500		2340	90	Liu *et al*., 2011
Dark fermentation effluent	53 610	Batch mode MFC (MFC-BM)	**99**		**220**		1 000	1.31	3 163	80	Pasupuleti *et al*., 2015
		Semi-continuous MFC (MFC-SCM)					2 000	9.06			
		Continuous MFC (MFC-CM)						15.53			

Table 2.8: Performance and characteristics of (laboratory scale) single-chambered air-cathode MFC technology used for the treatment of wastewater (WW) reported in literature

Substrate	Substrate strength	Process used	Anode Chamber		Surface area		R_{ext}	PD_{ASA}	PD_{ACV}	ε_{COD}	Reference
	mg COD/l		V_T	V_w	SA_A	SA_C	Ω	mW/m²	mW/m³	%	
			ml		cm²						
Synthetic WW (acetic acid)	7 000	Tubular MFC	**138**	**102**	2430	90	53	286		92	Gajda *et al*., 2015
Domestic WW	300	Tubular single chamber MFC	28				1 114	1 210 720 1 114		n/s	Liu *et al*., 2005
Domestic WW	246 280 379	Flat plate MFC (FPMFC)	**450**	27	**100**		470	56 43 72		58 79 42	Min & Logan, 2004
WW	20	Floating MFC				**300** **600** **1200**	100	750^^^ 500^^^ 125^^^			Martinucci *et al*., 2015
Synthetic WW (glucose)	3 400 6 400 9 600 16 000	Bench scale WW treatment plant	***36 000***	n/s	160	160	250	1.06 60.6 67.3 65.1		84 83 92 98	Aldrovandi *et al*., 2009
Synthetic WW	620	MFC-MBR	**1000**	880	**400**	**38.26**	1 000	*45*			Wang *et al*., 2016

Table 2.8: Performance and characteristics of (laboratory scale) single-chambered air-cathode MFC technology used for the treatment of wastewater (WW) reported in literature

Substrate	Substrate strength	Process used	Anode Chamber		Surface area		R_{ext}	PD_{ASA}	PD_{ACV}	ε_{COD}	Reference
	mg COD/l		V_T	V_w	SA_A	SA_C	Ω	mW/m^2	mW/m^3	%	
			ml		cm^2						
Synthetic WW (glucose and glutamate)	300^^	Tubular MFC	**7 854**	n/s	465	89	10	1.3		90	Jang *et al*., 2004
Synthetic WW (acetate)		Cube shape membrane-less air-cathode MFC (MLAC-MFC)	230		36	36	10	750	12 000		Tugtas *et al*., 2011
Synthetic WW (glucose)	880	Upflow mode membrane-less MFC (ML-MFC)	**4 712**				96		536	34	Zhuwei *et al*., 2008
Synthetic WW (sucrose)	325	Tubular mediator-less and ML-MFC	**10 603**	**4595**	211 140.43 70.21	210.64 140.43 70.21	100	4.66 6.45 10.9 8.6 7.4		88.24	Ghangrekar & Shinde, 2007
Domestic WW Hospital WW	429 332	Tubular MFC	390	210	n/s				66 000 80 000	22	Rabaey *et al*., 2005
Primary clarifier effluent	303	Single chamber MFC with separator electrode assembly (SEA)		130				328		62 - 94	Ahn *et al*., 2014
		Single chamber MFC with closely spaced electrode assembly (SPA)				35	1 000	282		81 - 93	

Table 2.8: Performance and characteristics of (laboratory scale) single-chambered air-cathode MFC technology used for the treatment of wastewater (WW) reported in literature

Substrate	Substrate strength	Process used	Anode Chamber		Surface area		R_{ext}	PD_{ASA}	PD_{ACV}	ε_{COD}	Reference
	mg COD/l		V_T	V_w	SA_A	SA_C	Ω	mW/m²	mW/m³	%	
			ml		cm²						
Synthetic WW (glucose)	300 - 1 000	Cube shaped MFC	**188**	n/s	750				124 000		Song *et al*., 2010
n/s		Floating type MFC (FT-MFC)	**255**	n/s	**0.97**	**0.97**		8			An *et al*., 2009
n/s	n/s	Cassette-electrode MFC (CE-MFC)		1 000	**136**	**130**				> 80	Miyahara *et al*., 2015
Brewery and domestic WW	1 200	DC-MFC	250	200	6			392.16		> 95	Larrosa-Guerrero *et al*., 2010

* All figures in *italics* and **bold** have been converted and/or calculated from the original data by the author of the thesis according to the calculations shown in Appendix A (section A.2).

*** Wastewater (WW); not specified (n/s); total volume (V_T); working volume (V_w); anode surface area (SA_A); cathode surface area (SA_C); external resistance (R_{ext}); COD removal efficiency (ε_{COD}); mg BOD/l (^); kg COD/m^3.day (^^); mA/m^2 (^^^); mA (^^^^)

CHAPTER THREE

RESEARCH METHODOLOGY AND DESIGN

CHAPTER THREE:
RESEARCH METHODOLOGY AND DESIGN

3.1. Background

In order to meet the objectives (refer to Chapter 1, section 1.4) of the study, an existing 6 compartment laboratory scale anaerobic baffled reactor (ABR) was modified to incorporate microbial fuel cell (MFC) technology for the biological treatment of industrial biodiesel wastewater (BDWW) while generating electricity. A full-scale biodiesel manufacturing company employing alkali-transesterification of waste vegetable oil (WVO) was chosen as the industrial partner from whom the wastewater was collected. The successful reduction of organic material (i.e. chemical oxygen demand (COD) and fats, oils and grease (FOG)) at ambient temperature including the by-product (i.e. electricity) produced by the system was the main reason for using this novel technology which operated for 225 days. The system was designed so that the ABR, which had a net liquid (working) volume of 90.32 L, was used as the anodic chamber of the single-chamber membrane-less floating air-cathode MFC. This chapter provides a description of the materials and methods used to evaluate the performance of the ABR-MFC system.

3.2. Description of materials

3.2.1. Microorganisms

Activated sludge (AS) and anaerobic granular sludge (AGS) were used as inoculum and biocatalyst. AS was obtained from the Athlone Wastewater Treatment Plant (Cape Town, South Africa). AGS was collected from a full-scale up-flow anaerobic sludge blanket (UASB) reactor at South African Breweries (SAB) (Cape Town, South Africa).

The ABR-MFC system was inoculated with equal volumes (50/50 v/v%) of AS and AGS. The sludge mixture (i.e. AS and AGS) was allowed to acclimatise to diluted BDWW prior to initialising experimental test work so as to prevent complete system failure. Refer to Tables H.2 and H.3 in Appendix H for more information on AS and AGS, respectively.

3.2.2. Substrate

Industrial BDWW was obtained from a local full-scale biodiesel manufacturing plant (Cape Town, South Africa) employing alkali-transesterification of WVO. The industrial partner used a methoxide

catalyst (i.e. potassium hydroxide (KOH) and methanol (CH_3OH)) during the production of biodiesel. Biodiesel from the wet-washing purification step of the manufacturing process was supplied by the industrial partner. This wastewater, which was used for all experiments, was collected in 25 litre air-tight containers. The wastewater was stored at room temperature (i.e. 21 °C) prior to feeding into the lab-scale ABR-MFC.

Prior to system inoculation, a sample of the BDWW was sent to an outside independent South African National Accreditation System (SANAS) accredited laboratory for a full chemical analysis (refer to Table H.1 in Appendix H for more information on the full-strength BDWW). It was found that the wastewater had average carbon (as COD), nitrogen (as Nitrate-N (NO_3^--N)) and phosphorous (as total phosphate (TP)) concentrations of 246 575 mg/l, 0.0858 mg/l, and 0.205 mg/l, respectively. The nutrients (i.e. nitrogen and phosphorous) concentrations in the BDWW were therefore adjusted to the optimum carbon:nitrate:phosphate (C:N:P) ratio (150:1.1:0.2) for the biological treatment of BDWW suggested by Phukingngam *et al.* (2011). Refer to Appendix F for calculations on nutrient substrate adjustment and Section 2.6.2. for more information on the C:N:P ratio. Subsequent to substrate adjustment and dilution, BDWW was fed to the lab-scale ABR-MFC system via a peristaltic pump (Watson Marlow 520S) at a hydraulic retention time (HRT) of 10 days and organic loading rate (OLR) of 0.58 kg COD/m^3.day. The long stabilization period used during this study is supported by the recommendations of Barber and Stuckey (1999) who suggests the use of low OLRs and long HRTs during start-up. This promotes the development of methanogenic bacteria in every compartment of the reactor.

3.2.3. Electrodes

Carbon fibre brush electrodes (Mill-Rose, United States of America (USA)) were used as the anode electrodes in each of the 6 anodic chamber compartments of the bench-scale single-chamber ABR-MFC. Each of these electrodes had a total surface area of 57.01 m^2 (refer to Appendix G (Figure G.1 and Table G.1) for a schematic drawing of the carbon fibre brush anode electrode, the specifications and surface area calculations).

The floating carbon air-cathodes used in this study were constructed in the same manner as Yang *et al*. (2014), using the phase-inversion method (refer to Appendix G section G.2 for cathode preparation and construction). Yang and co-workers (2014), developed these air-cathodes to be used in cube-shaped MFCs to eliminate the need for expensive catalysts (i.e. platinum (Pt)) by using a polyvinylidene fluoride (PVDF) binder and an activated carbon catalyst. The floating air-cathode electrodes had an average total (projected) surface area of 362.98 cm^2 (refer to Appendix

G (Table G.2) for cathode electrode specifications and a sample calculation on cathode surface area).

The 6-carbon fibre brush anode electrodes were connected in parallel with the 6 floating air-cathode electrodes by using insulated copper wire. The external circuit was completed with a 1 000 Ω resistor (i.e. colour coded tubular wire wound). The total surface area of the 6 carbon-fibre anodes and 6 floating air-cathode electrodes was found to be 342.07 m^2 and 2 173.27 cm^2, respectively.

3.2.4. Multimeter

A digital multimeter, Top T820, (Communica (Pty) Ltd, South Africa) was connected in series with the system (i.e. over a resistor) to measure the potential difference (i.e. voltage) and current (i.e. amperage) produced by the lab-scale ABR-MFC.

3.3. Experimental procedures

3.3.1. System construction

An existing 6 compartment ABR (Figure 3.1) was modified into a hybrid ABR-MFC system (Figure 3.2.a and 3.2.b). A process flow diagram and a schematic drawing of the ABR-MFC system can be found in Figure 3.2.a and 3.2.b, respectively. The ABR, which was used as the anodic chamber of the hybrid ABR-MFC, had a volume of 120.44 L (L x W x H = 105 cm x 31 cm x 37 cm) and a working volume of 90.32 L (refer to Appendix B for details regarding the ABR-MFC working volume).

According to Barber and Stuckey (1999) the implementation of a recycle stream in an ABR could cause the treatment system to return to a single-phase digestion system. This would result in a decrease in overall efficiency while microbial communities are disrupted and hydraulic dead space is increased. It was therefore decided not to incorporate a recycle stream for the ABR-MFC system during this study.

In order for the modification of the existing ABR to take place, the lid of the ABR had to be removed. This was done by carefully removing all silicon, glue and plastic welding that held the lid of the ABR intact.

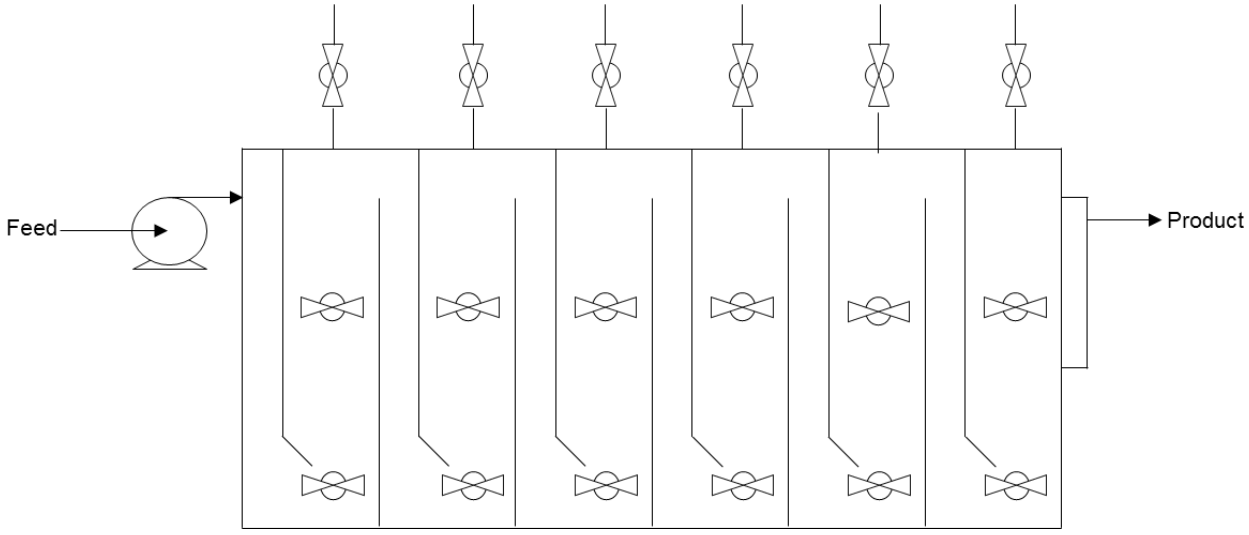

Figure 3.1: Schematic of the lab-scale ABR before modification

The electrode configuration of each cell was done by placing the floating air-cathode through the twisted titanium core of the carbon fibre brush anode. The chosen electrode configuration was used to obtain the smallest distance (± 2 mm) between the anode and cathode electrodes to eliminate limitation of system performance due to a long distance between the anode and cathode which results in a high internal resistance of the system (Kakarla *et al*., 2015). Insulated copper wire (i.e. crocodile grip type) was then used to connect the 6 anode and cathode electrodes in parallel.

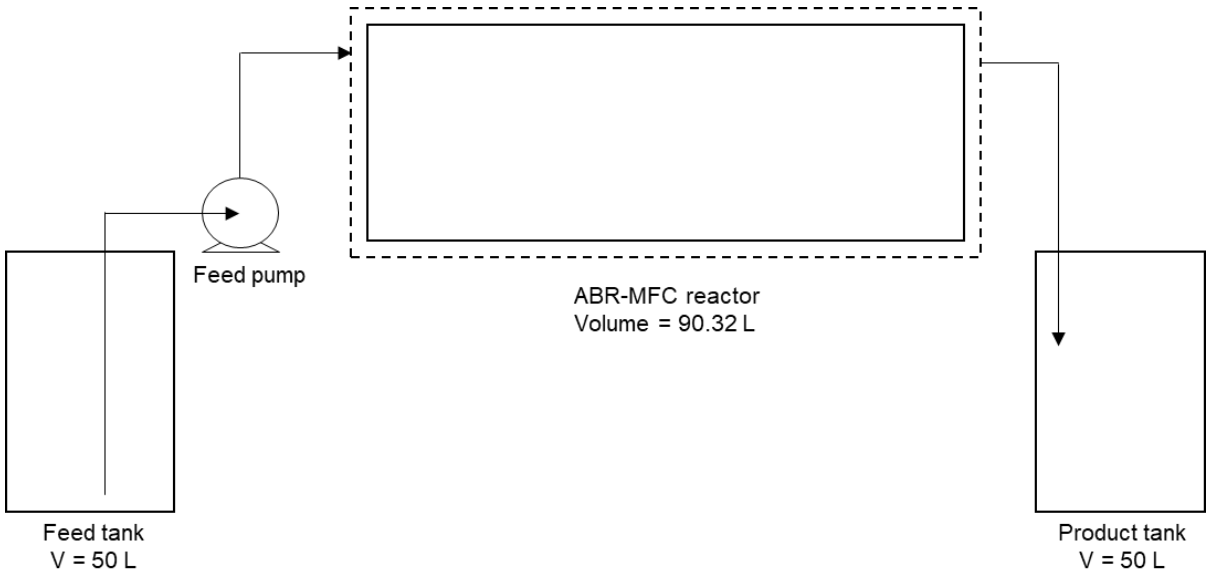

Figure 3.2.a: Process flow diagram of the lab-scale ABR-MFC system

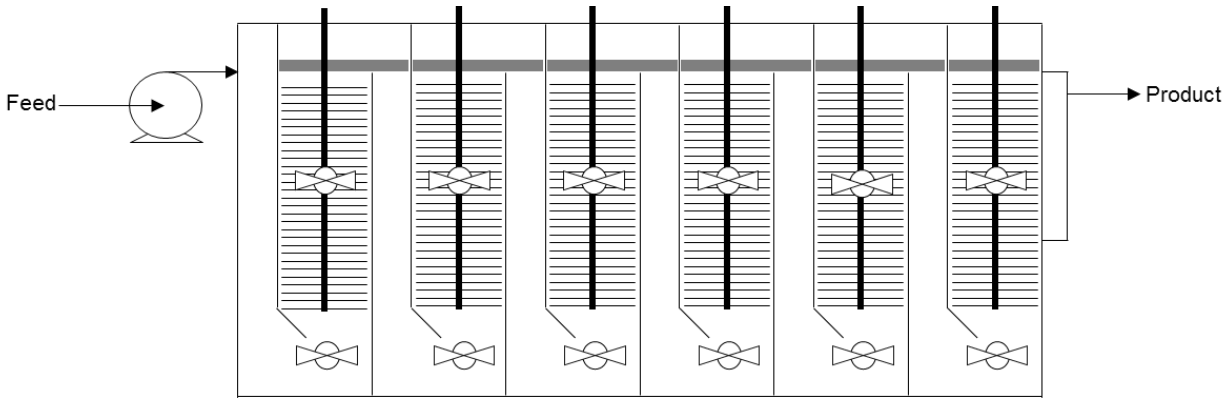

Figure 3.3.b: Schematic of the lab-scale ABR-MFC system

The external circuit was then closed with a 1 000 Ω external resistor (i.e. colour coded tubular wire wound) which completed the external circuit and the modification of the ABR into a hybrid ABR-MFC system (Figure 3.2.a and 3.2.b).

3.3.2. Experimental design

The experimental design depicted in Table 3.1 was suggested in order to analyse the influence of one independent variable (Phukingngam *et al*., 2011), feed concentration (i.e. OLR), on the COD removal in BDWW via biological treatment in the ABR-MFC system. The operating ranges selected for the independent variable (i.e. feed concentration) was established by considering the initial wastewater characterisation (refer to Table 2.3 in section 2.4.1).

The feed flow rate was chosen to remain constant at an HRT of 10 days, while the feed concentration was chosen to be 0.58, 1.15, 1.98 and 3.46 kg COD/m^3.day as indicated in Table 3.1 (refer to Appendix C for details regarding flow rate determinations). The ABR-MFC was operated without a recycle to minimize operational cost and power consumption (Grobicki & Stuckey, 1991).

After inoculation and system stabilisation (± 2 months), experimental run 1 was initiated by feeding the ABR-MFC with diluted BDWW at an OLR of 1.15 kg COD/m^3.day. Subsequently, run 2 was initiated by increasing the strength of the BDWW to an OLR of 1.98 kg COD/m^3.day. The feed concentration was then increased to 3.46 kg COD/m^3.day for the third and final OLR.

The chosen HRT at which the ABR-MFC operated (Table 3.1) was chosen as a basis from the study conducted by Phukingngam *et al*. (2011). Complete mineralisation of organic matter via microorganisms was observed as a result of longer digestion time (i.e. longer HRT) in a study conducted by Sukkasem *et al*. (2011) wherein the performance of an upflow bio-filter circuit (UBFC) for the treatment of BDWW was investigated.

Table 3.1: Experimental design for the treatment of BDWW

Experimental Condition	Feed Conditions			System Conditions	
	Description	COD [mg/l]	OLR [kg/m^3.day]	Q_{feed} [ml/min]	HRT [days]
1	Stabilisation	5 633	0.58	6.51	10
2	Low	10 979	1.15		
3	Medium	18 944	1.98		
4	High	33 356	3.46		

3.3.3. System inoculation and start-up procedure

Start-up of the system was done in a similar manner to An *et al.* (2009), who studied the potential for organic matter removal of a surface floating MFC structure, and Phukingngam *et al*. (2011) who investigated the performance of an ABR for organic matter removal and biogas production from BDWW. The working volume of the ABR-MFC was 80% filled with a mixture of equal parts (50/50 v/v%) AS and AGS which was used as the inoculum (An *et al*., 2009) for the ABR-MFC. The system was fed with diluted BDWW at an OLR of 0.58 kg COD/m^3.day for approximately 2 months (Phukingngam *et al*., 2011) in order to prevent bacterial shock in the anodic chamber of the ABR-MFC (Feng *et al*., 2010). An experimental design can be found in Table 3.1 wherein each OLR was applied to the hybrid ABR-MFC for 28 days in order to allow system stabilisation to occur as in the work of Feng *et al*. (2010).

3.3.4. Substrate adjustment

According to Phukingngam *et al*. (2011), the optimum C:N:P ratio for the biological treatment of BDWW is 150:1.1:0.2. The C:N:P ratio of the full-strength BDWW, having an initial COD concentration of 145 796 mg/l (refer to Table 4.1 in Section 4.1), was adjusted to 145796:1069.17:194.39 (150:1.1:0.2) by means of the addition of urea (CH_4N_2O) and potassium dihydrogen phosphate (KH_2PO_4) as the nitrogen (N) and phosphorous (P) sources, respectively. Initially 228.38 mg urea and 86.26 mg KH_2PO_4 was added per litre of BDWW. Refer to Appendix F.1. for calculations regarding the C:N:P ratio that was used and Appendix F.2. for procedure on substrate dilution and adjustment.

After nutrient addition and dilution with tap water to the relevant OLR, the pH of the wastewater frequently decreased from an average of 10.81 (refer to Table 4.1 in Section 4.1) to below 6 (refer

to Table H.4. in Appendix H) which was not in the optimal pH range (i.e. 6.8 to 7.4) for biological treatment (Khanal, 2008). Subsequent to nutrient addition, either sodium hydroxide (NaOH) or phosphoric acid (H_3PO_4) was used to adjust the pH of the feed to within the optimal pH range, after dilution with tap water, to respective OLRs of 0.58, 1.15, 1.98 and 3.46 kg COD/m^3.day.

3.4. Substrate analysis (chemicals, consumables and equipment)

Samples were collected daily from the feed and product tanks of the ABR-MFC system. Analysis of both the feed and product were done daily in duplicate for the following parameters: temperature, pH, total dissolved solids (TDS), salinity (salt), and electrical conductivity (EC) using a PCSTestr35 handheld multiparameter. The following parameters were analysed in duplicate every second day: turbidity using a TN-100 Turbidimeter ISO 7027 compliant nephelometric method, total suspended solids (TSS) using the ESS Method 350.2, and total COD (tCOD) using Merck COD solution A, (Cat. No. 1.14679.0495 and 1.14538.0065) and Merck COD Solution B (Cat. No. 1.14680.0495 and 1.14539.0495). Total phosphate concentration using Merck Spectroquant Phosphate cell tests for orthophosphate and total phosphorous (Cat. No. 1.14729.0001) and nitrogen concentration using Merck Spectroquant Nitrate cell tests (Cat. No. 1.14773.0001) were analysed weekly in duplicate. Biological oxygen demand (BOD) and FOG were determined by an independent SANAS accredited laboratory 2 weeks into the OLR testing, for each OLR. Current and voltage was measured daily using a Top T820 multimeter. Refer to Appendix D for all the analytical procedures.

The efficiency of the ABR-MFC was assessed according to the COD removal achieved by the system. Liu and Ramnarayanan (2004) demonstrated wastewater treatment and electricity generation by assessing the system they operated for removal of organic matter in the form of COD and BOD. Microbes contained within the anodic chamber were responsible for wastewater treatment and electricity generation (Mahendra & Mahavarkar, 2013).

CHAPTER FOUR

RESULTS AND DISCUSSION OF THE ABR-MFC OPERATIONAL PERFORMANCE

CHAPTER FOUR:
RESULTS AND DISCUSSION OF THE ABR-MFC OPERATIONAL PERFORMANCE

4.1. Introduction

The anaerobic treatment of biodiesel wastewater (BDWW), in which the total chemical oxygen demand (COD) was found to be 145 796 mg/l (Table 4.1), was studied at laboratory scale. Diluted BDWW was fed to a hybrid anaerobic baffled reactor microbial fuel cell (ABR-MFC), with a hydraulic retention time (HRT) of 10 days, at respective organic loading rates (OLR) of 0.58, 1.15, 1.98 and 3.46 kg COD/m^3.day which is in line with the work of Gao *et al*. (2004) and Phukingngam *et al*. (2011), who reported HRTs of 10.5 to 389 hours and OLRs ranging from 0.5 to 3.0 kg COD/m^3.day, respectively. The OLRs chosen for this study are also in accordance with the work of Siles *et al*. (2011) who studied OLRs ranging from 0.40 to 3.00 g COD/m^3.day for combined physical-chemical and biological treatments for BDWW. This chapter provides a description of the results obtained during the current study thereby evaluating the performance of the ABR-MFC system.

The results achieved in this study were not all obtained on the same day of sampling. Samples were kept at 4˚C, when not analysed on the day of sampling, to ensure minimum (biological) degradation of biological chemical demand (BOD), COD, total nitrate-nitrogen (NO_3^-N), fecal and total coliforms, total suspended solids (TSS), volatile suspended solids (VSS), alkalinity, acidity, and sulphate (Fulhage *et al*., 2017). All feed and product parameters were measured in duplicate. The average obtained from these results have been plotted in Figures 4.1 to 4.8 and 4.13 to 4.15 (refer to Appendix J for figures not displayed in this chapter, namely the daily operational parameters (i.e. temperature (Figure J.1), turbidity (Figure J.2), nitrates (Figure J.3), nitrogen (Figure J.4), total phosphate (TP) (Figure J.5), ortho-phosphate (OP) (Figure J.6), volatile suspended solids (VSS) (Figure J.7)). Experimental data can be found in Appendix H (Tables H.4, H.5, H.6 and H.7)). ABR-MFC efficiency data can be found in Appendix H (Table H.8). This chapter also includes a section on the fats, oils and grease (FOG) removal efficiency obtained by the ABR-MFC system.

The standard deviation of the results (measured in duplicate) were used to introduce error bars on all graphs presented in this chapter. The size of the error bars depicted in Figures 4.1, 4.2, 4.3, 4.4, 4.5, 4.6, 4.7, 4.8, 4.13, 4.14 and 4.15 (and Figures J.1 to J.7 depicted in Appendix J) suggests that the results were repeatable.

4.2. Full strength biodiesel wastewater

BDWW was collected from a local commercial biodiesel manufacturing company. The average, minimum and maximum values of the 5 respective samples which were analysed are indicated in Table 4.1 (refer to Table H.1 in Appendix H for summarised raw data on full strength BDWW samples). A chemical analysis (i.e. potability analysis) of 2 full strength BDWW samples was conducted by an outside independent South African National Accreditation System (SANAS) accredited laboratory. The average of these results is depicted in Tables 4.2 and 4.3.

Table 4.1: Average full strength BDWW characteristics

	Temp	pH	EC	TDS	Salt	COD	TSS	Turbidity	FOG
	°C		µS/cm	ppm	ppm	mg/l	mg/l	NTU	mg/l
Min	19.6	9.67	661	471	371	100595	0.01	470	900
Max	23.8	11.97	793	560	630	301125	0.44	1000	900
Ave	22.0	10.81	735	522	459	145796	0.18	895	900

Table 4.2: Chemical potability analysis of full strength BDWW – parameters which meets the industrial wastewater discharge standard limits

Temp	pH	EC	Na	Fe	Cl	B	Cu	Zn	TP	SO_4^-	TDS
°C		mS/cm	mg/l	mg/l	mg/l	mg/l	mg/l	mg/l	mg/l	mg/l	mg/l
17.1	10.55	1.2	133.9	1.5	17.9	<0.08	<0.02	0.37	0.2275	101	691

Table 4.3: Chemical potability analysis of full strength BDWW – parameters not specified and does not meet (i.e. FOG and COD) the industrial wastewater discharge standard limits

K	Ca	Mg	Mn	F	NH_4-N	NO_3-N	CO_3^{2-}	HCO_3^-	FOG	COD	BOD
mg/l	mg/l	mg/l	mg/l	mg/l	mg/l	mg/l	mg/l	mg/l	mg/l	mg/l	mg/l
733.5	<0.06	13.1	<0.03	0.45	6.705	<0.38	414.5	1103.45	900	246575	167738

The industrial wastewater discharge standard limits imposed by the City of Cape Town (2011) (refer to Table 2.2 in Section 2.3) suggests that the following parameters, depicted in Table 4.1 and 4.2, for the full strength BDWW meets the industrial wastewater discharge standard limits: pH, conductivity, TDS, chlorine (Cl), total sulphates (SO_4^{2-}), total copper (Cu), TP, sodium (Na), total iron (Fe), total zinc (Zn), total boron (B) and TSS.

Unfortunately, the COD and FOG contained in this wastewater does not meet the industrial wastewater discharge standard limits stipulated by the City of Cape Town (2011). The COD of this wastewater ranges from 100 595 mg/l to 301 125 mg/l (Table 4.1). The amount of COD permitted

to be present in the water is anything less than 5 000 mg/l (Table 2.2) which makes the full-strength BDWW, on average, approximately 140 800 mg/l over the allowed limit prior to treatment. The amount of FOG contained in the full-strength BDWW was found to be 900 mg/l, which is 500 mg/l over the allowed discharge limit of 400 mg/l stipulated by the City of Cape Town. It is therefore evident that this wastewater should be treated prior to disposal into the municipal sewer system to contribute towards environmental remediation.

The BOD:COD ratio for the BDWW used in this study was found to be 0.68. According to Zaher & Hammam (2014), the biodegradation index (BI) of 0.68 deems this wastewater fairly biodegradable and can be effectively treated via biological treatment.

4.3. Daily operational analysis

The ABR-MFC was operated at ambient conditions (i.e. room temperature (21 °C) and atmospheric pressure (101.325 kPa)) for the duration of this study. The average, minimum and maximum values of the daily operational parameters (i.e. temperature, pH, EC, TDS and salinity) for respective ABR-MFC feed and product samples are depicted in Tables 4.4 and 4.5 (refer to Appendix H (Tables H.4 and H.5) for daily operational experimental data on the ABR-MFC feed and product BDWW samples).

Table 4.4: Summarised daily operational parameters for ABR-MFC feed samples

	Temp °C	pH	EC µS/cm	TDS ppm	Salt ppm
Min	9.9	4.74	190	136	106
Max	25.4	8.41	1789	1270	1045
Ave	18.5	6.64	653	464	390

Table 4.5: Summarised daily operational parameters for ABR-MFC product samples

	Temp °C	pH	EC µS/cm	TDS ppm	Salt ppm
Min	8.8	4.17	2	293	274
Max	24.8	8.34	1866	1215	996
Ave	17.3	6.63	753	537	448

The EC, TDS and salinity of the respective ABR-MFC feed and product samples followed similar trends of increasing (Figures 4.6 and 4.7). The EC, TDS and salinity of product samples (Table 4.5) were on average 100 µS/cm, 73 mg/l and 58 mg/l more than the EC, TDS and salinity of the ABR-MFC feed samples (Table 4.4) which was respectively found to be 653 µS/cm, 464 mg/l and

390 mg/l over the study period of 225 days. There was thus no significant difference in ABR-MFC feed and product samples for these parameters. It is therefore recommended that a membrane based (i.e. nanofiltration (NF), ultrafiltration (UF) and reverse osmosis (RO)) post-treatment step is included to remove EC, TDS and salinity from the BDWW once the contaminants (i.e. COD and FOG), which could cause membrane fouling, has been removed (Jacobson *et al*., 2011).

4.3.1. ABR-MFC pH

The daily operational parameter, pH, of the ABR-MFC feed (and product) were measured to monitor the system as a feed-back process control. The pH of the ABR-MFC feed was thus adjusted to the optimal pH (6.5 – 7.5) for microbial growth in bioreactor systems (Water and Wastewater Measuring Solutions, 2002) using sodium hydroxide (NaOH) and phosphoric acid (H_3PO_4).

Although the pH of the feed samples decreased to below 6.5 on day 33, the pH of the product constantly remained above 7.0 until day 90 where a decrease can be observed in Figure 4.1. The pH of the product decreased until day 208 of ABR-MFC operation where an increase in product pH can be observed. This observation in the product pH can be due to an increase in feed pH on day 201.

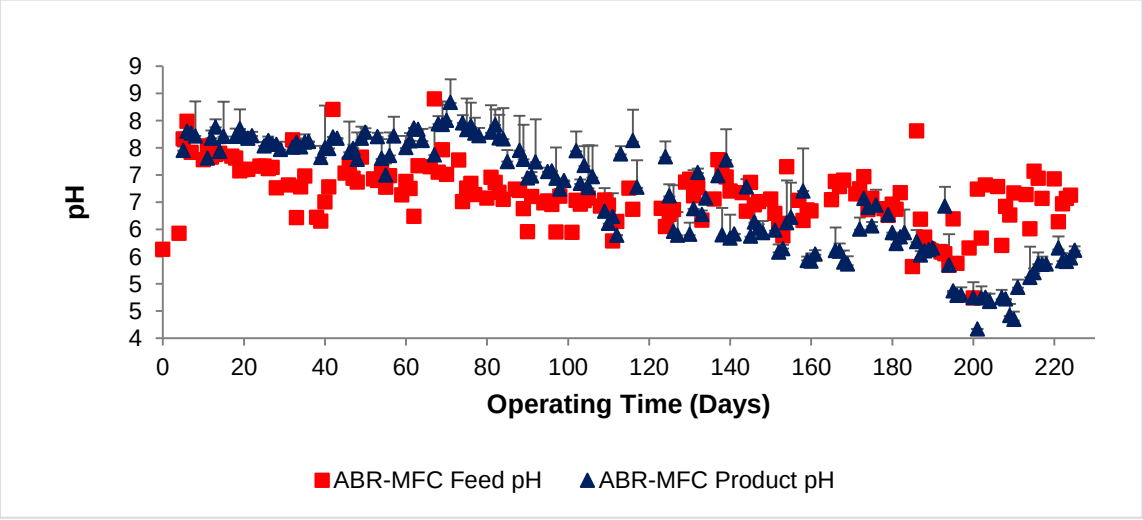

Figure 4.1: pH of ABR-MFC feed and product samples

The decrease in pH of the ABR-MFC feed to below 6.0 on day 97 (and again on days 101, 111, 153, 185, 188, 189, 192, 193, 194, 196, 199, 202 and 207) of ABR-MFC operation might have affected the microbial metabolism causing a decrease in organic matter removal (Pirsaheb *et al*.,

2015) since common wastewater bacteria function well between pH levels ranging from 6.0 to 8.5 in bioreactors (Jou & Huang, 2003). Nonetheless, the average pH of the respective feed (i.e. 6.64) and product (i.e. 6.63) samples shows an insignificant difference of 0.01. However, the treatment efficiency observed (Figure 4.2) by the ABR-MFC in this study contravenes the statement made by Pirsaheb and co-workers (2015) since the decrease in pH did not have a significant effect on the organic matter removal achieved. It is possible that the latter could be due to a very small decrease below the optimum pH range specified.

According to literature, the optimal pH range for a bioreactor is between 6.5 and 7.5 which will ensure optimal biological activity (Jou & Huang, 2003). This statement is supported by Florencio *et al*. (1996) and Pirsaheb *et al*. (2015), who claims that a neutral pH is best for methanogenesis. A recycle stream can be introduced to the ABR-MFC system to adjust the pH of the feed stream (Grobicki & Stuckey, 1991), thus possibly eliminating the need for adjusting the feed pH by adding NaOH and H_3PO_4.

Significant acid fermentation (i.e. acidogenesis) occurs at pH levels below 7.0 (Gerardi, 2003). A decrease in methanogenic activity can therefore be expected once the pH changes from the neutral pH range (Barber & Stuckey, 1999). The latter occurs since the four degradation stages (i.e. hydrolysis, acidogenesis, acetogenesis and methanogenesis) of anaerobic treatment are dependent on each other. An increase in acid(s) and thus loss of alkalinity and a decrease in pH consequently indicates inhibition of the fourth stage, methanogenesis (Pirsaheb *et al*., 2015; Henze *et al*., 2008; Gerardi, 2003). Products within the system can therefore be considered to be mainly hydrogen gas (H_2) and acids (i.e. acetic acid (CH_3CO_2H) and acetate ($CH_3CO_2^-$)) (Seijan *et al*., 2016; Henze *et al*., 2008). Consequently, a build-up of products from acetogenesis will occur which causes the pH to decrease further due to an increase of volatile fatty acid (VFA) (i.e. acetate) in the system (Pirsaheb *et al*., 2015; Henze *et al*., 2008). According to Von Sperling and De Lemos Chernicharo (2005), a large amount of VFA consumption reduces the buffering capacity of the substrate and is thus indicated by a small decrease in pH. Suehara *et al*,. (2005) states that the formation of VFA is attributed to the degradation of FOG.

The buffering capacity of the ABR-MFC system can thus be increased by supplying the system with sufficient alkalinity (i.e. a measure of the buffering capacity of water (Pirsaheb *et al*., 2015)) to prevent a decrease in pH and consequently reactor instability (Florencio *et al*., 1996). Supplying the ABR-MFC system with sodium bicarbonate ($NaHCO_3$) and potassium dihydrogen orthophosphate (KH_2PO_4) (Florencio *et al*., 1996) or urea (CH_4N_2O) (0.007 g/gCOD) and diammonium hydrogen phosphate ($NH_4H_2PO_4$) (0.0006 g/gCOD) (Pirsaheb *et al*., 2015) as

sources of alkalinity, can assist in maintaining the optimum pH as well as buffering the effect caused by VFA thereby ensuring effective digestion (Phukingngam *et al*., 2011).

In a study conducted by Phukingngam *et al*. (2011), excessive accumulation of VFA in BDWW caused a decrease in pH creating an environment unfavourable for methanogenesis (Veljković *et al*., 2014). This occurred due to decelerated utilisation of organic matter caused by OLRs higher than 1.5 kg COD/m^3.day which was found to be the optimal OLR for the study conducted by Phukingngam *et al*. (2011). Barber and Stuckey (1999) also reported that an increase in VFA resulted in a decrease in pH.

In biological wastewater treatment, acetogenesis and methanogenesis occur simultaneously (Pirsaheb *et al*., 2015). When treating wastewaters containing methanol (CH_3OH), the COD removal efficiency and thus the stability of the treatment system, is highly dependent on whether methanol is consumed by methylotropic methanogens or acetogens and directly converted to methane (CH_4) or acetate, respectively (Florencio *et al*., 1996). It is therefore necessary to limit the VFA content within the ABR-MFC to as little as 200 mg/l acetic acid, which have been reported as the optimum VFA content for biological wastewater treatment. Maintaining a low VFA content in the ABR-MFC is therefore essential for continued digestion (Pirsaheb *et al*., 2015).

Although methanogenesis (i.e. production of methane and carbon dioxide (CO_2) by methanogenic bacteria (Gerardi, 2003)) is considered to be a significant part of biogas production in anaerobic digesters, this study used an alternative approach to bioenergy (i.e. bioelectricity) production (i.e. MFC technology). The focus of this study was thus wastewater treatment while generating bioelectricity via MFC technology as a by-product. This approach is considered safer, when compared to the use of biogas on-site, for the treatment of BDWW at biodiesel companies since highly flammable chemicals (i.e. methanol) are used during the production of biodiesel (Steiman *et al*., 2016). Bioelectricity (which can be converted to run a pump used to feed BDWW to the ABR-MFC) could therefore be a safer alternative for biodiesel companies once more research has been conducted with regards to increasing electricity production in an ABR-MFC system.

Although KH_2PO_4 and urea have been used in this study as combined pH buffers and nutrients for microorganisms, the pH of the feed and product of the ABR-MFC system fluctuated. According to Bodkhe (2009), methanogens effectively consume VFA when constant pH values are obtained. It is therefore recommended to maintain alkalinity within the ABR-MFC below 200 mg/l acetic acid by using either $NaHCO_3$ or $NH_4H_2PO_4$ as suggested by Florencio *et al*. (1996) and Pirsaheb *et al*. (2015).

4.4. ABR-MFC performance

This section reflects the findings of the ABR-MFC performance for the duration of the study of 225 days. The findings include information regarding the treatment efficiency of the ABR-MFC during this time. Refer to Appendix H (Tables H.4, H.5, H.6 and H.7) for summarised feed and product experimental data. Diluted biodiesel wastewater was biologically treated using an ABR-MFC. The average, minimum and maximum values of the daily operational parameters of respective ABR-MFC feed and product samples are indicated in Tables 4.4 and 4.5. System performance parameters are indicated in Tables 4.6 and 4.7.

The industrial wastewater discharge limits stipulated by the City of Cape Town (2011) suggests that the following parameters for the ABR-MFC product meets the industrial wastewater discharge standard limits: pH, TDS, EC, TSS, FOG and TP (Table 4.4 and 4.6).

The only parameter that did not meet the industrial wastewater discharge standard limits after biological treatment with the ABR-MFC is the COD which ranges from 1 605 to 13 590 mg/l (average = 5 844 mg/l) (Table 4.7). The amount of COD permitted to be present in the water is anything less than 5 000 mg/l (Table 2.2). The treated wastewater thus remains over the allowed limit with approximately 8 590 mg/l (average = 844 mg/l) (Table 4.7). It is therefore evident that the wastewater should still be further treated prior to disposal into the municipal sewer system.

Table 4.6: Summarised system performance – ABR-MFC feed samples

	COD mg/l	TSS mg/l	VSS mg/l	Turbidity NTU	FOG mg/l	NO_3^- mg/l	N mg/l	TP mg/l	OP mg/l
Min	5213	0.01	1.33	225	1280	1.22	0.28	0.10	11.10
Max	37230	64.30	65.85	1000	269540	12.15	2.74	4.05	25.30
Ave	13906	4.54	7.68	855	91164	6.05	1.37	1.79	18.17

Table 4.7: Summarised system performance – ABR-MFC product samples

	COD mg/l	TSS mg/l	VSS mg/l	Turbidity NTU	FOG mg/l	NO_3^- mg/l	N mg/l	TP mg/l	OP mg/l
Min	1605	0.00	0.42	19	46	0.09	0.00	0.10	8.10
Max	13590	2.66	3.63	452	100	1.62	0.37	0.50	25.00
Ave	5844	0.16	1.57	85	73	0.54	0.11	0.18	15.86

Figure 4.2 depicts the COD of the ABR-MFC feed and product, as well as the COD removal achieved by the lab-scale ABR-MFC. The maximum removal capacity of the ABR-MFC was found to be 79.84% at an OLR of 0.58 kg COD/m^3.day and an HRT of 10 days. Despite the strong fluctuations in ABR-MFC feed COD, varying daily between 5 213 mg/l and 37 230 mg/l (Table 4.6),

the ABR-MFC product quality was consistent with regards to COD up until day 195 where a maximum of 11 068 mg/l was observed. The product COD then remained in the range of 11 000 mg/l until shutdown on day 225. The strong fluctuations in ABR-MFC feed can be attributed to a change in OLR from 0.58 kg COD/m^3.day (stabilisation period) to OLRs 1 (1.15 kg COD/m^3.day), 2 (1.98 kg COD/m^3.day) and 3 (3.46 kg COD/m^3.day) on days 144, 172 and 200 of ABR-MFC operation, respectively.

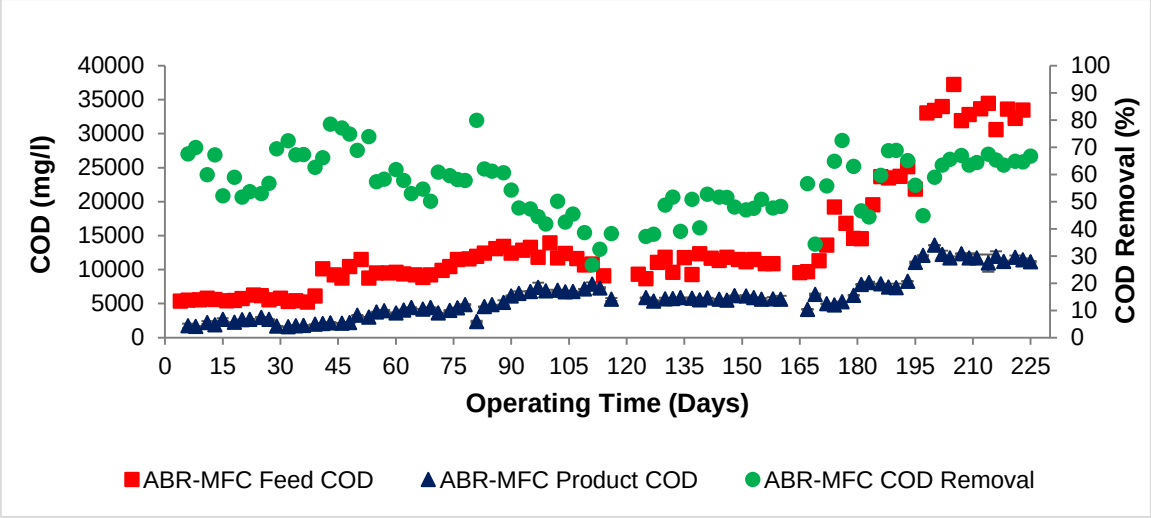

Figure 4.2: COD of ABR-MFC feed and product samples (and COD removal – ABR-MFC efficiency)

The ABR-MFC operated for 225 days during which the average feed and product COD was found to be 13 906 mg/l (Table 4.6) and 5 844 mg/l (Table 4.7), respectively. The average COD removal during operation was thus found to be 56.62%. The low COD removal observed during experimental operation suggests that anaerobic digestion was incomplete (Pirsaheb *et al*., 2015), thus not all organic matter was converted to final products resulting in excessive COD in the product stream.

According to Phukingngam *et al*. (2011) who achieved a 99% COD removal efficiency in an ABR treating BDWW, a chemical pre-treatment of biodiesel wastewater followed by biological treatment should increase the removal of organic matter. They operated ABRs at various OLRs and found that OLRs ranging from 0.5 to 1.5 kg COD/m^3.day were most effective and regarded an OLR of 1.5 kg COD/m^3.day as the optimal OLR since a removal efficiency of 99% was achieved. It was therefore decided to study OLRs ranging from 0.5 to 3.0 kg COD/m^3.day.

In their study, BDWW was pre-treated with chemical coagulation and sedimentation due to a significantly high FOG content (3 270 mg/l) which could inhibit microorganism activity in any biological treatment process (Phukingngam *et al*., 2011). The FOG content was reduced to 130 mg/l by adding polyaluminum chloride ($Al_2Cl(OH)_5$) (62.5 mg/l) and a cation polymer (1.25 mg/l) to the BDWW after adjusting the pH from 10.3 to 4.0 using sulphuric acid (H_2SO_4) (Phukingngam *et al*., 2011). The latter was done to recover the free fatty acid (FFA) content of the BDWW since the long-chain fatty acids contained in BDWW show acute toxicity towards anaerobic digestion (Siles *et al*., 2011). Urea, K_2HPO_4, and iron(II) chloride ($FeCl_2$) was added to the pre-treated BDWW to achieve a carbon:nitrate:phosphate:iron (C:N:P:Fe) ratio of 150:1.1:0.2:0.33 since the BDWW contained very low amounts of nitrogen (N) (14 mg/l) while total phosphate (TP) was undetected (Phukingngam *et al*., 2011).

4.4.1. ABR-MFC stabilisation

This section reflects on the findings of the ABR-MFC during the stabilisation period of 143 days when the ABR-MFC was operated without MFC technology. The findings include information regarding the treatment efficiency of the ABR-MFC during this time. Refer to Appendix H (Tables H.4, H.5, H.6 and H.7) for summarised feed and product experimental data. The ABR-MFC stabilisation period was prolonged (> 2 months) since MFC anode and cathode electrode materials were obtained later than expected. The ABR-MFC operated at an OLR of 0.58 kg COD/m^3.day and an HRT of 10 days during this period.

It is evident from Figure 4.3 that the feed COD is directly proportional to the product COD. The average COD in respective feed and product samples of the ABR-MFC was found to be 9 264 mg/l (Table 4.8) and 4 239 mg/l (Tables 4.9). However, the feed and product COD is indirectly proportional to the removal of COD. During this period, the ABR-MFC achieved an average COD removal of 55.84%.

The EC, TDS and salinity (Figures 4.6 and 4.7) of ABR-MFC feed and product samples was found to be similar while having respective differences of 155 μS/cm, 115 mg/l, and 98 mg/l in the feed and product samples (Tables 4.8 and 4.9). The feed pH ranged from 5.64 to 8.41 (Table 4.8) while the pH of the product samples ranged from 5.85 to 8.34 (Table 4.9). Nonetheless, the average feed and product pH (refer to Figure 4.1) was found to be 6.81 (Table 4.8) and 7.30 (Table 4.9), respectively.

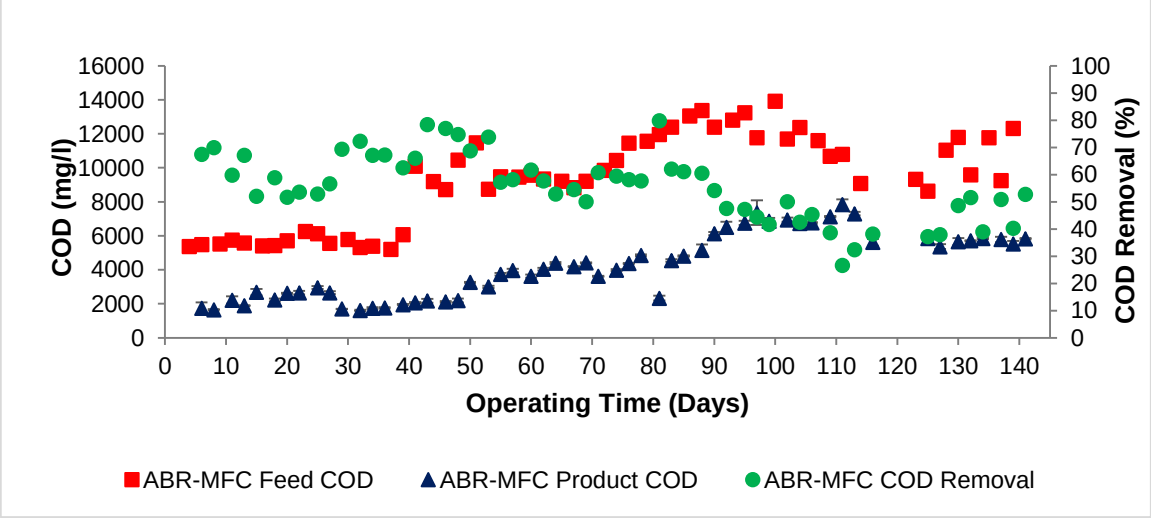

Figure 4.3: COD of ABR-MFC feed and product samples (and COD removal – ABR-MFC efficiency) during system stabilisation

Table 4.8: Summarised daily operational parameters for ABR-MFC feed samples during system stabilisation

	Temp °C	pH	EC µS/cm	TDS ppm	Salt ppm	COD mg/l	TSS mg/l	VSS mg/l	Turbidity NTU
Min	9.9	5.64	190	136	106	5213	0.01	1.33	225
Max	25.4	8.41	682	485	395	13920	15.67	16.43	1000
Ave	18.8	6.81	491	349	284	9264	2.14	4.46	799

Table 4.9: Summarised daily operational parameters for ABR-MFC product samples during system stabilisation

	Temp °C	pH	EC µS/cm	TDS ppm	Salt ppm	COD mg/l	TSS mg/l	VSS mg/l	Turbidity NTU
Min	8.8	5.85	2	293	274	1605	0.00	0.92	19
Max	24.8	8.34	1641	1165	938	7843	2.66	1.41	166
Ave	17.4	7.30	646	464	382	4222	0.14	1.08	47

It is evident from Figure 4.4 that the TSS contained in the BDWW was successfully reduced from an average of 2.14 mg/l to 0.14 mg/l (Tables 4.8 and 4.9) during the stabilisation period thus removing 86.98% TSS. It is observed (Figure 4.4) that the TSS contained in the feed samples increased over time, while the TSS contained in the product samples remained constantly low. Nonetheless, the TSS removal observed is indirectly proportional to the TSS contained in feed samples. The experimental data depicted in Figure 4.4 contains a few potential outliers which could be due to human error. Refer to Figure 4.5 for a complete representation of TSS in feed and products samples for this study.

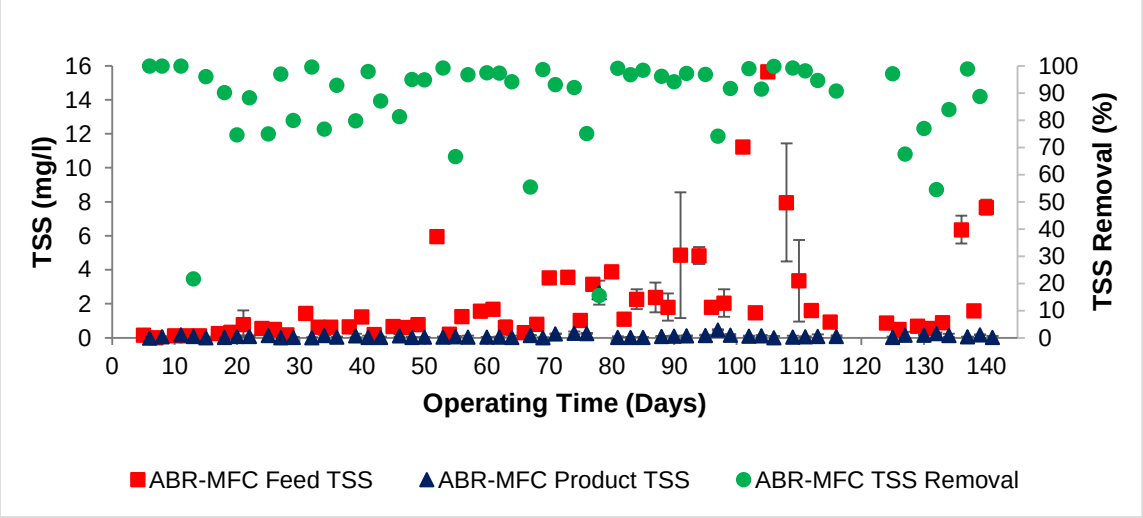

Figure 4.4: TSS of ABR-MFC feed and product samples (and TSS removal – ABR-MFC efficiency) during system stabilisation

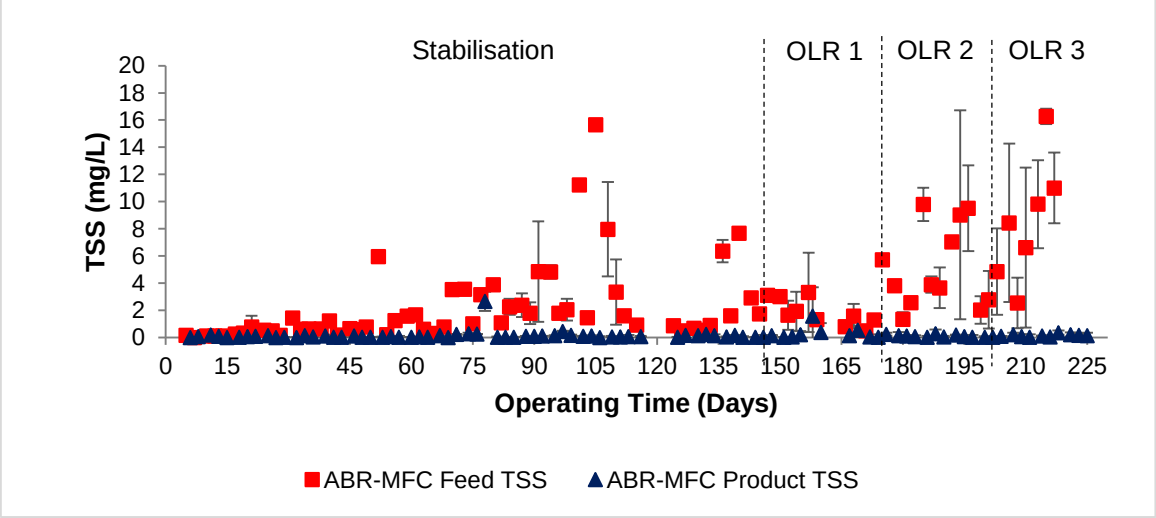

Figure 4.5: TSS of ABR-MFC feed and product samples

4.4.2. Effect of OLR's on ABR-MFC performance

Three different OLRs (1.15, 1.98, and 3.46 kg COD/m^3.day) were investigated during this study. This section reflects on the performance (i.e. COD-, FOG-, TSS-removal) as well as some of the daily operation parameters (i.e. EC, TDS and salinity) measured for the three OLRs. The ABR-MFC was operated at a constant HRT of 10 days.

The EC, TDS and salinity (Figure 4.6 and 4.7)) of ABR-MFC feed and product samples were found to be very similar. The EC, TDS and salinity of the product samples (Table 4.11) were 8 µS/cm

and 2 mg/l higher, and 8 mg/l lower than feed samples (Table 4.10), respectively which was found to be on average 921 µS/cm, 654 mg/l, and 565 mg/l.

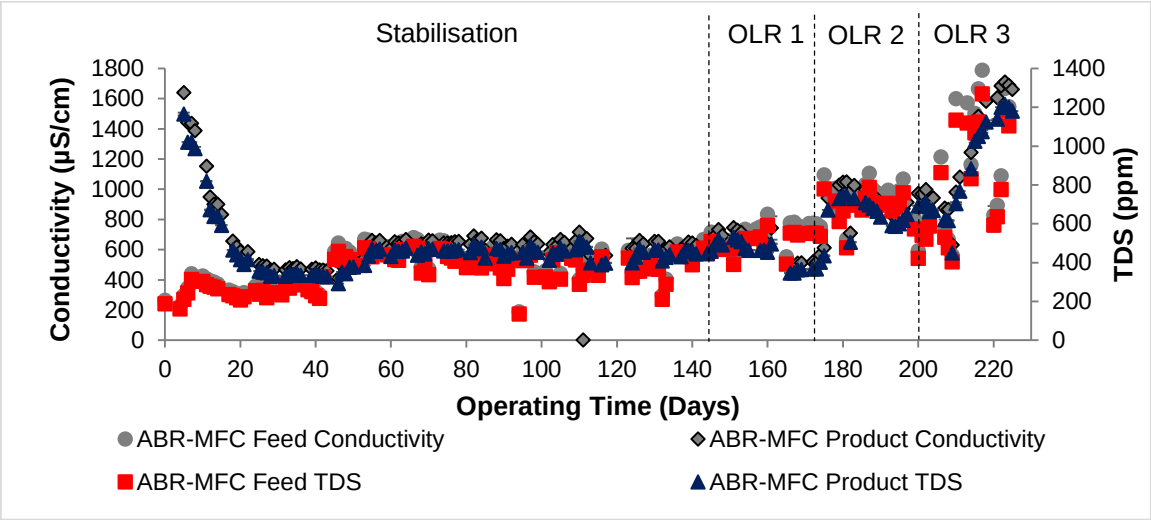

Figure 4.6: EC and TDS of ABR-MFC feed and product samples

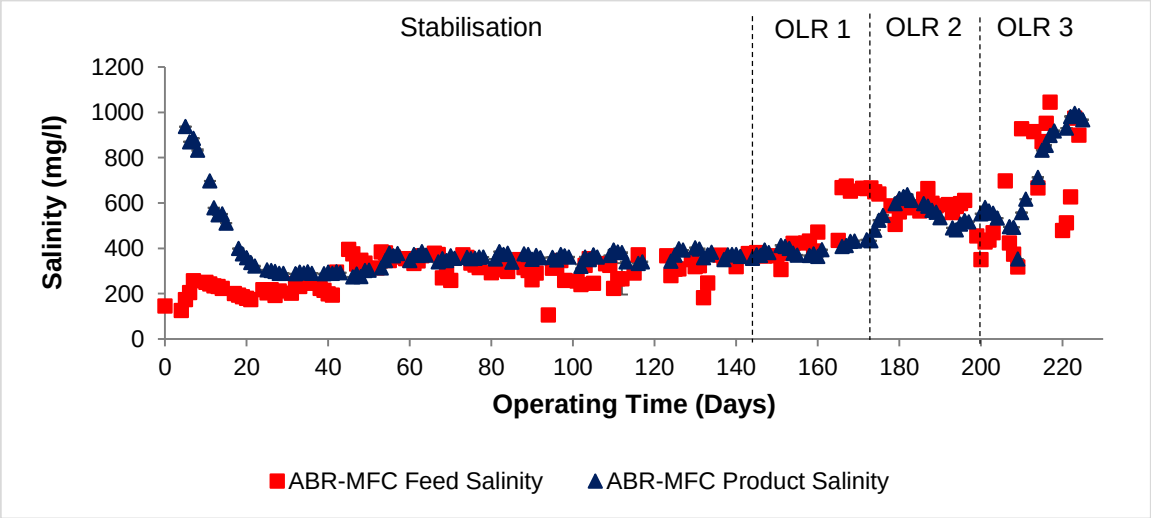

Figure 4.7: Salinity of ABR-MFC feed and product samples

The feed pH ranged from 4.74 to 7.82 (Table 4.10) while the pH of the product samples ranged from 4.17 to 6.79 (Table 4.11). Nonetheless, the average feed and product pH was found to be 6.37 (Table 4.10) and 5.54 (Table 4.11) for the duration of OLRs 1 to 3.

Table 4.10: Summarised daily operational parameters for ABR-MFC feed samples (OLR 1, 2 and 3)

	Temp °C	pH	EC µS/cm	TDS ppm	Salt ppm
Min	10.7	4.74	551	392	306
Max	24.0	7.82	1789	1270	1045
Ave	17.9	6.37	921	654	565

Table 4.11: Summarised daily operational parameters for ABR-MFC product samples (OLR 1, 2 and 3)

	Temp °C	pH	EC µS/cm	TDS ppm	Salt ppm
Min	10.5	4.17	488	346	353
Max	23.3	6.79	1866	1215	996
Ave	17.3	5.54	929	656	557

Figure 4.8 depicts the COD of both feed and product samples, as well as the COD removal for the 3 OLRs investigated during this study. The average COD in the feed and product samples were found to be 21 688 mg/l (Table 4.12) and 8 516 mg/l (Table 4.13), respectively. During operation, the ABR-MFC was able to remove 57.87% COD at an HRT of 10 days. The COD removal achieved by the ABR-MFC system can be compared to the work of Sukkasem *et al*. (2011) who removed 50% COD from BDWW by using an upflow bio-filter circuit (UBFC).

Although strong COD fluctuations can be observed (Figure 4.8) in the ABR-MFC feed samples, the COD of the ABR-MFC product samples remained relatively stable while the COD removal of the ABR-MFC system followed the same trend as the COD of ABR-MFC feed samples. In order to increase system efficiency (i.e. COD removal), a recycle stream can be introduced to the ABR-MFC, thereby diluting the ABR-MFC feed thus reducing the toxicity of the feed for microorganisms (Grobicki & Stuckey, 1991).

Suehara and co-workers (2005) conducted biological treatment on BDWW using an oil degradable yeast (i.e. *Rhodotoula mucilaginosa*). The microbial growth inhibitor was found to be the solid content (i.e. TSS) of the BDWW in this study. They found that the growth of the microorganisms was inhibited by a solid concentration above 2.14 g/l. The BDWW used in this study contained low concentrations of TSS (Table 4.12). The TSS of the BDWW was reduced from an average of 8.48 mg/l (Table 4.12) to 0.18 mg/l (Table 4.13), thus removing 93.53% TSS. The TSS contained in the BDWW treated by the ABR-MFC is much lower than the TSS reported by Suehara *et al*. (2005). It can be assumed that the microbial growth in the ABR-MFC was thus not affected by the amount of TSS contained in the BDWW.

The C:N:P ratio of the feed was adjusted to 150:1.1:0.2 by adding urea and KH_2PO_4. This adjustment caused an increase in NO_3^--N and TP from <0.38 mg/l and 0.2275 mg/l (Table 4.3) to an average of 6.05 mg/l and 2.16 mg/l (Table 4.12), respectively. However, after treatment with the ABR-MFC system the treated BDWW product contained respective average NO_3^--N and TP concentrations of 0.54 mg/l and 0.19 mg/l (Table 4.13). The ABR-MFC thus removed 91.07% and 91.20% NO_3-N and TP, respectively.

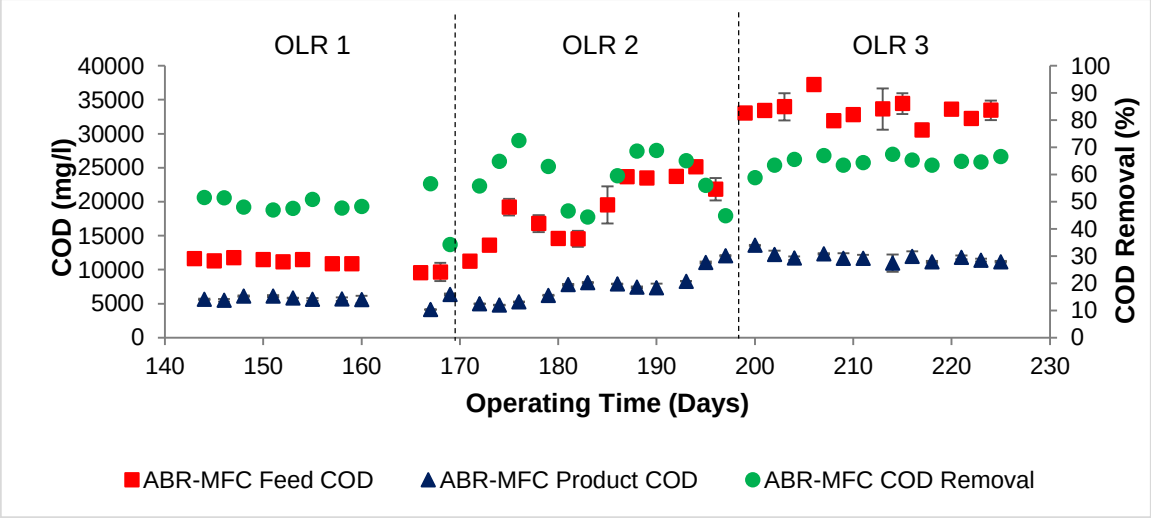

Figure 4.8: COD of ABR-MFC feed and product samples (and COD removal – ABR-MFC efficiency) for OLR 1-3

Table 4.12: Summarised system performance (OLR 1, 2 and 3) – ABR-MFC feed samples

	COD mg/l	TSS mg/l	VSS mg/l	Turbidity NTU	FOG mg/l	NO_3^- mg/l	N mg/l	TP mg/l	OP mg/l
Min	9538	0.50	2.24	347	1280	1.22	0.28	1.10	17.35
Max	37230	64.30	65.85	1000	269540	12.15	2.74	4.05	25.30
Ave	21688	8.48	9.85	951	91164	6.05	1.37	2.16	22.08

Table 4.13: Summarised system performance (OLR 1, 2 and 3) – ABR-MFC product samples

	COD mg/l	TSS mg/l	VSS mg/l	Turbidity NTU	FOG mg/l	NO_3^- mg/l	N mg/l	TP mg/l	OP mg/l
Min	4145	0.02	0.42	40	46	0.09	0.00	**0.10**	**13.75**
Max	13590	1.59	3.63	452	100	1.62	**0.37**	0.50	25.00
Ave	8516	0.18	1.92	147	73	0.54	0.11	0.19	19.08

4.4.2.1. FOG in the ABR-MFC system

The ABR-MFC reduced the FOG contained in the BDWW from 91 164 mg/l (Table 4.12) to 73 mg/l (Table 4.13). The FOG removal for OLRs 1, 2 and 3 in this study was found to be 96.41%, 97.31%

and 99.96% which resulted in an average FOG removal of 97.89%. These positive FOG removal results could be attributed to the fact that the small compartment to the left of compartment 1 (C1) turned into a fat trap during the stabilisation period (refer to Figure 4.9). The FOG removal achieved by the ABR-MFC can be compared to the work of Phukingngam *et al*. (2011) who reduced 82% of FOG contained in BDWW treated with an ABR at OLRs of 0.5, 1.0 and 1.5 kg COD/m^3.day.

Although the small compartment to the left of C1 had to be unblocked on day 116 of operation, there was no observable fat (i.e. FOG) in compartment 6 (C6) for the entire duration (225 days) of the study. The ABR-MFC therefore proves that a pre-treatment step in not necessary for BDWW for the successful removal of FOG. Figure 4.9 also illustrates the existence of larvae (i.e. maggots) which proves that the ABR-MFC can assist living organisms with BDWW as a food source.

Figure 4.9: Photograph of fat trap (left of C1) on day 181 (38 days since installation of MFC technology)

It is also evident from Figures 4.10 to 4.12 that the fat trapped in the fat trap of the ABR-MFC did not overflow out of the compartment. It can thus be said that the microorganisms living in the ABR-MFC successfully consumed the FOG contained in the BDWW.

Figure 4.10: Top view photograph of ABR-MFC on day 144 (on day of MFC technology installation)

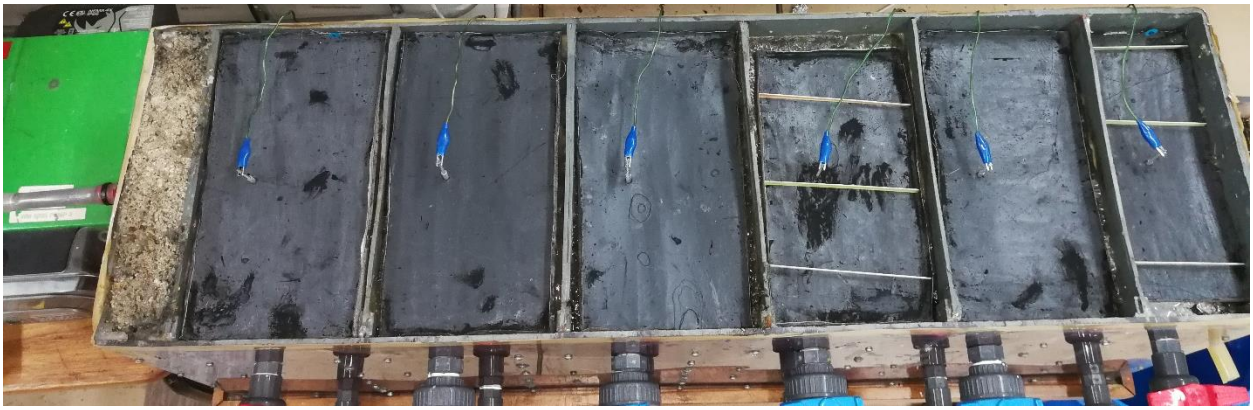

Figure 4.11: Top view photograph of ABR-MFC on day 148 (5 days since installation of MFC technology)

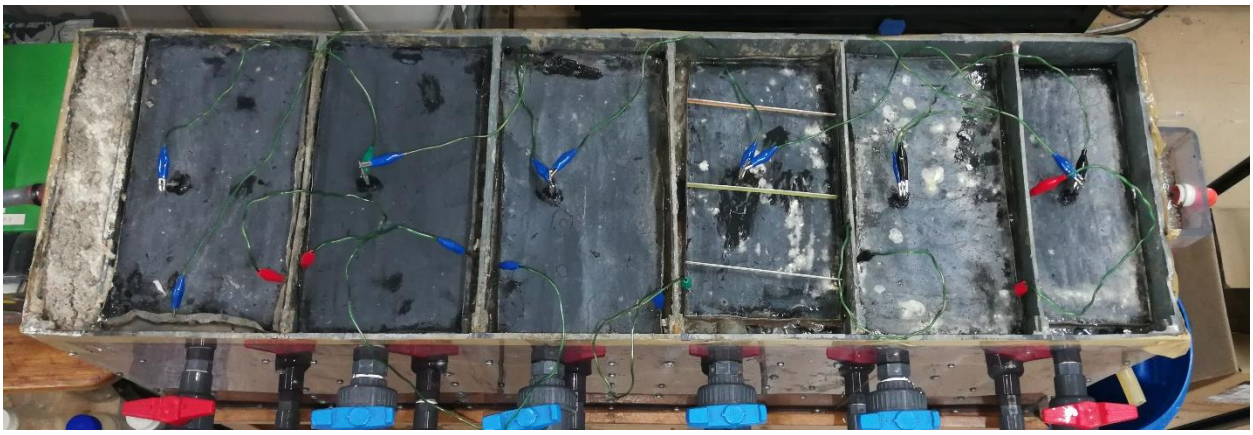

Figure 4.12: Top view photograph of ABR-MFC on day 161 (18 days since installation of MFC technology)

4.4.2.2. Effect of OLR 1 on ABR-MFC performance

This section reflects on the findings of the first OLR (1.15 kg COD/m^3.day) after system stabilisation. The findings include information regarding the treatment efficiency of the hybrid ABR-MFC system. Refer to Appendix H (Tables H.4, H.5, H.6 and H.7) for summarised feed and product experimental data for OLR 1. The ABR-MFC operated at an OLR of 1.15 kg COD/m^3.day and an HRT of 10 days during OLR 1 for a total of 28 days.

The EC, TDS and salinity (Figures 4.6 and 4.7) of the ABR-MFC feed and product samples was found to be approximately similar. The ABR-MFC feed (Table 4.14) was 52 µS/cm, 39 mg/l, and 46 mg/l higher than the product (Table 4.15) EC, TDS and salinity which was found to be on average 645 µS/cm, 456 mg/l, and 390 mg/l, respectively for OLR 1.

The feed pH ranged from 5.89 to 7.16 (Table 4.14) while the pH of product samples ranged from 5.37 to 6.79 (Table 4.15). Nonetheless, the average feed and product pH (refer to Figure 4.1) was found to be 6.52 (Table 4.14) and 5.86 (Table 4.15), respectively for OLR 1.

Table 4.14: Summarised daily operational parameters for ABR-MFC feed samples (OLR 1)

	Temp °C	pH	EC µS/cm	TDS ppm	Salt ppm
Min	13.0	5.89	551	392	306
Max	21.5	7.16	837	593	675
Ave	18.2	6.52	697	495	436

Table 4.15: Summarised daily operational parameters for ABR-MFC product samples (OLR 1)

	Temp °C	pH	EC µS/cm	TDS ppm	Salt ppm
Min	13.7	5.37	488	346	357
Max	20.9	6.79	747	531	433
Ave	17.3	5.86	645	456	390

It is evident from Figure 4.13 that the feed and product COD is directly proportional to the COD removal. The COD in the feed and product remained relatively constant for the duration of OLR 1. The average COD concentration found in the ABR-MFC feed and product samples for OLR 1 was 10 979 mg/l (Table 4.16) and 5 666 mg/l (Table 4.17). The constant feed and product COD concentrations resulted in a relatively constant COD removal of 48.3% for OLR 1. Unfortunately,

there is no experimental data available for days 162 and 165 since the ABR-MFC system was moved to a new location during this time.

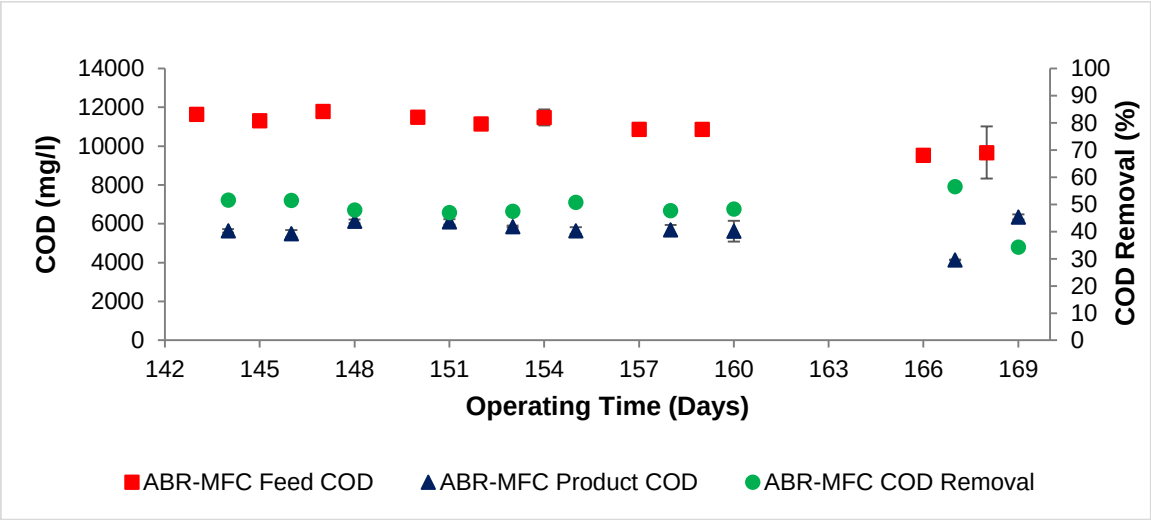

Figure 4.13: COD of ABR-MFC feed and product samples (and COD removal – ABR-MFC efficiency) for OLR 1

Table 4.16: Summarised system performance (OLR 1) – ABR-MFC feed samples

	COD mg/l	TSS mg/l	VSS mg/l	Turbidity NTU	FOG mg/l	NO_3^- mg/l	N mg/l	TP mg/l	OP mg/l
Min	9538	0.81	2.48	531	1280	1.70	0.38	1.30	17.35
Max	11783	3.32	4.48	1000	1280	5.95	1.34	1.65	20.35
Ave	10979	2.14	3.33	920	1280	3.43	0.78	1.52	18.55

Table 4.17: Summarised system performance (OLR 1) – ABR-MFC product samples

	COD mg/l	TSS mg/l	VSS mg/l	Turbidity NTU	FOG mg/l	NO_3^- mg/l	N mg/l	TP mg/l	OP mg/l
Min	4145	0.02	0.92	45	46	0.43	0.10	0.10	13.75
Max	6353	1.59	3.50	210	46	1.62	0.37	0.20	16.40
Ave	5666	0.32	1.76	85	46	0.83	0.19	0.13	15.05

The C:N:P ratio of the feed was adjusted to 150:0.05:0.02 by adding urea and KH_2PO_4 as sources of nitrogen and phosphorous, respectively. This adjustment thus caused an increase in NO_3^--N and TP from <0.38 mg/l (Table 4.3) and 0.2275 mg/l (Table 4.2) to an average of 3.43 mg/l and 1.52 mg/l (Table 4.16), respectively. However, after treatment with the ABR-MFC system the treated BDWW contained average NO_3^--N and TP concentrations of 0.83 mg/l and 0.19 mg/l, respectively (Table 4.17), thereby removing 76.75% NO_3-N and 91.31% TP. Increasing the C:N:P ratio of the BDWW used as feed in the ABR-MFC from 150:0.05:0.02 to 150:1.1:0.2 should

increase the COD removal of the ABR-MFC to a comparable removal efficiency (98 -100%) at an OLR of 1.0 kg COD/m^3.day (Phukingngam *et al*., 2011).

A possible explanation for the low COD removal achieved by the ABR-MFC when comparing the results to the removal efficiencies achieved by Phukingngam *et al*. (2011) could be that the amount of COD contained in the raw BDWW used in their study was much lower (i.e. 56 400 mg/l) than the COD concentration of the BDWW used in this study (i.e. 145 796 mg/l). The latter could account for the low COD removal efficiency achieved by the ABR-MFC at OLR 1.

The FOG of the ABR-MFC feed and product samples for OLR 1 was found to be an average of 1 280 mg/l (Table 4.16) and 46 mg/l (Table 4.17), respectively. The ABR-MFC thus removed 96.41% FOG (refer to section 4.3.2.1 for overall FOG removal explanation) which is comparable to the work of Phukingngam *et al*. (2011).

The TSS of the BDWW used in OLR 1 was reduced from an average of 2.14 mg/l (Table 4.16) to 0.32 mg/l (Table 4.17), thus removing 84.68% TSS. Low TSS removal efficiencies were achieved in other studies where BDWW were treated biologically. Silva and co-workers (2013) obtained TSS removal efficiencies of 30.43%, 38.46% and 32.84% at respective OLRs of 1.18, 1.23 and 1.29 kg COD/m^3.day when treating industrial BDWW using an anaerobic sequencing batch reactor (ASBR). Other studies have shown TSS removal efficiencies of 41.96% (1.29 kg COD/m^3.day) (Selma *et al*., 2010) and 32.43% (1.5 kg COD/m^3.day) (Bezerra *et al*., 2011) when treating BDWW using ASBRs.

The average VSS of the BDWW used in OLR 1 was reduced from 3.33 mg/l (Table 4.16) to 1.76 mg/l (Table 4.17), thus removing 46.76% of the VSS contained in the BDWW. The VSS removal achieved by the ABR-MFC can thus be comparable to the removal efficiencies of 53.23% (1.29 kg COD/m^3.day) (Selma *et al*., 2010) and 50.00% (1.50 kg COD/m^3.day) (Bezerra *et al*., 2011) achieved in other studies where biological treatment was applied to BDWW.

4.4.2.3. Effect of OLR 2 on ABR-MFC performance

This section reflects the findings of the second OLR (1.98 kg COD/m^3.day). The findings include information regarding the treatment efficiency of the hybrid ABR-MFC system. Refer to Appendix H (Tables H.4, H.5, H.6 and H.7) for summarised feed and product experimental data for OLR 2. The ABR-MFC was operated at an HRT of 10 days, for a total of 28 days.

The EC, TDS and salinity (Figures 4.6 and 4.7) of the ABR-MFC feed and product samples were found to be approximately similar. The ABR-MFC feed (Table 4.18) samples were 78 μS/cm,

56 mg/l, and 61 mg/l higher than the EC, TDS and salinity of the product (Table 4.19) which was found to be on average 854 µS/cm, 607 mg/l, and 544 mg/l, respectively for OLR 2.

The feed pH ranged from 5.32 to 7.82 (Table 4.18) while the pH of product samples ranged from 4.79 to 6.58 (Table 4.19). Nonetheless, the average feed and product pH (refer to Figure 4.1) was found to be 6.22 (Table 4.18) and 5.79 (Table 4.19), respectively for OLR 2.

Table 4.18: Summarised daily operational parameters for ABR-MFC feed samples (OLR 2)

	Temp °C	pH	EC µS/cm	TDS ppm	Salt ppm
Min	10.7	5.32	671	477	506
Max	21.3	7.82	1106	789	667
Ave	16.5	6.22	932	663	605

Table 4.19: Summarised daily operational parameters for ABR-MFC product samples (OLR 2)

	Temp °C	pH	EC µS/cm	TDS ppm	Salt ppm
Min	10.5	4.79	517	368	434
Max	20.9	6.58	1050	746	637
Ave	16.0	5.79	854	607	544

It is evident from Figure 4.14 that the feed COD is directly proportional to the COD removal for OLR 2. However, the feed COD and COD removal is indirectly proportional to the product COD. The average COD contained in the ABR-MFC feed and product samples was found to be 18 944 mg/l (Table 4.20) and 7 600 mg/l (Table 4.21), respectively. Although the feed COD did not remain constant for the duration of OLR 2, the product COD followed an indirectly proportional trend to the feed COD which resulted in an inconsistent COD removal which was 59.15% on average.

The variation in feed COD (Figure 4.14) can be attributed to a fresh BDWW batch (refer to Appendix H – Table H.1) obtained from the industrial partner that contained a visible layer of oil. It is therefore possible that more (or less) oil entered the ABR-MFC feed during the feed make-up process thereby causing a variation in feed concentration (Figure 4.14).

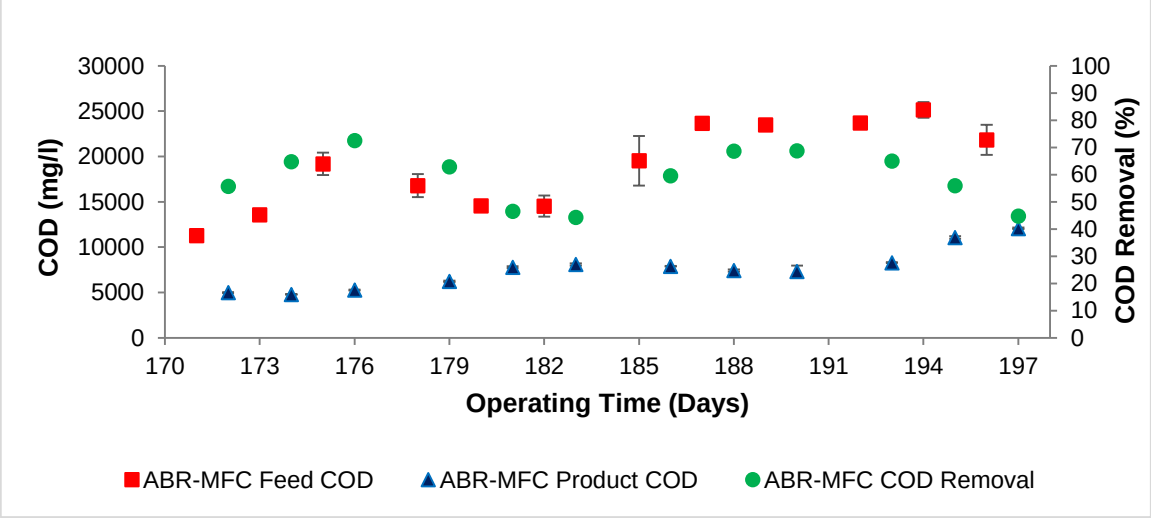

Figure 4.14: COD of ABR-MFC feed and product samples (and COD removal – ABR-MFC efficiency) for OLR 2

Table 4.20: Summarised system performance (OLR 2) – ABR-MFC feed samples

	COD mg/l	TSS mg/l	VSS mg/l	Turbidity NTU	FOG mg/l	NO_3^- mg/l	N mg/l	TP mg/l	OP mg/l
Min	11270	0.50	2.24	347	2673	1.22	0.28	1.10	21.90
Max	25140	9.80	10.88	1000	2673	12.15	2.74	2.95	25.30
Ave	18944	4.85	6.12	928	2673	6.76	1.53	1.80	23.49

Table 4.21: Summarised system performance (OLR 2) – ABR-MFC product samples

	COD mg/l	TSS mg/l	VSS mg/l	Turbidity NTU	FOG mg/l	NO_3^- mg/l	N mg/l	TP mg/l	OP mg/l
Min	4785	0.02	0.42	40	72	0.09	0.02	0.10	14.55
Max	12063	0.28	2.42	234	72	0.53	0.12	0.10	21.70
Ave	7600	0.12	1.73	100	72	0.22	0.05	0.10	17.20

The C:N:P ratio of the feed was adjusted to 150:0.05:0.01 by adding urea and KH_2PO_4. This adjustment caused an increase in average NO_3^--N and TP from <0.38 mg/l and 0.2275 mg/l (Table 4.3) to 6.76 mg/l and 1.80 mg/l (Table 4.20), respectively. However, after treatment with the ABR-MFC system the treated BDWW contained respective average NO_3^--N and TP concentrations of 0.22 mg/l and 0.10 mg/l (Table 4.21), thereby removing 95.71% NO_3-N and 93.70% TP.

The FOG of ABR-MFC feed and product samples for OLR 2 was found to be 2 673 mg/l (Table 4.20) and 72 mg/l (Table 4.21), respectively. The ABR-MFC thus removed 97.31% FOG (refer to section 4.3.2.1 for overall FOG removal explanation) which is comparable to the work of Phukingngam *et al*. (2011).

The average TSS of the BDWW used in OLR 2 was reduced from 4.85 mg/l (Table 4.20) to 0.12 mg/l (Table 4.21), thus removing 95.88% TSS. Low TSS removal efficiencies were achieved in other studies where BDWW were treated biologically. Silva and co-workers (2013) obtained TSS removal efficiencies of 14.29% and 35.52% at respective OLRs of 2.38 and 2.52 kg COD/m^3.day when treating industrial BDWW using an ASBR. Other studies have shown TSS removal efficiencies of 31.91% (2.44 kg COD/m^3.day) (Selma *et al*., 2010) and 9.76% (3.00 kg COD/m^3.day) (Bezerra *et al*., 2011) when treating BDWW using ASBRs.

The average VSS of the BDWW used in OLR 2 was reduced from 6.12 mg/l (Table 4.20) to 1.73 mg/l (Table 4.21), thus removing 61.08% of the VSS contained in the BDWW. Other studies achieved VSS removal efficiencies of 26.85% (2.44 kg COD/m^3.day) (Selma *et al*., 2010) and 20.00% (3.00 kg COD/m^3.day) (Bezerra *et al*., 2011) which is much lower than the 61.08% TSS removal achieved by the ABR-MFC during OLR 2.

4.4.2.4. Effect of OLR 3 on ABR-MFC performance

This section reflects the findings of the third OLR (3.46 kg COD/m^3.day). The findings include information regarding the treatment efficiency of the hybrid ABR-MFC system. Refer to Appendix H (Tables H.4, H.5, H.6 and H.7) for summarised feed and product experimental data for OLR 3. The ABR-MFC operated at an HRT of 10 days, for a period of 28 days.

The EC, TDS and salinity (Figures 4.6 and 4.7) of the ABR-MFC feed and product samples was found to fall within the same range. However, unlike in OLRs 1 and 2, the product (Table 4.23) EC, TDS and salinity was 149 μS/cm, 95 mg/l, and 78 mg/l, respectively higher than the feed (Table 4.22) samples which was found to be an average of 1 112 μS/cm, 789 mg/l, and 641 mg/l, respectively for OLR 3.

The feed pH ranged from 4.74 to 7.08 (Table 4.22) while the pH of product samples ranged from 4.17 to 5.66 (Table 4.23). Nonetheless, the average feed and product pH (refer to Figure 4.1) was found to be 6.38 (Table 4.22) and 5.01 (Table 4.23), respectively for OLR 3.

It is evident from Figure 4.15 that the feed and product COD is directly proportional to the COD removal achieved by the ABR-MFC for OLR 3. The COD in the feed and product remained relatively constant for the duration of OLR 3. The constant feed (33 356 mg/l (Table 4.24)) and product (11 809 mg/l (Table 4.25)) COD resulted in a constant COD removal of 64.55% for the duration of OLR 3.

Table 4.22: Summarised daily operational parameters for ABR-MFC feed samples (OLR 3)

	Temp °C	pH	EC µS/cm	TDS ppm	Salt ppm
Min	15.5	4.74	564	404	318
Max	24.0	7.08	1789	1270	1045
Ave	19.2	6.38	1112	789	641

Table 4.23: Summarised daily operational parameters for ABR-MFC product samples (OLR 3)

	Temp °C	pH	EC µS/cm	TDS ppm	Salt ppm
Min	14.9	4.17	633	451	353
Max	23.3	5.66	1866	1215	996
Ave	18.4	5.01	1261	884	719

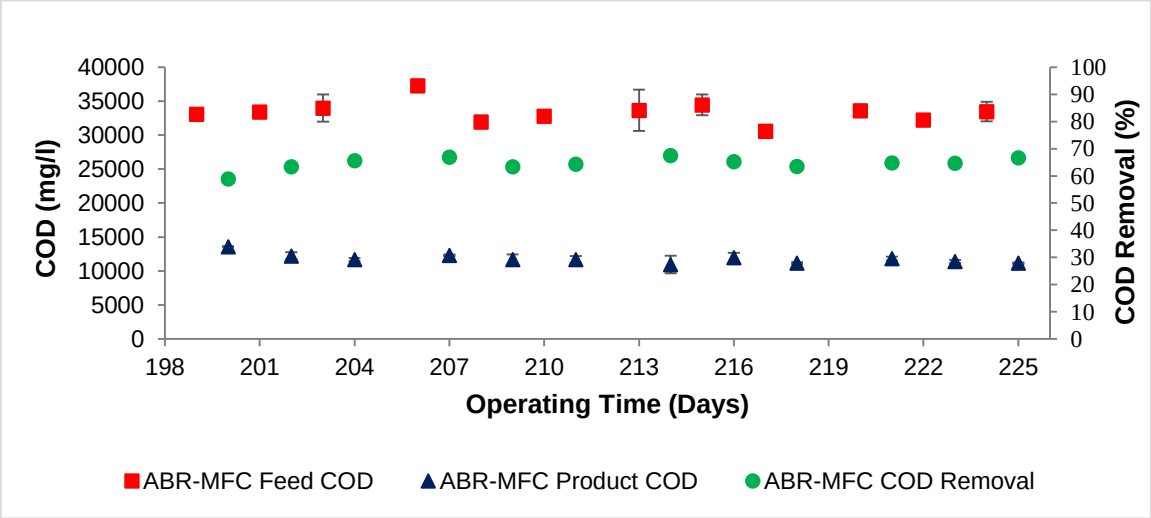

Figure 4.15: COD of ABR-MFC feed and product samples (and COD removal – ABR-MFC efficiency) for OLR 3

The C:N:P ratio of the feed was adjusted to 150:0.03:0.01 by adding urea and KH_2PO_4. This adjustment caused an increase in NO_3^--N and TP from <0.38 mg/l and 0.2275 mg/l (Table 4.3) to an average of 7.31 mg/l and 3.01 mg/l (Table 4.24), respectively. However, after treatment with the ABR-MFC system the treated BDWW contained average NO_3^--N and TP concentrations of 0.64 mg/l and 0.33 mg/l, respectively (Table 4.25), thereby removing 89.18% NO_3-N and 89.06% TP.

The FOG of ABR-MFC feed and product samples for OLR 3 was found to be 269 540 mg/l (Table 4.24) and 100 mg/l (Table 4.25), respectively. The ABR-MFC thus removed 99.96% FOG

(refer to section 4.3.2.1 for overall FOG removal explanation) which is comparable to the work of Phukingngam *et al*. (2011).

Table 4.24: Summarised system performance (OLR 3) – ABR-MFC feed samples

	COD mg/l	TSS mg/l	VSS mg/l	Turbidity NTU	FOG mg/l	NO_3^- mg/l	N mg/l	TP mg/l	OP mg/l
Min	30563	2.03	3.57	1000	269540	4.80	1.08	2.00	18.25
Max	37230	64.30	65.85	1000	269540	11.45	2.59	4.05	25.00
Ave	33356	17.40	19.02	1000	269540	7.31	1.65	3.01	23.31

Table 4.25: Summarised system performance (OLR 3) – ABR-MFC product samples

	COD mg/l	TSS mg/l	VSS mg/l	Turbidity NTU	FOG mg/l	NO_3^- mg/l	N mg/l	TP mg/l	OP mg/l
Min	10958	0.03	0.62	130	100	0.40	0.00	0.10	22.25
Max	13590	0.37	3.63	452	100	1.24	0.28	0.50	25.00
Ave	11809	0.13	2.25	247	100	0.64	0.12	0.33	23.98

The average TSS of the BDWW used in OLR 3 was reduced from 17.40 mg/l (Table 4.24) to 0.13 mg/l (Table 4.25), thus removing 98.55% of the TSS contained in the BDWW. Low TSS removal efficiencies were achieved in other studies where BDWW were treated biologically. Silva *et al*. (2013) obtained TSS removal efficiencies of 21.50% and 23.31% at respective OLRs of 3.71 and 3.77 kg COD/m^3.day when treating industrial BDWW using an ASBR. Other studies have shown TSS removal efficiencies of 9.92% (3.82 kg COD/m^3.day) (Selma *et al*., 2010) and 34.48% (4.50 kg COD/m^3.day) (Bezerra *et al*., 2011) when treating BDWW using ASBRs.

The average VSS of the BDWW used in OLR 3 was reduced from 19.02 mg/l (Table 4.24) to 2.25 mg/l (Table 4.25), thus removing 75.25% of the VSS contained in the BDWW. Other studies reported VSS removal efficiencies of 22.77% (3.82 kg COD/m^3.day) (Selma *et al*., 2010) and 21.95% (4.50 kg COD/m^3.day) (Bezerra *et al*., 2011) when treating BDWW applying biological treatment. The ABR-MFC achieved a much higher (i.e. 75.25%) TSS removal efficiency compared to the latter studies.

4.4.4. Biofilm formation and gas production

The formation of a biofilm layer on the surface of the wastewater in the ABR-MFC was first observed on day 3 of operation. The thickness of the biofilm layer observed grew in size until day 116 when the ABR had to be opened due to clogging of the fat trap. Nonetheless, the thickness

of the biofilm layer remained consistent after day 116 until day 144 when MFC technology was installed into the existing ABR. There was no observable oil (FOG removal = 97.89%) or sludge washout in the ABR-MFC product.

Each compartment developed a unique layer of sludge which was observed to decrease in thickness (representing a stair-like structure when observing the layer from the front-view of the ABR) as the wastewater moved through the compartments from compartment 1 (C1) to compartment 6 (C6). It is speculated that the four degradation stages (i.e. hydrolysis, acidogenesis, acetogenesis, and methanogenesis) of anaerobic digestion (refer to Section 2.5.1 for a complete description of the four degradation stages) occur in the different compartments of the ABR-MFC. This statement is supported by the work of Barber and Stuckey (1999) who reported that acidogenic bacteria dominates in the front compartments (where substrate concentrations are higher) while methanogenic bacteria dominates towards the end of the reactor. Photographic evidence of the development of different microbial populations (i.e. microorganisms and algae) in the separate compartments of the ABR can be observed in Tables 4.26 and 4.27. When referring to Table 4.26 (day 116) and the literature consulted (Barber & Stuckey, 1999) it is speculated that compartment 2 (C2) and compartment 3 (C3) are similar, while compartment 4 (C4) and compartment 5 (C5) are similar. It is speculated that hydrolysis occurs in C1, acidogenesis occurs in C2 and C3, acetogenesis occurs in C4 and C5, and methanogenesis occurs in C6.

Pink algae were observed on the sides of the ABR on day 35. According to Gerardi (2003), methanogenic bacteria can be pink. The formation of bubbles within and under the biofilm layer was observed from day 15 to 144 (implementation of MFC technology) as depicted in the figures in Tables 4.26 and 4.27. Although the bubbles grew larger over time and varied in shape they never burst. It was therefore concluded that there was to some extent of gas formation. It is however recommended that the gas be captured in future and analysed for methane and/or hydrogen. It is therefore possible that the ABR-MFC could generate a second source of energy as a by-product.

The ABR did not produce an unpleasant odour. It can therefore be said that the biogas mainly contained methane which is odourless (Gerardi, 2003). A flammability test was performed on the biogas on day 200 (day 65 since installation of MFC technology). During the flammability test a blue flame was observed, which burnt for a few seconds before going out. It is therefore recommended that the biogas produced is captured and analysed.

Table 4.26: Top view of the ABR after removing the ABR lid

Day	ABR-MFC
116	
133	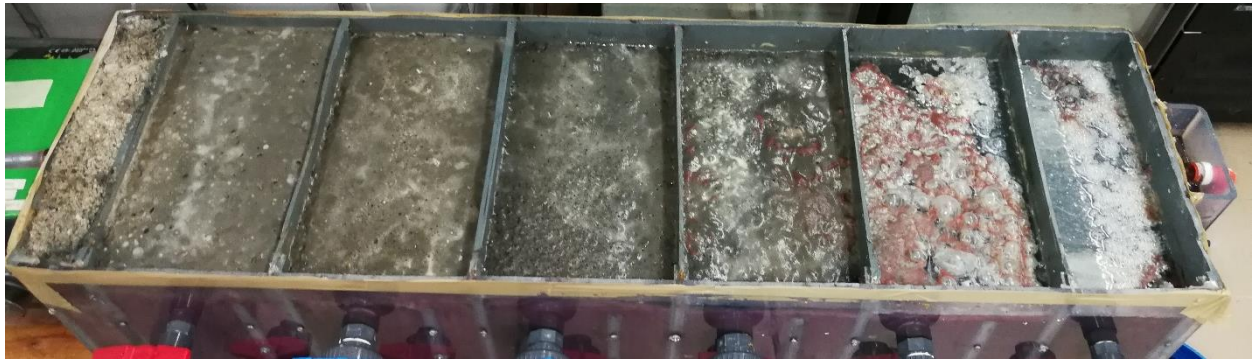

Table 4.27: Top view of individual ABR-MFC compartments after removing the ABR lid

Day 116					
C1 and fat trap	C2	C3	C4	C5	C6
					
Day 133					
C1 and fat trap	**C2**	**C3**	**C4**	**C5**	**C6**
					

4.5. Chapter summary

Although it has been proven that the ABR is capable of effectively treating a wide range of wastewaters with varying strength (0.45 – 1 000 g/l COD) at OLRs ranging from 0.40 to 28.00 kg COD/m^3.day (Barber & Stuckey, 1999), the average COD removal obtained during this study was 57.33%. Nonetheless, the ABR-MFC achieved a 10.85% higher COD removal with OLR 2 than with OLR 1. In OLR 3, the ABR-MFC achieved a 16.25% higher COD removal than with OLR 1. From Table 4.28 it is evident that OLR 3 was thus the most efficient when comparing the 3 OLRs regarding COD removal efficiency.

Table 4.28: Summarised ABR-MFC performance

	Parameter	Units	OLR 1	OLR 2	OLR 3
ABR-MFC	OLR	kg COD/m^3.day	1.15	1.98	3.46
	COD Removal	%	48.30	59.15	64.55
	FOG Removal	%	96.41	97.31	99.96
	TSS Removal	%	84.68	95.88	98.55
	VSS Removal	%	46.76	61.08	75.25
	NO_3-N Removal	%	76.75	95.71	89.18
	TP Removal	%	91.31	93.70	89.06
Feed	C:N:P	-	150:0.05:0.02	150:0.05:0.01	150:0.03:0.01
	COD	mg/l	10979	18944	33356
	pH	-	6.52	6.22	6.38
	TDS	ppm	495.00	663.00	789.00
	Salt	ppm	436.00	605.00	641.00
	NO^3-N	mg/l	3.43	6.76	7.31
	TP	mg/l	1.52	1.80	3.01
Product	COD	mg/l	5665	7600	11809
	pH	-	5.86	5.79	4.01
	EC	µS/cm	645.00	854.00	1261.00
	TDS	ppm	456.00	607.00	884.00
	Salt	ppm	390.00	544.00	719.00
	NO^3-N	mg/l	0.83	0.22	0.64
	TP	mg/l	0.13	0.10	0.33

The FOG removal achieved by the ABR-MFC increased as the OLR of the BDWW increased from OLR 1 (96.41%) to OLR 2 (97.31%) to OLR 3 (99.96%). OLR 3 was thus the most efficient when comparing the 3 OLRs for FOG removal efficiency. The same trend was followed for the TSS and VSS removal achieved by the ABR-MFC which increased as the OLR increased from OLR 1

(84.68% and 46.76%) to OLR 2 (95.88% and 61.08%) to OLR 3 (98.55% and 75.25%). OLR 3 was thus the most efficient when comparing the 3 OLRs for TSS and VSS removal efficiency.

The ABR-MFC achieved a 76.75% NO_3-N removal for OLR 1, followed by a 95.71% removal for OLR 2 and an 89.18% removal for OLR 3. The most NO_3-N was removed during OLR 2. The same trend follows for TP removal achieved by the ABR-MFC which was 91.31% for OLR 1, 93.70% for OLR 2 (highest TP removal) and 89.06% for OLR 3.

It is therefore evident from the experimental findings (Table 4.28) that OLR 3 is the most effective OLR to treat BDWW without the need for a pre-treatment step and the use of a recycle stream. However, more research should be conducted to increase system efficiency regarding the COD removal achieved by the lab-scale ABR-MFC system. It is therefore recommended to further increase the OLR steadily thereby finally feeding the ABR-MFC with full strength BDWW (i.e. average COD 145 796 mg/l).

CHAPTER FIVE

RESULTS AND DISCUSSION OF POWER GENERATION BY THE ABR-MFC SYSTEM

CHAPTER FIVE:
RESULTS AND DISCUSSION OF POWER GENERATION BY THE ABR-MFC SYSTEM

5.1. Introduction

The possibility of generating power using a hybrid anaerobic baffled reactor microbial fuel cell (ABR-MFC) was investigated at laboratory scale. The substrate (i.e. industrial biodiesel wastewater (BDWW)) was diluted and fed to the ABR-MFC as an energy source for the microorganisms. An existing 6-compartment ABR was modified into a hybrid ABR-MFC by transforming each compartment of the ABR into an MFC cell. Each compartment contained a carbon fibre brush anode electrode and a floating carbon air-cathode. All cells were connected in parallel and the external circuit was completed with a 1 000 Ω resistor (i.e. colour coded tubular wire wound) using insulated copper wire. This chapter provides a description of the results obtained during the current study thereby evaluating the maximum power output generated by the ABR-MFC system.

This chapter reflects the findings of the ABR-MFC power generation for the duration of the last 82 days (since day 144 of ABR-MFC operation) of the experimental study. The findings include information regarding the power generation of the ABR-MFC during this time. Refer to Appendix I (Tables I.1, I.2, I.3, I.4 and I.5) for summarised experimental data on electrical current (Table I.1), potential difference (Table I.2), power density (PD) (normalised to anode chamber volume (ACV) (Table I.3)), PD (normalised to cathode surface area (CSA) (Table I.4)) and PD (normalised to anode surface area (ASA) (Table I.5)) for the ABR-MFC and individual compartments.

Power generation (i.e. voltage and current) was measured daily. The results obtained for the generation of power (and chemical oxygen demand (COD) removal) have been plotted in Figure 5.1. The electrical current and voltage obtained by the ABR-MFC have been plotted in Figures 5.2 and 5.3 (refer to Appendix J (Figures J.8 and J.9) for figures not displayed in this chapter. This includes the PD of individual ABR-MFC compartments (experimental data can be obtained in Appendix I (Tables I.1, I.2, I.3, I.4 and I.5))).

The PD is normalised to the ACV, CSA and ASA in order to assess MFC power generation specific to system architecture (Logan, 2008). The latter eases comparison between different MFC systems. The amount of microorganisms that are contained in the anode chamber (i.e. ACV) as well as the surface area (i.e. CSA and ASA) available for microorganisms to grow on directly affects the amount of power generated by the system (Logan, 2008). The PD results achieved in

this study are presented in three possible ways (i.e. normalised to ACV, CSA and ASA) since PD in literature is inconsistently reported using these three representations. Refer to section 2.8.5 for a more complete explanation on PD.

Polarisation curves portray the performance of an MFC system by illustrating how well the system maintains voltage as a function of current generation (Logan, 2008). Polarisation and power density curves for each OLR (i.e. 1.15, 1.98 and 3.46 kg COD/m^3.day) were plotted in Figure 5.5. These results were then used to evaluate the maximum PD of the ABR-MFC system.

Experimental data for system polarisation, performed for each organic loading rate (OLR) under investigation (i.e. 1.15, 1.98 and 3.46 kg COD/m^3.day), is indicated in Appendix I (Tables I.6, I.7 and I.8). Polarisation data has been plotted in Figures 5.5 (experimental data can be found in Appendix I (Tables I.6, I.7 and I.8)).

5.2. Power generation (ABR-MFC power generation performance)

Figure 5.1 depicts the PD (normalised to ACV and CSA) and feed concentration (i.e. COD) of the ABR-MFC for the three OLRs (i.e. 1.15, 1.98 and 3.46 kg COD/m^3.day) under investigation. It is evident from Figure 5.1 that the ABR-MFC PD (normalised to ACV) is directly proportional to the PD (normalised to CSA) and thus directly proportional to the feed COD concentration. There is no noticeable relationship between PD and COD removal for the ABR-MFC.

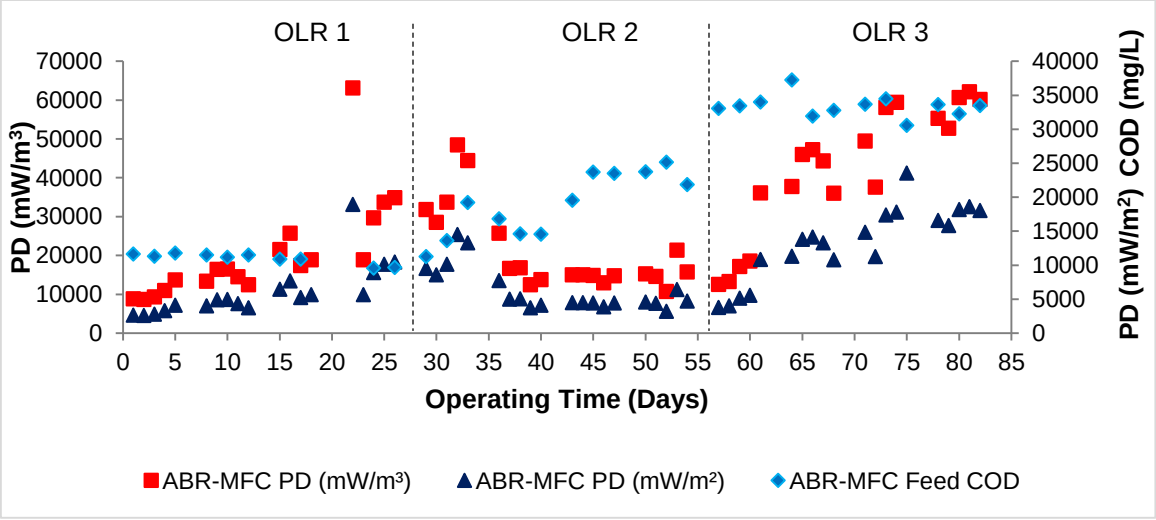

Figure 5.1: ABR-MFC PD (normalised to ACV and CSA) and feed concentration (i.e. COD)

There is no power generation data available between days 18 and 22 since the ABR-MFC system was moved to a new location during this time. Refer to Appendix I for electrical current (Table I.1) and voltage generation (Table I.2) experimental data and Figures 5.2 and 5.3 for electrical current and voltage graphs.

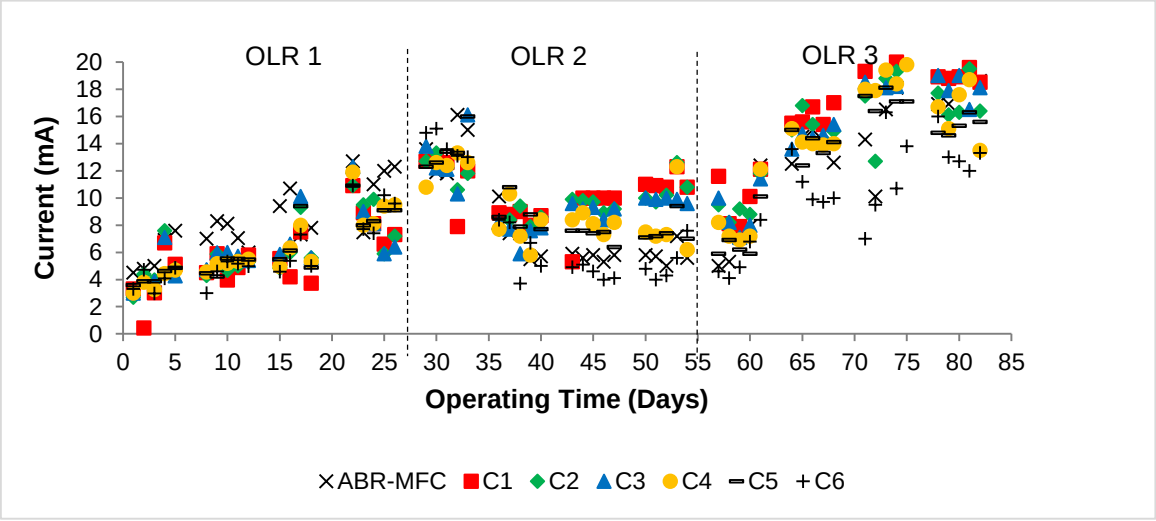

Figure 5.2: Electrical current generation of ABR-MFC and individual compartments

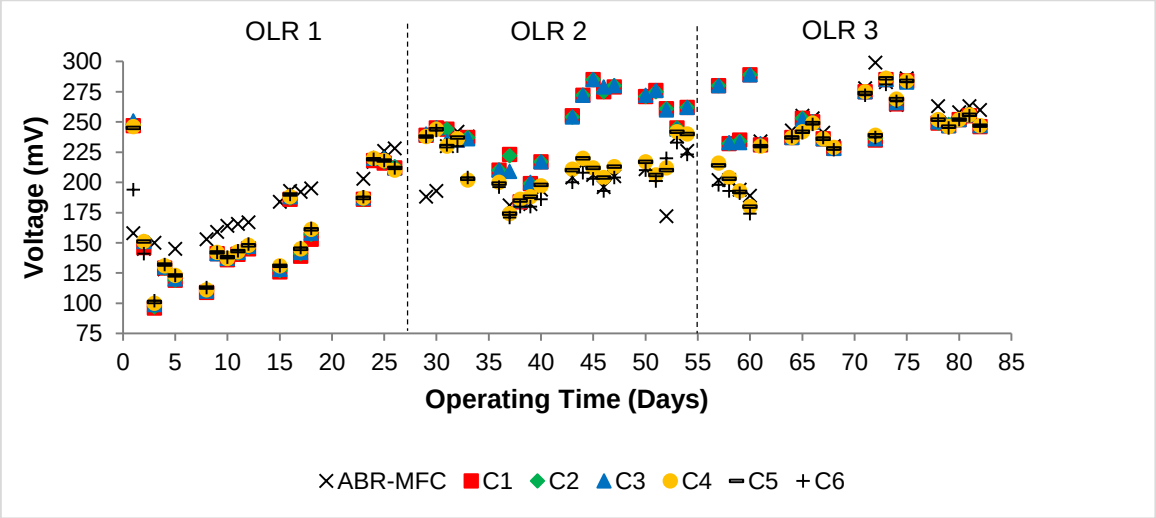

Figure 5.3: Voltage (potential difference) of ABR-MFC and individual compartments

The PD increases between OLR 1 and OLR 2 (Figure 5.1) where a direct relationship between PD and COD removal is observed. This spike observed (Figure 5.1) in PD between days 22 to day 33 could be attributed to vigorous mixing within the ABR-MFC system due to moving the

system to a new location during days 18 to 22. It can thus be said that vigorous mixing increases ABR-MFC PD due to better wastewater-microorganism contact since the performance of the ABR-MFC system is largely dependent on the hydrodynamic behaviour of the treatment system (Barber & Stuckey, 1999).

Logan (2008) states that the anaerobic chamber can be mixed to maintain homogenous conditions within the reactor. It is therefore recommended to include a recycle stream which should increase mixing within the ABR-MFC system since sufficient mixing should be ensured in order to obtain better wastewater-microorganism contact. The latter controls mass transfer and thus the ABR-MFC performance (Barber & Stuckey, 1999).

The average system PD of the 3 OLRs of the ABR-MFC was found to be 44 131 mW/m^3 (ACV) (Table 5.1) [13 225 mW/m^2 (CSA) (Table 5.2) and 6.75 mW/m^3 (ASA) (Table 5.3)] at an average COD feed concentration of 21 688 mg/l (Table 4.12). The system PD achieved by the ABR-MFC, 44 131 mW/m^3 (ACV), can be compared to the work of Cha *et al*. (2010) and You *et al*. (2007) who achieved respective PDs of 16 700 mW/m^3 and 50 200 mW/m^3. Ghangrekar and Shinde (2007) achieved a PD of 6.45 mW/m^2 which is comparable to the PD achieved by the ABR-MFC, 6.75 mW/m^2 (ASA) (Table 5.3).

Table 5.1: ABR-MFC summarised PD (normalised to ACV) for OLRs 1 to 3

	PD_{ACV}^{C1}	PD_{ACV}^{C2}	PD_{ACV}^{C3}	PD_{ACV}^{C4}	PD_{ACV}^{C5}	PD_{ACV}^{C6}	$PD_{ACV}^{ABR-MFC}$
				mW/m^3			
Min	129 010	129 749	111 450	101 571	75 239	81 750	12 554
Max	398 078	426 130	404 193	440 703	366 745	473 196	78 565
Ave	286 661	260 979	260 353	279 959	234 800	263 226	44 131

Table 5.2: ABR-MFC summarised PD (normalised to CSA) for OLRs 1 to 3

	PD_{CSA}^{C1}	PD_{CSA}^{C2}	PD_{CSA}^{C3}	PD_{CSA}^{C4}	PD_{CSA}^{C5}	PD_{CSA}^{C6}	$PD_{CSA}^{ABR-MFC}$
				mW/m^2			
Min	38 663	38 885	33 401	30 435	22 548	24 487	3 762
Max	119 299	127 708	121 136	132 056	109 907	141 739	23 543
Ave	85 909	78 214	78 027	83 889	70 365	78 846	13 225

Table 5.3: ABR-MFC summarised PD (normalised to ASA) for OLR 1 to 3

	PD_{ASA}^{C1}	PD_{ASA}^{C2}	PD_{ASA}^{C3}	PD_{ASA}^{C4}	PD_{ASA}^{C5}	PD_{ASA}^{C6}	$PD_{ASA}^{ABR-MFC}$
				mW/m^2			
Min	1.13	6.75	6.69	5.74	6.87	5.31	2.03
Max	100.48	109.59	105.23	98.63	90.80	80.34	18.48
Ave	45.31	44.11	44.01	39.55	38.16	30.98	6.75

From Tables 5.1, 5.2 and 5.3 it is evident that the highest PD can be estimated by normalising the PD to the ACV. The highest average PD was thus obtained in compartment 1 (C1), 286 661 mW/m^3 (ACV). However, the maximum PD was obtained in compartment 4 (C4), 440 703 mW/m^3 (ACV) while the ABR-MFC system PD (ACV) fluctuated between 12 554 mW/m^3 and 78 565 mW/m^3. Graphical representation of the PD (normalised to ACV and CSA) of the ABR-MFC and individual compartments can be found in Figures 5.2 and 5.3.

5.2.1. Effect of OLR 1 on power generation

This section reflects on the findings of ABR-MFC power generation for the first OLR (1.15 kg COD/m^3.day) after system stabilisation. Refer to Appendix I (Tables I.1, I.2, I.3, I.4 and I.5) for summarised power generation data for OLR 1. The ABR-MFC operated at an OLR of 1.15 kg COD/m^3.day and an HRT of 10 days during OLR 1.

The average system PD of the ABR-MFC was found to be 20 442 mW/m^3 (ACV) (Table 5.4), 6 126 mW/m^2 (CSA) (Table 5.5) and 4.81 mW/m^2 (ASA) (Table 5.6) at a feed concentration of 10 979 mg COD/l (Table 4.16) for OLR 1. These results are comparable to the work of Jang and co-workers (2004) who achieved 1.30 mW/m^2 (ASA) and Ghangrekar and Shinde (2007) who achieved 10.13, 6.45 and 4.66 mW/m^2 (ASA). The PD achieved in this study also compares well with the PDs reported by Logan *et al*. (2007) (29 000 mW/m^3), Tugtas *et al*. (2011) (12 000 mW/m^3) and Mardanpour *et al*. (2012) (20 200 mW/m^3) who used modified (i.e. addition of 1 g/l acetate in 50 mM phosphate buffer and vitamins) primary clarifier overflow, acetate containing synthetic wastewater and dairy wastewater as respective substrates.

It is evident from Tables 5.4 and 5.5 that compartment 6 (C6) achieved the highest PD, 442 554 mW/m^3 (ACV) and 132 561 mW/m^2 (CSA). However, from Table 5.6 it can be seen that compartment 3 (C3) achieved the highest PD (20.56 mW/m^2) when normalising the PD to the ASA.

Table 5.4: ABR-MFC summarised PD (normalised to ACV) for OLR 1

	PD_{ACV}^{C1}	PD_{ACV}^{C2}	PD_{ACV}^{C3}	PD_{ACV}^{C4}	PD_{ACV}^{C5}	PD_{ACV}^{C6}	$PD_{ACV}^{ABR-MFC}$
				mW/m^3			
Min	4464	26264	25678	25628	27763	31297	8651
Max	302222	296620	329803	367457	304258	442554	63145
Ave	72658	78321	78971	91503	82365	114513	20442

Table 5.5: ABR-MFC summarised PD (normalised to CSA) for OLR 1

	PD_{CSA}^{C1}	PD_{CSA}^{C2}	PD_{CSA}^{C3}	PD_{CSA}^{C4}	PD_{CSA}^{C5}	PD_{CSA}^{C6}	$PD_{CSA}^{ABR-MFC}$
				mW/m²			
Min	1338	7871	7696	7679	8320	9375	2592
Max	90572	88895	98841	110108	91180	132561	18922
Ave	21775	23366	23667	27419	24683	34301	6126

Table 5.6: ABR-MFC summarised PD (normalised to anode ASA) for OLR 1

	PD_{ASA}^{C1}	PD_{ASA}^{C2}	PD_{ASA}^{C3}	PD_{ASA}^{C4}	PD_{ASA}^{C5}	PD_{ASA}^{C6}	$PD_{ASA}^{ABR-MFC}$
				mW/m²			
Min	1.13	6.75	6.69	5.74	6.87	5.31	2.03
Max	76.28	76.28	85.87	82.24	75.33	75.14	14.85
Ave	18.34	20.05	20.56	20.48	20.39	19.44	4.81

5.2.2. Effect of OLR 2 on power generation

This section reflects on the findings of ABR-MFC power generation for OLR 2 (1.98 kg COD/m^3.day) after system stabilisation. The findings include information regarding the coulombic efficiency of the hybrid ABR-MFC system. Refer to Appendix I (Tables I.1, I.2, I.3, I.4 and I.5) for summarised power generation data for OLR 2. The ABR-MFC operated at an OLR of 1.98 kg COD/m^3.day and an HRT of 10 days during OLR 2.

The average PD of the ABR-MFC was found to be 21 114 mW/m^3 (ACV) (Table 5.7), 6 327 mW/m^2 (CSA) (Table 5.8) and 4.97 mW/m^2 (ASA) (Table 5.9) at a feed concentration of 18 944 mg COD/l (Table 4.20) for OLR 2. The volumetric PD (ACV) achieved during OLR 2 is significantly higher than the volumetric PDs reported by Logan *et al*. (2007) (2 300 mW/m^3), Tugtas *et al*. (2011) (4 100 mW/m^3), Wang *et al*. (2011) (3 150 mW/m^3), A. Wang *et al*. (2012) (1 000 mW/m^3), Liu *et al*. (2011) (2 340 mW/m^3), and Pasupuleti *et al*. (2015) (2 106 mW/m^3). Logan *et al*. (2007) proved that high PDs are attributed to the high surface areas and porous structures of carbon fibre brush anodes. Tugtas *et al*. (2011) demonstrated that spunbonded olefin sheets is a cost-effective alternative to polytetrafluoroethylene (PTFE) coating and can be used as a diffusion layer in air-cathode MFCs. Wang *et al*. (2011) and A. Wang *et al*. (2012) combined an MFC with a membrane bioreactor (MBR) for simultaneous wastewater treatment and energy recovery. Liu *et al*. (2011) concluded that MFCs can be integrated with the activated sludge process to generate electricity. Pasupuleti *et al*. (2015) concluded that continuous power generation can exist when employing a stack of MFCs for wastewater treatment thereby reducing the external power consumption of the treatment unit.

It is evident from Tables 5.7 and 5.8 that C6 achieved the highest PD, 379 079 mW/m^3 (ACV) and 113 548 mW/m^2 (CSA). However, from Table 5.9 it can be seen that compartment 2 (C2) achieved the highest average PD (43.97 mW/m^2) when normalising the PD to the ASA.

Table 5.7: ABR-MFC summarised PD (normalised to ACV) for OLR 2

	PD_{ACV}^{C1}	PD_{ACV}^{C2}	PD_{ACV}^{C3}	PD_{ACV}^{C4}	PD_{ACV}^{C5}	PD_{ACV}^{C6}	$PD_{ACV}^{ABR-MFC}$
				mW/m^3			
Min	93917	107221	73534	85457	96578	68805	10690
Max	219626	222238	255979	245995	230110	379079	48430
Ave	173903	170958	163312	154408	141614	166277	21114

Table 5.8: ABR-MFC summarised PD (normalised to CSA) for OLR 2

	PD_{CSA}^{C1}	PD_{CSA}^{C2}	PD_{CSA}^{C3}	PD_{CSA}^{C4}	PD_{CSA}^{C5}	PD_{CSA}^{C6}	$PD_{CSA}^{ABR-MFC}$
				mW/m^2			
Min	28146	32134	22038	25607	28943	20610	3203
Max	65819	66603	76716	73712	68960	113548	14513
Ave	52117	51235	48944	46268	42439	49806	6327

Table 5.9: ABR-MFC summarised PD (normalised to ASA) for OLR 2

	PD_{ASA}^{C1}	PD_{ASA}^{C2}	PD_{ASA}^{C3}	PD_{ASA}^{C4}	PD_{ASA}^{C5}	PD_{ASA}^{C6}	$PD_{ASA}^{ABR-MFC}$
				mW/m^2			
Min	23.71	27.58	19.15	19.13	23.91	11.68	2.51
Max	55.44	57.16	66.65	55.06	56.97	64.36	11.39
Ave	43.90	43.97	42.52	34.56	35.06	28.23	4.97

Compartmental PDs doubled from OLR 1 to OLR 2 when comparing the average PD (ASA) (Tables 5.6 and 5.9) of the ABR-MFC. It can thus be said that an increase in OLR results in increased power generation.

5.2.3. Effect of OLR 3 on power generation

This section reflects on the findings of ABR-MFC power generation for OLR 3 (3.46 kg COD/m^3.day) after system stabilisation. The findings include information regarding the coulombic efficiency of the hybrid ABR-MFC system. Refer to Appendix I (Tables I.1, I.2, I.3, I.4 and I.5) for summarised power generation data for OLR 3. The ABR-MFC operated at an OLR of 3.46 kg COD/m^3.day and an HRT of 10 days during OLR 3.

The average PD of the ABR-MFC was found to be 44 131 mW/m^3 (ACV) (Table 5.10), 13 225 mW/m^2 (CSA) (Table 5.11) and 10.38 mW/m^2 (ASA) (Table 5.12) at a feed concentration

of 33 356 mg COD/l (Table 4.24) for OLR 3. The volumetric PD (ACV) achieved in OLR 3 is comparable to the PD achieved by You *et al*. (2007) who attained a PD of 50 200 mW/m^3 using a graphite granule membrane-less tubular air-cathode MFC.

It is evident from Tables 5.10 and 5.11 that C6 achieved the highest PD, 473 196 mW/m^3 (ACV) and 141 739 mW/m^2 (CSA). However, from Table 5.12 it can be seen that C1 achieved the highest PD (72.36 mW/m^2) when normalising the PD to the ASA.

Table 5.10: ABR-MFC summarised PD (normalised to ACV) for OLR 3

	PD_{ACV}^{C1}	PD_{ACV}^{C2}	PD_{ACV}^{C3}	PD_{ACV}^{C4}	PD_{ACV}^{C5}	PD_{ACV}^{C6}	$PD_{ACV}^{ABR-MFC}$
				mW/m^3			
Min	129010	129749	111450	101571	75239	81750	12554
Max	398078	426130	404193	440703	366745	473196	78565
Ave	286661	260979	260353	279959	234800	263226	44131

Table 5.11: ABR-MFC summarised PD (normalised to CSA) for OLR 3

	PD_{CSA}^{C1}	PD_{CSA}^{C2}	PD_{CSA}^{C3}	PD_{CSA}^{C4}	PD_{CSA}^{C5}	PD_{CSA}^{C6}	$PD_{CSA}^{ABR-MFC}$
				mW/m^2			
Min	38663	38885	33401	30435	22548	24487	3762
Max	119299	127708	121136	132056	109907	141739	23543
Ave	85909	78214	78027	83889	70365	78846	13225

Table 5.12: ABR-MFC summarised PD (normalised to ASA) for OLR 3

	PD_{ASA}^{C1}	PD_{ASA}^{C2}	PD_{ASA}^{C3}	PD_{ASA}^{C4}	PD_{ASA}^{C5}	PD_{ASA}^{C6}	$PD_{ASA}^{ABR-MFC}$
				mW/m^2			
Min	32.56	33.37	29.02	22.73	18.63	13.88	2.95
Max	100.48	109.59	105.23	98.63	90.80	80.34	18.48
Ave	72.36	67.12	67.78	62.66	58.13	44.69	10.38

Compartmental PDs tripled from OLR 1 to OLR 3 when comparing the average PD (ASA) (Tables 5.6 and 5.12) of the ABR-MFC. It can thus be said that an increase in OLR results in increased power generation.

5.3. ABR-MFC performance

Polarisation and PD curves were obtained by initially applying different circuit resistances (i.e. 0 Ω to 10 000 Ω) to the ABR-MFC in 15-minute intervals and recording the corresponding potential difference (i.e. voltage) of the system which is illustrated as ABR-MFC voltage as a function of external resistance in the curve depicted in Figure 5.4. The respective curves (Figure 5.4) for

OLR 1, 2 and 3 follows the same trend as the typical external resistance versus MFC voltage curve for an MFC which shows a sharp increase in cell voltage followed by a stable increase as the corresponding resistance is increased (Logan, 2008).

System polarisation for OLR 1, 2 and 3 were performed on days 24, 52 and 80 of the ABR-MFCs operation (refer to Appendix I (Tables I.6, I.7 and I.8) for polarisation data of OLR 1, 2 and 3). The polarisation information was obtained after leaving the system in open circuit mode (OCM) overnight thereby achieving a stable MFC under steady-state conditions as described by (Logan, 2008).

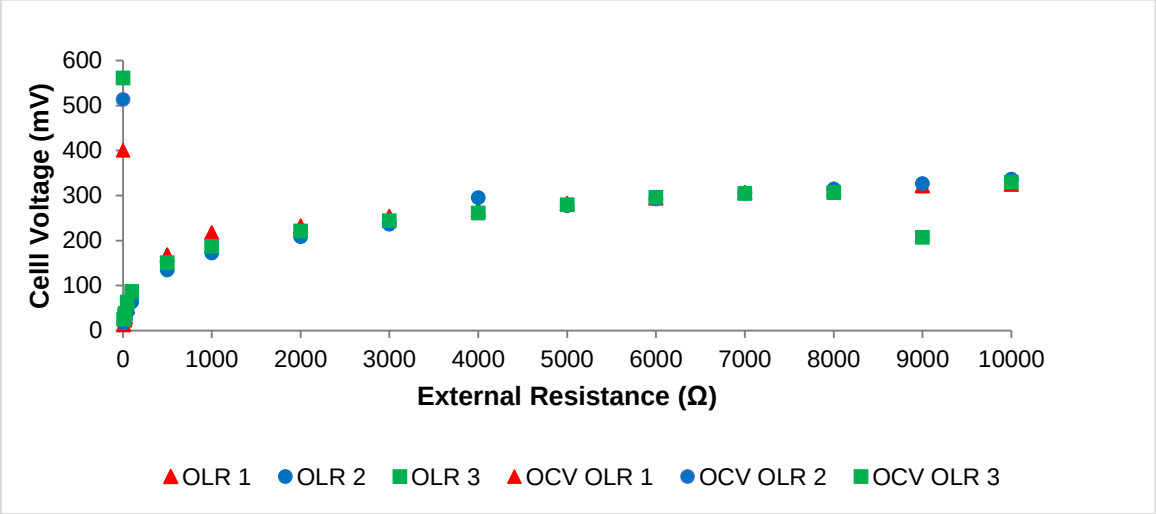

Figure 5.4: External resistance vs. ABR-MFC voltage (OLR 1 – 3)

The maximum voltage of the ABR-MFC was obtained during OCM for all three OLRs. The open circuit voltage (OCV) of the ABR-MFC was found to be 400 mV for OLR 1, 513 mV for OLR 2 and 561 mV for OLR 3 (Figure 5.4). The OCVs obtained during OLR 1, 2 and 3 was 700 mV, 587 mV and 539 mV respectively lower than the theoretical maximum cell voltage of 1.1 V under OCM conditions (Logan, 2008).

The OCV obtained during OLR 1 (400 mV) was the lowest OCV attained during this study and is comparable with the OCVs achieved by Ieropoulos *et al*. (2008) (between 440 and 450 mV at MFC stack configurations), Min & Angelidaki (2008) (393 mV) and Inoue *et al*. (2012) (390 mV). The second highest OCV attained by the ABR-MFC was during OLR 2 (513 mV) and is comparable with the OCVs achieved by Liu *et al*. (2011) (534 mV) and Xu *et al*. (2016) (500 mV). Ortiz-Martínez *et al.* (2016) achieved an OCV of 498 mV when using ceramic separators in MFCs

while Wang *et al*., (2016) achieved an OCV of 490 mV in a hybrid MFC-MBR which is also in-line with the OVC achieved by the ABR-MFC for OLR 2. The highest OCV achieved by the ABR-MFC was observed during OLR 3 (561 mV). The OCV achieved in OLR 3 is comparable with the OCVs achieved by Cha *et al*. (2010) (594 mV) and Yoo *et al*. (2011) (560 mV) when performing polarization tests on single chamber MFCs. The ABR-MFC achieved a lower OVC than the OCVs reported by You *et al*. (2007) and Song *et al*. (2010) who achieved OCVs of 710 mV and 650 mV, respectively, however, these results are still in line with the OCV achieved in OLR 3.

The low OCV obtained during OLR 1 (400 mV) could be due to oxygen permeability through the diffusion layer on the floating carbon air-cathodes (Prakash *et al*., 2009; Song *et al*., 2010) since oxygen is considered an electron acceptor in the cathode (Song *et al*., 2010). This observation could be due to the fact that the biofilm on the cathode have not yet been fully developed on day 24 when the polarisation of OLR 1 was performed. Prakash *et al*. (2009) concluded that a much higher PD is expected if the OCV could be increased by reducing the thickness of the membrane (i.e. separator) used. Song *et al*. (2010) also reported that the OCV could affect the maximum PD achieved by the system.

It is evident from Figure 5.4 that the same trend is followed by the three OLRs when considering the increasing cell voltage with respect to increasing the external resistance of the ABR-MFC. During all three OLRs the cell voltage sharply increases as the external resistance is increased until 1 000 Ω after which a stable increase in cell voltage is observed despite the respective outliers during OLR 2 (at 4 000 Ω) and 3 (at 9 000 Ω). The OCVs obtained during OLRs 1, 2 and 3 was higher than the ABR-MFC voltage when different external resistances were applied.

It is possible that the increase in OCV (from 400 mV to 516 mV and 561 mV) during this study could be attributed to an increase in OLR and an increased removal efficiency (i.e. COD) when considering OLR 1 (48.30%), 2 (59.15%) and 3 (64.55%) (Song *et al*., 2010). It is therefore concluded that the increase in OCV is attributed to an increase in OLR when treating BDWW using an ABR-MFC.

5.3.1. ABR-MFC polarisation

Current and current density (normalised to CSA) was calculated from the corresponding potential (i.e. voltage) measurements at the specified external resistances to obtain the polarisation curves (Figure 5.5) for OLRs 1, 2 and 3. The calculated current and current density (CSA) were then used

to calculate the power and subsequently the PD (normalised to CSA) at the specified external resistances to obtain the PD (normalised to CSA) curves (Figure 5.5) for OLR 1, 2 and 3.

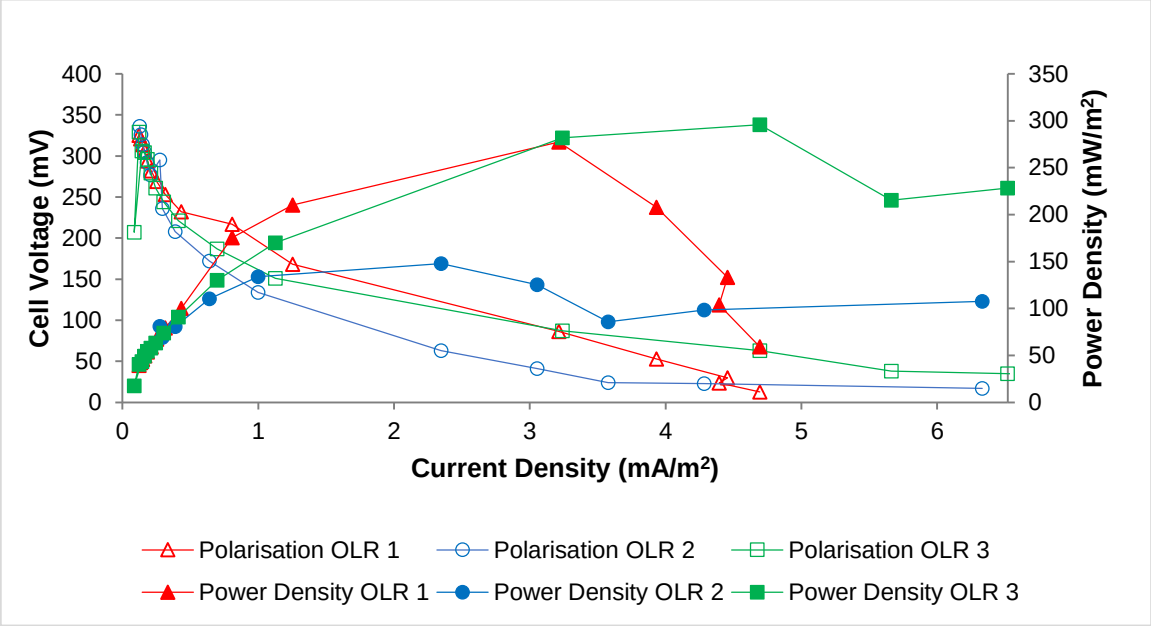

Figure 5.5: Polarisation and PD (CSA) curves (OLR 1 – 3)

The polarisation curves illustrated in Figure 5.5 depicts how well the MFC maintains voltage as a function of current generation thereby characterising the performance of the MFC (Logan, 2008).

5.3.1.1. Internal resistance

The internal resistance of a system consists of activation-, ohmic- and concentration-losses (Mahadevan *et al*., 2014; Logan, 2008). A significant amount of power is lost due to the internal resistance (Prakash *et al*., 2009) since the internal resistance of a system limits its overall performance (Kakarla *et al*., 2015).

The internal resistance of the ABR-MFC for all experiments (OLRs 1, 2 and 3) were determined using Equation 2.7 and was found to be 340.15 Ω, 487.97 Ω and 280.69 Ω, respectively (refer to sample calculation in Appendix E). Y. Wang *et al*. (2012) and Song *et al*. (2015) achieved respective internal resistances of 365 Ω and 328 Ω which is comparable to the internal resistance achieved by the ABR-MFC for OLR 1. The internal resistance achieved by the ABR-MFC during OLR 2 (487.97 Ω) is comparable with the internal resistance reported by Ortiz-Martínez *et*

al. (2016) who achieved an internal resistance of 539.1 Ω when evaluating the performance of ceramic MFCs assembled with different separator structures (e.g. absence of ionic liquid over ceramic surface, layer of ionic liquid with and without PTFE) in MFCs. The internal resistance obtained during OLR 3 (280.69 Ω) is in line with the internal resistance reported by Song *et al*. (2015) who achieved an internal resistance of 282 Ω using a PVDF layer on the solution side of an air-cathode MFC.

Liu *et al*. (2009) proved that by improving the operating conditions of the MFC (i.e. increasing the anode surface area and the electrical conductivity). The internal resistance was reduced from 317 Ω to 35 Ω, using glucose as substrate, by using excess sludge thereby increasing the PD achieved by the MFC. Min and Angelidaki (2008) identified the high internal resistance (35 Ω) of the electrolyte (i.e. ohmic) as the main limitation for achieving higher electricity generation in a submersible MFC.

According to Sukkasem *et al*. (2011), a large internal resistance (10 kΩ) is usually attributed to a greater distance between the anode and cathode electrodes, the electrode material and a low degree of biodegradation. Nandy *et al*. (2015) agrees that the electrode material and electrode spacing has a significant effect on the performance of an MFC. A smaller carbon fibre brush anode diameter provides a shorter distance along the fibre for electrons to get to the titanium (Ti) current collector. This decreases the internal resistance of the system and enhances the performance of the MFC (Lanas *et al*., 2014). According to Yuan *et al*. (2010), the internal resistance of an MFC is mostly attributed to ohmic losses within the system. Song *et al*. (2010) stated that it is possible that the increased maximum PD could be obtained by an increased OCV and a reduced internal resistance – of which a large portion consists of ohmic resistances associated with the electrode resistances. The ohmic losses observed during this study is described in Section 2.3.1.2.

5.3.1.2. Activation losses

The sharp decline in cell voltage initially observed at low current densities (< 0.40 mA/m^2) in the polarisation curves (Figure 5.5) of all three experimental conditions is attributed to activation losses (Du *et al*., 2007; Cha *et al*., 2010; Lázaro *et al*., 2011) which occurs at the anode and cathode electrodes (Logan, 2008). According to You *et al*. (2007), activation losses occurs due to a limitation of microbial metabolism at the anode and oxygen reduction at the cathode. The activation losses occur due to the energy that must be overcome by the reacting species (Du *et al*., 2007) and is thus the limiting step owing to very slow reaction kinetics of oxygen reduction at the cathode (Du *et al*., 2007; Yousefi *et al*., 2015).

The activation losses for the ABR-MFC ranged from 253 to 321 mV for OLR 1, 208 to 326 mV for OLR 2 and 221 to 329 mV for OLR 3 (refer to Figure 5.5). The activation losses observed in the ABR-MFC is much lower than the activation losses for a typical MFC which should range between 600 and 800 mV (section 2.8.1 – Figure 2.3) (Logan, 2008). According to Blackall *et al*. (2007) and Logan (2008), these activation losses can be overcome by using improved catalysts at the cathode while Song *et al*. (2010) and Mahadevan *et al*. (2014) suggests the addition a catalyst (i.e. Pt) to the cathode electrode.

5.3.1.3. Ohmic losses

It is evident from Figure 5.5 that all three experimental conditions followed a constant decrease in cell voltage while the cell voltage of OLR 2 and 3 stabilised after respective current densities of 3.58 and 5.66 mA/m^2. The constant decrease in all experiments (OLR 1, 2 and 3) represents a linear relationship between the cell voltage and the current density of the ABR-MFC and attributed to ohmic losses within the ABR-MFC which is mostly attributed to the internal resistance of the system (Yuan *et al*., 2010).

It is evident from Figure 5.5 that ohmic resistance is dominant in all three experimental conditions (OLR 1, 2 and 3). The ohmic losses for a typical MFC ranges between 300 and 600 mV (section 2.8.1 – Figure 2.3) (Logan, 2008). The ohmic losses for the ABR-MFC ranged from 12.6 to 321 mV for OLR 1, 17.0 to 208 mV for OLR 2 and 25.0 to 221 mV for OLR 3.

When comparing the three polarization curves of the ABR-MFC, a faster rate of change is observed during the polarisation of OLR 2 which suggests a higher ohmic resistance resulting in a faster decrease in cell voltage (Ortiz-Martínez *et al*., 2016). The latter is supported by the high internal resistance observed during OLR 2 which was found to be 487.97 Ω. The gradual decrease in cell voltage during OLR 3 suggests that there is a slow decrease in internal resistance which can be attributed to biofilm maturation over a long period of time (Lefebvre *et al*., 2013).

The ohmic losses can be overcome by reducing the distance between the anode and cathode electrodes (Logan *et al*., 2006; Du *et al*., 2007; Singh *et al*., 2010; Yao *et al*., 2014; Xu *et al*., 2016), membrane resistance (Lázaro *et al*., 2011; Huang *et al*., 2012), solution resistance (Huang *et al*., 2012), electrical resistance of the electrodes (Song *et al*., 2010; Lázaro *et al*., 2011; Huang *et al*., 2012) and current collectors (Lázaro *et al*., 2011; Huang *et al*., 2012) as well as increasing the conductivity of the current collector (Song *et al*., 2010) and the substrate to the maximum that can be tolerated by the bacteria (Logan *et al*., 2006; Singh *et al*., 2010). By overcoming the ohmic losses the internal resistance of the system is reduced which can thus

increase electricity generation since electrons generated in the anodic chamber during oxidation of the substrate will travel a shorter path to reach the cathode (Nandy *et al*., 2015).

5.3.1.4. Concentration losses

According to Mahadevan *et al*. (2014), the typical polarization curve of an MFC ends with a sharp decline in measured cell voltage. However, the sharp decrease in cell voltage on the polarisation curves for the ABR-MFC (Figure 5.5) does not exist. The latter suggests that the ABR-MFC does not have major concentration losses. It can therefore be said that the ABR-MFC reached electrical equilibrium during all three OLRs (1, 2 and 3) which is dependent on the anode and cathode electrodes (Mahadevan et al., 2014).

Since concentration losses were absent during this study it can be said that the ABR-MFC has the ability to maintain the initial substrate concentration in the bulk fluid (Du *et al*., 2007). The latter could be attributed to sufficient mixing (i.e. natural convective flow) of substrate (i.e. BDWW) within the system and atributed to the design of the ABR. This might have enhanced the mass transfer rate by minimising the concentration gradient between the bulk fluid and the electrode surface (Oh *et al*., 2010).

5.3.2. ABR-MFC maximum power density

The maximum power density (PD) for the three experimental conditions (OLR 1, 2 and 3) were determined by using the PD peak method (refer to section 2.8.1.1 for method description). The maximum PDs (CSA) (Figure 5.5) achieved by the ABR-MFC during OLR 1, 2 and 3 were determined to be 277.42 mW/m^2, 147.84 mW/m^2 and 295.68 mW/m^2 at respective current densities of 3.21 mA/m^2, 2.35 mA/m^2 and 4.69 mA/m^2. The corresponding external resistances for OLR 1 and 2 was 100 Ω while the maximum PD of OLR 3 was observed at an external resistance of 50 Ω.

The maximum PD achieved during OLR 1 (277.42 mW/m^2) is comparable with the work of Rahimnejad *et al*. (2011) who achieved a maximum PD of 274 mW/m^2. The ABR-MFC performed better when comparing the maximum PD observed to the maximum PD achieved by Liu *et al*. (2009) who attained a maximum PD of 220.7 mW/m^2 (at a current density of 0.11 mA/m^2) and Min and Angelidaki (2008) who achieved a maximum power density of 218 mW/m^2.

The ABR-MFC achieved a higher maximum PD when comparing the results of OLR 2 (147.84 mW/m^2) to the work of Miyahara *et al*. (2013) (100 mW/m^2) who conducted wastewater treatment using cassette electrode configurations, as well as Kondaveeti e*t al*. (2014) (118 mW/m^2) and Nandy *et al*. (2015) (124.46 mW/m^2) who respectively used Nafion® membranes as a separators in dual-chamber MFCs. However, the maximum PD obtained during OLR 2 is comparable with the work of Song *et al*. (2015) who achieved 147.84 mW/m^2 using an MFC with a polyvinylidene fluoride (PVDF) layer on the solution side of the air-cathodes.

The ABR-MFC achieved a lower maximum PD during OLR 3 (295.68 mW/m^2) than the PDs reported by Zuo *et al*. (2006) (475 mW/m^2) and Song *et al*. (2010) (311.2 mW/m^2) who respectively used corn stover- and synthetic- wastewater as substrate, both in single-chamber air cathode MFCs. Kakarla *et al*. (2015) achieved 370 mW/m^2 using an air-cathode MFC with oxygen supply from an externally connected algal bioreactor which is approximately 75 mW/m^2 more than the maximum PD achieved by the ABR-MFC for OLR 3. Rahimnejad *et al*. (2011), Min *et al*. (2005) and Gajda *et al*. (2015) reported respective maximum PDs of 274 mW/m^2, 261 mW/m^2 and 286 mW/m^2 when using glucose, swine wastewater and domestic wastewater. These results are lower than the maximum PD achieved by the ABR-MFC for OLR 3. Nonetheless, the maximum PD achieved during OLR 3 is comparable with the maximum PDs achieved by Logan *et al*. (2007) (300 mW/m^2) when using a carbon paper anode (air-cathode MFC), Ahn *et al*. (2014) (282 mW/m^2) when using carbon fibre brush anodes in MFCs treating domestic wastewater, Tugtas *et al*. (2011) (280 mW/m^2) treated synthetic wastewater in air-cathode MFCs and Lanas *et al*. (2014) (280 mW/m^2) who reported that the distance between the anode (i.e. carbon fibre brush) and the cathode is more important than the total surface area of the carbon fibre brush anode.

It is evident from Figure 5.5 that OLR 2 achieved the lowest maximum PD (147.84 mW/m^2) when comparing the three experimental conditions (OLR 1, 2 and 3). It is evident that a lower internal resistance results in a higher maximum PD (Song *et al*., 2010). According to Ahn *et al*. (2014), a higher PD is achieved at higher OLRs. The latter is observed in Figure 5.5 where OLR 3 achieved the highest maximum PD.

The low maximum PD achieved during OLR 2 could be due to a lower electrical conductivity (EC) in the feed substrate (Logan *et al*., 2006; Singh *et al*., 2010) when comparing the EC of the BDWW during OLR 2 (932 μS/cm (Table 4.18)) and 3 (1 112 μS/cm (Table 4.22)). The effect of the EC can directly be related to the maximum PDs achieved during these OLRs. The highest feed EC was measured during OLR 3 (1 112 μS/cm) which corresponds to the highest PD (295.68 mW/m^2) (Figure 5.5) achieved during this study.

5.4. Chapter summary

The internal resistance of a typical MFC system consists of activation-, ohmic- and concentration-losses (Mahadevan *et al*., 2014; Logan, 2008). During system polarisation it was found that activation- and ohmic-losses were present during all three OLRs. It was concluded that a high internal resistance, attributed to ohmic losses, limits the overall system performance of the ABR-MFC (Kakarla *et al*., 2015). It was however concluded that sufficient mixing of BDWW within the ABR-MFC resulted in the absence of concentration losses.

The maximum PD for the three experimental conditions (OLR 1, 2 and 3) were determined by using the PD peak method. It is evident from Table 5.13 that the highest PD was obtained during OLR 3. There is no significant difference between the PDs of OLR 1 (20 442 mW/m^3 (ACV), 6 126 mW/m^2 (CSA), 4.81 mW/m^2 (ASA)) and OLR 2 (21 114 mW/m^3 (ACV), 6 327 mW/m^2 (CSA), 4.97 mW/m^2 (ASA)). However, the PDs obtained during OLR 3 (44 131 mW/m^3 (ACV), 13 225 mW/m^2 (CSA), 10.38 mW/m^2 (ASA)) were nearly double that of OLRs 1 and 2. The ABR-MFC attained the highest OCV (561 mV), maximum PD (296 mW/m^2) and the lowest internal resistance (281 Ω) during OLR 3 when compared to that of OLR 1 and 2. It was concluded that a lower internal resistance (Song *et al*., 2010) and a higher OLR (Ahn *et al*., 2014) resulted in a higher maximum PD.

Table 5.13: Summarised ABR-MFC performance with regard to power generation

	Parameter	Units	OLR 1	OLR 2	OLR 3
ABR-MFC	**OLR**	**kg COD/m^3.day**	1.15	1.98	3.46
	COD Removal	**%**	48.3	59.15	64.55
	PD_{ACV}	**mW/m^3**	20442.04	21113.71	44131.14
	PD_{CSA}	**mW/m^2**	6125.76	6327.03	13224.55
	PD_{ASA}	**mW/m^2**	4.81	4.97	10.38
	OCV	**mV**	400	513	561
	PD_{max}	**mW/m^2**	277.42	147.84	295.61
	ID_{max}	**mA/m^2**	3.21	2.35	4.69
	R_{int}	**Ω**	340.15	487.97	280.69

It is therefore evident from the experimental findings (Table 5.13) that OLR 3 is the most effective OLR to treat BDWW and generate electricity simultaneously without the need for a pre-treatment step and the use of a recycle stream. However, more research should be conducted to increase system efficiency regarding COD removal and the maximum PD achieved by the laboratory scale ABR-MFC system. It is therefore recommended to further increase the OLR steadily thereby ultimately feeding the ABR-MFC with full strength BDWW (i.e. average COD of 150 000 mg/l).

CHAPTER SIX

CONCLUSIONS AND RECOMMENDATIONS

CHAPTER SIX:
CONCLUSIONS AND RECOMMENDATIONS

6.1. Conclusions

The possibility of reducing the chemical oxygen demand (COD) in untreated industrial biodiesel wastewater (BDWW), obtained from a commercial biodiesel company located in the Western Cape, was evaluated using an anaerobic baffled reactor (ABR) equipped with microbial fuel cell (MFC) technology at ambient temperature in order to meet the industrial wastewater discharge standard limits as anticipated by the City of Cape Town (2011).

1. The results of this study lead to the following conclusions concerning the parameters which do not meet the industrial wastewater discharge standards in the BDWW:

All parameters measured during this study met the industrial wastewater discharge standard limits except for the COD and fats, oils and grease (FOG) for the full strength BDWW. The COD and FOG of full strength BDWW was approximately 296 125 mg/l and 500 mg/l over the allowed limit prior to anaerobic biological treatment of diluted BDWW. It was therefore concluded that the BDWW should be treated prior to disposal into the municipal sewer system to reduce the COD to a value below 5 000 mg/l.

After treatment with the ABR-MFC, the FOG and COD contained within the BDWW was reduced by 97.89% and 57.87%, respectively. Therefore, the only parameter which did not meet the industrial wastewater discharge standard limits, after treatment with the ABR-MFC, was the COD.

2. The results of this study lead to the following conclusions concerning pH and carbon:nitrate:phosphate (C:N:P) ratio adjustments prior to treatment with the ABR-MFC:

Although the pH of the ABR-MFC feed decreased to a value below 6, the pH of the ABR-MFC feed remained relatively constant during the study period of 225 days. It is however concluded that the pH was too low. The low organic matter (i.e. COD) removal could therefore be attributed to the acidity within the ABR-MFC caused by an accumulation of volatile fatty acids (VFA) since the alkalinity of the ABR-MFC was not monitored.

The C:N:P ratio used during this study (150:0.05:0.01) was lower than the optimal C:N:P ratio (150:1.1:0.2) suggested by Phukingngam *et al*. (2011). The nitrogen and phosphorous

concentrations of the BDWW were thus increased to obtain the optimal C:N:P ratio. The treatment efficiency of the ABR-MFC increased from 48.30% to 64.55% over the study period. It can thus be concluded that a pre-treatment step is not necessary for BDWW when adjusting the pH and C:N:P ratio of the ABR-MFC feed.

3. The results of this study lead to the following conclusions concerning the maximum power output generated by the ABR-MFC system:

The ABR-MFC obtained a power density (PD) of 44 131 mW/m^3 (normalised to anode chamber volume) during organic loading rate (OLR) 3 which was nearly double the PD of OLRs 1 and 2. During this OLR (3), the ABR-MFC achieved an open circuit voltage (OCV) of 561 mV, a maximum PD of 296 mW/m^2 and a low internal resistance (281 Ω).

4. The results of this study lead to the following conclusions concerning the treatment efficiency of the ABR-MFC:

The BDWW was deemed fairly biodegradable with regard to the biological oxygen demand (BOD):COD ratio which was found to be 0.68. It is concluded that the ABR-MFC successfully reduced the COD, FOG, total suspended solids (TSS), nitrate nitrogen (NO_3-N), and total phosphate (TP) by 64.55%, 99.96%, 98.55%, 89.18%, and 89.06%, respectively during OLR 3 which was deemed the most effective OLR for this study.

It is concluded that OLR 3 (3.46 kg COD/m^3.day) was the most effective and efficient OLR to treat BDWW and generate electricity simultaneously without the need for a pre-treatment step and the use of a recycle stream.

6.2. Recommendations

The following recommendations have been proposed for further studies:

- Introduce a post-treatment step which includes the use of membrane technology (i.e. nanofiltration (NF), ultrafiltration (UF) and reverse osmosis (RO)) to ensure that the COD is further reduced to below the industrial discharge standard limits imposed by the City of Cape Town (City of Cape Town, 2011). The use of membrane technology will also ensure the reduction of electrical conductivity (EC), total dissolved solids (TDS) and salinity contained in the treated BDWW.
- Introduce a recycle stream to increase mixing in the ABR-MFC system to ensure adequate wastewater-microorganism contact. The use of a recycle stream will control mass transfer and thus better ABR-MFC performance.
- Monitor the alkalinity of the system in order to monitor VFA accumulation.
- Maintain the pH of the ABR-MFC feed between 6.5 and 7.5 so as to ensure that a build-up of products from acetogenesis (i.e. VFA) does not occur, and that optimal biological activity and therefore COD removal from the BDWW occurs (Pirsaheb *et al*., 2015; Florencio *et al*., 1996).
- Limit the amount of VFA content within the ABR-MFC to below 200 mg/l acetic acid by providing the system with sufficient alkalinity within the ABR-MFC in order to ensure continuous digestion of organic material (Pirsaheb *et al*., 2015).
- Supply alkalinity to the ABR-MFC in the form of sodium bicarbonate ($NaHCO_3$) and dipotassium hydrogen phosphate (K_2HPO_4) (Florencio *et al*., 1996) or urea (CH_4N_2O) (0.007 g/gCOD) and diammonium hydrogen phosphate ($NH_4H_2PO_4$) (0.0006 g/gCOD) (Pirsaheb *et al*., 2015) so as to maintain the optimum pH as well as to ensure effective digestion and production of quality biogas (i.e. 50-75% methane) (Phukingngam *et al*., 2011).
- Increase the C:N:P ratio of the BDWW used as feed in the ABR-MFC from 150:0.05:0.02 to 150:1.1:0.2 (Phukingngam *et al*., 2011) to ensure optimal biological activity and therefore COD removal (Ammary, 2004; Thompson *et al*., 2006; Ajeng *et al*., 2010).
- Introduce mixing to the ABR-MFC system by implementing a recycle stream which will assist (the system):
    a. In adjusting the pH of the ABR-MFC feed thus possibly eliminating the need for adjusting the feed pH by adding sodium hydroxide (NaOH) and phosphoric acid (H_3PO_4).

b. In increasing the maximum PD of the system and possibly system efficiency (i.e. COD removal) since sufficient mixing should be ensured in order to obtain better wastewater-microorganism contact (Barber & Stuckey, 1999).
c. In diluting the ABR-MFC feed thus reducing the toxicity of the feed for microorganisms (Grobicki & Stuckey, 1991) and possibly increasing the treatment efficiency of the ABR-MFC system.

- Capture and analyse the gas produced by the ABR-MFC system as a possible additional source of bioenergy.
- Further increase the OLR from 3.46 kg COD/m^3.day thereby finally feeding the ABR-MFC with full strength BDWW.
- Up-scale the ABR-MFC system to a pilot- and then full-scale system to be implemented at biodiesel production companies to eliminate penalties liable by these companies as a result of the waste discharge charge system (WDCS).
- Maximise the PD achieved by the lab-scale ABR-MFC system by using improved catalysts at the cathode and by adding platinum to the cathode electrode.

REFERENCES

Ahn, Y., Hatzell, M.C., Zhang, F. & Logan, B.E. 2014. Different Electrode Configurations to Optimize Performance of Multi-Electrode Microbial Fuel Cells for Generating Power or Treating Domestic Wastewater. *Journal of Power Sources*, 249: 440–445.

Ajeng, D., Liberty, H. & Soewondo, P. 2010. *The Influence of Water Addition of Biowaste to CNP Ratio in Mechanical Biological Treatment (MBT) Process*. Institut Teknologi Bandung: Bandung.

Aldrovandi, A., Marsili, E., Stante, L., Paganin, P., Tabacchioni, S. & Giordano, A. 2009. Sustainable Power Production in a Membrane-Less and Mediator-Less Synthetic Wastewater Microbial Fuel Cell. *Bioresource Technology*, 100(13): 3252–3260.

Amjad, Z. 2010. *The Science and Technology of Industrial Water Treatment*. London: International Water Association.

Ammary, B.Y. 2004. Nutrients Requirements in Biological Industrial Wastewater Treatment. *African Journal of Biotechnology*, 3(4): 236–238.

An, J., Kim, D., Chun, Y. & Lee, S. 2009. Floating-Type Microbial Fuel Cell (FT-MFC) for Treating Organic-Contaminated Water. *Environmental Science and Technology*, 43(5): 1642–1647.

Arora, R. 2012. *Microbial Biotechnology: Energy and Environment*. Cambridge: Centre for Agriculture and Bioscience.

Atadashi, I.M., Aroua, M.K., Aziz, A.R.A. & Sulaiman, N.M.N. 2011. Refining Technologies for the Purification of Crude Biodiesel. *Applied Energy*, 88(12): 4239–4251.

Austic, G. & Lobdell, S. 2009. *Treatment, Disposal and Reuse of Biodiesel Derived Waste Products*. Pittsboro: Piedmont Biofuels & Chatam Environmental Consulting.

Bachmann, A., Beard, V.L. & McCarthy, P.L. 1982. Comparison of Fixed-Film Reactors with a Modified Sludge Blanket Reactor. *Fixed Film Biological Processes for Wastewater Treatment*: 1–20.

Bachmann, A., Beard, V.L. & Perry, L.M. 1985. Performance Characteristics of the Anaerobic Baffled Reactor. *Water Research*, 19(1): 99–106.

Barber, W.P. & Stuckey, D.C. 1999. The Use of the Anaerobic Baffled Reactor (ABR) for Wastewater Treatment: A Review. *Water Research*, 33(7): 1559–1578.

Berrios, M. & Skelton, R.L. 2008. Comparison of Purification Methods for Biodiesel. *Chemical Engineering Journal*, 144(3): 459–465.

Bezerra, R.A., Rodrigues, J.A.D., Ratusznei, S.M., Canto, S.A.C. & Zaiat, M. 2011. Effect of Organic Load on the Performance and Methane Production of an AnSBBR Treating Effluent from Biodiesel Production. *Applied Biochemical Biotechnology*, (165): 347–368.

Bitton, G. 1998. *Formula Handbook for Environmental Engineers and Scientists*. New York: John Wiley.

Blackall, L.L., Keller, J., Gross, P., Rabaey, K., Rodrı, J., Batstone, D., Verstraete, W. & Nealson, K.H. 2007. Microbial ecology meets electrochemistry : electricity-driven and driving communities. *The IInternational Society for Microbial Ecology (ISME) Journal*, 1: 9–18.

Bodkhe, S.Y. 2009. A Modified Anaerobic Baffled Reactor for Municipal Wastewater Treatment. *Journal of Environmental Management*, 90(8): 2488–2493.

Bretschneider, F. & De Weille, R.J. 2006. *Introduction to Electrophysiological Methods and Instrumentation*. Amsterdam: Academic.

Bwapwa, J.K., Foxon, K.M. & Buckley, C.A. 2010. Analysis of an Anaerobic Baffled Reactor Treating Complex Particulate Wastewater in an ABR Membrane Bioreactor Unit (MBR-ABR). Report, University of Kwazulu-Natal, Durban.

Cameron, N. 2015. Addressing South Africa's Energy Crisis with a Long-Term Solution. *Hi-Tech Security Solutions Magazine*. [23 May 2016].

Cha, J., Choi, S., Yu, H., Kim, H. & Kim, C. 2010. Directly Applicable Microbial Fuel Cells in Aeration Tank for Wastewater Treatment. *Bioelectrochemistry*, 78(1): 72–79.

Chavalparit, O. & Ongwandee, M. 2009. Optimizing Electrocoagulation Process for the Treatment of Biodiesel Wastewater Using Response Surface Methodology. *Journal of Environmental Sciences*, 21(11): 1491–1496.

Cheremisinoff, N.P. 1996. *Biotechnology for Waste and Wastewater Treatment*. New Jersey: Noyes.

City of Cape Town. 2011. *City of Cape Town: Water and Industrial Effluent By-law, 2006.* Cape Town. [3 July 2016].

City of Cape Town. 2012. *Wastewater and Industrial Effluent Bylaw*. Cape Town. [3 July 2016].

City of Cape Town. 2016a. City's Mayco Recommends Implementation of Level 3 Water Restrictions. *Media Office*. http://www.capetown.gov.za/Media-and-news/City's Mayco recommends implementation of Level 3 water restrictions [18 September 2017].

City of Cape Town. 2016b. Council to Implement Water Restrictions. *Media Office*. http://www.capetown.gov.za/Media-and-news/Council to implement water restrictions [18 September 2017].

City of Cape Town. 2017a. Driving Water Consumption Down to 500 Million Litres a Day: Level 5 Water Restrictions Announced. *Media Office*. http://www.capetown.gov.za/Media-and-news/Driving water consumption down to 500 million litres a day Level 5 restrictions announced [18 September 2017].

City of Cape Town. 2017b. Drought crisis: Level 4 Water Restrictions Recommended. *Media Office*. http://www.capetown.gov.za/Media-and-news/Drought crisis Level 4 water restrictions recommended [18 September 2017].

City of Cape Town. 2017c. Drought Crisis: Level 4B Restrictions from 1 July 2017. *Media Office*. http://www.capetown.gov.za/Media-and-news/Drought crisis Level 4b restrictions from 1 July 2017 [18 September 2017].

City of Cape Town. 2017d. Water Crisis: Stricter Water Restrictions from Tomorrow. *Media Office*. http://www.capetown.gov.za/Media-and-news/Water crisis stricter water restrictions from tomorrow [18 September 2017].

City of Cape Town. 2018. Day Zero now likely to happen - new emergency measures. *Media Office*. [14 May 2018]

Cloete, K. 2016. South Africa Faces Potential 1.1Bn Cubic Metre Water Deficit by 2035 - WRC. *Creamer Media*. http://www.engineeringnews.co.za/article/south-africa-faces-potential-11bn-cubic-metre-water-deficit-by-2035-wrc-2016-05-19/rep_id:4136 [23 May 2016].

Daud, N.M., Bdullah, S.R.S., Hasan, H.A. & Yaakob, Z. 2014. Production of biodiesel and its wastewater treatment technologies: A review. *Process Safety and Environmental Protection*, 94(October): 487–508.

Daud, Z., Awang, H., Latif, A.A.A., Nasir, N., Ridzuan, M.B. & Ahmad, Z. 2015. Suspended Solid,

Color, COD and Oil and Grease Removal from Biodiesel Wastewater by Coagulation and Flocculation Processes. *Procedia - Social and Behavioral Sciences*, 195: 2407–2411.

Davis, R. 2018. #CapeWaterGate: In the end, what was Day Zero all about? *Daily Maverick*.

De la Harpe, J. & Ramsden, P. 2008. *Guide to the National Water Act*. Pretoria: Department of Water Affairs and Forestry.

Denita, A. 2018. Level 6 water restrictions take effect in CT. *Cape Talk*.

Department of Minerals and Energy. 2007. *Biofuels Industrial Strategy of the Republic of South Africa*. Pretoria: Department of Minerals and Energy.

Drioli, E. & Giorno, L. 2010. *Comprehensive Membrane Science and Engineering*. Oxford: Elsevier.

Du, Z., Li, H. & Gu, T. 2007. A State of the Art Review on Microbial Fuel Cells: A Promising Technology for Wastewater Treatment and Bioenergy. *Biotechnology Advances*, 25: 464–482.

Environment News South Africa. 2015. Prepare for Power Load Shedding Which Could Last 12 Hours. *Environment SA*. http://www.environment.co.za/south-africas-energy-crisis/prepare-for-power-load-shedding-which-could-last-12-hours.html [24 May 2016].

Environmental Business Specialists. 2015. Chemical Oxygen Demand Testing. *EBS - Wastewater Training and Consulting*. [12 Februay 2016].

Faisal, M. & Unno, H. 2001. Kinetic Analysis of Palm Oil Mill Wastewater Treatment by a Modified Anaerobic Baffled Reactor. *Biochemical Engineering Journal*, 9: 25–31.

Feng, Y., Lee, H., Wang, X., Liu, Y. & He, W. 2010. Continuous Electricity Generation by a Graphite Granule Baffled Air–Cathode Microbial Fuel Cell. *Bioresource Technology*, 101(2): 632–638.

Florencio, L., Field, J.A., van Langerak, A. & Lettinga, G. 1996. pH-Stability in Anaerobic Bioreactors Treating Methanolic Wastewaters. *Water Science and Technology*, 33(3): 177–184.

Fulhage, C.D., Porter, J. & Sievers, D. 2017. Collecting and Preserving Waste and Wastewater Samples for Analysis. *University of Missouri. MU Extension*. https://extension2.missouri.edu/g1895 [28 August 2018].

Gajda, I., Greenman, J., Melhuish, C. & Ieropoulos, I. 2015. Simultaneous Electricity Generation and Microbially-Assisted Electrosynthesis in Ceramic MFCs. *Bioelectrochemistry*, 104: 58–64.

Gao, M., Yang, M., Li, H., Yang, Q. & Zhang, Y. 2004. Comparison Between a Submerged Membrane Bioreactor and a Conventional Activated Sludge System on Treating Ammonia-Bearing Inorganic Wastewater. *Journal of Biotechnology*, 108(3): 265–269.

Garche, J., Dyer, C.K., Moseley, P.T., Ogumi, Z., Rand, D.A.J. & Scrosati, B. 2009. *Encyclopedia of Electrochemical Power Sources*. Amsterdam: Elsevier.

Garverick, L. 1994. *Corrosion in the Petrochemical Industry*. Russel: ASM.

Gerardi, M.H. 2003. *The Microbiology of Anaerobic Digesters*. M. H. Gerardi, ed. New Jersey: John Wiley.

Ghangrekar, M.M. & Shinde, V.B. 2007. Performance of Membrane-Less Microbial Fuel Ccell Treating Wastewater and Effect of Electrode Distance and Area on Electricity Production. *Bioresource Technology*, 98(15): 2879–2885.

Gil, J. a., Krzeminski, P., van Lier, J.B., van der Graaf, J.H.J.M., Wijffels, T. & Prats, D. 2011.

Analysis of the Filterability in Industrial MBRs. Influence of activated sludge Parameters and Constituents on Filterability. *Journal of Membrane Science*, 385–386(1): 96–109.

Gray, N.F. 2004. *Biology of Wastewater Treatment*. 2nd ed. Singapore: World Scientific.

Grobicki, a & Stuckey, D.C. 1991. Performance of the Anaerobic Baffled Reactor Under Steady-State and Shock Loading Conditions. *Biotechnology and Bioengineering*, 37(4): 344–355.

Gude, V.G. 2016. Wastewater Treatment in Microbial Fuel Cells - An Overview. *Journal of Cleaner Production*, 122: 287–307.

Hawker, D. 2015. SA Water Crisis Map: What You Need to Know. *eNCA*.

Henze, M., Van Loosdrecht, M.C.M., Ekama, G.A. & Brdjanovic, D. 2008. *Biological Wastewater Treatment: Principles, Modelling and Design*. London: IWA.

Huang, Y., He, Z., Kan, J., Manohar, A.K., Nealson, K.H. & Mansfeld, F. 2012. Electricity generation from a floating microbial fuel cell. *Bioresource Technology*, 114: 308–313.

HWT. 2013. Industrial Effluent Treatment. *HWT Water Treatment*. http://hwt.co.za/industrial-effluent/ [6 June 2016].

Ieropoulos, I., Greenman, J. & Melhuish, C. 2008. Microbial Fuel Cells Based on Carbon Veil Electrodes: Stack Configuration and Scalability. *International Journal of Energy Research*, (32): 1228–1240.

Inoue, S., Parra, E.A., Higa, A., Jiang, Y., Wang, P., Buie, C.R., Coates, J.D. & Lin, L. 2012. Structural optimization of contact electrodes in microbial fuel cells for current density enhancements. *Sensors & Actuators A: Physical*, 177: 30–36.

Jacobson, K.S., Drew, D.M. & He, Z. 2011. Use of a Liter-Scale Microbial Desalination Cell As a Platform to Study Bioelectrochemical Desalination with Salt Solution or Artificial Seawater. *Environment Science and Technology*, 45(10): 4652–4657.

Jang, J.K., Pham, T.H., Chang, I.S., Kang, K.H., Moon, H., Cho, K.S. & Kim, B.H. 2004. Construction and Operation of a Novel mediator- and Membrane-Less Microbial Fuel Cell. *Process Biochemistry*, 39(8): 1007–1012.

Jou, C.-J.G. & Huang, G.-C. 2003. A Pilot Study for Oil Refinery Wastewater Treatment Using a Fixed-Film Bioreactor. *Advances in Environmental Research*, 7(2): 463–469.

Judd, S. 2010. *The MBR Book: Principles and Applications of Membrane Bioreactors for Water and Wastewater Treatment*. 2nd ed. Burlington: Butterworth-Heinemann.

Judd, S. & Judd, C. 2006. *The MBR book: Principles and Applications of Membrane Bioreactors in Water and Wastewater Treatment*. Amsterdam: Elsevier.

Kakarla, R., Rae, J., Jeon, B. & Min, B. 2015. Enhanced Performance of an Air–Cathode Microbial Fuel Cell with Oxygen Supply From an Externally Connected Algal Bioreactor. *Bioresource Technology*, 195: 210–216.

Khanal, S.K. 2008. *Anaerobic Biotechnology for Bioenergy Production: Principles and Applications*. Iowa: Wiley-Blackwell.

Kim, T., An, J., Kyung, J. & Seop, I. 2015. Coupling of Anaerobic Digester and Microbial Fuel Cell for COD Removal and Ammonia Recovery. *Bioresource Technology*, 195: 217–222.

Kleine, J., Peinemann, K. V. & Schuster, C. 2002. Multifunctional System for Treatment of Wastewaters From Adhesive-Producing Industries: Separation of Solids and Oxidation of

Dissolved Pollutants Using Doted Microfiltration Membranes. *Chemical Engineering Science*, 57(9): 1661–1664.

Kondaveeti, S., Lee, J., Kakarla, R., Kim, H.S. & Min, B. 2014. Low-cost separators for enhanced power production and field application of microbial fuel cells (MFCs). *Electrochimica Acta*, 132: 434–440.

Kumar, R.V. & Sarakonsri, T. 2010. Introduction to Electrochemical Cells. In K. E. Aifantis, S. A. Hackney, & R. V. Kumar, eds. *High Energy Density Lithium Batteries: Materials, Engineering, Applications*. Germany: Wiley-VCH Verlag GmbH & Co. KGaA: 1–26.

Lanas, V., Ahn, Y. & Logan, B.E. 2014. Effects of carbon brush anode size and loading on microbial fuel cell performance in batch and continuous mode. *Journal of Power Sources*, 247: 228–234.

Larrosa-Guerrero, A., Scott, K., Katuri, K.P., Godinez, C., Head, I.M. & Curtis, T. 2010. Open Circuit Versus Closed Circuit Enrichment of Anodic Biofilms in MFC: Effect on Performance and Anodic Communities. *Applied Microbiology and Biotechnology*, 87(5): 1699–1713.

Lázaro, M.J., Calvillo, L., Celorrio, V., Pardo, J.I., Perathoner, S. & Moliner, R. 2011. Study and application of Vulcan XC-72 in low temperature fuel cells: 41–68.

Lee, A.H. & Nikraz, H. 2014. BOD:COD Ratio as an Indicator for Pollutants Leaching from Landfill. *Journal of Clean Energy Technologies*, 2(3): 263–266.

Lefebvre, O., Tan, Z., Shen, Y. & Ng, H.Y. 2013. Optimization of a microbial fuel cell for wastewater treatment using recycled scrap metals as a cost-effective cathode material. *Bioresource Technology*, 127: 158–164.

Leung, D.Y.C., Wu, X. & Leung, M.K.H. 2009. A Review on Biodiesel Production Using Catalyzed Transesterification. *Applied Energy*, 87(4): 1083–1095.

Li, Z., Yao, L., Kong, L. & Liu, H. 2008. Electricity Generation Using a Baffled Microbial Fuel Cell Convenient for Stacking. *Bioresource Technology*, 99(6): 1650–1655.

Liu, H., Cheng, S. & Logan, B.E. 2005. Power Generation in Fed-Batch Microbial Fuel Cells as a Function of Ionic Strength, Temperature, and Reactor Configuration. *Environmental Science and Technology*, 39(14): 5488–5493.

Liu, H. & Ramnarayanan, R. 2004. Production of Electricity during Wastewater Treatment Using a Single Chamber Microbial Fuel Cell. *Environmental Science Technology*, 38(7): 2281–2285.

Liu, X.W., Wang, Y.P., Huang, Y.X., Sun, X.F., Sheng, G.P., Zeng, R.J., Li, F., Dong, F., Wang, S.G., Tong, Z.H. & Yu, H.Q. 2011. Integration of a Microbial Fuel Cell with Activated Sludge Process for Energy-Saving Wastewater Treatment: Taking a Sequencing Batch Reactor as an Example. *Biotechnology and Bioengineering*, 108(6): 1260–1267.

Liu, Z., Li, X., Jia, B., Zheng, Y., Fang, L., Yang, Q., Wang, D. & Zeng, G. 2009. Production of electricity from surplus sludge using a single chamber floating-cathode microbial fuel cell. *Water Science and Technology*, 60(9): 2399–2404.

Logan, B., Cheng, S., Watson, V. & Estadt, G. 2007. Graphite Fiber Brush Anodes for Increased Power Production in Air-Cathode Microbial Fuel Cells. *Environmental Science and Technology*, 41(9): 3341–3346.

Logan, B.E. 2008. *Microbial Fuel Cells*. New Jersey: Wiley-Blackwell.

Logan, B.E., Hamelers, B., Rozendal, R., Schroder, U., Keller, J., Freguia, S., Aelterman, P., Verstraete, W. & Rabaey, K. 2006. Microbial Fuel Cells: Methodology and Technology.

Environmental Science & Technology, 40(17): 5181–5192.

Mahadevan, A., Gunawardena, D.A. & Fernando, S. 2014. Biochemical and Electrochemical Perspectives of the Anode of a Microbial Fuel Cell. In *Technology and Applications of Microbial Fuel Cells*. London: InTech: 96.

Mahendra, B.G. & Mahavarkar, S. 2013. Treatment of Wastewater and Electricity Generation Using Microbial Fuel Cell Technology. *International Journal of Research in Engineering and Technology*: 277–282.

Mardanpour, M.M., Nasr Esfahany, M., Behzad, T. & Sedaqatvand, R. 2012. Single chamber microbial fuel cell with spiral anode for dairy wastewater treatment. *Biosensors amd Bioelectronics*, 38(1): 264–269.

Martinucci, E., Pizza, F., Perrino, D., Colombo, A., Trasatti, S.P.M., Lazzarini Barnabei, A., Liberale, A. & Cristiani, P. 2015. Energy Balance and Microbial Fuel Cells Experimentation at Wastewater Treatment Plant Milano-Nosedo. *International Journal of Hydrogen Energy*, 40(42): 14683–14689.

Min, B. & Angelidaki, I. 2008. Innovative Microbial Fuel Cell for Electricity Production from Anaerobic Reactors. *Journal of Power Sources*, 180(1): 641–647.

Min, B., Kim, J., Oh, S., Regan, J.M. & Logan, B.E. 2005. Electricity generation from swine wastewater using microbial fuel cells. *Water research*, 39(20): 4961–4968.

Min, B. & Logan, B.E. 2004. Continuous Electricity Generation from Domestic Wastewater and Organic Substrates in a Flat Plate Microbial Fuel Cell. *Environmental Science & Technology*, 38(21): 5809–5814.

Miyahara, M., Hashimoto, K. & Watanabe, K. 2013. Use of cassette-electrode microbial fuel cell for wastewater treatment. *Journal of Bioscience and Bioengineering*, 115(2): 176–181.

Miyahara, M., Yoshizawa, T., Kouzuma, A. & Watanabe, K. 2015. Floating Boards Improve Electricity Generation from Wastewater in Cassette-Electrode Microbial Fuel Cells. *Journal of Water and Environment Technology*, 13(3): 221–230.

Mushwana, M.L. & Fourie, C.H. 2009. *Report of the Public Protector in terms of Section 182(1)(b) of the Constitution of the Republic of South Africa, 1996 and Sections 8(1) and 8(2)(b)(i) of the Public Protector Act, 1994.* Pretoria: Public Protector South Africa.

Nandy, A., Kumar, V., Mondal, S., Dutta, K., Salah, M. & Kundu, P.P. 2015. Performance evaluation of microbial fuel cells: Effect of varying electrode configuration and presence of a membrane electrode assembly. *New Biotechnology*, 32(2): 272–281.

National Planning Commision. 2011. *National Development Plan: Vision for 2030*. Pretoria: Government of the Republic of South Africa.

News24. 2017. Level 5 Water Restrictions Implemented in Cape Town. *News24*. http://www.news24.com/SouthAfrica/News/level-5-water-restrictions-implemented-in-cape-town-20170903.

Nill, K. 2016. *Glossary of Biotechnology & Agrobiotechnology Terms*. 5th ed. Mankato: CRC.

Oh, S.T., Rae, J., Premier, G.C., Ho, T., Kim, C. & Sloan, W.T. 2010. Sustainable wastewater treatment : How might microbial fuel cells contribute. *Biotechnology Advances*, 28(6): 871–881.

Ortiz-Martínez, V.M., Gajda, I., Salar-García, M.J., Greenman, J., Hernández-fernández, F.J. & Ieropoulos, I. 2016. Study of the effects of ionic liquid-modified cathodes and ceramic separators on MFC performance. *Chemical Engineering Journal*, 291: 317–324.

Padaki, M., Surya Murali, R., Abdullah, M.S., Misdan, N., Moslehyani, A., Kassim, M. a., Hilal, N. & Ismail, A.F. 2015. Membrane Technology Enhancement in Oil–Water Separation: A Review. *Desalination*, 357: 197–207.

Pasupuleti, S.B., Srikanth, S., Mohan, S.V. & Pant, D. 2015. Continuous Mode Operation of Microbial Fuel Cell (MFC) Stack with Dual Gas Diffusion Cathode Design for the Treatment of Dark Fermentation Effluent. *International Journal of Hydrogen Energy*, 40(36): 12424–12435.

Payi, B. 2017. Level 4B Water Restrictions Enacted in Cape Town. *IOL News*. https://www.iol.co.za/news/south-africa/western-cape/level-4b-water-restrictions-enacted-in-cape-town-10095498 [18 September 2017].

Pegram, G.C., Weston, D. & Reddy, S.T. 2014. Implementation of the Waste Discharge Charge System. *Water Practice & Technology*, 9(2): 125–134.

Permana, D., Rosdianti, D., Ishmayana, S., Rachman, S.D., Putra, H.E., Rahayuningwulan, D. & Hariyadi, H.R. 2015. Preliminary Investigation of Electricity Production Using Dual Chamber Microbial Fuel Cell (DCMFC) with *Saccharomyces cerevisiae* as Biocatalyst and Methylene Blue as an Electron Mediator. *Procedia Chemistry*, 17: 36–43.

Phukingngam, D., Chavalparit, O., Somchai, D. & Ongwandee, M. 2011. Anaerobic Baffled Reactor Treatment of Biodiesel-Processing Wastewater with High Strength of Methanol and Glycerol: Reactor Performance and Biogas Production. *Chemical Papers*, 65(5): 644–651.

Pirsaheb, M., Rostamifar, M., Mansouri, A.M., Zinatizadeh, A.A.L. & Sharafi, K. 2015. Performance of an Anaerobic Baffled Reactor (ABR) Treating High Strength Baker's Yeast Manufacturing Wastewater. *Journal of the Taiwan Institute of Chemical Engineers*, 47: 137–148.

Pitakpoolsil, W. & Hunsom, M. 2013. Adsorption of Pollutants from Biodiesel Wastewater Using Chitosan Flakes. *Journal of the Taiwan Institute of Chemical Engineers*, 44(6): 963–971.

Pletcher, D. & Walsh, F.C. 1993. *Industrial Electrochemistry*. 2nd ed. Glasgow: Blackie Academic & Professional.

Povrenović, D.S., Stojković, I.J., Stamenković, O.S. & Veljković, V.B. 2014. Purification Technologies for Crude Biodiesel Obtained by Alkali-Catalyzed Transesterification. *Renewable and Sustainable Energy Reviews*, 32: 1–15.

Prakash, G.K.S., Viva, F.A., Bretschger, O., Yang, B., El-Naggar, M. & Nealson, K. 2009. Inoculation procedures and characterization of membrane electrode assemblies for microbial fuel cells. *Journal of Power Sources*.

Pretorius, W. & Le Cordeur, M. 2016. Nersa Approves 9.4% Electricity Price Hike. *fin24*.

Prokkola, H., Heiska, E., Roppola, K., Kuokkanen, T. & Jaakko, R. 2007. Comparison Study of Different BOD Tests in the Determination of BOD7 Evaluated in a Model Domestic Sewage. *Journal of Automated Methods and Management in Chemistry*, 2007(39761): 1–4.

Qin, L., Fan, Z., Xu, L., Zhang, G., Wang, G., Wu, D., Long, X. & Meng, Q. 2015. A Submerged Membrane Bioreactor with Pendulum Type Oscillation (PTO) for Oily Wastewater Treatment: Membrane Permeability and Fouling Control. *Bioresource Technology*, 183: 33–41.

Rabaey, K., Angenent, L.T., Schroder, U. & Keller, J. 2010. *Bioelectrochemical Systems: From Extracellular Electron Transfer to Biotechnological Application*. London: IWA.

Rabaey, K., Clauwaert, P., Aelterman, P. & Verstraete, W. 2005. Tubular Microbial Fuel Cells for Efficient Electricity Generation. *Environmental Science and Technology*, 39(20): 8077–8082.

Rabaey, K. & Verstraete, W. 2005. Microbial Fuel Cells: Novel Biotechnology for Energy

Generation. *Trends in Biotechnology*, 23(6): 291–298.

Rahimnejad, M., Ghoreyshi, A.A., Najafpour, G. & Jafary, T. 2011. Power generation from organic substrate in batch and continuous flow microbial fuel cell operations. *Applied Energy*, 88(11): 3999–4004.

Rattanapan, C., Sawain, A., Suksaroj, T. & Suksaroj, C. 2011. Enhanced Efficiency of Dissolved Air Flotation for Biodiesel Wastewater Treatment by Acidification and Coagulation Processes. *Desalination*, 280(1–3): 370–377.

Ravindra, P. 2015. *Advances in Bioprocess Technology*. New York: Springer.

Rayment, C. & Sherwin, S. 2003. *Introduction to Fuel Cell Technology*. Notre Dame: University of Notre Dame.

Ren, L., Ahn, Y. & Logan, B.E. 2014. A Two-Stage Microbial Fuel Cell and Anaerobic Fluidized Bed Membrane Bioreactor (MFC-AFMBR) System for Effective Domestic Wastewater Treatment. *Environmental Science and Technology*, 48: 4199–4206.

Republic of South Africa. 1996. *Constitution of the Republic of South Africa, No. 108 of 1996*. South African Government.

Republic of South Africa. 1998a. National Environmental Management Act, No. 107 of 1988. *Government Gazette*, 401(19519): 1–37.

Republic of South Africa. 1998b. *National Water Act, No. 36 of 1998*.

Seijan, V., Bhatta, R., Malik, P.K., Madiajagan, B., Al-Hosni, Y.A.S., Sullivan, M. & Gaughan, J.B. 2016. Livestock as Sources of Greenhouse Gases and Its Significance to Climate Change. In B. L. Moya & J. Pouys, eds. *Greenhouse Gases*. ExLi4EvA: 243–259.

Selma, V.C., Cotrim, L.H.B., Rodrigues, J.A.D., Ratusznei, S.M., Zaiat, M. & Foresti, E. 2010. ASBR Applied to the Treatment of Biodiesel Production Effluent: Effect of Organic Load and Fill Time on Performance and Methane Production. *Applied Biochemical Biotechnology*, (162): 2365–2380.

Siles, J.A., Gutiérrez, M.C., Martín, M.A. & Martín, A. 2011. Physical-Chemical and Biomethanization Treatments of Wastewater from Biodiesel Manufacturing. *Bioresource Technology*, 102(10): 6348–6351.

Siles, J.A., Martín, M.A., Chica, A.F. & Martín, A. 2010. Anaerobic Co-Digestion of Glycerol and Wastewater Derived from Biodiesel Manufacturing. *Bioresource Technology*, 101(16): 6315–6321.

Silva, R.C., Rodrigues, J.A.D., Ratusznei, S.M. & Zaiat, M. 2013. Anaerobic Treatment of Industrial Biodiesel Wastewater by an ASBR for Methane Production. *Applied Biochemical Biotechnology*, 170: 105–118.

Singh, D., Pratap, D., Baranwal, Y., Kumar, B. & Chaudhary, R.K. 2010. Microbial fuel cells: A green technology for power generation. *Annals of Biological Research*, 1(3): 128–138.

Singh, K. 2016. Desperate Residents 'Drinking Sewage Water' as Taps Run Dry. *NEWS24*. http://www.news24.com/SouthAfrica/News/desperate-senekal-residents-drinking-sewage-water-as-taps-run-dry-20160104 [23 May 2016].

Smil, V. 2015. *Power Densities: A Key to Understanding Energy Sources and Uses*. 1st ed. Massachusettes: MIT.

Song, J., Liu, L., Yang, Q., Liu, J., Yu, T., Yang, F. & Crittenden, J. 2015. PVDF Layer as a

Separator on the Solution-Side of Air-Cathodes: The Electricity Generation, Fouling and Regeneration. *RSC Advances*, 5(65): 52361–52368.

Song, Y.-C., Yoo, K.S. & Lee, S.K. 2010. Surface Floating, Air-Cathode Microbial Fuel Cell with Horizontal Flow for Continuous Power Production from Wastewater. *Journal of Power Sources*, 195(19): 6478–6482.

Spellman, F.R. 2004. *Mathematics Manual for Water and Wastewater Treatment Plant Operators*. New York: Boca Raton: CRC Press.

Spellman, F.R. 2013. *Handbook of Water and Wastewater Treatment Plant Operations, Third Edition*. New York: Boca Raton: CRC Press.

Spellman, F.R. 2014. *Water and Wastewater Treatment Plant Operations*. 3rd ed. New York: Boca Raton: CRC Press.

Spiegel, C. 2007. *Designing and Building Fuel Cells*. K. P. McCoombs & L. Hagar, eds. New York: McGraw-Hill.

Steiman, M., Altemose, C., Buffington, D.E., Cauffman, G.R., Ferguson, M., Frier, M.C., Holland, L.J., Lloyd, W.A., Lumley-Sapanski, K., Perez, J.M., Roth, G.W. & Young, J. 2016. Safety in Small-Scale Biodiesel Production. *eXtension.org*. http://articles.extension.org/pages/29265/safety-in-small-scale-biodiesel-production [20 November 2017].

Stewart, M. & Arnold, K. 2009. *Emulsions and Oil Treating Equipment: Selection, Sizing and Troubleshooting*. 1st ed. Burlington: Gulf Professional.

Suehara, K., Kawamoto, Y., Fujii, E., Kohda, J., Nakano, Y. & Yano, T. 2005. Biological Treatment of Wastewater Discharged from Biodiesel Fuel Production Plant with Alkali-Catalyzed Transesterification. *Journal of Bioscience and Bioengineering*, 100(4): 437–442.

Sukkasem, C., Laehlah, S., Hniman, A., Sompong, O., Boonsawang, P., Rarngnarong, A., Nlsoa, M. & Klrdtongmee, P. 2011. Upflow Bio-Filter Circuit (UBFC): Biocatalyst Microbial Fuel Cell (MFC) Configuration and Application to Biodiesel Wastewater Treatment. *Bioresource Technology*, 102(22): 10363–10370.

Tchobanoglous, G., Burton, F.L. & Stensel, H.D. 2003. *Wastewater Engineering: Treatment and Reuse*. 4th ed. New York City: McGraw-Hill.

Templeton, M.R. & Butler, D. 2011. *Introduction to Wastewater Treatment*. London: Butler and Ventus.

Thelwell, E. 2014. South Africa's Looming Water Disaster. *NEWS24*.

Thompson, L.J., Gray, V., Lindsay, D. & von Holy, A. 2006. Carbon : Nitrogen : Phosphorus Ratios Influence Biofilm Formation by Enterobacter Cloacae and Citrobacter Freundii. *Journal of Applied Microbiology*, 101(5): 1105–13.

Tugtas, A.E., Cavdar, P. & Calli, B. 2011. Continuous Flow Membrane-Less Air Cathode Microbial Fuel Cell with Spunbonded Olefin Diffusion Layer. *Bioresource Technology*, 102(22): 10425–10430.

Van der Nest, G. 2015. The Economic Consequences of Load Shedding in South Africa and the State of the Electrical grid. *Tralac*. http://www.tralac.org/discussions/article/7000-the-economic-consequences-of-load-shedding-in-south-africa-and-the-state-of-the-electrical-grid.html [24 May 2016].

Veljković, V.B., Stamenković, O.S. & Tasić, M.B. 2014. The Wastewater Treatment in the Biodiesel Production with Alkali-Catalyzed Transesterification. *Renewable and Sustainable*

Energy Reviews, 32: 40–60.

Von Meier, A. 2006. *Electric Power Systems: A Conceptual Introduction*. 1st ed. New Jersey: John Wiley.

Von Sperling, M. 2007. *Basic Principles of Wastewater Treatment*. 2nd ed. Brazil: International Water Association.

Von Sperling, M. & De Lemos Chernicharo, C.A. 2005. *Biological Wastewater Treatment in Warm Climate Regions*. UK: International Water Association.

Wafler, M. 2010. *Anaerobic Baffled Reactor*. Wolhusen: Sustainable Sanitation and Water Management (SSWM).

Wang, A., Cheng, H., Ren, N., Cui, D., Lin, N. & Wu, W. 2012. Sediment microbial fuel cell with floating biocathode for organic removal and energy recovery. *Frontiers of Environmental Science and Engineering in China*, 6(4): 569–574.

Wang, J. 2004. Performance and Characteristics of an Anaerobic Baffled Reactor. *Bioresource Technology*, 93: 205–208.

Wang, J., Bi, F., Ngo, H., Guo, W., Jia, H., Zhang, H. & Zhang, X. 2016. Evaluation of Energy-Distribution of a hybrid Microbial Fuel Cell – Membrane Bioreactor (MFC – MBR) for Cost-Effective Wastewater Treatment. *Bioresource Technology*, 200: 420–425.

Wang, Y., Liu, X., Li, W., Li, F., Wang, Y., Sheng, G., Zeng, R.J. & Yu, H. 2012. A microbial Fuel Cell–Membrane Bioreactor Integrated System for Cost-Effective Wastewater Treatment. *Applied Energy*, 98: 230–235.

Wang, Y.K., Sheng, G.P., Li, W.W., Huang, Y.X., Yu, Y.Y., Zeng, R.J. & Yu, H.Q. 2011. Development of a Novel Bioelectrochemical Membrane Reactor for Wastewater Treatment. *Environmental Science and Technology*, 45(21): 9256–9261.

Warden Biomedia. 2014. Types of Biological Treatment. *Warden Plastics Limited*. http://www.wardenbiomedia.com/process/types.htm [10 July 2016].

Water Research Commission. 2015. Background to Current Drought Situation in South Africa. *Water Reseach Commission Drought Factsheet 1*: 2015. http://www.wrc.org.za/SiteCollection Documents/ Background to current drought situation in South Africa (3).pdf 10 August 2017.

Water Research Commission. 2016. WRC Study Investigates Quantification of Drought Shocks in South African Industries. *Water Research Commission*. http://www.wrc.org.za/News/Pages/ WRCstudyinvestigatesquantificationofdroughtshocksinSouthAfricanindustries.aspx [25 May 2016].

Water and Wastewater Measuring Solutions. 2002. *Determination of Biochemical Oxygen Demand (BOD).* Germany: Weilheim.

Xu, L., Zhao, Y., Doherty, L., Hu, Y. & Hao, X. 2016. Promoting the bio-cathode formation of a constructed wetland-microbial fuel cell by using powder activated carbon modified alum sludge in anode chamber. *Scientific Reports*, 6(May): 1–9.

Yadav, G., Kumar, R. & Sen, R. 2015. Fermentation Techniques in Bioenergy Production. In S.-K. Kim & C.-G. Lee, eds. *Marine Bioenergy: Trends and Developmentsnergy*. Florida: CRC: 111–134.

Yang, J. 2013. *Membrane Bioreactor for Wastewater Treatment*. 1st ed. Bookboon.

Yang, W., He, W., Zhang, F., Hickner, M.A. & Logan, B.E. 2014. Single-Step Fabrication Using a

Phase Inversion Method of Poly(Vinylidene Fluoride) (PVDF) Activated Carbon Air Cathodes for Microbial Fuel Cells. *Environmental Science and Technology Letters*, 1(10): 416–420.

Yang, W., Kim, K.-Y. & Logan, B.E. 2015. Development of Carbon Free Diffusion Layer for Activated Carbon Air Cathode of Microbial Fuel Cells. *Bioresource Technology*, 197: 318–322.

Yao, S., He, Y., Li, Y. & Xi, H. 2014. Effect of the Membrane Electrode Assemble Design on the Performance of Single Chamber Microbial Fuel Cells. *Energy Procedia*, 61: 1947–1951.

Yoo, K., Song, Y.C. & Lee, S.K. 2011. Characteristics and continuous operation of floating air-cathode microbial fuel cell (FA-MFC) for wastewater treatment and electricity generation. *KSCE Journal of Civil Engineering*, 15(2): 245–249.

You, S., Zhao, Q., Zhang, J., Jiang, J., Wan, C., Du, M. & Zhao, S. 2007. A Graphite-Granule Membrane-Less Tubular Air-Cathode Microbial Fuel Cell for Power Generation Under Continuously operational Conditions. *Journal of Power Sources*, 173(1): 172–177.

Yousefi, V., Mohebbi-Kalhori, D., Samimi, A. & Salari, M. 2015. ScienceDirect Effect of separator electrode assembly (SEA) design and mode of operation on the performance of continuous tubular microbial fuel cells (MFCs). *International Journal of Hydrogen Energy*, 41(1): 597–606.

Yu, L., Han, M. & He, F. 2013. A Review of Treating Oily Wastewater. *Arabian Journal of Chemistry*, 10(2): 1–10.

Yuan, X.-Z., Song, C., Wang, H. & Zhang, J. 2010. *Electrochemical Impedance Spectroscopy in PEM Fuel Cells: Fundamentals and Applications*. New York: Springer.

Zaher, K. & Hammam, G. 2014. Correlation between Biochemical Oxygen Demand and Chemical Oxygen Demand for Various Wastewater Treatment Plants in Egypt to Obtain the Biodegradability Indices. *International Journal of Sciences: Basic and Applied Research*, 13(1): 42–48.

Zhang, X., He, W., Ren, L., Stager, J., Evans, P.J. & Logan, B.E. 2015. COD Removal Characteristics in Air-Cathode Microbial Fuel Cells. *Bioresource Technology*, 176: 23–31.

Zhang, X., Xia, X., Ivanov, I., Huang, X. & Logan, B.E. 2014. Enhanced Activated Carbon Cathode Performance for Microbial Fuel Cell by Blending Carbon Black. *Environmental Science and Technology*, 48(3): 2075–2081.

Zhong, C., Zhang, B., Kong, L. & Ni, J. 2011. Electricity Generation from Molasses Wastewater by an Anaerobic Baffled Stacking Microbial Fuel Cell. *Journal of Chemical Technology Biotechnology*, 86(July 2010): 406–413.

Zhuwei, D.U., Qinghai, L.I., Meng, T. & Shaohua, L.I. 2008. Electricity Generation Using Membrane-less Microbial Fuel Cell during Wastewater Treatment. *Chinese Journal of Chemical Engineering*, 16(5): 772–777.

Zuo, Y., Maness, P.-C. & Logan, B.E. 2006. Electricity Production from Steam Exploded Corn Stover Biomass. *Energy Fuels*, 20(12): 1716.

APPENDICES

APPENDIX A:
Conversions and calculations reported in literature

A.1. Conversions and calculations in section 2.4

The following conversions and calculations are derived from the original data found in literature. Converted and calculated values can be found in Tables 2.3 and 2.4.

A.1.1. Sukkasem *et al*., 2011:

a. Average pH:

$$\frac{(10+1)+(10-1)}{2}=10$$

b. Average chemical oxygen demand (COD):

Conversion:

$$(218\ \pm 30\ g/l)\ \times\ (1000\ mg/g) = 218\,000\ \pm 30\,000\ mg/l$$

Average COD:

$$\frac{(218\,000+30\,000)+(218\,000-30\,000)}{2}=218\,000\ mg/l$$

c. Total suspended solids (TSS) conversion:

$$79.39\ g/l\ \times\ 1000\ mg/g\ = 79\,390\ mg/l$$

d. External resistance:

$$10\ \Omega\ \times\ 1000\ \Omega/k\Omega\ = 10\,000\ \Omega$$

e. Microbial fuel cell (MFC) volume:

Table A.1: MFC compartmental volumes

Location	Volume [l]
Pre-fermentation tank	8.0
Influent adjustment tank	8.0
Void volume per bottle	0.5
Up-flow anaerobic filter (UFAF) 1	1.0
UFAF 2	1.0
Biofilter Circuit (BFC) 1	1.0
BFC 2	1.0
BFC Cathode (granular activated carbon)	0.6

$$V_T = UFAF\ 1 + UFAF\ 2 + BFC\ 1 + BFC\ 2 = 1l + 1l + 1l + 1l = 4l$$

$$V_W = V_T - V_{Void} = 4l - (4 \times 0.5l) = 2l$$

A.1.2. Phukingngam *et al*., 2011:

a. COD conversion:

$(56.4\ g/l)\ \times\ (1000\ mg/g) = 56\ 400\ mg/l$

b. Fats, oils and grease (FOG) conversion:

$(3.27\ g/l)\ \times\ (1000\ mg/g) = 3\ 270\ mg/l$

c. TSS conversion:

$(0.4\ g/l)\ \times\ (1000\ mg/g) = 400\ mg/l$

A.1.3. Suehara *et al*., 2005:

a. COD conversion:

$(14.8\ g/l)\ \times\ (1000\ mg/g) = 14\ 800\ mg/l$

b. FOG conversion:

$(15.1\ g/l)\ \times\ (1000\ mg/g) = 15\ 100\ mg/l$

c. TSS conversion:

$(2.67\ g/l)\ \times\ (1000\ mg/g) = 2\ 670\ mg/l$

A.1.4. Pitakpoolsil & Hunsom, 2013:

a. Average pH:

$$\frac{(9.25 + 10.26)}{2} = 9.8$$

b. Average COD:

$$\frac{(29\ 595 + 54\ 362)}{2} = 41\ 979\ mg/l$$

c. Average biological oxygen demand (BOD):

$$\frac{(1\ 492 + 2\ 286)}{2} = 1\ 889\ mg/l$$

d. Average FOG:

$$\frac{(1\ 040 + 1\ 710)}{2} = 1\ 375\ mg/l$$

e. Average TSS:

$$\frac{(670 + 690)}{2} = 680\ mg/l$$

f. TSS removal %:

$$\varepsilon_{TSS} = \frac{OC_{feed}^{TSS} - OC_{product}^{TSS}}{OC_{feed}^{TSS}} \times 100 = \frac{680\ mg/l\ - 70\ mg/l}{680\ mg/L} \times 100 =\ 89.7\ \%$$

A.1.5. Daud *et al*., 2015:

a. Average pH:

$$\frac{(4.5 + 5.5)}{2} = 5$$

A.1.6. Siles *et al*., 2010 and Siles *et al*., 2011:

a. Average pH:

$$\frac{(10.35 + 0.03) + (10.35 - 0.03)}{2} = 10.4$$

b. Average COD:

Conversion:

$$(428 \pm 12\ g/l) \times (1000\ mg/g) = 4288\,000 \pm 12\,000\ mg/l$$

Average COD:

$$\frac{(428\,000 + 12\,000) + (428\,000 - 12\,000)}{2} = 428\,000\ mg/l$$

A.1.7. Rattanapan *et al*., 2011:

a. Average pH:

$$\frac{(8.5 + 10.5)}{2} = 9.5$$

b. Average COD:

$$\frac{(60\,000\ mg/l + 150\,000\ mg/l)}{2} = 105\,000\ mg/l$$

c. Average BOD:

$$\frac{(30\,000\ mg/l + 60\,000\ mg/l)}{2} = 45\,000\ mg/l$$

d. Average FOG:

$$\frac{(7\,000\ mg/l + 15\,000\ mg/l)}{2} = 11\,000\ mg/l$$

A.1.8. Kakarla *et al*., 2015:

a. Air MFC: Current density:

$$1.21\ A/m^2 \times 1000\ mA/A = 1\,210\ mA/m^2$$

b. Air from algal bioreactor (ABR*) MFC: Current density:

$7.8\ A/m^2\ \times\ 1000\ mA/A\ =\ 780\ mA/m^2$

c. Air MFC: Maximum power density (PD):

$0.44\ W/m^2\ \times\ 1000\ mW/W\ =\ 440\ mW/m^2$

d. Air from ABR* MFC: Maximum PD:

$0.37\ W/m^2\ \times\ 1000\ mW/W\ =\ 370\ mW/m^2$

e. Anode working volume:

Conversion:

$$\frac{205\ ml}{1000\ ml/dm^3} = 0.205\ dm^3$$

f. MFC volume:

$V_T = V_T^{Anode} + V_T^{Cathode}$

$V_T = 0.21\ dm^3 + 0.045\ dm^3 = 0.255\ dm^3$

g. Air-cathode working volume:

$V_W^{Cathode} = V_T^{Anode} + V_T^{Cathode}$

$V_W^{Cathode} = 0.205\ dm^3 + 0.045\ dm^3 = 0.25\ dm^3$

h. Air form ABR* working volume:

$V_W = V_T^{Anode} + V_T^{Cathode} + V_W^{ABR*}$

$V_W = 0.205\ dm^3 + 0.045\ dm^3 + 0.58\ dm^3 = 0.83\ dm^3$

A.1.9. Wang *et al*., 2012:

a. Averaged current:

$$\frac{(1.9\ mA + 0.4\ mA) + (1.9\ mA - 0.4\ mA)}{2} = 1.9\ mA$$

b. Maximum PD:

$0.053\ W/m^2\ \times\ 1000\ mW/W\ =\ 53\ mW/m^2$

A.1.10. Mahendra & Mahavarkar, 2013:

Table A.2: Anode and cathode electrodes (graphite rods) dimensions

Dimensions	Length	Diameter	Radius
[mm]	90	2	1
[m]	0.09	0.002	0.001

a. Conversions:

   Length:

   $$\frac{90\ mm}{1000\ mm/m} = 0.09\ m$$

   Diameter:

   $$\frac{2\ mm}{1000\ mm/m} = 0.002\ m$$

b. Radius:

   $$r = \frac{d}{2} = \frac{0.002\ m}{2} = 0.001\ m$$

c. Electrode volume:

   $$V_{Electrode} = \pi r^2 L = \pi(0.001)^2(0.09\ m) = 2.827\ \times 10^{-7}\ m^3$$

d. Electrode surface area:

   $$SA_{Electrode} = (2\pi rL) + (2\pi r^2) = \left(2\pi(0.001\ m)(0.09\ m)\right) + (2\pi(0.001\ m)^2)$$

   $$SA_{Electrode} = (5.65\ \times 10^{-4}\ m^2) + \ (6.28\ \times 10^{-6}\ m^2) = \ 5.72\ \times 10^{-4}\ m^2$$

   Conversion:

   $$(5.72\ \times 10^{-4}\ m^2)\ \times\ (10\ 000\ cm^2/m^2) = 5.72\ cm^2$$

A.1.11. Kim *et al*., 2015:

a. Anode working volume:

   Conversion:

   $$\frac{320\ ml}{1000\ ml/dm^3} = 0.32\ dm^3$$

A.1.12. Liu & Ramnarayanan, 2004:

a. Anode working volume:

   Conversion:

   $$\frac{388\ ml}{1000\ ml/dm^3} = 0.388\ dm^3$$

b. 8 x Graphite rods (anode electrodes):

Table A.3: Anode electrodes (graphite rods) dimensions

Dimensions	Length	Diameter	Radius
[mm]	150	6.15	3.075
[cm]	15	0.615	0.3075

Conversions:

Length:

$$\frac{150\ mm}{10\ mm/cm} = 15\ cm$$

Diameter:

$$\frac{6.15\ mm}{10\ mm/cm} = 0.615\ cm$$

c. Radius:

$$r = \frac{d}{2} = \frac{0.615\ cm}{2} = 0.3075\ cm$$

d. Electrode surface area:

$$SA_{Electrode} = (2\pi rL) + (2\pi r^2) = \left(2\pi(0.3075\ cm)(15\ cm)\right) + (2\pi(0.3075\ cm)^2)$$

$$SA_{Electrode} = (28.98\ cm^2) + (0.59\ cm^2) = 29.58\ cm^2$$

A.2. Conversions and calculations in section 2.9

The following conversions and calculations are derived from the original data found in literature. Converted and calculated values can be found in Table 2.7.

A.2.1. Zhong *et al*., 2011

a. Total MFC volume:

$$V_T = Length\ (L) \times Width(W) \times Height(H)$$

$$V_T = 34.5\ cm \times 6\ cm \times 12\ cm$$

$$V_T = 2\ 484\ cm^3$$

$$V_T = 2\ 484\ ml$$

A.2.2. Li *et al*., 2008

a. Total MFC volume:

$$V_T = L \times W \times H$$

$$V_T = 25.5\ cm \times 11.5\ cm \times 25\ cm$$

$$V_T = 7\ 331.25\ cm^3$$

$$V_T = 7\ 331.25\ ml$$

A.2.3. Sukkasem *et al*., 2011

$$\varepsilon_{COD} = \frac{OC_{feed}^{COD} - OC_{product}^{COD}}{OC_{feed}^{COD}} \times 100$$

$$\varepsilon_{COD} = \frac{30\ g/l - 15\ g/l}{30\ g/l} \times 100$$

$$\varepsilon_{COD} = 50\ \%$$

A.2.4. Mahendra & Mahavarkar, 2013

a. Anode surface area:

$$SA_A = 2\pi rL + 2\pi r^2$$

$$SA_A = 2\pi(0.2)(9) + 2\pi(0.2)^2$$

$$SA_A = 11.56\ cm^2$$

A.2.5. Liu & Ramnarayanan, 2004

a. Total MFC volume:

$$V_T = \pi r^2 L$$

$$V_T = \pi(3.25)^2(15)$$

$$V_T = 497.75\ cm^3$$

$$V_T = 497.75\ ml$$

b. Anode (8) surface area:

$$SA_A = 8 \times (2\pi rL + 2\pi r^2)$$

$$SA_A = 8 \times (2\pi(0.3075)(15) + 2\pi(0.3075)^2)$$

$$SA_A = 8 \times 29.84\ cm^2$$

$$SA_A = 238.75\ cm^2$$

A.2.6. Kim *et al*., 2015

a. Total MFC volume:

$$V_T = L \times W \times H$$

$$V_T = 4\ cm \times 6\ cm \times 6\ cm$$

$$V_T = 216\ cm^3$$

$V_T = 216\ ml$

A.2.7. Kakarla *et al*., 2015

a. Distance between electrodes conversion:

$3\ cm\ \times 10\ mm/cm = 30\ mm$

b. PD conversion:

$0.63\ W/m^2\ \times\ 1000\ mW/W\ =\ 630\ mW/m^2$

A.2.8. Zhang *et al*., 2015

a. Total MFC volume:

$V_T = L\ \times\ W\ \times\ H$

$V_T = 4\ cm\ \times\ 4\ cm\ \times\ 4\ cm$

$V_T = 64\ cm^3$

$V_T = 64\ ml$

A.2.9. Min & Angelidaki, 2008

a. Distance between electrodes conversion:

$3\ cm\ \times 10\ mm/cm = 30\ mm$

b. Anode surface area (SA):

$SA_A = L\ \times\ W$

$SA_A = 4\ cm\ \times\ 4\ cm$

$SA_A = 16\ cm^2$

A.2.10. You *et al*., 2007

a. PD conversion:

$50.2\ W/m^3\ \times\ 1000\ mW/W\ =\ 52\ 000\ mW/m^3$

b. Anode surface area:

$SA_A = SA_{Anode\ 1} + SA_{rod}$

$SA_A = (\ SA_{Anode\ 1}) + (2\pi rL +\ 2\pi r^2)$

$SA_A = (\,31\ cm^2) + (2\pi(0.5)(5) + \ 2\pi(0.5)^2)$

$SA_A = (\,31\ cm^2) + (17.27\ cm^2)$

$SA_A = 48.28\ cm^2$

A.2.11. Pasupuleti *et al*., 2015

a. Total MFC volume:

$V_T = L\ \times\ W\ \times\ H$

$V_T = 11\ cm\ \times\ 11\ cm\ \times\ 0.82\ cm$

$V_T = 99.22\ cm^3$

$V_T = 99.22\ ml$

b. Anode (2) surface area:

$SA_A = 2\ \times\ (L\ \times\ W)$

$SA_A = 2\ \times\ (11\ cm\ \times\ 10\ cm)$

$SA_A = 2\ \times\ 110\ cm^2$

$SA_A = 220\ cm^2$

A.2.12. Gajda *et al*., 2015

a. Total MFC volume:

$V_T = \pi r^2 L$

$V_T = \pi(2.1)^2(10)$

$V_T = 138\ cm^3$

$V_T = 138\ ml$

b. MFC working volume:

$V_W = \pi r^2 L$

$V_W = \pi(1.8)^2(10)$

$V_W = 101.79\ cm^3$

$V_W = 101.79\ ml$

A.2.13. Min & Logan, 2004

a. Total MFC volume:

$V_T = L\ \times\ W\ \times\ H$

$V_T = 15\ cm\ \times\ 15\ cm\ \times\ 2\ cm$

$V_T = 450\ cm^3$

$V_T = 450\ ml$

b. Anode surface area:

$SA_A = L\ \times\ W$

$SA_A = 10\ cm\ \times\ 10\ cm$

$SA_A = 100\ cm^2$

A.2.14. Martinucci *et al*., 2015

a. Anode surface area (1):

$SA_A = L\ \times\ W$

$SA_A = 20\ cm\ \times\ 15\ cm$

$SA_A = 300\ cm^2$

b. Anode surface area (2):

$SA_A = L\ \times\ W$

$SA_A = 20\ cm\ \times\ 30\ cm$

$SA_A = 600\ cm^2$

c. Anode surface area (3):

$SA_A = L\ \times\ W$

$SA_A = 40\ cm\ \times\ 30\ cm$

$SA_A = 1\ 200\ cm^2$

A.2.15. Aldrovandi *et al*., 2009

a. Total MFC volume:

$V_T = 18\ l + 18\ l$

$V_T = 36\ l$

$V_T = 36\ 000\ ml$

A.2.16. Wang *et al*., 2016

a. Total MFC volume:

$V_T = L\ \times\ W\ \times\ H$

$V_T = 10\ cm\ \times\ 10\ cm\ \times\ 10\ cm$

$V_T = 1\,000\ cm^3$

$V_T = 1\,000\ ml$

b. Anode (2) surface area:

$SA_A = 2\ \times\ (L\ \times\ W)$

$SA_A = 2\ \times\ (20\ cm\ \times\ 10\ cm)$

$SA_A = 2\ \times\ 200\ cm^2$

$SA_A = 400\ cm^2$

c. Cathode (2) surface area:

$SA_C = 2\pi rL + \ 2\pi r^2$

$SA_C = 2\pi(0.3)(20) + \ 2\pi(0.3)^2$

$SA_C = 38.26\ cm^2$

A.2.17. Jang *et al*., 2004

a. Total MFC volume:

$V_T = \pi r^2 L$

$V_T = \pi(5)^2(100)$

$V_T = 7\,853.98\ cm^3$

$V_T = 7\,853.98\ ml$

A.2.18. Zhuwei *et al*., 2008

a. Total MFC volume:

$V_T = \pi r^2 L$

$V_T = \pi(5)^2(60)$

$V_T = 4\,712\ cm^3$

$V_T = 4\,712\ ml$

A.2.19. Ghangrekar & Shinde, 2007

a. Total MFC volume:

$V_T = \pi r^2 L$

$V_T = \pi(7.5)^2(60)$

$V_T = 10\,602.88\ cm^3$

$V_T = 10\,602.88\,ml$

b. MFC working volume:

$V_W = \pi r^2 L$

$V_W = \pi(7.5)^2(26)$

$V_W = 4\,594.58\,cm^3$

$V_W = 4\,594.58\,ml$

A.2.20. Song *et al*., 2010

a. Total MFC volume:

$V_T = L \times W \times H$

$V_T = 15\,cm \times 50\,cm \times 2.5\,cm$

$V_T = 187.50\,cm^3$

$V_T = 187.50\,ml$

A.2.21. An *et al*., 2009

a. Total MFC volume:

$V_T = \pi r^2 L$

$V_T = \pi(2.5)^2(13)$

$V_T = 255.25\,cm^3$

$V_T = 255.25\,ml$

b. Anode surface area:

$SA_A = 2\pi rL + 2\pi r^2$

$SA_A = 2\pi(2.5)(0.06) + 2\pi(0.06)^2$

$SA_A = 0.97\,cm^2$

c. Cathode surface area:

$SA_C = 2\pi rL + 2\pi r^2$

$SA_C = 2\pi(2.5)(0.06) + 2\pi(0.06)^2$

$SA_C = 0.97\,cm^2$

A.2.22. Miyahara *et al*., 2015

a. Total MFC volume:

$V_W = 1\ L$

$V_W = 1\ 00\ ml$

b. Anode (2) surface area:

$SA_A = 2\ \times\ 68\ cm^2$

$SA_A = 136\ cm^2$

c. Cathode (2) surface area:

$SA_C = 2\ \times 65\ cm^2$

$SA_C = 130\ cm^2$

APPENDIX B:
Determination of ABR-MFC working volume

B.1. Anaerobic baffled reactor (ABR) total volume

Table B.1: ABR-MFC dimensions

Dimensions [cm]	ABR-MFC	Baffles	Separators	Anode Electrodes
Length	105	31	31	-
Width	31	1	1	-
Height	37	33.5	30.8	19.99
Diameter	-	-	-	10.16

$$V_T^{ABR} = L \times W \times H$$
$$V_T^{ABR} = 105\ cm \times 31\ cm \times 37\ cm$$
$$V_T^{ABR} = 120435\ cm^3$$
$$V_T^{ABR} = 120.44\ l$$

B.2. Volume of 6 baffles

$$V_{Baffle} = L_{Baffle} \times W_{Baffle} \times H_{Baffle}$$
$$V_{Baffle} = 31\ cm \times 1\ cm \times 33.5\ cm$$
$$V_{Baffle} = 1038.50\ cm^3$$
$$V_{Baffle} = 1.04\ l$$

The ABR contains 6 identical baffles. Therefore, the volume of 1 baffle is multiplied by 5 in order to obtain the total baffle volume.

$$V_T^{Baffle} = V_{Baffle} \times 6$$
$$V_T^{Baffle} = 1.04\ l \times 6$$
$$V_T^{Baffle} = 6.23\ l$$

B.3. Volume of 5 separators

$$V_{Separator} = L_{Separaor} \times W_{Separator} \times H_{Separator}$$
$$V_{Separator} = 31\ cm \times 1\ cm \times 30.8\ cm$$

$$V_{Separator} = 954.8\ cm^3$$
$$V_{Separator} = 0.96\ l$$

The ABR contains 5 identical separators. Therefore, the volume of 1 separator is multiplied by 6 in order to obtain the total separator volume.

$$V_T^{Separator} = V_{Separator} \times 5$$
$$V_T^{Separator} = 0.96\ l \times 5$$
$$V_T^{Separator} = 4.77\ l$$

B.4. Volume of 6 carbon fibre brush anode electrodes

The volume of 6 identical carbon fibre anode electrodes was determined by the displacement of water in a measuring cylinder. One anode electrode was submerged in 80 ml water. It was found that the displacement of one anode electrode equated to 15 ml (0.015 L) of water. The volume of 1 anode electrode was then multiplied by 6 in order to obtain the total anode electrode volume.

$$V_T^{Anode} = V_{Anode} \times 6$$
$$V_T^{Anode} = 0.015\ l \times 6$$
$$V_T^{Anode} = 0.09\ l$$

B.5. Total void volume

Table B.2: Void volume in ABR-MFC

Dimensions [cm]	ABR-MFC	Baffles
Length	105	31
Width	31	1
Height	6.2	6.2

B.5.1. ABR-MFC void volume

$$V_{Void}^{ABR} = L_{Void}^{ABR} \times W_{Void}^{ABR} \times H_{Void}^{ABR}$$

$$V_{Void}^{ABR} = 105\ cm\ \times\ 31\ cm\ \times\ 6.2\ cm$$
$$V_{Void}^{ABR} = 20\ 181\ cm^3$$
$$V_{Void}^{ABR} = 20.18\ l$$

B.5.2. Volume of baffles in void volume

$$V_{Void}^{ABR} = L_{Void}^{Baffle}\ \times\ W_{Void}^{Baffle}\ \times\ H_{Void}^{Baffle}$$
$$V_{Void}^{ABR} = 31\ cm\ \times\ 1\ cm\ \times\ 6.2\ cm$$
$$V_{Void}^{ABR} = 192.2\ cm^3$$
$$V_{Void}^{ABR} = 0.19\ l$$

The ABR contains 6 baffles. Therefore, the void volume of one baffle is multiplied by six in order to obtain the total void volume of the baffles.

$$V_{Total\ Void}^{Baffle} = V_{Baffle}\ \times 6$$
$$V_{Total\ Void}^{Baffle} = 0.19\ l\ \times 6$$
$$V_{Total\ Void}^{Baffle} = 1.15\ l$$

B.6. ABR working volume

$$V_W^{ABR} = V_T^{ABR} - V_T^{Baffle} - V_T^{Separator} - V_{Void}^{ABR} + V_{Total\ Void}^{Baffles}$$
$$V_W^{ABR} = 120.44\ l - 6.23\ l - 4.77\ l - 20.18\ l + 1.15\ l$$
$$V_W^{ABR} = 90.41\ l$$

B.7. ABR-MFC working volume

$$V_W^{ABR-MFC} = V_W^{ABR} - V_T^{Anode}$$
$$V_W^{ABR-MFC} = 90.41\ l - 0.09\ l$$
$$V_W^{ABR-MFC} = 90.32\ l$$

APPENDIX C:
Determination of system conditions

C.1. Flow rate determination for set hydraulic retention time (HRT)

Sample calculation for flow rate of HRT of 10 days (OLR 1) (using Equation 2.3):

$$HRT = \frac{V_W^{ABR}}{Q_{feed}}$$

$$Q_{feed} = \frac{V_W^{ABR}}{HRT}$$

$$Q_{feed} = \frac{90.32\ l}{10\ days}$$

$$Q_{feed} = 9.03\ l/day$$

Converting from l/day to ml/min:

$$\frac{9.03\ l/day\ \times\ 1000\ ml/l}{24\ h/day\ \times\ 60\ min/h} = 6.27\ ml/min$$

Steps for setting flow rate to HRT of 10 days

1. Set the peristaltic pump (Watson Marlow 520S) to a flow rate of 6 ml/min and HRT of 10 days.
2. Place measuring cylinder below product outlet stream.
3. Use a stopwatch to measure and record the time.
4. Record treated substrate volume in the measuring cylinder.
5. Calculate flow rate from recorded data (refer to sample calculation below).
6. If desired HRT is not obtained, increase/decrease the flow rate on the peristaltic pump and repeat steps 2 to 5 until desired HRT is obtained.

Sample calculation for flow rate determination via the bucket-and-stopwatch method:

Table C.1: ABR-MFC flow rate measurements

Trial [No.]	Time [min]	Volume [ml]	Flow Rate [ml/min]
1	10	65	6.5
2	10	66	6.6
Average	10	65.5	6.55

The average volumetric flow rate was determined as follows:

$$Q_{feed} = \frac{V_{ave}}{t_{ave}}$$

$$Q_{feed} = \frac{65.5\ ml}{10.0\ min}$$

$$Q_{feed} = \ 6.55\ ml/min$$

Sample calculation for HRT from flow rate:

Converting from ml/min to l/day:

$$\frac{6.55\ ml/min\ \times\ 60\ min/h\ \times 24\ h/day}{1000\ ml/min} = 9.43\ l/day$$

$$HRT = \frac{V_W^{ABR}}{Q_{feed}}$$

$$HRT = \frac{90.32\ l}{9.43\ l/day}$$

$$HRT = 9.58\ days$$

C.2. Organic loading rate (OLR) determination

Sample calculation for determining OLR (using a combination of Equations 2.3 and 2.4):

$$OLR = OC_{feed}^{COD} \times \frac{V_W^{ABR}}{Q_{feed}}$$

$$OLR = \frac{OC_{feed}^{COD}}{HRT}$$

$$OLR = \frac{10\ 979\ mg\ COD/l}{9.58\ day}$$

$$OLR = \ 1\ 146.53\ mg\ COD/l.day$$

$$OLR = \ 1.15\ kg\ COD/m^3.day$$

APPENDIX D:
Analytical procedures

D.1. Daily operational parameters

Steps for calibrating the pH of the PCSTestr35:

1. Remove sensor cap of PCSTestr35.
2. Press and release the “ON/OFF” button to switch on the PCSTestr35.
3. Press and release the “MODE” button to select the pH mode.
4. Immerse the sensor into the 4.01 pH buffer.
5. Press and release the “CAL” button.
6. Allow the pH value on the display to stabilise.
7. Press and release the “MODE” button to confirm the calibration value.
8. Remove PCSTestr35 from pH buffer and rinse the protected sensor with distilled water.
9. Repeat steps 4 to 8 for pH buffers 7.01 and 10.01.
10. Press and release the “CAL” button to return to measurement mode.

Steps for calibrating the conductivity of the PCSTestr35:

1. Remove sensor cap of PCSTestr35.
2. Press and release the “ON/OFF” button to switch on the PCSTestr35.
3. Press and release the “MODE” button to select the conductivity mode.
4. Immerse the sensor in the 1413 µS conductivity buffer.
5. Press and release the “CAL” button.
6. Allow the conductivity value on the display to stabilise.
7. Press and release the “MODE” button to confirm the calibration value.
8. Remove PCSTestr35 from conductivity buffer and rinse the protected sensor with distilled water.
9. Press and release the “CAL” button to return to measurement mode.

Steps for calibrating the total dissolved solids (TDS) of the PCSTestr35:

1. Remove sensor cap of PCSTestr35.
2. Press and release the “ON/OFF” button to switch on the PCSTestr35.
3. Press and release the “MODE” button to select the TDS mode.
4. Immerse the sensor in the 300 ppm TDS buffer.

5. Press and release the “CAL” button.
6. Press the “HOLD” or “CAL” button(s) to manually adjust the TDS value on the display to the value of the calibration solution (i.e. 300 ppm).
7. Press and release the “MODE” button to confirm the calibration value.
8. Remove PCSTestr35 from TDS buffer and rinse the protected sensor with distilled water.
9. Press and release the “CAL” button to return to measurement mode.

Steps for determining daily operational parameters:

1. Transfer 50 ml of sample into a glass beaker.
2. Remove sensor cap of PCSTestr35.
3. Press and release the “ON/OFF” button to switch on the PCSTestr35.
4. Immerse the sensor into the sample.
5. Press and release the “MODE” button to select the parameter to be measured (e.g. pH).
6. The reading for the chosen parameter will be displayed on the screen.
7. Record displayed reading once the reading has stabilised.
8. Press and release the “MODE” button to measure remaining parameters (i.e. TDS, conductivity and salinity) using the PCSTestr35.
9. Remove PCSTestr35 from the sample and rinse the protected sensor with distilled water.
10. Carefully dry the casing of the protected sensor.
11. Repeat steps 1 to 8 for new samples to be tested.
12. Press and release the “ON/OFF” button to switch off the PCSTestr35.
13. Replace sensor cap of PCSTestr35 once all samples have been tested.

D.2. Turbidity determination

Steps for calibrating the TN-100 turbidimeter:

1. Place the CAL 1 standard (800 NTU) into the TN-100 turbidimeter.
2. Align the arrow on the calibration vial with the arrow on the TN-100 turbidimeter.
3. Cover the calibration vial with the supplied light shield cap.
4. Press and release the “ON/OFF” button to switch on the TN-100 turbidimeter.
5. Press and release the “CAL” button once.
6. Press the “READ/ENTER” button to start the calibration.
7. Once calibrated, the TN-100 turbidimeter displays “CAL 2 100 NTU”.

8. Repeat steps 1 to 7 for CAL 2 (100 NTU), CAL 3 (20.0 NTU) and CAL 4 (0.02 NTU).
9. The display shows “STbY” once successfully calibrated.

Steps for determining turbidity:

1. Fill a clean and dry sample vial with the sample (approximately 10 ml) to be measured up to the mark indicated on the sample vial.
2. Cap the sample vial with the supplied screw cap.
3. Ensure vial is clean and dry by wiping the sample vial with the supplied lint-free cloth.
4. Place sample vial into the TN-100 turbidimeter.
5. Align the arrow on the sample vial with the arrow on the TN-100 turbidimeter.
6. Cover the sample vial with the supplied light shield cap.
7. Press and release the “ON/OFF” button to switch the TN-100 turbidimeter on.
8. Press and release the “READ/ENTER” button once.
9. The measured reading is then displayed on the screen of the TN-100 turbidimeter.
10. Remove sample vial from TN-100 turbidimeter.
11. Repeat steps 1 to 10 for additional samples.
12. Press “ON/OFF” button to switch the TN-100 turbidimeter off.

D.3. COD determination

Steps for determining total COD [High Range]

1. Set TR420 Thermoreactor to a set temperature of 148 °C for 2 hours.
2. Add 1.0 ml sample to a clean and dry test cell.
3. Add 2.2 ml Merck COD solution A (Cat. No. 1.14679.0495) to test cell.
4. Add 1.8 ml Merck COD solution B (Cat. No. 1.14680.0495) to test cell.
5. Close test cell containing mixture tightly.
6. Mix solution in test cell vigorously using the vortex mixer.
7. Place test cell into pre-heated TR420 Thermoreactor and allow solution to react for 2 hours at 148 °C.
8. Remove reacted test cell from TR420 Thermoreactor and allow to cool for 10 minutes.
9. Mix solution in test cell vigorously using the vortex mixer.
10. Allow solution to cool to room temperature for 30 minutes.

11. Place test cell into NOVA60 Spectroquant to measure COD concentration of sample using code 024 for high range measurements.

Steps for determining total COD [Low Range]

1. Set TR420 Thermoreactor to a set temperature of 148 °C for 2 hours.
2. Add 0.3 ml sample to a clean and dry test cell.
3. Add 2.85 ml Merck COD solution A (Cat. No. 1.14538.0065) to test cell.
4. Add 3.0 ml Merck COD solution B (Cat. No. 1.14539.0495) to test cell.
5. Close test cell containing mixture tightly.
6. Mix solution in test cell vigorously using the vortex mixer.
7. Place test cell into pre-heated TR420 Thermoreactor and allow solution/mixture to react for 2 hours at 148 °C.
8. Remove reacted test cell from TR420 Thermoreactor and allow to cool for 10 minutes.
9. Mix solution in test cell vigorously using the vortex mixer.
10. Allow solution to cool to room temperature for 30 minutes.
11. Place test cell into NOVA60 Spectroquant to measure COD concentration of sample using code 023 for low range measurements.

D.3.1: Determination of BOD:COD ratio

1 litre full-strength biodiesel wastewater (BDWW) was analysed by an outside independent South African National Accredited System (SANAS) accredited laboratory. It was found that the BOD and COD of the full-strength BDWW was 78 503 mg/l and 115 400 mg/l, respectively. Refer to Table 4.1 for full chemical analysis of full-strength BDWW.

$$BOD : COD$$
$$78\,503\ mg/l : 115\,400\ mg/l$$
$$0.68 : 1$$

D.4. Solids determination

D.4.1. TSS

Steps for determining TSS:

1. Connect the Büchner funnel to the vacuum-pressure pump.
2. Place pre-weighed reinforced glass filter paper into the Büchner funnel.
3. Switch on the vacuum-pressure pump.
4. Pipette 10 ml sample onto the filter paper contained in the Büchner funnel.
5. Switch off the vacuum-pressure pump once all sample has been vacuumed into the flask.
6. Remove filter paper from the Büchner funnel and place in the oven at 80 °C for 1 hour.
7. Weigh dried filter paper.
8. Calculate TSS using Equation D.1 – refer to sample calculation.

Sample calculation of TSS determination (OLR 1):

$$TSS = \frac{m_{post\,(g)} - m_{pre\,(g)}}{V_{sample\,(ml)}} \times 1000\,ml/l \qquad \text{(Eq. D.1)}$$

$$TSS = \frac{0.2579\,mg - 0.2271\,mg}{10\,ml} \times 1000\,ml/l$$

$$TSS = 3.08\,mg/l$$

D.4.2. Volatile suspended solids (VSS)

Steps for determining VSS:

1. Determine TSS using method described in D.4.1.
2. Place filter paper (used to determine TSS) in oven at 550 °C for 30 minutes.
3. Carefully, remove combusted filter paper from oven and allow to reach room temperature.
4. Weigh combusted filter paper.
5. Calculate VSS using Equation D.2 – refer to sample calculation.

Sample calculation of VSS determination (OLR 1):

$$VSS = \frac{m_{post\,(mg)} - m_{combust\,(mg)}}{V} \times 1000\,ml/l \qquad \text{(Eq. D.2)}$$

$$VSS = \frac{0.2579\,mg\ -\ 0.2176\,mg}{10\,ml} \times 1000\,ml/l$$

$$VSS = 4.03\,mg/l$$

D.5. Total nitrates (as nitrogen) determination

Steps for determining ammonium concentration

1. Place 1 level micro-spoon of reagent NO_3-1 into a clean and dry test cell.
2. Using a pipette, add 5 ml of reagent NO_3-2 into the test cell containing reagent NO_3-1.
3. Close test cell containing mixture tightly.
4. Shake test cell vigorously using vortex mixer until NO_3-1 reagent has dissolved completely.
5. Using a pipette, add 1.5 ml sample to the mixture in the test cell.
6. Allow the solution to react for 10 minutes.
7. Transfer sample to 10 mm clean and dry cuvette.
8. Place reference test cell into NOVA60 Spectroquant with the barcode in the forward-facing position to select the nitrate measurement option.
9. Place 10 mm test cell containing solution mixture into NOVA60 Spectroquant to measure nitrate content.

D.6. Phosphorous determination

D.6.1. Total phosphate (TP) determination

Steps for determining TP concentration [samples with low COD concentration]

1. Set TR420 Thermoreactor to a set temperature of 120 °C for 30 minutes.
2. Add 1 ml sample to clean and dry test cell.
3. Add 1 dose P-1K to test cell.
4. Close test cell containing mixture tightly.
5. Shake test cell and mix vigorously using vortex mixer.
6. Place test cell into TR420 Thermoreactor and allow solution/mixture to react at 120 °C for 30 minutes.
7. Remove reacted test cell from TR420 Thermoreactor and allow to cool to room temperature for 30 minutes.

8. Place test cell into NOVA60 Spectroquant with the barcode in forward position to measure TP concentration of sample.

Steps for determining TP concentration [samples with high COD concentration]

1. Set TR420 Thermoreactor to a set temperature of 120 °C for 30 minutes.
2. Add 1 ml sample to clean and dry test cell.
3. Add 2 doses P-1K to test cell.
4. Close test cell containing mixture tightly.
5. Shake test cell and mix vigorously using vortex mixer.
6. Place test cell into TR420 Thermoreactor and allow solution/mixture to react at 120 °C for 30 minutes.
7. Remove reacted test cell from TR420 Thermoreactor and allow to cool to room temperature for 30 minutes.
8. Place test cell into NOVA60 Spectroquant with the barcode in forward position to measure TP concentration of sample.

D.6.2. Ortho-phosphate (OP) determination

Steps for determining OP concentration

1. Digest sample by following "*steps for determining TP concentration*".
2. Shake test cell containing mixture vigorously using the vortex mixer.
3. Add 5 drops P-2K to test cell.
4. Close test cell and mix vigorously using vortex mixer.
5. Add 1 dose P-3K to test cell.
6. Close test cell and mix vigorously using vortex mixer until P-3K reagent has dissolved.
7. Leave test cell containing solution/mixture to stand for 5 minutes.
8. Place test cell into NOVA60 Spectroquant to with the barcode in the forward-facing position to measure OP concentration of sample.

APPENDIX E:
Removal Efficiency

E.1. Determination of organic matter removal efficiency

The performance of the ABR-MFC system was evaluated according to its organic matter (i.e. COD and FOG) removal efficiency by using Equations 2.2 and E.1, as well as the TSS- (Equation E.2), VSS- (Equation E.3), NO_3^-- (Equation E.4) and TP- (Equation E.5) removal efficiencies.

E.1.1. COD removal

The average COD removal efficiency of the ABR-MFC was calculated by using equation 2.4 and the average COD values (OLR 1) recorded for the feed and product, respectively.

$$\varepsilon_{COD} = \frac{OC_{feed}^{COD} - OC_{product}^{COD}}{OC_{feed}^{COD}} \times 100$$

$$\varepsilon_{COD} = \frac{10\,979\ mg/l - 5\,770\ mg/l}{10\,979\ mg/l} \times 100$$

$$\varepsilon_{COD} = 48.30\%$$

E.1.2. FOG removal

The average FOG removal efficiency of the ABR-MFC was calculated by using the average FOG values (OLR 1) recorded for the feed and product, respectively.

$$\varepsilon_{FOG} = \frac{OC_{feed}^{FOG} - OC_{product}^{FOG}}{OC_{feed}^{FOG}} \times 100 \qquad \text{(Eq. E.1)}$$

$$\varepsilon_{FOG} = \frac{1\,280\ mg/l - 46\ mg/l}{1\,280\ mg/l} \times 100$$

$$\varepsilon_{FOG} = 96.41\%$$

E.1.3. TSS removal

The average TSS removal efficiency of the ABR-MFC was calculated by using the average TSS values (OLR 1) recorded for the feed and product, respectively.

$$\varepsilon_{TSS} = \frac{OC_{feed}^{TSS} - OC_{product}^{TSS}}{} \times 100 \qquad \text{(Eq. E.2)}$$

$$\varepsilon_{TSS} = 84.68\%$$

E.1.4. VSS removal

The average VSS removal efficiency of the ABR-MFC was calculated by using the average VSS values (OLR 1) recorded for the feed and product, respectively.

$$\varepsilon_{VSS} = \frac{OC_{feed}^{VSS} - OC_{product}^{VSS}}{OC_{feed}^{VSS}} \times 100 \quad \text{(Eq. E.3)}$$

$$\varepsilon_{VSS} = \frac{3.33\ mg/l - 1.76\ mg/l}{3.33\ mg/l} \times 100$$

$$\varepsilon_{VSS} = 47.15\%$$

E.1.5. Nitrate nitrogen (NO_3-N) removal

The average NO_3-N removal efficiency of the ABR-MFC was calculated by using the average NO_3-N values (OLR 1) recorded for the feed and product, respectively.

$$\varepsilon_{NO_3} = \frac{OC_{feed}^{NO_3} - OC_{product}^{NO_3}}{OC_{feed}^{NO_3}} \times 100 \quad \text{(Eq. E.4)}$$

$$\varepsilon_{NO_3} = \frac{3.43\ mg/l - 0.83\ mg/l}{3.43\ mg/l} \times 100$$

$$\varepsilon_{NO_3} = 76.75\%$$

E.1.6. TP removal

The average TP removal efficiency of the ABR-MFC was calculated by using the average TP values (OLR 1) recorded for the feed and product, respectively.

$$\varepsilon_{TP} = \frac{OC_{feed}^{TP} - OC_{product}^{TP}}{O_{feed}^{TP}} \times 100 \quad \text{(Eq. E.5)}$$

$$\varepsilon_{TP} = \frac{1.52\ mg/l - 0.13\ mg/l}{1.52\ mg/l} \times 100$$

$$\varepsilon_{TP} = 91.31\%$$

E.2. Internal resistance

The internal resistance of each OLR was calculated by using the PD peak method (section 2.7.2.1.1) and Equation 2.7. The internal resistance of the ABR-MFC for OLR 1 was determined as follows:

$$P_{max} = \frac{OCV^2 R_{ext}}{(R_{int} + R_{ext})^2} \quad \text{(Eq. 2.7)}$$

$$R_{int} = \sqrt{\frac{OCV^2 R_{ext}}{P_{max}}} - R_{ext}$$

$$R_{int} = \sqrt{\frac{(400^2)(100)}{277.42}} - 100$$

$$R_{int} = 340.15\ \Omega$$

APPENDIX F:
Substrate preparation

F.1. Nutrient adjustment

The optimal carbon:nitrate:phosphate (C:N:P) ratio for BDWW is 150:1.1:0.2 (Phukingngam *et al*., 2011) where C is COD (as $C_{optimal}^{ratio}$), N is total nitrate (NO_3^-) (as $N_{optimal}^{ratio}$) and P is total phosphate (TP) (as $P_{optimal}^{ratio}$).

The COD (as $C_{available}$) (Table 4.1), NO_3^- (as $N_{available}$) (Table 4.3) and TP (as $P_{available}$) (Table 4.2) of the sample should be determined prior to adjusting the wastewater. The following sample calculation results in a C:N:P ratio of 145796:1069.17:194.39 which is equivalent to the optimal C:N:P ratio (150:1.1:0.2) for BDWW proposed by Phukingngam *et al*., (2011).

Table F.1: BDWW characterisation

Wastewater characterisation	Value [mg/l]
COD (as $C_{available}$)	145796
NO_3^- (as $N_{available}$)	0.38
TP (as $P_{available}$)	0.2275

F.1.1. Basis of calculation

$$Basis = \frac{C_{available}}{C_{optimal}^{ratio}}$$

$$Basis = \frac{145796\ mg/l}{150\ mg/l}$$

$$Basis = 97.19$$

F.1.2. Optimal amount of NO_3^- required per litre of BDWW

$$N_{optimal}^{sample} = Basis\ \times\ N_{optimal}^{ratio}$$

$$N_{optimal}^{sample} = 97.19\ \times 1.1$$

$$N_{optimal}^{sample} = 106.91\ mg/l$$

F.1.3. Optimal amount of phosphorous required per litre of BDWW

$$P_{optimal}^{sample} = 97.19\ \times\ P_{optimal}^{ratio}$$

$$P_{optimal}^{sample} = 61.76\ \times 0.2$$

$$P_{optimal}^{sample} = 19.44\ mg/l$$

F.1.4. NO_3^- required

$$N_{required} = N_{optimal}^{sample} - N_{available}$$
$$N_{required} = 106.91 - 0.38$$
$$N_{required} = 106.53\ mg/l$$

Amount of urea (CH_4N_2O) to add:

Table F.2: Elemental composition of urea (CH_4N_2O)

Element	Composition [%]	Molecular weight [g/mol]
C	19.999	12.0107
H	6.713	1.00794
N	46.646	14.0067
O	26.641	15.99903
CH_4N_2O	100.00	60.05489

$$\%N = \frac{Mr_N}{Mr_{Urea}} \times 100$$
$$\%N = \frac{2 \times 14.0067\ g/mol}{60.05489\ g/mol} \times 100$$
$$\%N = \frac{28.0134\ g/mol}{60.05489\ g/mol} \times 100$$
$$\%N = 46.646\%$$

Basis:

100 mg urea contains 46.646 mg N

$$Ratio = \frac{N_{required}}{N_{available}}$$
$$Ratio = \frac{106.53\ mg\ N/l}{46.646\ mg\ N/100\ mg\ urea}$$
$$Ratio = 2.28$$

$$Amount\ Urea\ to\ add = 100\ mg\ urea\ \times\ 2.28$$
$$Amount\ Urea\ to\ add = 228.38\ mg\ urea/l$$

F.1.5. TP required

$$P_{required} = P_{optimal}^{sample} - P_{available}$$
$$P_{required} = 19.44 - 0.2275$$
$$P_{required} = 19.21\ mg/l$$

Amount of potassium dihydrogen orthophosphate (KH_2PO_4) to add:

Table F.3: Elemental composition of potassium dihydrogen ortho-phosphate (KH_2PO_4)

Element	Composition [%]	Molecular weight [g/mol]
K	28.731	39.0983
H	1.481	1.00794
P	22.761	30.9738
O	47.027	15.9990
KH_2PO_4	100.00	136.084

$$\%P = \frac{Mr_P}{Mr_{KH_2PO_4}} \times 100$$
$$\%P = \frac{30.9738\ g/mol}{139.084\ g/mol} \times 100$$
$$\%P = 22.27\ \%$$

Basis:

100 mg KH_2PO_4 contains 22.27 mg P

$$Ratio = \frac{P_{required}}{P_{available}}$$
$$Ratio = \frac{19.21\ mg\ P/l}{22.27\ mg\ P/100\ mg\ KH_2PO_4}$$
$$Ratio = 0.86$$

$$Amount\ KH_2PO_4\ to\ add = 100\ mg\ KH_2PO_4\ \times\ 0.86$$
$$Amount\ KH_2PO_4\ to\ add = 86.26\ mg\ KH_2PO_4/l$$

F.2. Substrate dilution

Steps for dilution of substrate (OLR 1 = 1.15 kg COD/m^3.day)

1. Adjust C:N:P ratio of 20 L BDWW with urea and KH_2PO_4 to obtain an optimal C:N:P ratio of 150:1.1:0.2.
2. Add 80 L tap water.
3. Use PCTestr35 to check that pH is in the range of 6.8 and 7.2.
4. Add sodium hydroxide (NaOH) if pH is below 6.5 to obtain a pH close to 7.
5. Add phosphoric acid (H_3PO_4) if pH is above 7.5 to obtain a pH close to 7.

APPENDIX G:
Anode and cathode electrodes

G.1. Carbon fibre brush anode surface area determination

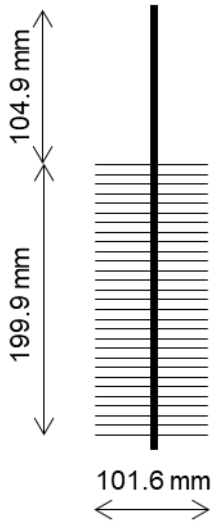

Figure G.1: Schematic of carbon fibre brush anode electrode.

Table G.1: Carbon fibre brush dimensions

		Dimension	
Brush	Diameter	[m]	0.1016
	Radius	[m]	0.0508
	Length	[m]	0.1999
	Length (overall)	[m]	0.3048
	Cylindrical Area	[m^2]	0.0800
Fibre Tips	Diameter	[m]	7.20×10^{-6}
	Radius	[m]	3.60×10^{-6}
	Length	[m]	0.0508
	Surface Area	[m^2/tip]	1.15×10^{-6}
	Tips	[m^{-2}]	6.20×10^{8}
		[per brush]	4.96×10^{7}
	Active Surface Area	[m^2]	57.01

G.1.1. Cylindrical area

$$A_{brush} = 2\pi r(r + l)$$
$$A_{brush} = 2\pi(0.0508\ m)(0.0508\ m + 0.1999\ m)$$
$$A_{brush} = 0.08\ m^2$$

G.1.2. Fibre area

$$A_{fibre} = 2\pi r(r + l)$$
$$A_{fibre} = 2\pi(3.6 \times 10^{-6}\, m)\left((3.6 \times 10^{-6}\, m) + 0.0508\, m\right)$$
$$A_{fibre} = 1.15 \times 10^{-6}\, m^2$$

G.1.3. Conversion

$$400\,000\ tips/in^2 \times 1550\ in^2/m^2 = 620\,000\,000\ tips/m^2$$

G.1.4. Number of fibre tips per brush

$$Fibre\ tips = 620\,000\,000\ tips/m^2 \times A_{brush}$$
$$Fibre\ tips = 620\,000\,000\ tips/m^2 \times 0.08\, m^2$$
$$Fibre\ tips = 49\,611\,932\ tips$$

G.1.4.1. Active surface area per carbon fibre brush anode electrode

$$SA_{anode} = Fibre\ tips \times A_{fibre}$$
$$SA_{anode} = 49\,611\,932\ ips \times 1.15 \times 10^{-6}\, m^2$$
$$SA_{anode} = 57.01\, m^2$$

G.1.4.2. Active surface area of 6 carbon fibre brush anode electrodes

$$SA_T^{Anode} = SA_{anode} \times 6$$
$$SA_T^{Anode} = 57.01\, m^2 \times 6$$
$$SA_T^{Anode} = 342.07\, m^2$$

G.2. Floating carbon air-cathode preparation

Dimensions of stainless steel mesh and quantities of chemicals mentioned below varied for the 6-floating air-cathodes that was prepared (refer to Table G.2). The size of the stainless-steel mesh and quantities of 10% polyvinylidene fluoride (PVDF) solution, carbon black powder and activated

carbon powder used are based on the floating air-cathode in the 6th compartment of the lab-scale ABR-MFC.

G.2.1. Materials required for floating air-cathode preparation:

1. PVDF powder (~ 534 000 Da, Sigma Aldrich)
2. N,N-dimethylacetamide (DMAc) (Anhydrous (99.8%), Sigma Aldrich)
3. Activated carbon powder (Norit SX Plus, Cabot Corporation)
4. Carbon black powder (Vulcan XC-72, Cabot Corporation)
5. 50 x 50 stainless steel mesh (Type 304)

G.2.2. Steps for preparation of 10% PVDF solution (300 ml):

1. Transfer 240 ml DMAc solution to a clean and dry volumetric flask.
2. Weigh 30 g PVDF powder using a clean and dry weighing boat and a calibrated balance.
3. In a fume hood, transfer the 30 g PVDF powder to the volumetric flask containing the 240 ml DMAc solution.
4. Swirl the volumetric flask gently to ensure that the PVDF powder completely dissolves.
5. Fill the volumetric flask containing the dissolved PVDF and DMAc solution to 300 ml using pure DMAc solution.
6. Transfer the final 10% PVDF solution prepared in steps 1 to 5 into a clean and dry glass bottle for future use.

Table G.2: Floating carbon air-cathode dimensions used for producing cathodes

Dimensions		Compartment					
		C1	C2	C3	C4	C5	C6
Length	[cm]	30.20	30.20	30.20	28.20	30.00	28.10
Width	[cm]	15.90	16.20	16.40	15.10	15.70	11.50
Activated Carbon	[g]	15.25	15.50	15.67	13.66	14.98	10.75
Carbon Black	[g]	1.52	1.55	1.57	1.37	1.50	1.07
10 % PVDF Solution	[ml]	50.82	51.67	52.24	45.54	49.94	35.83

G.3. Projected surface area for floating air-cathode cathode electrode

$$SA_{cathode} = (L - (wall\ height \times 2)) \times (W - (wall\ height \times 2)$$

$$SA_{cathode} = (30.20\ cm - (1\ cm \times 2)) \times (15.90\ cm\ (1\ cm \times 2)$$

$$SA_{cathode} = (28.20\ cm) \times (13.90\ cm)$$
$$SA_{cathode} = \ 391.98\ cm^2$$

G.4. Steps for floating carbon air-cathode preparation (C1):

1. Cut the stainless-steel mesh into a 30.2 cm x 15.9 cm (Table G.2) rectangular block using a sterile pair of scissors.
2. Weigh 15.25 g activated carbon (AC) powder using a clean dry weighing boat and a calibrated balance.
3. Transfer the 15.25 g of activated carbon (CB) powder into a clean dry glass beaker.
4. Weigh 1.52 g CB powder using a clean and dry weighing boat and a calibrated balance.
5. Transfer the 1.52 g CB powder to the glass beaker containing the AC powder.
6. In a fume hood, using a pipette, add 50.82 ml of the 10% PVDF solution (prepared as described) to the powder contained in the glass beaker.
7. Mix the contents in the glass beaker using a glass stirring rod until a smooth paste of AC/CB/PVDF forms.
8. Using a spatula, spread the AC/CB/PVDF mixture evenly onto the stainless-steel mesh (NOTE: the degree of waterproofness of the electrode depends on the smoothness of the electrode surface – complete step in 2 minutes).
9. Immerse the carbon coated electrode into deionised water for 15 minutes with the uncoated stainless-steel side facing upwards.
10. Air-dry the cathode for 8 hours in a fume hood.

APPENDIX H:
Experimental data – BDWW treatment

H.1. Full strength BDWW

Table H.1: Summarised raw data for full strength BDWW

Day	Temp °C	SD	pH	SD	EC µS/cm	SD	TDS ppm	SD	Salt ppm	SD	COD mg/l	SD	TSS mg/L	SD	Turbidity NTU	SD	NO_3^- mg/l	SD	TP mg/l	SD
0	22.20	0.00	11.20	0.01	767	2.12	544	1.41	426	0.71	107030	1400	0.25	0.18	1704	2.83				
31	23.75	0.07	10.50	0.02	661	8.49	471	5.66	416	9.19	112393	1128	0.01	0.02	952	1.41				
40	23.45	0.07	9.67	0.00	736	4.24	523	2.83	460	2.12	100595	1867	0.03	0.04	948	8.49				
76	21.70	0.14	11.97	0.16	673	0.00	479	0.71	371	0.00	135768	117	0.11	0.08	470	2.83	0.49	0.07	4.60	0.14
144	19.60	0.14	10.44	0.01	779	4.95	554	3.54	450	2.83	117865	1089	0.44	0.05	1000	0.00	0.31	0.01	5.75	0.07
180	21.15	0.21	11.12	0.01	793	7.78	560	0.71	630	212.84	301125	11667	0.25	0.09	1000	0.00	0.40	0.01	6.40	0.14

H.2. Sludge used for inoculation

Table H.2: Summarised raw data for activated sludge (AS)

Day	Temp °C	SD	pH	SD	EC µS/cm	SD	TDS ppm	SD	Salt ppm	SD	COD mg/l	SD	TSS mg/l	SD	Turbidity NTU	SD
0	17.50	0.42	6.68	0.00	863.00	2.83	613.00	1.41	508.00	1.41	1705.00	233.35	0.06	0.19	5.01	0.76

Table H.3: Summarised raw data for activated granular sludge (AGS)

Day	Temp °C	SD	pH	SD	EC µS/cm	SD	TDS ppm	SD	Salt ppm	SD	COD mg/l	SD	TSS mg/l	SD	Turbidity NTU	SD
0	16.95	0.35	7.21	0.01	2.21	0.01	1565	0.01	1350	0.00	1902.50	88.39	0.26	0.01	93.15	0.07

H.3. Daily operational data

Table H.4: Daily operational data for ABR-MFC feed samples

Day	Temp °C	SD	pH	SD	EC µS/cm	SD	TDS ppm	SD	Salt ppm	SD
0	21.9	0.00	5.64	0.05	266	0.71	189	1.41	146	0.71
4	22.5	0.07	5.93	0.01	229	0.00	163	0.00	126	0.00
5	23.7	0.07	7.67	0.02	298	0.71	211	0.00	173	0.00
6	23.1	0.00	7.99	0.01	346	1.41	245	0.71	205	0.71
7	18.3	0.78	7.42	0.00	443	3.54	314	1.41	258	0.71
10	23.6	0.07	7.29	0.01	427	1.41	304	0.71	251	0.71
11	24.2	0.07	7.54	0.01	408	0.71	287	2.83	243	0.00
12	24.4	0.00	7.33	0.00	394	1.41	280	1.41	235	0.71
13	24.1	0.07	7.38	0.01	386	2.12	274	0.71	232	0.71
14	16.5	0.42	7.40	0.00	373	1.41	266	0.71	224	0.71
17	19.1	0.21	7.35	0.00	333	0.00	236	0.00	200	0.00
18	18.0	0.35	7.32	0.01	323	0.71	229	0.00	193	0.00
19	22.7	0.14	7.08	0.00	310	0.00	220	0.00	187	0.00
20	23.5	0.00	7.10	0.00	293	0.00	208	0.00	179	0.00
21	23.3	0.00	7.11	0.01	316	1.41	226	0.71	173	0.00
24	22.9	0.21	7.17	0.01	359	2.83	256	3.54	218	3.54
25	23.2	0.00	7.17	0.01	335	2.12	238	0.71	204	0.71
26	25.4	0.07	7.12	0.01	362	0.00	257	0.00	218	0.00
27	25.1	0.00	7.15	0.01	309	2.83	220	2.12	193	0.71
28	21.6	0.28	6.77	0.02	348	0.00	247	0.00	212	0.00
31	24.3	0.07	6.82	0.00	330	0.71	234	0.00	202	0.00
32	23.5	0.00	7.65	0.00	398	0.71	283	0.71	244	0.00
33	24.4	0.07	6.22	0.00	380	0.71	270	0.71	231	0.00
34	24.6	0.07	6.79	0.01	425	0.00	302	0.00	258	0.00
35	23.3	0.07	6.99	0.01	403	1.41	287	0.71	246	0.71
38	17.4	0.57	6.23	0.01	366	1.41	261	0.71	223	0.71
39	18.7	0.78	6.16	0.01	353	0.71	251	0.71	215	0.71
40	22.9	0.14	6.51	0.01	325	0.71	231	0.71	199	0.00
41	21.5	0.07	6.79	0.01	305	0.71	217	0.71	193	0.00
42	21.1	0.14	8.21	0.00	463	0.00	329	0.00	295	0.00
45	19.4	0.42	7.04	0.01	588	2.12	418	1.41	395	0.00
46	22.3	0.07	7.21	0.01	644	0.00	459	0.71	375	0.00

Table H.4: Daily operational data for ABR-MFC feed samples

Day	Temp °C	SD	pH	SD	EC µS/cm	SD	TDS ppm	SD	Salt ppm	SD
47	21.3	0.35	6.94	0.00	579	0.00	412	0.00	331	0.71
48	20.8	0.28	6.87	0.00	608	1.41	432	1.41	348	0.71
49	22.2	0.07	7.33	0.01	586	1.41	417	0.71	335	0.71
52	23.3	0.07	6.93	0.01	544	2.12	387	2.12	313	1.41
53	19.8	0.14	6.90	0.03	670	2.12	478	2.12	385	2.12
54	20.1	0.21	7.07	0.01	664	1.41	472	0.00	380	0.00
55	19.2	0.42	6.78	0.00	606	0.71	431	0.71	346	0.71
56	20.9	0.14	6.99	0.00	629	2.12	448	1.41	361	0.00
59	21.1	0.07	6.64	0.01	620	1.41	442	0.71	354	0.00
60	21.2	0.00	6.89	0.01	611	0.71	435	1.41	349	0.00
61	21.6	0.07	6.76	0.01	584	2.83	416	1.41	334	0.71
62	20.7	0.07	6.24	0.01	580	0.71	413	0.71	345	0.71
63	17.2	0.14	7.17	0.01	656	0.00	468	0.71	367	2.12
66	16.7	0.21	7.16	0.01	682	0.71	485	0.00	379	0.00
67	18.1	0.00	8.41	0.02	669	0.71	476	0.71	373	0.00
68	17.9	0.07	7.06	0.01	488	0.71	347	0.00	270	0.71
69	18.2	0.14	7.47	0.01	564	2.83	402	2.12	314	2.12
70	13.3	0.42	7.02	0.01	476	1.41	339	0.71	259	0.00
73	18.5	0.07	7.28	0.01	665	1.41	474	0.71	372	0.71
74	15.9	0.42	6.52	0.02	659	1.41	469	1.41	360	0.71
75	19.9	0.49	6.76	0.01	600	10.61	433	0.71	334	0.00
76	17.7	2.26	6.85	0.01	595	5.66	424	4.24	326	1.41
77	20.5	0.71	6.65	0.02	574	3.54	409	2.12	316	2.12
80	11.2	0.57	6.58	0.01	527	1.41	375	0.71	293	1.41
81	12.6	0.35	6.96	0.04	546	0.00	388	0.00	306	0.71
82	12.8	0.57	6.87	0.02	574	2.12	411	4.95	323	0.71
83	13.5	0.49	6.69	0.01	554	2.12	395	2.83	312	1.41
84	18.8	0.00	6.56	0.01	523	1.41	373	0.71	299	0.71
87	12.2	0.64	6.75	0.01	615	0.00	439	2.12	351	0.71
88	13.0	0.71	6.72	0.01	555	2.83	395	2.12	315	0.71
89	18.9	0.00	6.39	0.01	524	4.24	373	2.12	302	1.41
90	18.6	0.07	5.96	0.03	447	4.95	318	2.83	261	2.83
91	9.9	0.57	6.61	0.01	516	4.24	367	3.54	291	2.12
94	11.1	0.07	6.49	0.01	190	2.69	136	0.71	106	1.41

Table H.4: Daily operational data for ABR-MFC feed samples

Day	Temp °C	SD	pH	SD	EC µS/cm	SD	TDS ppm	SD	Salt ppm	SD
95	17.8	0.14	6.53	0.02	589	2.12	411	0.71	312	0.00
96	10.7	0.28	6.46	0.01	581	1.41	413	0.71	317	1.41
97	18.6	0.14	5.96	0.02	617	1.41	439	0.71	346	0.71
98	19.9	0.00	6.62	0.01	455	8.49	326	4.24	259	1.41
101	14.7	0.21	5.95	0.03	461	0.71	328	0.71	256	0.71
102	18.0	0.07	6.54	0.02	424	0.00	302	0.71	240	0.00
103	14.3	0.14	6.47	0.01	582	0.71	414	0.00	325	0.71
104	14.2	0.14	6.53	0.01	633	0.71	450	0.00	354	0.00
105	14.2	0.21	6.58	0.03	444	3.54	315	2.83	246	2.12
108	13.7	0.21	6.43	0.03	595	0.71	423	0.00	332	0.71
109	13.6	0.35	6.55	0.04	580	1.41	415	2.12	325	0.71
110	13.6	0.14	6.45	0.01	405	3.54	289	3.54	223	2.83
111	18.6	0.00	5.79	0.04	473	0.71	336	0.71	265	1.41
112	20.8	0.07	6.15	0.01	510	0.71	362	0.00	265	69.30
115	20.9	0.00	6.76	0.04	472	2.12	335	1.41	291	2.12
116	14.2	0.07	6.37	0.06	605	2.12	430	0.00	372	0.71
123	15.4	0.28	6.39	0.01	596	1.41	424	0.71	367	0.71
124	20.9	0.07	6.06	0.01	455	0.00	324	0.71	280	0.00
125	14.4	0.21	6.28	0.00	502	3.54	357	3.54	308	0.71
126	20.9	0.07	6.37	0.02	502	0.71	357	0.71	310	0.71
129	21.0	0.07	6.88	0.01	566	2.12	403	2.83	351	2.12
130	16.4	0.14	6.93	0.02	520	1.41	369	0.00	319	0.00
131	19.7	0.00	6.62	0.01	521	0.00	366	1.41	323	1.41
132	18.3	0.07	6.78	0.01	299	0.71	212	0.00	182	0.00
133	17.6	0.07	6.18	0.01	407	0.71	289	0.00	248	0.71
136	14.9	0.28	6.56	0.04	640	0.71	455	0.00	371	0.71
137	14.1	0.42	7.29	0.05	616	2.83	438	2.12	356	2.12
138	13.7	0.28	7.03	0.01	613	0.71	441	7.07	359	2.83
139	13.3	0.35	6.97	0.01	608	1.41	432	1.41	353	4.24
140	17.5	0.07	6.71	0.01	549	0.00	390	0.00	319	0.00
143	20.1	0.07	6.68	0.01	668	0.71	475	0.71	377	0.00
144	20.3	0.21	6.34	0.01	627	0.71	445	0.00	360	0.00
145	15.2	0.42	6.87	0.02	716	0.00	510	2.83	381	0.00
146	19.7	0.00	6.46	0.01	689	3.54	490	2.83	371	2.12

Table H.4: Daily operational data for ABR-MFC feed samples

Day	Temp °C	SD	pH	SD	EC µS/cm	SD	TDS ppm	SD	Salt ppm	SD
147	16.5	0.21	6.52	0.01	661	0.71	470	0.71	366	2.12
150	17.7	0.21	6.56	0.01	662	0.71	471	1.41	367	0.71
151	20.2	0.21	6.30	0.01	551	2.83	392	1.41	306	1.41
152	21.5	0.07	6.12	0.01	675	2.83	481	1.41	377	1.41
153	13.0	0.64	5.89	0.01	677	2.12	481	1.41	382	0.00
154	16.4	0.35	7.16	0.01	737	1.41	524	0.00	422	0.00
157	17.1	0.28	6.54	0.02	738	0.71	525	1.41	424	0.71
158	20.3	0.07	6.17	0.01	752	2.12	534	2.12	432	1.41
159	21.0	0.00	6.36	0.01	675	2.83	481	2.12	389	1.41
160	20.0	0.21	6.34	0.01	837	3.54	593	0.71	472	0.71
165	16.2	0.28	6.55	0.03	555	0.71	393	0.00	435	0.00
166	18.1	0.21	6.89	0.01	778	0.71	553	0.00	668	2.12
167	18.0	0.21	6.79	0.01	784	0.71	556	2.12	675	0.71
168	17.4	0.35	6.91	0.01	763	4.95	543	2.12	652	1.41
171	16.9	0.28	6.66	0.01	774	5.66	552	2.12	665	2.12
172	16.0	0.28	6.75	0.01	777	1.41	553	2.12	664	2.83
173	18.3	0.07	6.97	0.04	772	4.95	551	0.00	667	0.00
174	21.3	0.07	6.37	0.01	754	4.95	536	3.54	650	5.66
175	10.7	0.28	6.57	0.00	1097	0.71	781	0.71	640	0.71
178	11.1	0.21	6.39	0.01	1007	10.61	718	3.54	587	0.00
179	15.3	0.00	6.26	0.01	860	1.41	613	4.95	506	4.95
180	16.2	0.07	6.47	0.01	937	2.12	667	2.83	561	2.12
181	16.7	0.07	6.37	0.00	671	2.12	477	1.41	602	2.12
182	13.9	0.28	6.68	0.08	977	2.12	696	0.71	579	0.71
185	20.2	0.07	5.32	0.01	945	4.24	672	3.54	565	2.83
186	18.4	0.00	7.82	0.01	1033	5.66	733	5.66	617	5.66
187	16.0	0.14	6.19	0.01	1106	2.83	789	2.12	663	2.83
188	16.5	0.07	5.86	0.00	998	1.41	709	1.41	599	0.71
189	17.6	0.07	5.64	0.01	978	9.90	696	7.78	588	6.36
192	13.6	0.42	5.59	0.13	994	5.66	707	4.95	593	3.54
193	14.2	0.35	5.56	0.02	933	0.71	666	1.41	558	0.71
194	19.1	0.07	5.34	0.03	971	2.83	690	1.41	585	0.71
195	19.2	0.07	6.20	0.01	992	4.24	704	3.54	598	3.54
196	18.4	0.57	5.38	0.02	1069	4.24	761	1.41	612	2.12

Table H.4: Daily operational data for ABR-MFC feed samples

Day	Temp °C	SD	pH	SD	EC µS/cm	SD	TDS ppm	SD	Salt ppm	SD
199	17.1	0.28	5.66	0.00	808	5.66	575	3.54	455	2.83
200	16.8	0.07	4.74	0.01	594	4.95	423	2.12	351	2.12
201	17.6	0.28	6.74	0.06	760	2.12	541	0.71	428	0.71
202	18.4	0.07	5.85	0.02	732	0.71	522	2.12	437	1.41
203	18.5	0.14	6.82	0.01	828	0.71	590	0.71	469	0.71
206	18.7	0.14	6.79	0.00	1214	0.00	865	0.71	698	0.00
207	20.6	0.14	5.71	0.04	748	3.54	532	1.41	423	1.41
208	15.5	0.28	6.43	0.01	669	0.71	478	0.71	375	0.71
209	18.0	0.07	6.27	0.05	564	3.54	404	0.00	318	0.71
210	18.1	0.35	6.67	0.01	1600	14.85	1135	7.07	928	4.24
213	19.1	0.28	6.64	0.00	1574	6.36	1120	0.00	916	3.54
214	24.0	0.07	6.02	0.01	1164	1.41	832	1.41	667	2.83
215	19.6	0.21	7.08	0.02	1503	3.54	1070	0.00	871	1.41
216	19.1	0.28	6.94	0.01	1665	8.49	1125	7.07	952	2.12
217	20.5	0.07	6.57	0.01	1789	0.00	1270	0.00	1045	7.07
220	20.6	0.28	6.93	0.01	829	60.10	595	34.65	479	22.63
221	20.1	0.07	6.15	0.04	895	2.83	636	1.41	513	2.12
222	21.6	0.14	6.48	0.02	1089	11.31	776	5.66	628	2.12
223	20.9	0.00	6.58	0.01	1668	16.26	1185	7.07	975	9.19
224	19.4	0.07	6.63	0.01	1547	10.61	1105	7.07	900	5.66

Table H.5: Daily operational data for ABR-MFC product samples

Day	Temp °C	SD	pH	SD	EC µS/cm	SD	TDS ppm	SD	Salt ppm	SD
5	22.9	0.07	7.46	0.01	1641	1.41	1165	7.07	938	0.71
6	22.8	0.14	7.81	0.01	1444	3.54	1020	0.00	871	0.71
7	22.1	0.00	7.77	0.00	1437	1.41	1020	0.00	886	1.41
8	16.4	0.64	7.72	0.00	1389	7.78	987	8.49	834	3.54
11	23.9	0.07	7.32	0.01	1154	0.00	819	1.41	697	0.00
12	23.6	0.14	7.68	0.00	951	2.12	673	0.71	579	0.00
13	23.4	0.14	7.89	0.01	901	0.71	638	0.00	548	0.00
14	23.5	0.14	7.44	0.01	902	2.12	639	0.00	552	0.71
15	16.6	0.64	7.72	0.01	833	2.12	593	0.71	511	0.00
18	19.9	0.14	7.72	0.01	657	0.00	466	0.71	400	0.71
19	18.5	0.35	7.86	0.01	620	0.00	440	0.00	376	0.00
20	22.4	0.07	7.72	0.01	587	0.00	416	0.00	358	0.00
21	22.9	0.00	7.68	0.00	551	1.41	392	0.71	338	0.71
22	23.5	0.07	7.73	0.01	587	2.83	416	3.54	322	2.12
25	22.8	0.07	7.54	0.00	502	1.41	356	0.00	305	0.00
26	22.6	0.07	7.64	0.01	495	1.41	353	0.71	302	1.41
27	24.8	0.07	7.57	0.00	492	0.71	349	0.00	298	0.71
28	24.8	0.00	7.57	0.01	465	0.71	330	0.00	290	0.71
29	23.0	0.14	7.48	0.01	471	0.00	334	0.00	289	0.00
32	24.4	0.07	7.52	0.01	467	0.00	331	0.00	288	0.71
33	22.7	0.07	7.60	0.00	481	1.41	342	1.41	296	0.71
34	23.7	0.07	7.52	0.00	476	0.00	339	0.71	291	0.00
35	24.0	0.14	7.61	0.01	488	2.12	346	0.00	296	0.00
36	22.9	0.00	7.62	0.01	474	0.71	336	0.00	289	0.00
39	18.1	0.21	7.33	0.01	471	0.00	335	0.00	288	0.00
40	19.5	0.78	7.50	0.00	480	1.41	342	0.71	295	0.00
41	23.3	0.07	7.49	0.00	468	0.00	333	0.00	289	0.00
42	20.8	0.00	7.70	0.00	464	0.00	330	0.00	296	0.00
43	20.5	0.00	7.68	0.01	461	0.71	328	0.71	293	0.00
46	18.7	0.57	7.42	0.00	412	0.71	293	0.71	274	0.00
47	21.5	0.07	7.49	0.00	495	0.71	352	0.71	286	0.00
48	20.4	0.49	7.29	0.01	484	0.00	344	0.00	275	0.00
49	21.8	0.21	7.68	0.03	531	0.00	377	0.00	302	0.00
50	22.1	0.07	7.79	0.00	533	2.12	379	0.71	303	0.00

Table H.5: Daily operational data for ABR-MFC product samples

Day	Temp °C	SD	pH	SD	EC µS/cm	SD	TDS ppm	SD	Salt ppm	SD
53	22.8	0.07	7.71	0.01	545	0.71	387	0.00	313	0.00
54	17.9	0.35	7.31	0.01	609	2.83	434	2.12	347	2.12
55	18.6	0.21	7.00	0.00	662	1.41	472	1.41	379	1.41
56	17.3	0.42	7.36	0.00	646	0.71	460	0.71	368	0.71
57	17.7	0.35	7.72	0.00	662	0.00	471	0.00	377	0.00
60	21.0	0.21	7.51	0.01	608	1.41	432	1.41	347	0.71
61	20.6	0.14	7.63	0.00	654	1.41	466	0.71	374	0.71
62	21.6	0.00	7.87	0.01	645	0.71	459	0.00	369	0.71
63	20.5	0.00	7.85	0.01	647	1.41	461	0.71	386	0.71
64	15.9	0.21	7.64	0.01	668	0.71	476	1.41	371	0.71
67	15.4	0.49	7.38	0.01	617	7.07	439	4.95	341	3.54
68	17.0	0.14	7.95	0.01	640	0.71	455	1.41	355	0.00
69	15.7	0.42	7.93	0.01	626	1.41	446	0.71	347	0.71
70	15.1	0.28	8.01	0.01	664	2.12	472	1.41	367	0.00
71	9.1	0.42	8.34	0.01	661	3.54	470	2.12	357	0.71
74	17.6	0.14	7.96	0.00	646	1.41	460	1.41	360	1.41
75	18.2	0.57	7.84	0.01	646	4.24	460	2.83	355	0.71
76	19.0	0.42	7.91	0.03	647	0.71	461	0.71	356	0.00
77	19.6	0.28	7.77	0.01	654	0.00	466	0.00	361	0.00
78	20.2	0.14	7.73	0.02	657	0.71	467	0.00	361	0.00
81	9.8	0.49	7.79	0.01	636	2.12	452	1.41	353	0.00
82	9.7	0.28	7.93	0.01	692	1.41	493	0.71	386	0.00
83	12.2	0.42	7.69	0.01	663	1.41	472	0.71	373	0.00
84	11.2	0.57	7.67	0.01	676	4.24	481	2.83	379	1.41
85	17.8	0.21	7.25	0.00	596	2.12	424	0.71	340	0.71
88	10.7	0.64	7.46	0.01	667	7.07	474	4.95	376	2.83
89	10.8	0.64	7.29	0.00	660	7.78	469	4.95	373	3.54
90	17.6	0.00	6.95	0.00	609	0.00	434	0.71	352	0.71
91	18.1	0.07	6.99	0.01	624	2.83	446	1.41	368	1.41
92	8.8	0.78	7.25	0.01	637	0.00	452	0.00	359	1.41
95	9.2	0.07	7.07	0.01	635	0.71	452	0.71	360	1.41
96	17.5	0.00	7.08	0.00	598	1.41	425	1.41	349	0.71
97	9.2	0.57	6.95	0.01	686	5.66	488	3.54	373	2.12
98	18.4	0.00	6.74	0.01	655	0.71	464	1.41	367	1.41

Table H.5: Daily operational data for ABR-MFC product samples

Day	Temp °C	SD	pH	SD	EC µS/cm	SD	TDS ppm	SD	Salt ppm	SD
99	19.6	0.00	6.90	0.01	639	3.54	454	2.83	361	1.41
102	12.2	0.35	7.45	0.01	581	1.41	413	0.71	320	8.49
103	17.2	0.07	6.85	0.01	635	2.12	451	1.41	361	1.41
104	10.5	0.35	7.18	0.01	625	0.00	444	0.00	350	0.71
105	9.0	0.78	6.77	0.01	669	9.90	475	7.07	372	3.54
106	9.9	0.57	6.98	0.02	649	0.71	460	2.83	361	1.41
109	11.3	0.42	6.34	0.01	657	2.83	467	0.71	369	0.71
110	8.8	0.28	6.12	0.01	717	0.71	510	0.71	393	0.71
111	11.2	0.42	6.25	0.01	2	2.12	494	1.41	385	0.71
112	16.9	0.00	5.90	0.01	676	0.71	481	2.12	381	0.00
113	12.6	0.14	7.39	0.01	562	0.71	399	1.41	341	1.41
116	13.0	0.57	7.64	0.02	551	3.54	390	1.41	334	0.71
117	12.3	0.49	6.78	0.01	562	0.71	399	0.71	341	0.71
124	12.8	0.28	7.34	0.01	610	65.76	400	0.00	343	0.71
125	13.2	0.21	6.62	0.01	609	0.71	430	3.54	370	2.12
126	9.4	0.85	5.97	0.04	661	2.83	470	2.83	398	0.00
127	14.7	0.42	5.90	0.01	639	2.12	454	0.71	393	0.71
130	13.9	0.21	5.92	0.02	657	0.71	466	0.00	403	0.71
131	11.1	0.71	6.39	0.01	656	7.78	465	4.24	397	2.83
132	20.0	0.07	7.05	0.01	578	0.71	410	0.71	358	0.00
133	17.4	0.07	6.28	0.03	603	2.12	428	1.41	372	1.41
134	19.0	0.07	6.58	0.01	620	2.12	440	1.41	383	0.71
137	14.2	0.21	6.99	0.04	605	1.41	430	1.41	350	0.71
138	13.0	0.49	5.90	0.06	593	70.71	457	0.00	371	0.00
139	11.5	0.57	7.28	0.00	652	4.95	463	4.24	373	2.83
140	12.8	0.42	5.85	0.01	646	2.83	460	2.12	373	0.71
141	16.9	0.00	5.92	0.00	628	0.71	446	0.71	365	0.00
144	20.1	0.14	6.79	0.01	631	1.41	449	0.71	357	0.71
145	19.3	0.35	5.88	0.01	647	2.83	460	2.12	371	1.41
146	15.6	0.21	6.14	0.01	695	0.71	494	0.71	369	0.00
147	18.9	0.07	6.03	0.01	733	0.00	521	0.71	393	0.00
148	14.3	0.21	5.95	0.04	694	2.83	493	2.12	382	0.71
151	15.0	0.28	5.99	0.01	747	0.71	531	0.71	413	0.71
152	19.6	0.14	5.59	0.01	730	0.71	519	0.71	408	0.71

Table H.5: Daily operational data for ABR-MFC product samples

Day	Temp °C	SD	pH	SD	EC µS/cm	SD	TDS ppm	SD	Salt ppm	SD
153	20.9	0.07	5.65	0.00	716	2.12	508	1.41	400	0.71
154	13.9	0.78	6.13	0.02	666	6.36	474	3.54	379	0.71
155	14.4	0.64	6.23	0.01	655	1.41	465	0.71	370	1.41
158	13.7	0.78	6.71	0.00	654	0.71	464	0.00	369	0.71
159	20.6	0.07	5.43	0.00	656	0.00	466	0.00	375	0.00
160	19.1	0.14	5.42	0.01	639	2.12	454	0.71	365	0.00
161	19.8	0.07	5.55	0.01	744	77.07	497	1.41	394	1.41
166	15.4	0.42	5.62	0.04	488	0.71	346	1.41	408	1.41
167	18.2	0.14	5.60	0.00	489	0.71	347	0.00	413	0.71
168	17.0	0.21	5.40	0.11	511	0.71	363	0.00	430	0.00
169	16.6	0.14	5.37	0.02	514	2.12	365	1.41	433	2.12
172	17.0	0.21	6.01	0.01	519	0.00	369	0.00	438	0.00
173	15.3	0.35	6.58	0.01	517	0.71	368	0.71	434	0.00
174	18.1	0.21	6.41	0.01	566	0.00	402	0.00	481	0.71
175	20.9	0.07	6.07	0.01	614	3.54	436	1.41	524	1.41
176	10.6	0.28	6.45	0.01	943	0.00	671	0.00	546	0.71
179	10.8	0.07	6.27	0.01	1029	2.12	731	1.41	597	1.41
180	15.0	0.00	5.94	0.04	1048	4.24	746	4.95	620	3.54
181	16.0	0.07	5.74	0.01	1050	1.41	745	1.41	628	1.41
182	16.3	0.07	5.87	0.01	711	4.24	505	1.41	637	2.12
183	14.9	0.42	5.94	0.04	1027	2.83	731	2.83	611	1.41
186	19.7	0.21	5.78	0.01	1000	4.95	710	4.95	597	4.24
187	17.5	0.07	5.53	0.04	985	5.66	699	4.95	586	4.24
188	16.2	0.07	5.61	0.07	957	1.41	680	0.71	568	1.41
189	15.8	0.14	5.63	0.01	936	3.54	665	2.83	559	2.12
190	17.3	0.07	5.66	0.01	894	0.71	635	0.00	535	0.00
193	13.0	0.35	6.43	0.07	831	1.41	591	1.41	491	0.71
194	10.5	0.57	5.35	0.06	822	2.83	587	0.71	481	2.83
195	18.9	0.00	4.87	0.03	847	0.71	601	0.00	508	0.71
196	18.7	0.07	4.79	0.00	873	6.36	619	4.24	523	3.54
197	18.4	0.14	4.80	0.01	914	0.71	649	0.00	518	0.71
200	17.2	0.28	4.75	0.04	973	1.41	693	0.00	553	0.71
201	16.3	0.00	4.17	0.00	970	5.66	692	2.12	581	3.54
202	17.0	0.21	4.74	0.00	998	1.41	709	1.41	566	0.71

Table H.5: Daily operational data for ABR-MFC product samples

Day	Temp °C	SD	pH	SD	EC µS/cm	SD	TDS ppm	SD	Salt ppm	SD
203	17.8	0.07	4.76	0.01	934	2.83	664	2.12	555	4.24
204	17.8	0.14	4.68	0.04	943	0.00	670	0.71	534	0.71
207	18.5	0.14	4.75	0.03	876	0.71	622	0.00	496	0.71
208	19.2	0.00	4.73	0.02	867	4.24	617	1.41	493	0.00
209	14.9	0.21	4.42	0.01	633	0.71	451	0.00	353	0.71
210	17.2	0.14	4.35	0.03	982	7.07	705	5.66	558	1.41
211	19.0	0.14	4.94	0.01	1081	0.00	768	0.00	617	0.71
214	18.3	0.57	5.12	0.00	1245	1.41	884	0.71	713	0.00
215	23.3	0.07	5.21	0.01	1435	2.83	1025	7.07	833	0.71
216	17.2	0.21	5.37	0.01	1484	0.00	1050	0.00	855	0.00
217	18.1	0.14	5.36	0.03	1866	8.49	1075	7.07	898	0.71
218	20.1	0.00	5.37	0.01	1583	4.95	1125	7.07	919	2.12
221	17.8	0.21	5.66	0.03	1607	0.71	1140	0.00	931	0.00
222	18.9	0.14	5.43	0.01	1685	5.66	1200	0.00	981	2.83
223	19.8	0.00	5.42	0.01	1710	4.95	1215	7.07	996	1.41
224	20.1	0.00	5.48	0.01	1690	2.12	1200	0.00	985	0.00
225	20.6	0.07	5.62	0.01	1661	0.00	1180	0.00	968	0.71

H.4. ABR-MFC performance data

Table H.6: ABR-MFC performance – raw experimental data for feed samples

Day	COD mg/l	SD	TSS mg/l	SD	VSS mg/l	SD	Turbidity NTU	SD	FOG mg/l	NO_3^- mg/l	SD	N mg/l	SD	TP mg/l	SD	OP mg/l	SD
0	5725	212.13					244	2.83									
5	5373	3.54	0.17	0.02			283	0.00									
7	5493	208.60	0.01	0.00			303	0.00									
10	5525	7.07	0.13	0.01			304	0.71									
12	5760	77.78	0.12	0.04			343	31.11									
14	5588	208.60	0.13	0.03			419	0.71									
17	5423	74.25	0.26	0.04			489	11.31									
19	5433	74.25	0.33	0.02			512	2.83									
21	5720	148.49	0.78	0.83			853	7.78									
24	6265	21.21	0.56	0.07			900	16.26									
26	6133	116.67	0.50	0.06			807	2.83									
28	5558	31.82	0.17	0.01			500	3.54									
31	5793	88.39	1.44	0.01			1000	0.00									
33	5315	7.07	0.62	0.11			718	37.48									
35	5390	113.14	0.63	0.02			515	27.58									
38	5213	152.03	0.65	0.12			842	7.07									
40	6083	24.75	1.24	0.21			1000	0.00									
42	10110	84.85	0.20	0.01			562	1.41						2.40	0.28	17.20	0.28
45	9200	254.56	0.67	0.04			732	4.95						<0.5	0.00	12.60	0.28
47	8735	49.50	0.61	0.02			674	13.44						<0.5	0.00	12.35	0.21
49	10458	1856.16	0.79	0.01			953	12.02						<0.5	0.00	12.30	0.14
52	11478	130.81	5.96	0.18			684	14.85						<0.5	0.00	14.60	0.71
54	8743	45.96	0.21	0.11			530	2.83						<0.5	0.00	13.70	0.14
56	9478	88.39	1.25	0.05			1000	0.00						<0.5	0.00	13.30	0.00
59	9473	60.10	1.58	0.01			1000	0.00						<0.5	0.00	13.85	0.21
61	9580	155.56	1.69	0.07			1000	0.00						<0.5	0.00	11.35	0.35
63	9350	120.21	0.61	0.42			654	1.41						0.20	0.00	14.00	0.00
66	9225	0.00	0.32	0.18			535	0.71						0.20	0.00	12.40	0.00
68	8850	98.99	0.79	0.08			961	4.24						0.10	0.00	11.10	0.00
70	9228	286.38	3.53	0.17			936	21.92						1.85	0.07	21.95	0.21
73	9853	342.95	3.57	0.35			885	16.97						1.40	0.14	25.00	0.00
75	10448	434.87	1.03	0.18			1000	0.00						2.15	0.07	19.90	0.42
77	11465	98.99	3.15	0.01			1000	0.00						1.95	0.07	22.05	0.35

Table H.6: ABR-MFC performance – raw experimental data for feed samples

Day	COD mg/l	SD	TSS mg/l	SD	VSS mg/l	SD	Turbidity NTU	SD	FOG mg/l	NO_3^- mg/l	SD	N mg/l	SD	TP mg/l	SD	OP mg/l	SD
80	11570	339.41	3.89	0.19			866	22.63									
82	11965	134.35	1.10	0.19	2.12	0.23	1000	0.00									
84	12400	848.53	2.27	0.59	3.19	0.59	1000	0.00									
87	13068	562.15	2.38	0.87	3.29	0.33	1000	0.00									
89	13383	53.03	1.81	0.80	2.72	0.74	1000	0.00									
91	12403	1672.31	4.86	3.69	5.80	3.61	1000	0.00									
94	12816	244.66	4.84	0.49	5.99	0.03	1000	0.00									
96	13248	837.92	1.81	0.25	2.63	0.11	916	90.51									
98	11788	109.60	2.05	0.81	3.00	0.74	1000	0.00									
101	13920	593.97	11.24	0.44	12.06	0.44	856	96.17									
103	11695	120.21	1.48	0.13	2.33	0.12	1000	0.00									
105	12373	491.44	15.67	9.74	16.43	9.61	1000	0.00									
108	11603	38.89	7.97	3.47	8.76	3.47	1000	0.00									
110	10693	187.38	3.36	2.40	4.23	2.37	1000	0.00									
112	10808	406.59	1.61	0.06	2.46	0.08	1000	0.00									
115	9090	70.71	0.92	0.02	1.79	0.01	823	33.23									
124	9328	364.16	0.89	0.08	1.87	0.08	1000	0.00									
126	8640	205.06	0.51	0.00	1.45	0.02	536	0.71									
129	11050	98.99	0.70	0.05	1.64	0.03	1000	0.00									
131	11800	49.50	0.55	0.03	1.33	0.03	1000	0.00									
133	9600	311.13	0.90	0.02	1.96	0.10	1000	0.00									
136	11770	205.06	6.37	0.83	6.96	0.79	1000	0.00									
138	9250	21.21	1.60	0.10	2.44	0.08	1000	0.00									
140	12330	42.43	7.68	0.44	8.18	0.45	1000	0.00									
143	11645	162.63	2.93	0.21	3.83	0.28	1000	0.00									
145	11313	166.17	1.76	0.01	2.62	0.03	1000	0.00									
147	11783	208.60	3.11	0.11	3.96	0.08	966	7.07		1.70	0.28	0.38	0.06	1.60	0.14	17.95	0.07
150	11495	205.06	3.03	0.16	3.81	0.11	1000	0.00									
152	11150	127.28	1.65	1.07	2.48	1.00	531	5.66									
154	11473	413.66	1.94	1.44	3.28	1.50	704	28.99	1280	2.65	0.07	0.60	0.02	1.30	0.00	17.35	0.21
157	10868	321.73	3.32	2.91	4.48	2.49	1000	0.00									
159	10861	289.21	1.32	0.34	3.09	0.89	1000	0.00									
166	9538	236.88	0.81	0.01	2.63	0.33	1000	0.00									
168	9668	1339.97	1.58	0.91	3.14	0.20	1000	0.00		5.95	0.78	1.34	0.18	1.65	0.21	20.35	0.35

Table H.6: ABR-MFC performance – raw experimental data for feed samples

Day	COD mg/l	SD	TSS mg/l	SD	VSS mg/l	SD	Turbidity NTU	SD	FOG mg/l	NO_3^- mg/l	SD	N mg/l	SD	TP mg/l	SD	OP mg/l	SD
171	11270	28.28	0.50	0.28	2.71	0.24	347	4.95									
173	13590	98.99	1.29	0.27	2.24	1.47	1000	0.00									
175	19190	1230.37	5.72	0.31	6.95	0.61	1000	0.00		7.65	0.35	1.73	0.08	1.60	0.14	24.35	0.35
178	16790	1258.65	3.82	0.03	5.17	0.64	1000	0.00									
180	14580	127.28	1.36	0.51	2.87	0.41	1000	0.00									
182	14535	1166.73	2.57	0.18	3.88	1.19	1000	0.00	2673	1.22	0.17	0.28	0.04	1.10	0.42	21.90	0.00
185	19530	2729.43	9.80	1.22	10.17	0.30	1000	0.00									
187	23665	289.91	3.90	0.59	5.49	0.07	794	4.95									
189	23490	579.83	3.66	1.50	5.01	0.61	1000	0.00		6.00	0.14	1.36	0.03	1.55	0.07	22.40	0.28
192	23705	374.77	7.05	0.07	8.30	0.45	1000	0.00									
194	25140	876.81	9.03	7.68	10.88	7.83	1000	0.00									
196	21845	1661.70	9.51	3.15	9.71	1.29	1000	0.00		12.15	2.05	2.74	0.46	2.95	0.07	25.30	0.42
199	33053	456.08	2.03	1.00	3.57	0.35	1000	0.00									
201	33405	806.10	2.78	2.12	4.31	1.40	1000	0.00									
203	33968	2004.65	4.85	3.18	6.02	2.18	1000	0.00		4.80	0.42	1.08	0.10	4.05	0.07	18.25	0.07
206	37230	148.49	8.44	5.83	9.71	4.94	1000	0.00									
208	31920	912.17	2.55	1.85	4.53	2.50	1000	0.00									
210	32783	31.82	6.62	5.88	8.38	6.36	1000	0.00	269 540	11.45	2.62	2.59	0.59	2.20	0.28	25.00	0.00
213	33645	3033.49	9.81	3.24	11.59	3.61	1000	0.00									
215	34440	1527.35	16.26	0.57	17.79	0.16	1000	0.00									
217	30563	922.77	11.00	2.60	12.83	3.24	1000	0.00		5.10	0.14	1.15	0.03	3.80	0.85	25.00	0.00
220	33593	710.64	64.30	6.11	65.85	6.49	1000	0.00									
222	32228	243.95	39.46	4.86	41.50	3.90	1000	0.00									
224	33450	1442.50	40.72	6.87	42.20	7.55	1000	0.00		7.90	0.00	1.78	0.00	2.00	0.14	25.00	0.00

Table H.7: ABR-MFC performance – raw experimental data for product samples

Day	COD mg/l	SD	TSS mg/l	SD	VSS mg/l	SD	Turbidity NTU	SD	FOG mg/l	NO_3^- mg/l	SD	N mg/l	SD	TP mg/l	SD	OP mg/l	SD
5							44	0.57									
6	1745	332.34	0.00	0.06			31	0.07									
8	1653	31.82	0.07	0.00			21	0.07									
11	2218	215.67	0.18	0.09			32	0.07									
13	1890	21.21	0.09	0.01			45	4.45									
15	2678	187.38	0.01	0.06			32	0.57									
18	2225	77.78	0.02	0.01			74	0.07									
20	2625	28.28	0.09	0.05			34	0.07									
22	2655	106.07	0.09	0.06			36	0.85									
25	2953	81.32	0.14	0.41			166	7.78									
27	2655	84.85	0.01	0.02			21	0.14									
29	1703	10.61	0.03	0.01			27	0.00									
32	1605	35.36	0.01	0.02			36	0.07									
34	1745	56.57	0.15	0.01			29	0.64									
36	1763	38.89	0.05	0.02			24	0.78									
39	1953	10.61	0.13	0.10			32	0.78									
41	2065	35.36	0.03	0.11			38	1.70									
43	2175	106.07	0.03	0.04			22	0.14						<0.5	0.00	10.40	0.28
46	2113	53.03	0.13	0.08			38	0.28						<0.5	0.00	8.10	0.00
48	2198	109.60	0.03	0.03			32	3.61						<0.5	0.00	9.20	0.99
50	3263	31.82	0.04	0.01			19	0.69						<0.5	0.00	22.65	3.32
53	2998	60.10	0.04	0.03			23	0.85						<0.5	0.00	9.80	0.00
55	3735	77.78	0.07	0.03			20	0.47						<0.5	0.00	13.45	0.07
57	3960	98.99	0.04	0.08			20	0.01						<0.5	0.00	13.15	0.07
60	3625	91.92	0.04	0.00			32	0.71						<0.5	0.00	13.05	0.35
62	4048	74.25	0.04	0.02			28	1.91						<0.5	0.00	13.45	0.35
64	4400	49.50	0.04	0.09			24	0.92						<0.5	0.00	17.20	#DIV/0!
67	4190	14.14	0.14	0.01			37	0.64						<0.5	0.00	14.60	#DIV/0!
69	4415	28.28	0.01	0.01			33	0.71						<0.5	0.00	<0.5	0.00
71	3618	24.75	0.24	0.01			41	0.57						<0.5	0.00	14.55	0.07
74	3990	56.57	0.28	0.08			35	0.57						<0.5	0.00	13.70	0.00
76	4373	24.75	0.26	0.01			41	5.66						<0.5	0.00	14.00	0.00
78	4850	56.57	2.66	0.71			42	1.13						0.10	0.00	15.30	0.00
81	2333	144.96	0.03	0.05	1.03	0.06	35	1.70									

Table H.7: ABR-MFC performance – raw experimental data for product samples

Day	COD mg/l	SD	TSS mg/l	SD	VSS mg/l	SD	Turbidity NTU	SD	FOG mg/l	NO_3^- mg/l	SD	N mg/l	SD	TP mg/l	SD	OP mg/l	SD
83	4543	74.25	0.03	0.01	0.99	0.03	28	0.35									
85	4815	35.36	0.04	0.02	0.99	0.01	43	0.28									
88	5160	339.41	0.09	0.01	1.16	0.50	50	0.28									
90	6125	91.92	0.11	0.02	1.08	0.02	63	0.28									
92	6500	325.27	0.13	0.00	1.21	0.08	59	1.20									
95	6755	120.21	0.15	0.03	1.21	0.04	62	1.56									
97	7358	724.78	0.47	0.04	1.41	0.04	59	0.28									
99	6870	183.85	0.17	0.06	1.33	0.04	58	0.49									
102	6948	116.67	0.11	0.01	1.05	0.04	55	3.96									
104	6725	176.78	0.12	0.04	1.02	0.08	63	0.64									
106	6763	53.03	0.01	0.09	0.94	0.06	36	0.85									
109	7123	38.89	0.05	0.08	0.99	0.06	37	0.07									
111	7843	307.59	0.06	0.00	1.00	0.01	75	1.41									
113	7305	106.07	0.08	0.11	1.13	0.04	86	2.33									
116	5615	197.99	0.08	0.05	0.95	0.10	84	0.42									
125	5858	81.32	0.03	0.04	1.01	0.01	95	19.37									
127	5363	144.96	0.17	0.19	1.01	0.01	99	1.84									
130	5668	208.60	0.16	0.03	1.13	0.12	69	0.85									
132	5713	31.82	0.25	0.06	1.19	0.06	82	0.57									
134	5853	45.96	0.14	0.09	1.15	0.03	54	0.28									
137	5785	155.56	0.06	0.01	1.04	0.04	62	1.56									
139	5523	180.31	0.18	0.01	1.07	0.01	69	2.97									
141	5828	38.89	0.03	0.08	0.92	0.02	60	1.70									
144	5638	88.39	0.03	0.01	0.95	0.01	56	1.34									
146	5490	183.85	0.02	0.17	0.92	0.02	57	0.64									
148	6130	91.92	0.15	0.06	1.07	0.06	45	0.49		0.45	0.07	0.10	0.02	0.10	0.00	13.75	0.35
151	6098	137.89	0.03	0.00	0.95	0.01	58	0.07									
153	5853	45.96	0.05	0.01	0.97	0.01	51	0.14									
155	5648	173.24	0.23	0.24	3.14	0.23	57	0.14	46	0.43	0.32	0.10	0.07	0.10	0.00	15.00	0.00
158	5688	258.09	1.59	2.11	3.50	2.60	79	4.31									
160	5620	530.33	0.39	0.66	2.58	0.31	48	0.07									
167	4145	14.14	0.15	0.75	1.26	3.51	186	0.71									
169	6353	137.89	0.55	0.30	2.27	1.20	210	0.71		1.62	0.54	0.37	0.12	0.20	0.00	16.40	0.00
172	4983	60.10	0.06	0.00	1.98	0.28	118	0.71									

Table H.7: ABR-MFC performance – raw experimental data for product samples

Day	COD mg/l	SD	TSS mg/l	SD	VSS mg/l	SD	Turbidity NTU	SD	FOG mg/l	NO_3^- mg/l	SD	N mg/l	SD	TP mg/l	SD	OP mg/l	SD
174	4785	42.43	0.04	0.20	2.42	1.36	124	0.71									
176	5275	49.50	0.25	0.10	1.85	0.64	106	0.71		0.53	0.60	0.12	0.14	0.10	0.00	15.50	0.00
179	6223	81.32	0.16	0.25	1.28	0.31	126	0.71									
181	7790	106.07	0.13	0.07	2.20	0.76	81	0.28									
183	8090	113.14	0.08	0.08	1.42	0.71	49	1.13	72	0.09	0.00	0.02	0.00	0.10	0.00	14.55	0.07
186	7893	38.89	0.04	0.08	1.78	0.23	62	0.07									
188	7418	123.74	0.28	0.31	0.42	2.57	40	0.28									
190	7325	636.40	0.06	0.06	1.92	0.42	70	0.42		0.10	0.00	0.02	0.00	0.10	0.00	17.05	0.07
193	8288	17.68	0.20	0.03	2.04	0.03	234	0.71									
195	11068	137.89	0.08	0.03	1.66	1.19	73	0.42									
197	12063	88.39	0.02	0.17	1.75	0.75	123	1.41		0.15	0.07	0.03	0.02	0.10	0.00	21.70	0.00
200	13590	63.64	0.04	0.06	2.43	1.32	147	0.71									
202	12233	555.08	0.04	0.06	1.27	1.00	249	0.71									
204	11698	243.95	0.09	0.01	2.27	1.15	317	0.71		0.50	0.00	0.11	0.00	0.30	0.00	22.25	0.07
207	12325	98.99	0.23	0.13	2.44	0.08	325	4.24									
209	11690	735.39	0.07	0.18	1.72	0.48	452	0.71									
211	11693	512.65	0.03	0.21	2.08	0.51	405	0.71	100	0.40	0.28	0.09	0.06	0.40	0.00	23.65	0.64
214	10958	1283.40	0.13	0.01	2.11	0.27	294	3.54									
216	11955	728.32	0.06	0.11	2.74	0.88	183	2.83									
218	11175	141.42	0.37	0.16	3.41	1.77	200	2.83		1.24	0.23	0.28	0.05	0.50	0.00	25.00	0.00
221	11820	282.84	0.23	0.16	2.29	0.21	130	1.41									
223	11410	233.35	0.18	0.08	3.63	1.91	133	0.71									
225	11158	116.67	0.15	0.21	0.62	1.64	130	2.83		0.40	0.14	0.00	0.03	0.10	0.00	25.00	0.00

Table H. 8: ABR-MFC efficiency

Since Inoculation	Date	COD Removal	FOG Removal	TSS Removal	VSS Removal	NO3-N Removal	TP Removal
		%	%	%	%	%	%
6	05-04-17	67.52		100.00			
8	07-04-17	69.91		100.00			
11	10-04-17	59.86		100.00			
13	12-04-17	67.19		21.74			
15	14-04-17	52.08		96.15			
18	17-04-17	58.97		90.20			
20	19-04-17	51.68		74.63			
22	21-04-17	53.58		88.39			
25	24-04-17	52.87		75.00			
27	26-04-17	56.71		97.00			
29	28-04-17	69.37		80.00			
32	01-05-17	72.29		99.65			
34	03-05-17	67.17		76.80			
36	05-05-17	67.30		92.91			
39	08-05-17	62.54		79.84			
41	10-05-17	66.05		97.98			
43	12-05-17	78.49		87.18			
46	15-05-17	77.04		81.34			
48	17-05-17	74.84		95.04			
50	19-05-17	68.80		94.90			
53	22-05-17	73.88		99.33			
55	24-05-17	57.28		66.67			
57	26-05-17	58.22		96.79			
60	29-05-17	61.73		97.46			
62	31-05-17	57.75		97.33			
64	02-06-17	52.94		94.26			
67	05-06-17	54.58		55.56			
69	07-06-17	50.11		98.74			
71	09-06-17	60.80		93.20			
74	12-06-17	59.50		92.15			
76	14-06-17	58.15		75.12			
78	16-06-17	57.70		15.56			

Table H. 8: ABR-MFC efficiency

Since Inoculation	Date	COD Removal	FOG Removal	TSS Removal	VSS Removal	NO3-N Removal	TP Removal
		%	%	%	%	%	%
81	19-06-17	79.84		99.10			
83	21-06-17	62.04		96.80	50.94		
85	23-06-17	61.17		98.45	69.12		
88	26-06-17	60.51		96.21	64.84		
90	28-06-17	54.23		94.18	60.48		
92	30-06-17	47.59		97.33	79.22		
95	03-07-17	47.29		96.90	79.80		
97	05-07-17	44.46		74.24	46.39		
99	07-07-17	41.72		91.71	55.83		
102	10-07-17	50.09		99.02	91.29		
104	12-07-17	42.50		91.53	56.34		
106	14-07-17	45.34		99.90	93.94		
109	17-07-17	38.61		99.31	88.75		
111	19-07-17	26.65		98.21	76.45		
113	21-07-17	32.41		94.70	54.27		
116	24-07-17	38.23		90.81	46.93		
125	02-08-17	37.20		97.18	45.84		
127	04-08-17	37.93		67.65	30.10		
130	07-08-17	48.71		76.98	31.40		
132	09-08-17	51.59		54.55	10.90		
134	11-08-17	39.04		83.98	41.33		
137	14-08-17	50.85		98.98	85.13		
139	16-08-17	40.30		88.75	56.15		
141	18-08-17	52.74		99.67	88.08		
144	21-08-17	51.59		99.15	75.20		
146	23-08-17	51.47		98.86	61.05		
148	25-08-17	47.97		95.18	73.11	73.53	93.75
151	28-08-17	46.96		99.01	75.20		
153	30-08-17	47.51		97.26	60.61		
155	01-09-17	50.77	96.41	88.14	4.27	83.96	92.31
158	04-09-17	47.67		52.11	21.88		
160	06-09-17	48.25		70.45	16.50		

Table H. 8: ABR-MFC efficiency

Since Inoculation	Date	COD Removal	FOG Removal	TSS Removal	VSS Removal	NO3-N Removal	TP Removal
		%	%	%	%	%	%
167	13-09-17	56.54		81.48	52.09		
169	15-09-17	34.29		65.19	27.71	72.77	87.88
172	18-09-17	55.79		88.00	26.94		
174	20-09-17	64.79		96.90	-8.04		
176	22-09-17	72.51		95.63	73.38	93.14	93.75
179	25-09-17	62.94		95.81	75.24		
181	27-09-17	46.57		90.44	23.34		
183	29-09-17	44.34	97.31	96.89	63.40	92.62	90.91
186	02-10-17	59.59		99.59	82.50		
188	04-10-17	68.66		92.82	92.35		
190	06-10-17	68.82		98.36	61.68	98.33	93.55
193	09-10-17	65.04		97.16	75.42		
195	11-10-17	55.98		99.11	84.74		
197	13-10-17	44.78		99.79	81.98	98.77	96.61
200	16-10-17	58.88		98.03	31.93		
202	18-10-17	63.38		98.56	70.53		
204	20-10-17	65.56		98.14	62.29	89.58	92.59
207	23-10-17	66.89		97.27	74.87		
209	25-10-17	63.38		97.25	62.03		
211	27-10-17	64.33	99.96	99.55	75.18	96.51	81.82
214	30-10-17	67.43		98.67	81.79		
216	01-11-17	65.29		99.63	84.60		
218	03-11-17	63.44		96.64	73.42	75.69	86.84
221	06-11-17	64.81		99.64	96.52		
223	08-11-17	64.60		99.54	91.25		
225	10-11-17	66.64		99.63	98.53	94.94	95.00

APPENDIX I:
Experimental data – power generation

I.1. ABR-MFC voltage and current generation

Table I.1: ABR-MFC and individual compartment electrical current (since day 144 of ABR-MFC operation)

Day	Date	C1	C2	C3	C4	C5	C6	ABR-MFC
					mA			
1	21-08-17	3.30	2.70	3.00	3.00	3.60	3.30	4.50
2	22-08-17	0.44	4.38	3.93	3.79	3.87	4.71	4.80
3	23-08-17	3.03	3.97	3.85	3.27	3.88	2.97	5.00
4	24-08-17	6.70	7.60	7.10	4.43	4.62	4.09	6.90
5	25-08-17	5.11	4.80	4.28	4.70	4.85	4.87	7.60
8	28-08-17	4.50	4.29	4.72	4.55	4.47	3.00	7.00
9	29-08-17	5.89	5.87	5.96	5.16	4.23	4.59	8.30
10	30-08-17	3.96	4.68	5.99	5.19	5.54	5.34	8.10
11	31-08-17	4.88	5.00	5.70	5.34	5.51	5.16	7.05
12	01-09-17	5.79	5.31	5.41	5.49	5.48	4.98	5.99
15	04-09-17	5.54	4.84	5.84	4.96	5.50	4.57	9.40
16	05-09-17	4.21	5.98	6.61	6.32	6.13	5.37	10.70
17	06-09-17	7.50	9.30	10.10	8.00	9.40	7.30	7.30
18	07-09-17	3.74	5.59	5.59	5.32	4.88	4.99	7.80
22	11-09-17	10.90	10.90	12.30	11.90	10.90	10.90	12.70
23	12-09-17	8.90	9.50	9.00	8.00	8.00	7.70	7.48
24	13-09-17	8.10	9.90	8.10	8.10	8.30	7.40	11.00
25	14-09-17	6.60	5.90	5.90	9.40	9.10	10.20	12.00
26	15-09-17	7.30	7.20	6.40	9.50	9.10	9.60	12.30
29	18-09-17	12.70	12.70	13.80	10.80	12.30	14.80	13.60
30	19-09-17	12.90	13.30	12.20	12.60	12.60	15.10	11.90
31	20-09-17	12.60	12.20	12.10	12.40	13.40	13.60	11.80
32	21-09-17	7.90	10.60	10.30	13.30	13.30	13.10	16.10
33	22-09-17	12.00	11.80	16.10	12.60	16.00	13.00	15.00
36	25-09-17	8.90	7.70	8.20	7.70	8.60	8.40	10.10
37	26-09-17	8.80	8.40	7.70	10.30	10.80	8.20	7.40
38	27-09-17	9.00	9.40	5.90	7.20	7.90	3.70	7.40
39	28-09-17	8.00	7.90	7.60	5.80	8.80	6.70	5.50
40	29-09-17	8.70	8.60	7.80	8.40	7.70	5.00	5.70
43	02-10-17	5.30	9.90	9.60	8.40	7.60	4.90	5.90
44	03-10-17	10.00	9.80	9.20	8.90	7.60	5.10	5.60
45	04-10-17	10.00	9.70	9.30	8.10	7.40	4.60	5.80

Table I.1: ABR-MFC and individual compartment electrical current (since day 144 of ABR-MFC operation)

Day	Date	C1	C2	C3	C4	C5	C6	ABR-MFC
					mA			
46	05-10-17	10.00	8.90	8.40	7.30	7.50	4.00	5.30
47	06-10-17	10.00	9.20	9.20	8.20	6.40	4.10	5.80
50	09-10-17	11.00	10.00	10.00	7.50	7.10	4.80	5.80
51	10-10-17	10.90	9.70	9.90	7.20	7.20	4.00	5.70
52	11-10-17	10.80	10.20	10.00	7.30	7.40	4.30	5.00
53	12-10-17	12.30	12.60	9.90	12.30	9.40	5.60	7.20
54	13-10-17	10.80	10.80	9.60	6.20	7.00	7.60	5.60
57	16-10-17	11.60	9.50	10.00	8.20	5.90	4.60	5.00
58	17-10-17	8.10	8.20	8.20	7.20	6.90	4.10	5.30
59	18-10-17	7.90	9.20	7.10	6.90	6.20	4.90	7.10
60	19-10-17	10.10	8.80	8.00	7.20	5.90	6.80	7.90
61	20-10-17	12.10	11.80	11.40	12.10	10.10	8.40	12.40
64	23-10-17	15.50	15.00	13.60	15.10	15.00	13.60	12.50
65	24-10-17	15.60	16.80	14.70	14.10	12.40	11.20	14.50
66	25-10-17	16.70	15.40	14.40	14.00	14.40	9.90	15.00
67	26-10-17	15.40	14.30	14.60	13.90	13.30	9.70	14.80
68	27-10-17	17.00	14.90	15.40	14.00	14.10	10.00	12.60
71	30-10-17	19.30	17.50	18.50	18.00	17.50	7.00	14.30
72	31-10-17	20.40	12.70	20.10	17.90	16.40	9.50	10.10
73	01-11-17	20.10	18.80	18.10	19.40	18.10	16.30	16.50
74	02-11-17	20.00	19.30	18.20	18.40	17.10	10.70	18.10
75	03-11-17	20.10	22.00	21.20	19.80	17.10	13.80	22.10
78	06-11-17	18.90	17.70	19.00	16.70	14.80	16.00	16.90
79	07-11-17	18.80	16.10	17.90	15.10	14.60	13.00	16.90
80	08-11-17	18.90	16.30	19.00	17.60	15.30	12.70	18.90
81	09-11-17	19.60	19.50	16.50	18.70	16.30	12.00	19.00
82	10-11-17	18.50	16.40	18.10	13.50	15.60	13.30	18.60

Table I.2: ABR-MFC and individual compartment potential difference/voltage (since day 144 of ABR-MFC operation)

Day	Date	C1	C2	C3	C4	C5	C6	ABR-MFC
					mV			
1	21-08-17	247	248	251	246	245	194	158
2	22-08-17	146	151	151	151	151	141	145
3	23-08-17	96	97	99	100	101	102	150
4	24-08-17	129	129	130	131	132	132	128
5	25-08-17	119	119	120	123	123	123	145
8	28-08-17	109	110	110	111	113	113	153
9	29-08-17	141	141	141	142	142	142	159
10	30-08-17	136	137	137	137	138	138	164
11	31-08-17	141	142	142	143	143	144	166
12	01-09-17	145	146	147	148	148	149	167
15	04-09-17	126	127	128	131	131	131	184
16	05-09-17	186	187	188	188	190	190	193
17	06-09-17	139	141	142	145	145	146	192
18	07-09-17	153	157	158	161	161	162	195
22	11-09-17	399	399	398	394	394	393	400
23	12-09-17	186	186	187	187	187	188	203
24	13-09-17	218	220	220	220	219	219	217
25	14-09-17	216	217	220	218	218	218	226
26	15-09-17	212	213	212	210	212	212	228
29	18-09-17	239	239	240	238	238	238	188
30	19-09-17	245	245	245	244	244	243	193
31	20-09-17	244	244	234	230	230	231	230
32	21-09-17	235	235	235	236	237	230	242
33	22-09-17	237	237	236	202	203	204	238
36	25-09-17	210	210	210	200	199	196	205
37	26-09-17	223	222	209	174	174	171	181
38	27-09-17	184	184	185	186	185	180	183
39	28-09-17	199	199	200	188	188	180	182
40	29-09-17	217	217	217	197	198	186	194
43	02-10-17	255	254	254	211	210	200	204
44	03-10-17	272	272	272	220	220	208	215
45	04-10-17	285	285	285	212	212	203	206
46	05-10-17	275	275	279	204	204	193	196
47	06-10-17	279	280	280	213	213	204	205

Table I.2: ABR-MFC and individual compartment potential difference/voltage (since day 144 of ABR-MFC operation)

Day	Date	C1	C2	C3	C4	C5	C6	ABR-MFC
					mV			
50	09-10-17	271	271	272	217	217	210	211
51	10-10-17	276	275	276	206	206	201	206
52	11-10-17	261	261	260	212	210	220	172
53	12-10-17	245	245	244	242	242	233	238
54	13-10-17	262	262	262	240	240	223	226
57	16-10-17	280	280	280	216	214	198	202
58	17-10-17	232	232	233	204	203	193	202
59	18-10-17	235	234	233	193	192	191	194
60	19-10-17	289	289	289	180	180	174	189
61	20-10-17	231	231	232	230	230	230	234
64	23-10-17	237	237	237	237	237	238	243
65	24-10-17	253	253	252	242	242	241	255
66	25-10-17	250	250	250	249	249	248	253
67	26-10-17	236	236	236	236	236	237	241
68	27-10-17	228	228	228	229	228	227	230
71	30-10-17	275	275	275	275	274	272	278
72	31-10-17	235	236	236	239	239	237	299
73	01-11-17	285	286	285	286	286	281	283
74	02-11-17	265	266	266	269	269	267	264
75	03-11-17	284	284	283	284	284	283	286
78	06-11-17	249	249	250	252	252	251	263
79	07-11-17	247	248	247	246	246	245	251
80	08-11-17	252	252	252	252	252	252	258
81	09-11-17	255	256	256	256	256	255	263
82	10-11-17	246	247	247	247	247	247	260

I.2. ABR-MFC PD data

Table I.3: ABR-MFC and individual compartments PD (normalised to anode chamber volume)

Day	Date	C1 PD	C2 PD	C3 PD	C4 PD	C5 PD	C6 PD	System PD
					mW/m^3			
1	21-08-17	56641.93	45668.45	50729.62	57838.80	62486.72	66139.78	8837.78
2	22-08-17	4464.09	45668.45	39979.38	44851.72	41400.64	68609.95	8651.33
3	23-08-17	20213.48	45107.83	25678.08	25627.76	27763.37	31297.07	9322.55
4	24-08-17	60060.87	26264.13	62182.52	45481.83	43205.10	55775.61	10978.23
5	25-08-17	42256.64	66865.82	34601.24	45307.06	42263.55	61884.39	13697.93
8	28-08-17	34085.22	32184.80	34978.51	39581.96	35785.33	35022.47	13312.60
9	29-08-17	57711.39	56449.24	56615.06	57425.00	42554.73	67336.12	16403.96
10	30-08-17	37424.95	43728.77	55285.85	55725.10	54163.66	76132.03	16512.10
11	31-08-17	47596.84	48205.08	54529.29	59637.45	55822.17	76497.75	14492.80
12	01-09-17	58340.98	52874.74	53577.35	63679.11	57459.44	76658.92	12434.17
15	04-09-17	48507.34	41922.77	50360.43	50923.23	51044.99	61849.27	21499.04
16	05-09-17	54415.44	76268.23	83719.36	93118.91	82515.05	105408.34	25669.33
17	06-09-17	72444.13	89434.05	96622.07	90911.94	96563.94	110108.99	17421.98
18	07-09-17	39764.01	59856.64	59502.54	67127.50	55662.77	83514.64	18906.13
22	11-09-17	302222.31	296619.88	329803.14	367456.66	304257.88	442553.85	63144.73
23	12-09-17	115035.02	120513.97	113383.73	117245.05	105986.54	149553.18	18874.31
24	13-09-17	122706.80	148545.24	120053.36	139659.55	128777.90	167426.00	29670.57
25	14-09-17	99066.04	87319.77	87446.27	160600.65	140545.52	229722.61	33710.34
26	15-09-17	107543.92	104595.49	91407.63	156352.86	136677.29	210258.79	34858.88
29	18-09-17	210925.34	207015.32	223129.47	201448.32	207396.39	363903.09	31781.19
30	19-09-17	219625.58	222238.14	201368.96	240947.99	217810.84	379079.50	28548.13
31	20-09-17	213642.43	203025.47	190751.45	223517.98	218349.27	324562.22	33735.20
32	21-09-17	129009.62	169892.65	163069.11	245995.17	223315.62	311276.41	48430.02
33	22-09-17	197631.75	190735.36	255979.09	199473.34	230109.81	273981.09	44375.33
36	25-09-17	129878.25	110283.59	116011.16	120693.44	121246.90	170091.43	25736.45
37	26-09-17	136368.69	127184.19	108418.56	140458.95	133134.96	144862.85	16648.83
38	27-09-17	115076.72	117963.20	73534.37	104956.27	103542.33	68805.21	16832.79
39	28-09-17	110629.31	107221.29	102402.41	85457.22	117208.64	124593.21	12442.50
40	29-09-17	131191.63	127279.67	114030.48	129690.59	108012.75	96079.34	13745.17

Table I.3: ABR-MFC and individual compartments PD (normalised to anode chamber volume)

Day	Date	C1 PD	C2 PD	C3 PD	C4 PD	C5 PD	C6 PD	System PD
					mW/m^3			
43	02-10-17	93916.78	171502.23	164275.03	138907.18	113071.20	101244.90	14960.83
44	03-10-17	189014.90	181800.82	168586.71	153453.09	118455.54	109592.44	14965.80
45	04-10-17	198048.70	188546.06	178564.21	134581.02	111144.17	96471.93	14851.44
46	05-10-17	191099.62	166925.84	157888.35	116712.12	108395.32	79756.19	12912.35
47	06-10-17	193879.25	175689.87	173545.14	136885.17	96578.11	86409.42	14779.35
50	09-10-17	207151.99	184829.02	183246.43	127551.02	109153.38	104137.61	15211.91
51	10-10-17	209056.04	181930.41	184081.81	116241.89	105079.70	83062.14	14595.38
52	11-10-17	195880.59	181568.93	175162.02	121289.07	110095.64	97732.32	10689.86
53	12-10-17	209410.44	210541.39	162739.00	233283.18	161161.88	134800.35	21300.16
54	13-10-17	196631.09	192986.05	169449.05	116618.08	119022.32	175091.69	15731.49
57	16-10-17	225706.03	181418.89	188636.03	138813.13	89450.94	94095.77	12554.37
58	17-10-17	130587.06	129748.61	128717.14	115113.33	99234.86	81750.09	13307.63
59	18-10-17	129009.62	146826.53	111450.21	104368.48	84335.81	96688.88	17121.17
60	19-10-17	202836.61	173452.82	155759.46	101570.58	75239.11	122237.72	18559.33
61	20-10-17	194233.66	185906.62	178180.20	218110.29	164576.69	199597.09	36067.08
64	23-10-17	255274.35	242460.20	217147.01	280471.17	251859.72	334397.44	37756.32
65	24-10-17	274266.18	289888.28	249565.46	267422.18	212596.53	278857.38	45960.17
66	25-10-17	290123.97	262579.97	242532.03	273206.06	254027.63	253649.47	47172.10
67	26-10-17	252557.26	230170.10	232130.10	257092.70	222373.36	237501.94	44335.56
68	27-10-17	269346.23	231697.84	236549.58	251261.80	227757.70	234516.25	36022.33
71	30-10-17	368822.27	328224.96	342744.92	387943.20	339709.53	196704.38	49414.48
72	31-10-17	333138.76	204416.80	319576.38	335284.81	277690.40	232604.99	37537.55
73	01-11-17	398077.89	366711.68	347528.19	434841.22	366744.60	473195.93	58042.19
74	02-11-17	368301.09	350138.45	326151.69	387911.85	325887.35	295149.54	59395.82
75	03-11-17	396681.12	426129.78	404193.11	440703.47	344059.51	403471.25	78565.47
78	06-11-17	327030.52	300589.27	320007.55	329822.25	264229.54	414897.46	55247.91
79	07-11-17	322687.35	272319.30	297863.02	291121.98	254452.71	329045.92	52727.09
80	08-11-17	330970.65	280148.95	322567.61	347597.10	273156.22	330636.91	60611.48
81	09-11-17	347314.88	340467.32	284570.92	375184.18	295628.76	316132.03	62113.04
82	10-11-17	316252.50	276275.05	301191.10	261332.64	272986.18	339387.37	60111.80

Table I.4: ABR-MFC and individual compartments PD (normalised to cathode surface area)

Day	Date	C1 PD	C2 PD	C3 PD	C4 PD	C5 PD	C6 PD	System PD
					mW/m^2			
1	21-08-17	16974.88	13686.53	15203.52	17331.27	18726.11	19811.23	2648.37
2	22-08-17	1337.83	13518.52	11981.71	13439.72	12407.01	20551.14	2592.50
3	23-08-17	6057.73	7871.19	7695.65	7679.30	8320.17	9374.59	2793.64
4	24-08-17	17999.50	20039.24	18635.92	13628.53	12947.77	16706.79	3289.79
5	25-08-17	12663.79	11675.25	10369.89	13576.16	12665.61	18536.59	4104.79
8	28-08-17	10214.92	9645.57	10482.96	11860.65	10724.20	10490.48	3989.32
9	29-08-17	17295.39	16917.46	16967.37	17207.27	12752.87	20169.58	4915.69
10	30-08-17	11215.79	13105.22	16569.01	16697.90	16231.85	22804.27	4948.09
11	31-08-17	14264.18	14446.74	16342.27	17870.23	16728.87	22913.82	4342.98
12	01-09-17	17484.07	15846.21	16056.98	19081.30	17219.53	22962.09	3726.08
15	04-09-17	14537.05	12563.98	15092.88	15259.03	15297.24	18526.07	6442.51
16	05-09-17	16307.63	22857.08	25090.45	27902.87	24728.24	31573.57	7692.19
17	06-09-17	21710.61	26802.80	28957.36	27241.56	28938.43	32981.59	5220.75
18	07-09-17	11916.78	17938.64	17832.74	20114.60	16681.10	25015.63	5665.50
22	11-09-17	90572.29	88895.02	98841.06	110107.56	91180.47	132560.73	18922.25
23	12-09-17	34474.57	36117.24	33980.78	35132.22	31762.21	44796.53	5655.97
24	13-09-17	36773.71	44518.03	35979.65	41848.67	38592.36	50150.09	8891.22
25	14-09-17	29688.87	26169.16	26207.40	48123.62	42118.90	68810.15	10101.80
26	15-09-17	32229.58	31346.58	27394.61	46850.78	40959.66	62980.04	10445.98
29	18-09-17	63211.71	62041.13	66871.26	60363.53	62152.87	109002.01	9523.70
30	19-09-17	65819.07	66603.30	60349.70	72199.52	65273.89	113547.89	8554.87
31	20-09-17	64025.99	60845.39	57167.66	66976.66	65435.24	97218.01	10109.25
32	21-09-17	38662.58	50915.71	48871.35	73711.90	66923.57	93238.43	14512.77
33	22-09-17	59227.79	57162.13	76716.20	59771.73	68959.66	82067.15	13297.72
36	25-09-17	38922.90	33051.26	34768.21	36165.52	36335.46	50948.48	7712.31
37	26-09-17	40868.01	38116.26	32492.73	42088.21	39898.09	43391.61	4989.07
38	27-09-17	34487.07	35352.79	22038.04	31449.91	31029.72	20609.62	5044.20
39	28-09-17	33154.23	32133.51	30689.71	25607.06	35125.27	37320.13	3728.58
40	29-09-17	39316.51	38144.88	34174.61	38861.49	32369.43	28779.20	4118.94
43	02-10-17	28145.70	51398.09	49232.76	41623.22	33885.35	30326.47	4483.23
44	03-10-17	56645.42	54484.51	50524.96	45981.87	35498.94	32826.86	4484.72
45	04-10-17	59352.74	56506.01	53515.18	40326.90	33307.86	28896.80	4450.45

Table I.4: ABR-MFC and individual compartments PD (normalised to cathode surface area)

Day	Date	C1 PD	C2 PD	C3 PD	C4 PD	C5 PD	C6 PD	System PD
					mW/m^2			
46	05-10-17	57270.19	50026.57	47318.69	34972.52	32484.08	23889.83	3869.38
47	06-10-17	58103.21	52653.09	52010.98	41017.33	28942.68	25882.72	4428.85
50	09-10-17	62080.89	55392.04	54918.43	38220.37	32711.25	31192.94	4558.47
51	10-10-17	62651.51	54523.34	55168.79	34831.62	31490.45	24880.09	4373.72
52	11-10-17	58702.99	54415.01	52495.56	36344.00	32993.63	29274.33	3203.37
53	12-10-17	62757.72	63097.87	48772.41	69902.78	48297.24	40377.53	6382.91
54	13-10-17	58927.90	57836.64	50783.40	34944.34	35668.79	52446.23	4714.17
57	16-10-17	67641.30	54370.04	56533.68	41595.04	26806.79	28185.05	3762.10
58	17-10-17	39135.32	38884.80	38576.16	34493.45	29738.85	24487.08	3987.83
59	18-10-17	38662.58	44002.94	33401.31	31273.78	25273.89	28961.78	5130.61
60	19-10-17	60787.62	51982.67	46680.67	30435.40	22547.77	36614.58	5561.58
61	20-10-17	58209.42	55714.99	53400.10	65356.25	49320.59	59786.48	10808.03
64	23-10-17	76502.56	72663.72	65078.34	84042.55	75477.71	100164.01	11314.24
65	24-10-17	82194.18	86877.61	74794.06	80132.45	63711.25	83527.77	13772.64
66	25-10-17	86946.56	78693.48	72686.16	81865.58	76127.39	75977.10	14135.82
67	26-10-17	75688.28	68980.46	69568.73	77037.25	66641.19	71140.34	13285.80
68	27-10-17	80719.73	69438.31	70893.23	75290.03	68254.78	70246.02	10794.62
71	30-10-17	110531.47	98366.85	102719.67	116246.30	101804.67	58920.01	14807.78
72	31-10-17	99837.56	61262.37	95776.13	100467.33	83218.68	69673.53	11248.68
73	01-11-17	119299.01	109901.07	104153.21	130299.19	109906.58	141739.13	17393.20
74	02-11-17	110375.28	104934.18	97746.73	116236.91	97662.42	88407.86	17798.84
75	03-11-17	118880.42	127708.28	121135.52	132055.80	103108.28	120854.09	23543.30
78	06-11-17	98007.00	90084.62	95905.35	98830.49	79184.71	124276.65	16555.85
79	07-11-17	96705.40	81612.30	89268.70	87234.04	76254.78	98561.04	15800.45
80	08-11-17	99187.80	83958.79	96672.59	104156.69	81859.87	99037.60	18163.13
81	09-11-17	104085.97	102035.81	85285.09	112423.09	88594.48	94692.87	18613.09
82	10-11-17	94776.96	82797.81	90266.11	78307.74	81808.92	101658.67	18013.39

Table I.5: ABR-MFC and individual compartments PD (normalised to anode surface area)

Day	Date	C1 PD	C2 PD	C3 PD	C4 PD	C5 PD	C6 PD	System PD
					mW/m^2			
1	21-08-17	14.30	11.74	13.21	12.94	15.47	11.23	2.08
2	22-08-17	1.13	11.60	10.41	10.04	10.25	11.65	2.03
3	23-08-17	5.10	6.75	6.69	5.74	6.87	5.31	2.19
4	24-08-17	15.16	17.20	16.19	10.18	10.70	9.47	2.58
5	25-08-17	10.67	10.02	9.01	10.14	10.46	10.51	3.22
8	28-08-17	8.60	8.28	9.11	8.86	8.86	5.95	3.13
9	29-08-17	14.57	14.52	14.74	12.85	10.54	11.43	3.86
10	30-08-17	9.45	11.25	14.39	12.47	13.41	12.93	3.88
11	31-08-17	12.01	12.40	14.20	13.35	13.82	12.99	3.41
12	01-09-17	14.73	13.60	13.95	14.25	14.23	13.02	2.92
15	04-09-17	12.24	10.78	13.11	11.40	12.64	10.50	5.06
16	05-09-17	13.74	19.61	21.80	20.84	20.43	17.90	6.04
17	06-09-17	18.29	23.00	25.16	20.35	23.91	18.69	4.10
18	07-09-17	10.04	15.39	15.49	15.02	13.78	14.18	4.45
22	11-09-17	76.28	76.28	85.87	82.24	75.33	75.14	14.85
23	12-09-17	29.04	30.99	29.52	26.24	26.24	25.39	4.44
24	13-09-17	30.97	38.20	31.26	31.26	31.88	28.43	6.98
25	14-09-17	25.01	22.46	22.77	35.94	34.80	39.00	7.93
26	15-09-17	27.15	26.90	23.80	34.99	33.84	35.70	8.20
29	18-09-17	53.24	53.24	58.09	45.09	51.35	61.78	7.47
30	19-09-17	55.44	57.16	52.43	53.93	53.93	64.36	6.71
31	20-09-17	53.93	52.21	49.66	50.02	54.06	55.10	7.93
32	21-09-17	32.56	43.69	42.46	55.06	55.29	52.85	11.39
33	22-09-17	49.88	49.05	66.65	44.64	56.97	46.52	10.44
36	25-09-17	32.78	28.36	30.20	27.01	30.02	28.88	6.05
37	26-09-17	34.42	32.71	28.23	31.44	32.96	24.60	3.92
38	27-09-17	29.05	30.34	19.15	23.49	25.64	11.68	3.96
39	28-09-17	27.92	27.58	26.66	19.13	29.02	21.15	2.93
40	29-09-17	33.11	32.73	29.69	29.03	26.74	16.31	3.23
43	02-10-17	23.71	44.11	42.77	31.09	27.99	17.19	3.52
44	03-10-17	47.71	46.76	43.89	34.34	29.33	18.61	3.52
45	04-10-17	49.99	48.49	46.49	30.12	27.52	16.38	3.49

Table I.5: ABR-MFC and individual compartments PD (normalised to anode surface area)

Day	Date	C1 PD	C2 PD	C3 PD	C4 PD	C5 PD	C6 PD	System PD
					mW/m^2			
46	05-10-17	48.24	42.93	41.11	26.12	26.84	13.54	3.04
47	06-10-17	48.94	45.18	45.18	30.64	23.91	14.67	3.48
50	09-10-17	52.29	47.53	47.71	28.55	27.02	17.68	3.58
51	10-10-17	52.77	46.79	47.93	26.02	26.02	14.10	3.43
52	11-10-17	49.44	46.70	45.60	27.15	27.26	16.59	2.51
53	12-10-17	52.86	54.15	42.37	52.21	39.90	22.89	5.01
54	13-10-17	49.63	49.63	44.12	26.10	29.47	29.73	3.70
57	16-10-17	56.97	46.66	49.11	31.07	22.15	15.98	2.95
58	17-10-17	32.96	33.37	33.51	25.76	24.57	13.88	3.13
59	18-10-17	32.56	37.76	29.02	23.36	20.88	16.42	4.03
60	19-10-17	51.20	44.61	40.55	22.73	18.63	20.75	4.36
61	20-10-17	49.03	47.81	46.39	48.81	40.75	33.89	8.48
64	23-10-17	64.43	62.36	56.54	62.77	62.36	56.77	8.88
65	24-10-17	69.23	74.55	64.98	59.85	52.63	47.34	10.81
66	25-10-17	73.23	67.53	63.15	61.15	62.89	43.06	11.09
67	26-10-17	63.75	59.20	60.44	57.54	55.06	40.32	10.43
68	27-10-17	67.99	59.59	61.59	56.23	56.39	39.82	8.47
71	30-10-17	93.10	84.41	89.24	86.82	84.11	33.40	11.62
72	31-10-17	84.09	52.57	83.20	75.04	68.75	39.49	8.83
73	01-11-17	100.48	94.31	90.48	97.32	90.80	80.34	13.65
74	02-11-17	92.96	90.05	84.92	86.82	80.68	50.11	13.97
75	03-11-17	100.13	109.59	105.23	98.63	85.18	68.50	18.48
78	06-11-17	82.55	77.31	83.32	73.82	65.42	70.44	12.99
79	07-11-17	81.45	70.03	77.55	65.16	63.00	55.87	12.40
80	08-11-17	83.54	72.05	83.98	77.79	67.63	56.14	14.26
81	09-11-17	87.67	87.56	74.09	83.97	73.19	53.67	14.61
82	10-11-17	79.83	71.05	78.42	58.49	67.59	57.62	14.14

I.3. ABR-MFC polarisation data

Table I.6: ABR-MFC polarisation data for OLR 1

Date Measured	Day	Resistance Ω	Current mA	Voltage mV	Current (Calculated) mA	J_{ASA} mA/m^2	Power mW	PD_{CSA} mW/m^2
		0	7.10	400.00	-	-	-	-
		10000	15.10	325.00	0.03	0.12	10.56	39.34
		9000	16.30	321.00	0.04	0.13	11.45	42.65
		8000	15.40	314.00	0.04	0.15	12.32	45.91
		7000	15.00	306.00	0.04	0.16	13.38	49.83
		6000	14.60	294.00	0.05	0.18	14.41	53.66
		5000	15.30	282.00	0.06	0.21	15.90	59.24
		4000	14.40	269.00	0.07	0.25	18.09	67.38
13-09-17	24	3000	13.10	253.00	0.08	0.31	21.34	79.47
		2000	12.30	232.00	0.12	0.43	26.91	100.24
		1000	11.00	217.00	0.22	0.81	47.09	175.40
		500	9.00	168.00	0.34	1.25	56.45	210.26
		100	5.30	86.30	0.86	3.21	74.48	277.42
		50	3.00	52.80	1.06	3.93	55.76	207.69
		25	2.40	29.90	1.20	4.45	35.76	133.20
		20	1.90	23.60	1.18	4.40	27.85	103.73
		10	1.30	12.60	1.26	4.69	15.88	59.14

Table I.7: ABR-MFC polarisation data for OLR 2

Date Measured	Day	Resistance	Current	Voltage	Current (Calculated)	J_{ASA}	Power	PD_{CSA}
		Ω	mA	mV	mA	mA/m2	mW	mW/m^2
		0	15.90	513.00	-	-	-	-
		10000	10.60	336.00	0.03	0.13	11.29	42.05
		9000	10.60	326.00	0.04	0.13	11.81	43.98
		8000	10.10	314.00	0.04	0.15	12.32	45.91
		7000	9.10	305.00	0.04	0.16	13.29	49.50
		6000	9.00	292.00	0.05	0.18	14.21	52.93
		5000	8.90	277.00	0.06	0.21	15.35	57.16
		4000	7.50	295.00	0.07	0.27	21.76	81.04
11-10-17	52	3000	7.20	236.00	0.08	0.29	18.57	69.15
		2000	6.30	208.00	0.10	0.39	21.63	80.58
		1000	5.00	172.00	0.17	0.64	29.58	110.20
		500	4.20	134.00	0.27	1.00	35.91	133.77
		100	2.40	63.00	0.63	2.35	39.69	147.84
		50	1.80	41.00	0.82	3.05	33.62	125.23
		25	1.40	24.00	0.96	3.58	23.04	85.82
		20	1.40	23.00	1.15	4.28	26.45	98.52
		10	1.60	17.00	1.70	6.33	28.90	107.65

Table I.8: ABR-MFC polarisation data for OLR 3

Date Measured	Day	Resistance	Current	Voltage	Current (Calculated)	J_{ASA}	Power	PD_{CSA}
		Ω	mA	mV	mA	mA/m2	mW	mW/m^2
		0	41.00	561.00	-	-	-	-
		10000	24.00	329.00	0.03	0.12	10.82	40.32
		9000	23.70	207.00	0.02	0.09	4.76	17.73
		8000	20.20	306.00	0.04	0.14	11.70	43.60
		7000	22.60	304.00	0.04	0.16	13.20	49.18
		6000	22.10	296.00	0.05	0.18	14.60	54.39
		5000	22.40	279.00	0.06	0.21	15.57	57.99
		4000	17.20	261.00	0.07	0.24	17.03	63.44
08-11-17	80	3000	16.60	244.00	0.08	0.30	19.85	73.92
		2000	15.60	221.00	0.11	0.41	24.42	90.96
		1000	13.60	187.00	0.19	0.70	34.97	130.25
		500	10.40	151.00	0.30	1.12	45.60	169.86
		100	6.40	87.00	0.87	3.24	75.69	281.93
		50	4.80	63.00	1.26	4.69	79.38	295.68
		25	3.40	38.00	1.52	5.66	57.76	215.15
		20	3.30	35.00	1.75	6.52	61.25	228.15
		10	2.80	25.00	2.50	9.31	62.50	232.80

APPENDIX J:
Graphs

J.1. Daily operating parameters (daily operational analysis)

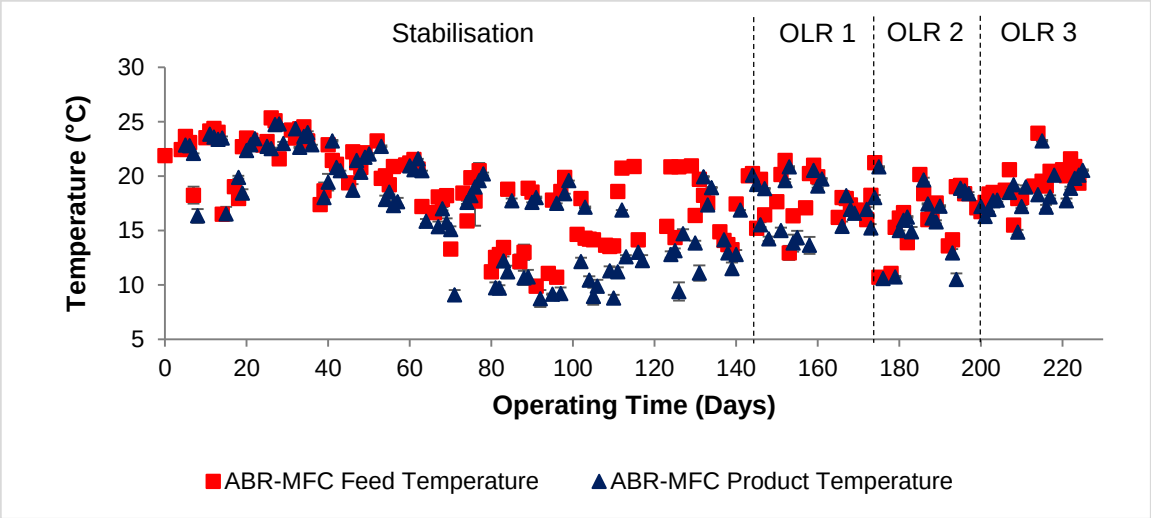

Figure J.1: Temperature of ABR-MFC feed and product samples

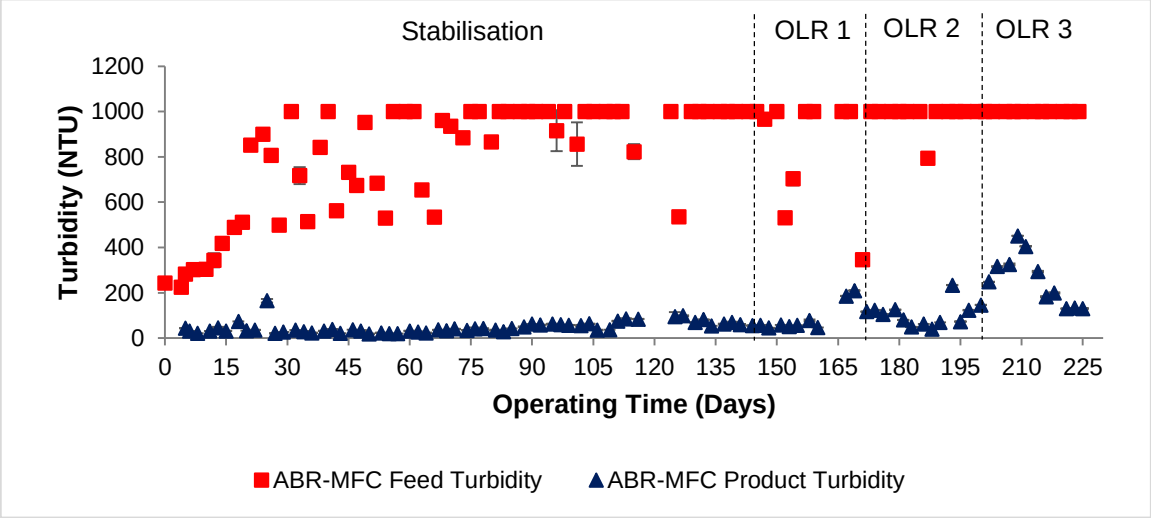

Figure J.2: Turbidity of ABR-MFC feed and product samples

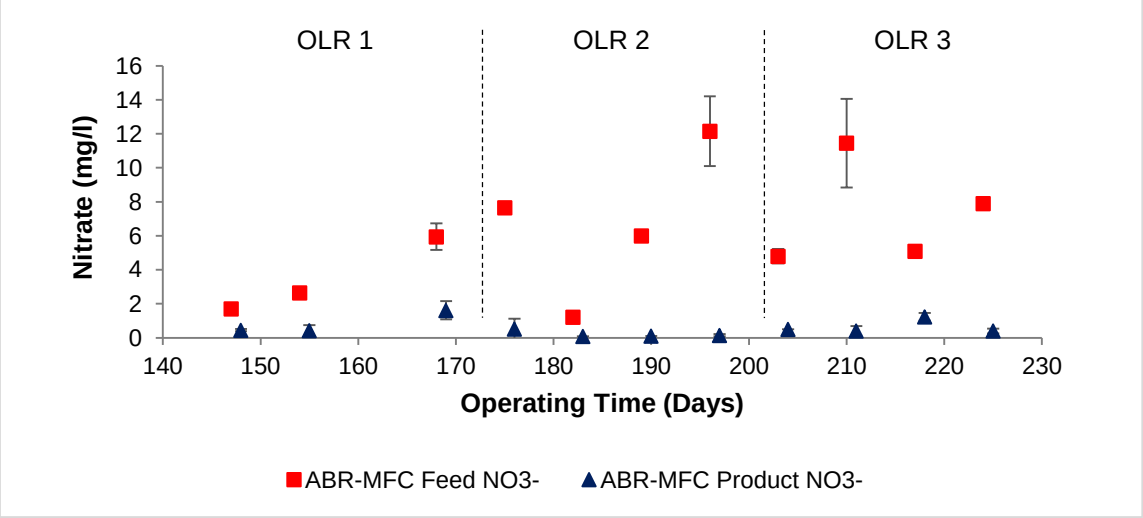

Figure J.3: Nitrate of ABR-MFC feed and product samples

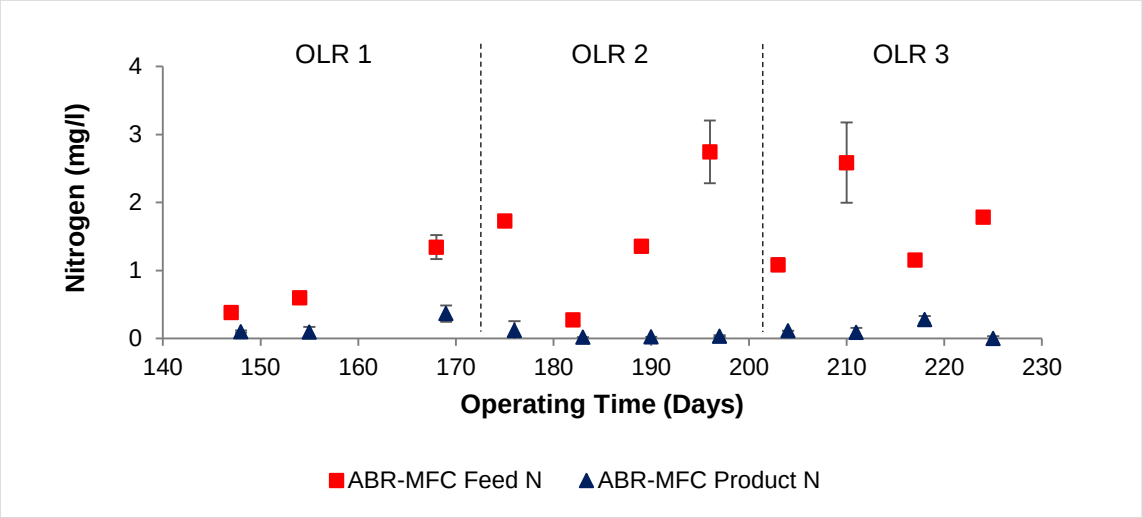

Figure J.4: Nitrogen of ABR-MFC feed and product samples

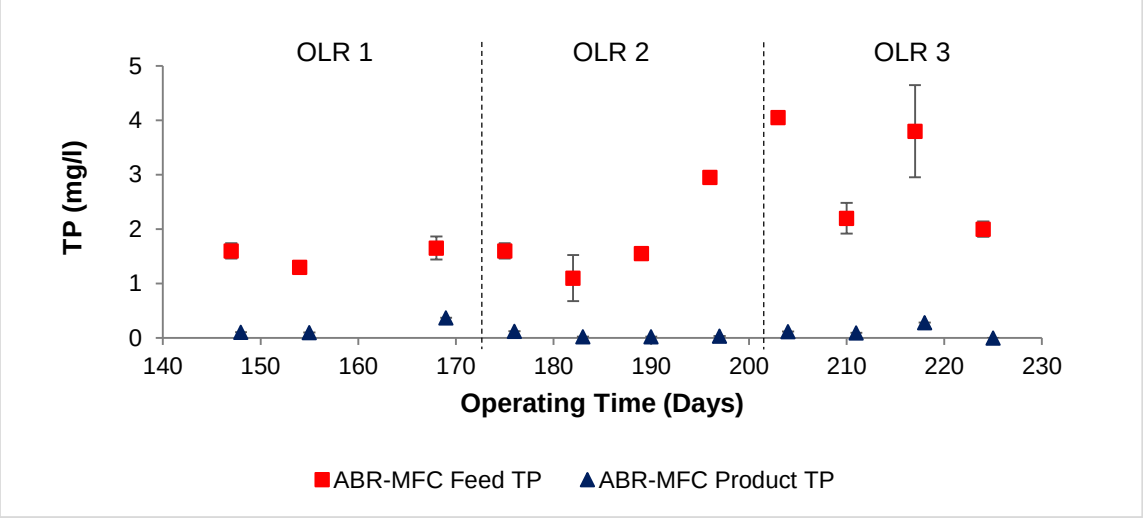

Figure J.5: TP of ABR-MFC feed and product samples

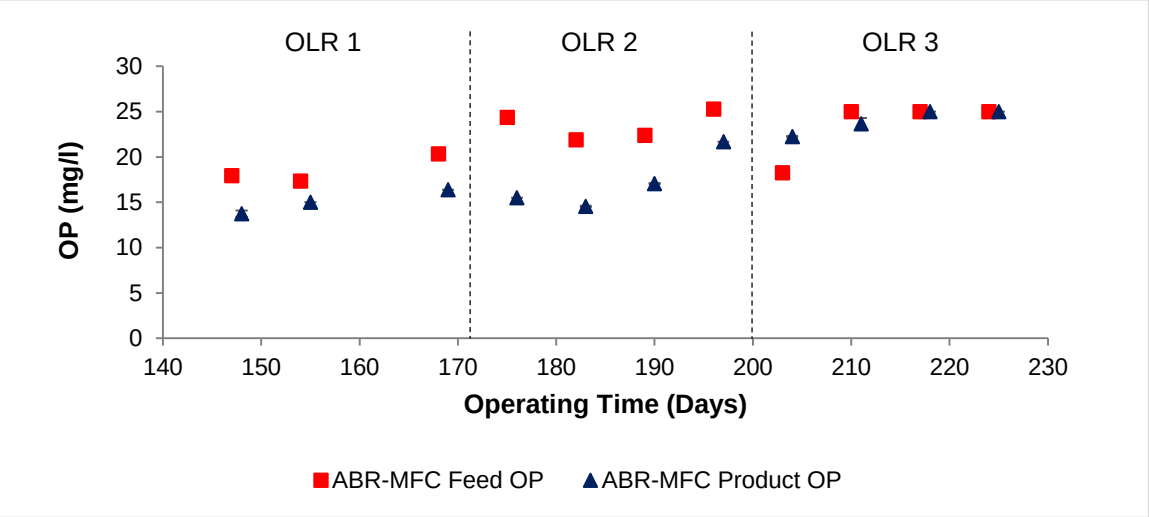

Figure J.6: OP of ABR-MFC feed and product samples

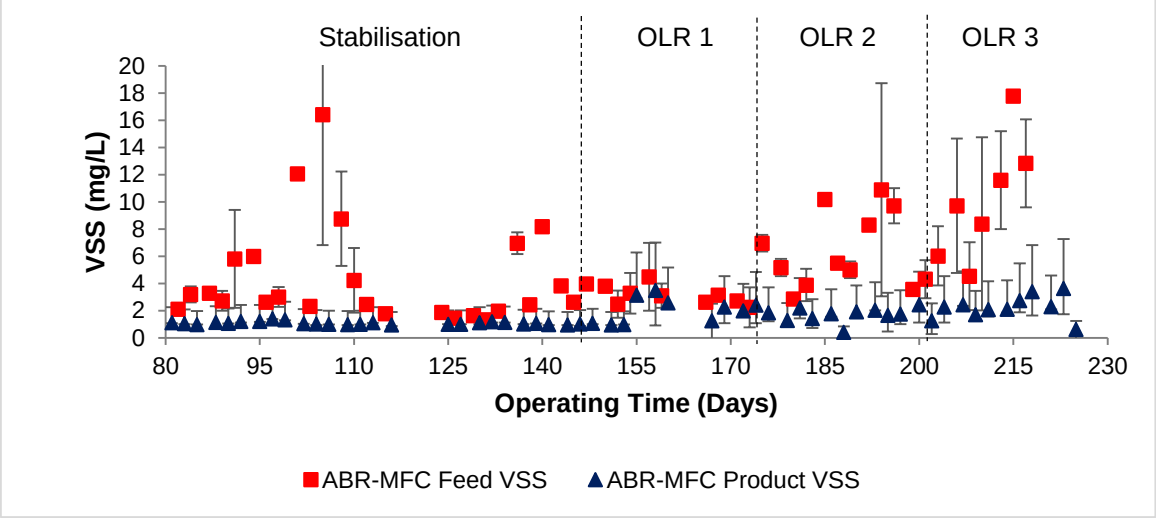

Figure J.7: VSS of ABR-MFC feed and product samples

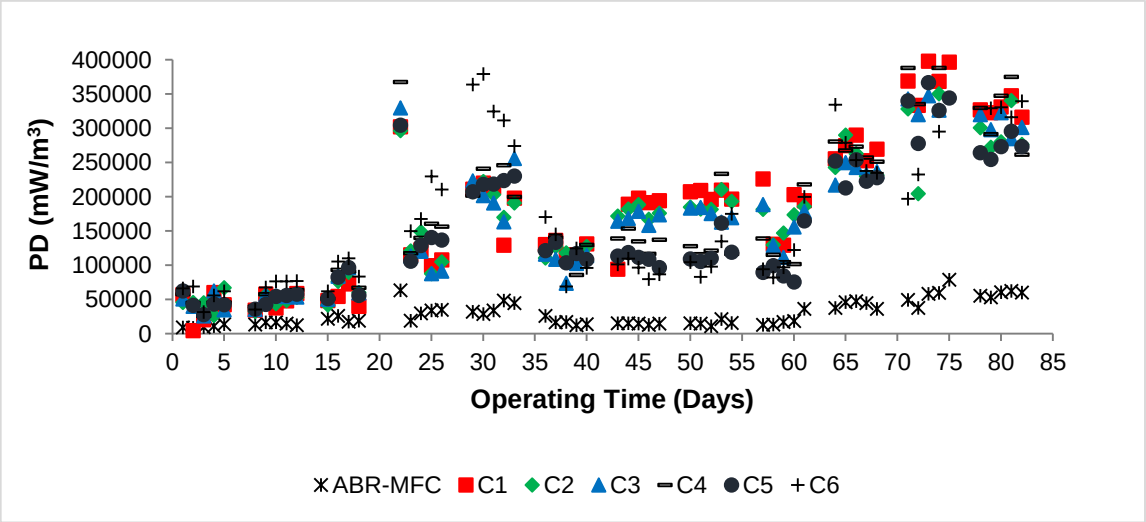

Figure J.8: PD (normalised to anode chamber volume) of ABR-MFC and individual compartments

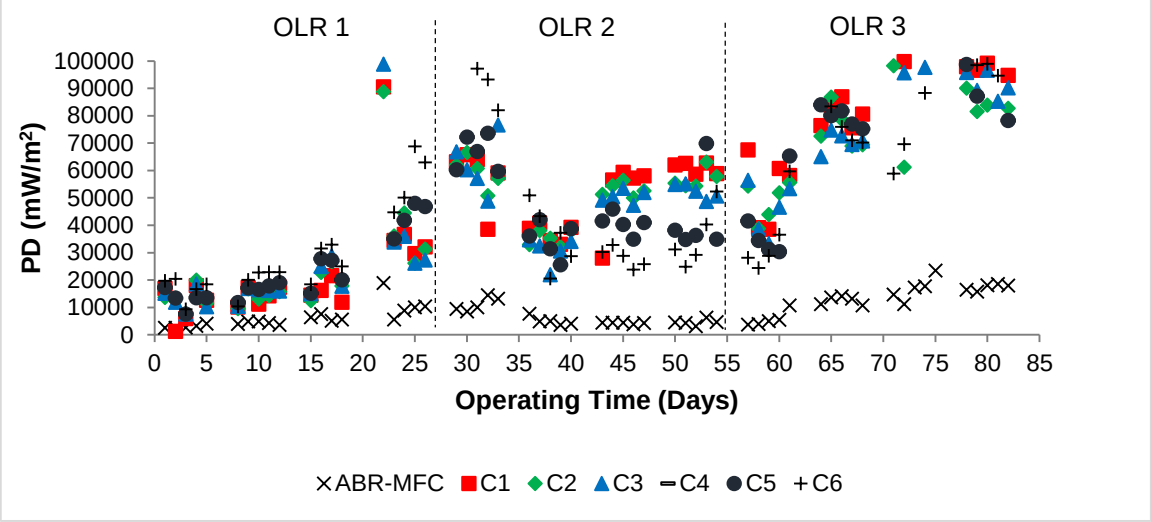

Figure J.9: PD (normalised to cathode surface area) of ABR-MFC and individual compartments

APPENDIX K
Unpublished article

K.1. Article 1 – Full article submitted for International Young Water Professional (IYWP) Conference 2017

Is it possible to successfully treat biodiesel wastewater and produce electricity simultaneously?

L. Grobbelaar*, D. De Jager, B. Godongwana*, and M.S. Sheldon****

* Department of Chemical Engineering, Cape Peninsula University of Technology, P.O. Box 652, Cape Town 8000, South Africa. E-mail: gloreeng@gmail.com; gdngwn@yahoo.com
** Department of Chemical Engineering, Cape Peninsula University of Technology, P.O. Box 1906, Bellville, 7635, South Africa. E-mail: dejagerd@cput.ac.za; sheldonm@cput.ac.za

Abstract

The disposal of untreated industrial biodiesel wastewater (BDWW), a highly-polluted effluent, may raise serious environmental concerns. The possibility of biologically treating industrial BDWW, thereby contributing to environmental remediation, was therefore evaluated in this study. Three individual anaerobic baffled reactor (ABR) treatment systems were evaluated. Two of these systems were modified by implementing microbial fuel cell (MFC) technology. The 2-compartment bench-scale ABR-MFC attained both a low chemical oxygen demand (COD) removal efficiency (9.3%) and a low power density (PD) (14.67 mW/m^3). The 6-compartment lab-scale ABR also achieved a low COD removal efficiency (13.1%), however the system effectively removed 94.1% fats, oils and grease (FOG). Following pH and C:N:P ratio adjustments, the 6-compartment lab-scale ABR-MFC, equipped with carbon fibre brush anodes and floating air-cathodes, reduced the COD (57.3%) in industrial BDWW while simultaneously generating power (28 560 mW/m^3 or 8 560 mW/m^2) as a by-product.

Keywords: Anaerobic baffled reactor (ABR); biodiesel wastewater (BDWW); bioelectricity; chemical oxygen demand (COD); microbial fuel cell (MFC) technology; wastewater treatment.

Introduction

The rising need for water for various uses in developing economic activities, along with an expanding global population has been a concern over the past decade. Society is being inattentive towards the rapid deterioration of water quality, thus further reducing a significant amount of water that can no longer be used without proper treatment. South Africa is facing important environmental challenges with growth in water usage outpacing supply (van der Nest, 2015).

As the international demand for biodiesel increases due to higher oil prices, government targets and incentives, the generation of biodiesel wastewater (BDWW) also increases (Department of Minerals and Energy, 2007). The global biodiesel industry uses up to 3 litres of potable water per litre of biodiesel produced, which resulted in the generation of an estimated 13 000 to 193 000 m^3/day of BDWW in 2011 (Veljković *et al*., 2014). Industries in South Africa are severely penalized if they do not meet the industrial wastewater discharge standard limits and therefore, methods for treating and re-using the wastewater are of great importance as this would aid in decreasing the operational costs of these industries, including biodiesel producing companies, due to a reduction in water usage from the municipality (Kleine *et al*., 2002).

BDWW is generally produced during the purification step of biodiesel production via the alkali-catalysed transesterification process of waste vegetable oil (Leung *et al*., 2009). The wet-washing purification process is effective in removing methanol, glycerol and any residual sodium

salts and soaps which were used or produced during biodiesel production (Veljković *et al.*, 2014). However, this purification process may at times cause serious environmental problems if the wastewater is not treated appropriately before discharge to municipal sewer systems (Veljković *et al*., 2014). The loss of fatty acid methyl esters (FAME) in the wastewater contributes to the generation of highly polluted wastewater (Daud *et al*., 2015), creating a major problem for the industry and the environment. Treatment prior to discharge is a necessity since the disposal of untreated BDWW may raise serious environmental concerns (i.e. disturbance of biological ecosystems) (Daud *et al*., 2014).

BDWW, a highly-polluted effluent, contains high concentrations of chemical oxygen demand (COD); total suspended solids (TSS); and fats, oils and grease (FOG). The nitrogen and phosphorous content in this wastewater is extremely low with a varying pH of between 3.3 and 11.2, creating an unfavourable environment for the growth of microorganisms, thus making it difficult for the wastewater to be degraded naturally (Daud *et al*., 2015). BDWW must therefore be effectively treated and comply with the industrial wastewater discharge standard limits prior to disposal (Veljković *et al*., 2014). Many studies have reported effective treatment of BDWW (De Gisi *et al*., 2013; Pitakpoolsil & Hunsom, 2013; Ramírez *et al*., 2012; and Siles *et al*., 2010), however to date literature implementing an anaerobic baffled reactor (ABR) equipped with microbial fuel cell (MFC) technology has not been reported.

A commercial biodiesel production company, located in the Western Cape (South Africa), discharges non-compliant wastewater directly to the municipal sewer system. Currently, the company is using an ineffective treatment system prior to disposal of the BDWW. The aim of this study was to evaluate the possibility of reducing the COD of the high-strength untreated industrial BDWW, using an ABR equipped with MFC technology, at ambient temperature, to meet the industrial wastewater discharge standard limits imposed by the City of Cape Town, while generating electricity as a by-product. The objectives of this study were to determine; 1) the treatment efficiency of the ABR-MFC, 2) the power generated by the ABR-MFC, and 3) whether the ABR-MFC can be regarded as a zero-waste discharge system.

Material and Methods

Three individual ABR treatment systems were evaluated. Industrial BDWW, with an initial COD of 27 370 mg/L was fed to a lab-scale ABR, while the BDWW fed to the bench- and lab-scale ABR-MFC's had an initial COD of 133 950 mg/L. The industrial BDWW was produced by a full-scale commercial biodiesel plant employing transesterification of waste vegetable oil.

Bench-scale ABR-MFC preliminary study

The viability of a 2-compartment bench-scale ABR-MFC, with a working volume of 2.3 L, was assessed in preliminary studies to determine whether it was feasible to incorporate existing ideas into an ABR-MFC on a larger scale; prior to economically investing in the initial materials required for the lab-scale ABR-MFC treatment system. Equal volumes of activated sludge and anaerobic granular sludge were used as inoculum. The system stabilized for 24 hours prior to feeding BDWW at an organic loading rate (OLR) of 0.9 kg COD/m^3.day for 3 weeks. Graphite electrodes were used as the anode and cathode of the single chamber bench-scale ABR-MFC system. The C:N:P ratio of BDWW was adjusted, by using urea and potassium dihydrogen orthophosphate (KH_2PO_4), to an optimal C:N:P ratio of 150:1.1:0.2 (Phukingngam *et al*., 2011), prior to dilution with tap water.

Lab-scale ABR study

A 6-compartment lab-scale ABR, with a working volume of 90.4 L, was evaluated for organic matter (i.e. COD and FOG) removal. After system inoculation (i.e. activated sludge) and stabilization (i.e. 7 days) BDWW was fed to the ABR at an OLR of 0.6 kg COD/m^3.day for 53 days.

Lab-scale ABR-MFC study

MFC technology was implemented into the existing 6-compartment lab-scale ABR, constructed with 5 mm thick plexiglass (L x H x W = 105 cm x 37 cm x 31 cm), to increase system efficiency and generate electricity as a by-product. Carbon fibre brush anode electrodes (Mill-Rose, 57 m^2) and floating carbon air-cathode electrodes were installed, thereby transforming the system into a hybrid ABR-MFC (Figure 1). The carbon air-cathode electrodes were manufactured at room temperature according to the single-phase inversion process described by Yang *et al*. (2014). Activated sludge and anaerobic granules were used as inoculum. The microorganisms present in the anodic chamber of the system were responsible for removing organic material (i.e. COD) contained within the BDWW, while releasing electrons for electricity generation. After system inoculation and stabilization (i.e. 30 days at 0.5 kg COD/m^3.day), BDWW was fed to the ABR-MFC at organic loading rates (OLR) of 1.2, 2.0 and 3.5 kg COD/m^3.day, respectively. The C:N:P ratio of BDWW feed was adjusted to 150:1.1:0.2 prior to dilution with tap water. The pH of the feed wastewater was maintained between 6.5 and 7.5 by adjusting the pH using sodium hydroxide and phosphoric acid.

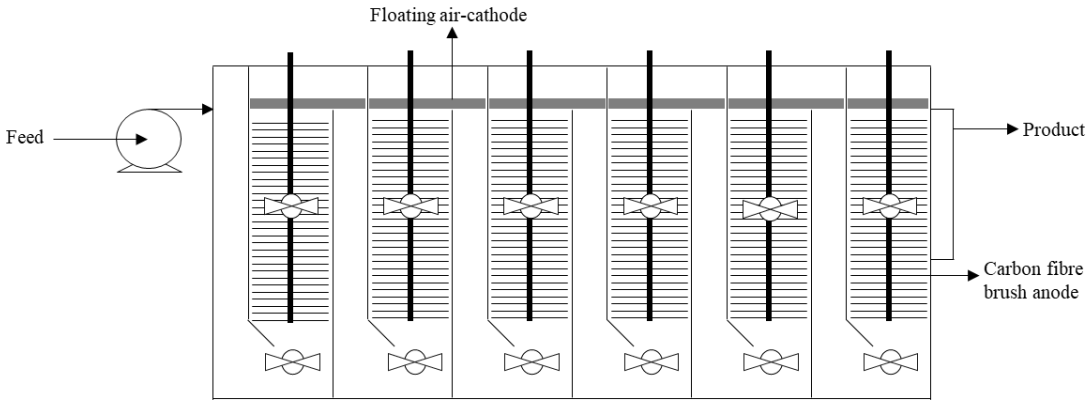

Figure 1: Schematic diagram of the 6-compartment lab-scale ABR-MFC.

The same analysis procedure was followed for all the studies. Samples collected from the feed and product tanks of the respective systems were analysed daily in duplicate for temperature, pH, conductivity, total dissolved solids (TDS) and salinity using a calibrated PCSTestr 35 handheld multiparameter. Turbidity (TN-100 turbidimeter, ISO 7027 compliant nephelometric method), COD (Merck COD Solution A, Cat. No. 1.14679.0495 and 1.14538.0065; Merck COD Solution B, Cat. No. 1.14680.0495 and 1.14539.0495) and TSS (ESS Method 350.2) were analysed in duplicate every second day. FOG was analysed by an outside independent South African National Accreditation System (SANAS) accredited laboratory for each OLR. Electricity generation (i.e. current and voltage) was monitored daily with a digital handheld multimeter (Top Tronic T820). All experiments were conducted at ambient conditions.

Results and Discussion

Bench-scale ABR-MFC performance

Biological treatment of BDWW (113 950 mg COD/L) was studied using a 2-compartment bench-scale ABR-MFC. BDWW was fed to the ABR-MFC at an OLR of 0.9 kg COD/m^3.day. Strong fluctuations in the ABR-MFC feed and product were observed (Figure 2). The ABR-MFC achieved an average COD removal of 9.3%. Although the feed wastewater was adjusted to obtain the optimal C:N:P ratio for biological treatment of BDWW (Phukingngam *et al*., 2011), the average pH of the feed was 5.3, explaining the low COD removal achieved by the system. Spillage and sludge washout could also be an attributing factor to the low removal efficiency observed.

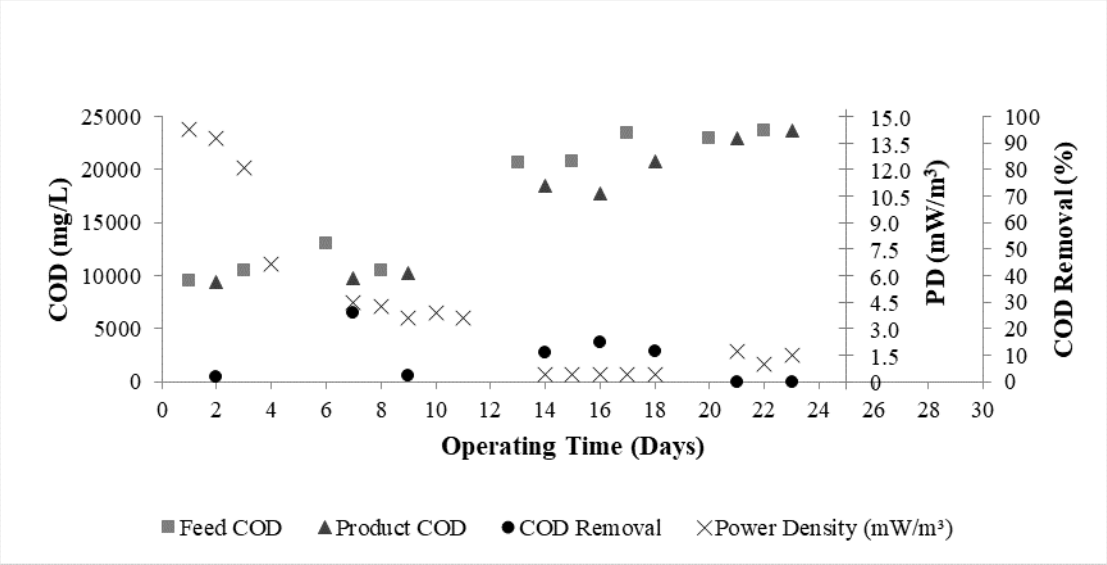

Figure 2: Treatment efficiency of the bench-scale ABR-MFC and the PD normalized to anode chamber volume (mW/m^3).

Respective maximum and average power densities (PD) of 14.7 mW/m^3 and 4.4 mW/m^3 were observed (Figure 2). The maximum PD was achieved during start-up and can be compared to the power generated (i.e. 35.6 mW/m^3) in the up-flow biofilter circuit system developed by Sukkasem *et al*. (2011). Power generation decreased significantly in week 3 and stabilized at 0.4 mW/m^3 when the ABR-MFC operated at an OLR of 0.9 kg COD/m^3.day. Initiation of the second OLR (1.9 kg COD/m^3.day) in week 4 caused power generation to increase to approximately 1.4 mW/m^3 and COD removal to decrease to 0%. It can therefore be said that an increase in OLR results in an apparent increase in the PD achieved by the system.

Lab-scale ABR performance

The anaerobic biological treatment of BDWW (27 370 mg COD/L) was studied in a lab-scale ABR. BDWW was fed to the ABR, at an OLR of 0.6 kg COD/m^3.day, which is in line with the work of Phukingngam *et al*. (2011) who reported OLRs ranging from 0.5 to 3.0 kg COD/m^3.day. The maximum COD removal capacity of the ABR was found to be 23.4%.

Although it has been proven that the ABR is capable of effectively treating a wide range of wastewaters with varying strength (0.45 – 1 000 mg COD/L) at OLRs ranging from 0.4 – 28.0 kg COD/m^3.day (Barber & Stuckey, 1999), the average COD removal obtained during the lab-scale ABR study was 13.1% (Figure 3). This indicated that anaerobic digestion was incomplete (Pirsaheb

et al., 2015). Phukingngam *et al*. (2011), who achieved 99% COD removal in an ABR treating BDWW, regarded 1.5 kg COD/m^3.day as the optimal OLR for the treatment of BDWW after operating ABRs at various OLRs.

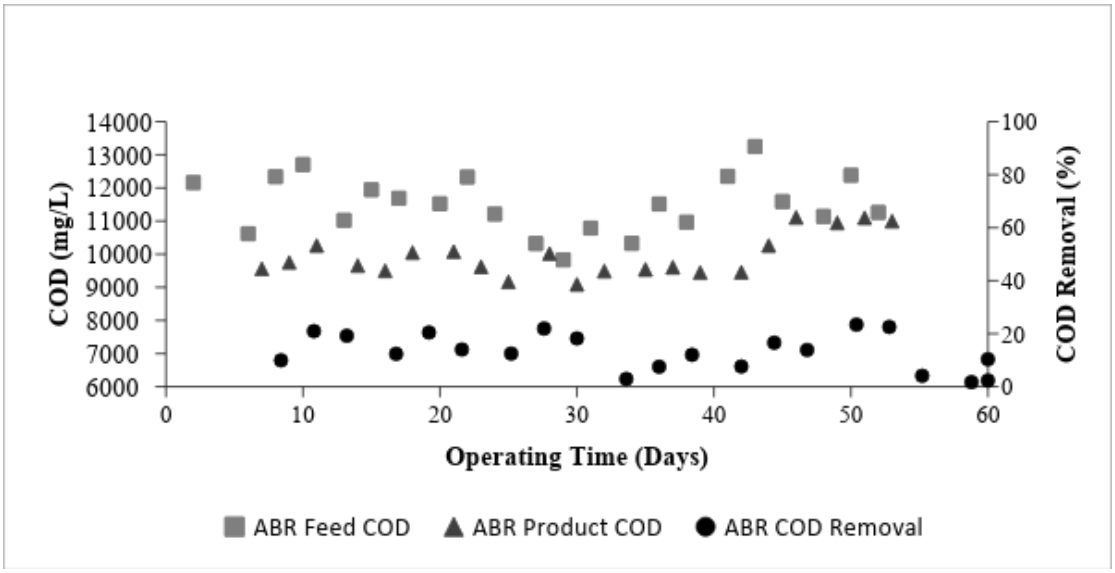

Figure 3: Treatment efficiency of the lab-scale ABR.

The pH of the ABR feed decreased from a maximum of 9.0 to 5.8 over the study period of 53 days. According to Jou and Huang (2003), the pH of influent wastewater should be maintained between 6.5 and 7.5 to ensure optimal biological activity during anaerobic conditions (Jou & Huang, 2003). A decrease in methanogenic activity can be expected once the pH deviates from this pH range which is optimal for methanogenesis since methanogens are pH sensitive (Barber & Stuckey, 1999). In a study conducted by Phukingngam *et al*. (2011), excessive accumulation of volatile fatty acids (VFA) in BDWW caused a decrease in pH creating an environment unfavourable for methanogenesis. It was therefore decided to maintain a neutral pH in future experiments to ensure optimal biological activity and therefore organic matter removal. Based on available literature the microbial metabolism was negatively affected by the low pH (5.8) of the influent BDWW in the lab-scale ABR system, thus causing a decrease in organic matter removal contained within the BDWW (Pirsaheb *et al*., 2015).

According to Siles *et al*. (2010), it becomes necessary to compensate for nutrient deficiency in the wastewater prior to feeding anaerobic systems. This would assist in activating microbial metabolism and growth within the system. It was therefore recommended that the nitrogen and phosphate levels be monitored in future experiments in order to ensure that the suggested C:N:P ratio for BDWW (150:1.1:0.2) is obtained (Phukingngam *et al*., 2011).

Despite the low COD removal efficiency (i.e. 13.1%) achieved by the ABR, the average FOG removal obtained during this study was 94.1%. Thus, removing nearly all the FOG in the influent wastewater with minimal sludge production. This high FOG removal efficiency attained by the system suggests that the ABR might be an appropriate pre-treatment technology for BDWW.

Lab-scale ABR-MFC performance

Maintaining a neutral feed pH and optimal C:N:P ratio (150:1.1:0.2) in the lab-scale ABR-MFC increased COD removal efficiency to an average of 57.3% (Figure 4). Florencio *et al*. (1996) and Pirsaheb *et al*. (2015) suggested that anaerobic treatment systems could be supplied with sodium bicarbonate and KH_2PO_4, or urea and $(NH_4)_2HPO_4$ as sources of alkalinity. The addition of these chemicals could assist in maintaining the optimum pH, as well as buffering the effect caused by VFA accumulation, resulting in effective digestion (Phukingngam *et al*., 2011).

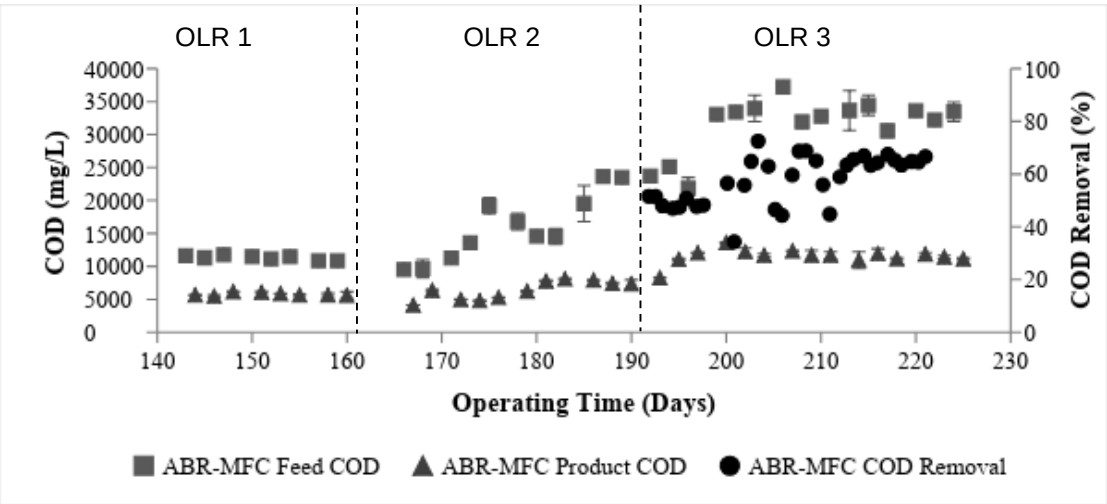

Figure 4: Treatment efficiency of the lab-scale ABR-MFC.

It is evident from Figure 4 that maintaining a neutral pH and an optimal C:N:P ratio in the ABR-MFC resulted in increased microbial activity thus resulting in a higher COD removal efficiency. The lab-scale ABR-MFC can be deemed as a zero-waste discharge system since the ABR-MFC was able to reduce 57.3% of COD and 97.9% FOG contained in the BDWW without any pre-treatment, apart from adjusting the pH and C:N:P ratio of the feed, without any sludge washout.

Considering the high fluctuations in the ABR-MFC feed COD (Figure 4), the COD in the product was affected by the change in OLR from 0.5 to 1.2 kg COD/m^3.day on day 169. However, the system stabilised again after approximately 20 days which proves that the lab-scale ABR-MFC is a robust system (Barber & Stuckey, 1999).

MFC technology was implemented into the lab-scale ABR on day 133 of experimental operation. The current and voltage generated by each compartment, as well as the total of all 6 compartments configured in series and parallel were measured. The power generated by the ABR-MFC was calculated using Ohm's law of: $P = I \times V$ where *P* represent power (mW), *I* current (mA) and *V* voltage (mV) (Spellman, 2014). After monitoring the power production of both series and parallel configurations, it was decided to operate the lab-scale ABR-MFC in closed circuit mode (i.e. 1 kΩ external resistance) configured in parallel since the parallel configuration produced a higher current.

The ABR-MFC attained an average PD of 28 560 mW/m^3 (8 560 mW/m^2) in closed circuit mode (Figure 5). These results can be compared to the PD (i.e. 12 000 mW/m^3 (750 mW/m^2) and

10 700 mW/m^3) obtained by Tugtas *et al*. (2011) and Feng *et al*. (2010), respectively. It is evident (Figure 5) that the power generation steadily increased as the BDWW strength was increased. Sukkasem *et al*. (2011), studied the treatment of BDWW in an up-flow biofilter circuit (UBFC) with electricity as a by-product. The UBFC obtained a PD of 35.6 mW/m^3 while reducing the COD in the BDWW by 50%. The lab-scale ABR-MFC therefore obtained a slightly higher treatment efficiency (i.e. 55.3%) for the treatment of BDWW while simultaneously generating a higher PD as by-product.

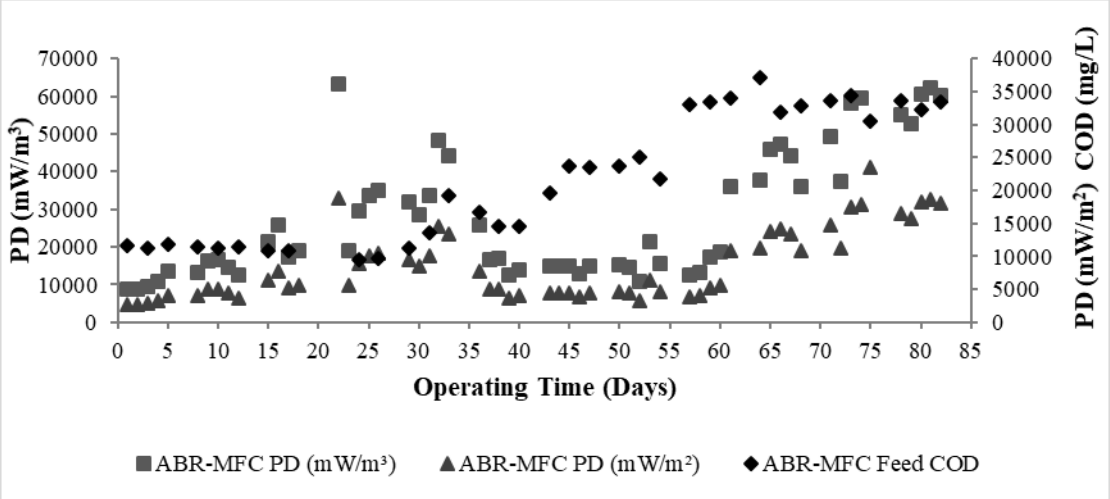

Figure 5: PD (normalized to anode chamber volume (mW/m^3) and cathode surface area (mW/m^2)) and treatment efficiency of lab-scale ABR-MFC.

Conclusions

The lab-scale ABR-MFC had an average treatment efficiency of 57.3% (COD removal) while generating power (28 560 mW/m^3 (8 560 mW/m^2)) as a by-product. The ABR-MFC removed 97.9% FOG from the BDWW which contributes to regarding the ABR-MFC as a robust zero-waste discharge system. However, currently more research is being conducted to increase system efficiency regarding COD removal and the PD achieved by the lab-scale ABR-MFC system.

Acknowledgement

This paper would not have been published without the support provided by the program committee of the International Young Water Professionals Conference organised by IWA, WISA and YWP-ZA. The financial assistance of the National Research Foundation (NRF) of South Africa is hereby acknowledged. Opinions expressed and conclusions arrived at, are those of the author and are not necessarily to be attributed to the NRF.

References

Barber, W.P. & Stuckey, D.C. 1999. The use of the anaerobic baffled reactor (ABR) for wastewater treatment: A review. *Water Research*, 33(7): 1559–1578.

Daud, N.M., Bdullah, S.R.S., Hasan, H.A. & Yaakob, Z. 2014. Production of biodiesel and its wastewater treatment technologies: A review. *Process Safety and Environmental Protection*, 94(October): 487–508.

Department of Minerals and Energy. 2007. *Biofuels Industrial Strategy of the Republic of South Africa*.

Feng, Y., Lee, H., Wang, X., Liu, Y. & He, W. 2010. Continuous electricity generation by a graphite granule baffled air–cathode microbial fuel cell. *Bioresource Technology*, 101(2): 632–638.

Florencio, L., Field, J.A., van Langerak, A. & Lettinga, G. 1996. pH-Stability in anaerobic bioreactors treating

methanolic wastewaters. *Water Science and Technology*, 33(3): 177–184.
De Gisi, S., Galasso, M. & De Feo, G. 2013. Full-scale treatment of wastewater from a biodiesel fuel production plant with alkali-catalyzed transesterification. *Environmental Technology*, 34(7): 861–870.
Jou, C.-J.G. & Huang, G.-C. 2003. A pilot study for oil refinery wastewater treatment using a fixed-film bioreactor. *Advances in Environmental Research*, 7(2): 463–469.
Kleine, J., Peinemann, K. V. & Schuster, C. 2002. Multifunctional system for treatment of wastewaters from adhesive-producing industries: Separation of solids and oxidation of dissolved pollutants using doted microfiltration membranes. *Chemical Engineering Science*.
Leung, D.Y.C., Wu, X. & Leung, M.K.H. 2009. A review on biodiesel production using catalyzed transesterification. *Applied Energy*, 87(4): 1083–1095.
Phukingngam, D., Chavalparit, O., Somchai, D. & Ongwandee, M. 2011. Anaerobic baffled reactor treatment of biodiesel-processing wastewater with high strength of methanol and glycerol: reactor performance and biogas production. *Chemical Papers*, 65(5): 644–651.
Pirsaheb, M., Rostamifar, M., Mansouri, A.M., Zinatizadeh, A.A.L. & Sharafi, K. 2015. Performance of an anaerobic baffled reactor (ABR) treating high strength baker's yeast manufacturing wastewater. *Journal of the Taiwan Institute of Chemical Engineers*, 47: 137–148.
Pitakpoolsil, W. & Hunsom, M. 2013. Adsorption of pollutants from biodiesel wastewater using chitosan flakes. *Journal of the Taiwan Institute of Chemical Engineers*, 44(6): 963–971.
Ramírez, X.M. V., Mejía, M.G.H., López, V.K.P., Vásquez, G.R. & Sepúlveda, J.M.M. 2012. Wastewater treatment from biodiesel production via a coupled photo-Fenton-aerobic sequential batch reactor (SBR) system. *Water Science and Technology*, 66(4): 824–830.
Siles, J.A., Martín, M.A., Chica, A.F. & Martín, A. 2010. Anaerobic co-digestion of glycerol and wastewater derived from biodiesel manufacturing. *Bioresource Technology*, 101(16): 6315–6321.
Spellman, F.R. 2014. *Water and Wastewater Treatment Plant Operations*. 3rd ed. New York: CRC Press.
Sukkasem, C., Laehlah, S., Hniman, A., Sompong, O., Boonsawang, P., Rarngnarong, A., Nlsoa, M. & Klrdtongmee, P. 2011. Upflow bio-filter circuit (UBFC): Biocatalyst microbial fuel cell (MFC) configuration and application to biodiesel wastewater treatment. *Bioresource Technology*, 102(22): 10363–10370.
Tugtas, A.E., Cavdar, P. & Calli, B. 2011. Continuous flow membrane-less air cathode microbial fuel cell with spunbonded olefin diffusion layer. *Bioresource Technology*, 102(22): 10425–10430.
Van der Nest, G. 2015. The economic consequences of load shedding in South Africa and the state of the electrical grid. *tralac*. http://www.tralac.org/discussions/article/7000-the-economic-consequences-of-load-shedding-in-south-africa-and-the-state-of-the-electrical-grid.html 24 May 2016.
Veljković, V.B., Stamenković, O.S. & Tasić, M.B. 2014. The wastewater treatment in the biodiesel production with alkali-catalyzed transesterification. *Renewable and Sustainable Energy Reviews*, 32: 40–60.
Yang, W., He, W., Zhang, F., Hickner, M.A. & Logan, B.E. 2014. Single-Step Fabrication Using a Phase Inversion Method of Poly(vinylidene fluoride) (PVDF) Activated Carbon Air Cathodes for Microbial Fuel Cells. *Environmental Science and Technology Letters*, 1(10).